2011

ISOLATION AND ELUCIDATION OF THE CHRYSOMYCIN BIOSYNTHETIC GENE CLUSTER AND ALTERING THE GLYCOSYLATION PATTERNS OF TETRACENOMYCINS AND MITHRAMYCIN-PATHWAY MOLECULES

Stephen Eric Nybo
University of Kentucky, senybo2@uky.edu

ISOLATION AND ELUCIDATION OF THE CHRYSOMYCIN BIOSYNTHETIC GENE CLUSTER AND ALTERING THE GLYCOSYLATION PATTERNS OF TETRACENOMYCINS AND MITHRAMYCIN-PATHWAY MOLECULES

DISSERTATION

A dissertation submitted in partial fulfillment of the
requirements for the degree of Doctor of Philosophy in the
College of Pharmacy at the University of Kentucky

By

Stephen Eric Nybo

Lexington, Kentucky

Director: Doctor Jürgen Rohr, Professor of Pharmaceutical Sciences

Lexington, Kentucky

2011

ABSTRACT OF DISSERTATION

ISOLATION AND ELUCIDATION OF THE CHRYSOMYCIN BIOSYNTHETIC GENE CLUSTER AND ALTERING THE GLYCOSYLATION PATTERNS OF TETRACENOMYCINS AND MITHRAMYCIN-PATHWAY MOLECULES

Natural products occupy a central role as the majority of currently used antibiotic and anticancer agents. Among these are type-II polyketide synthase (PKS)-derived molecules, or polyketides, which are produced by many representatives of the genus *Streptomyces.* Some type-II polyketides, such as the tetracyclines and the anthracycline doxorubicin, are currently employed as therapeutics. However, several polyketide molecules exhibit promising biological activity, but due to toxic side effects or solubility concerns, remain undeveloped as drugs.

Gilvocarcin V (GV) (topoisomerase II inhibitor) has a novel mechanism of action: [2+2] cycloaddition to thymine residues by the 8-vinyl side chain and cross-linking of histone H. Mithramycin blocks transcription of proto-oncogenes *c-myc* and *c-src* by forming an Mg^{2+}-coordinated homodimer in the GC-rich minor groove of DNA. The purpose of this research was to investigate the biosynthesis of several type II polyketide compounds (e.g. chrysomycin, elloramycin, and mithramycin) with the goal of improving the bioactivities of these drugs through combinatorial biosynthesis. Alteration of the glycosylation pattern of these molecules is one promising way to improve or alter the bioactivities of these molecules. To this end, an understanding of the glycosyltransferases and post-polyketide tailoring enzymatic steps involved in these biosynthetic pathways must be established. Four specific aims were established to meet these goals.

In specific aim 1, the biosynthetic locus of chrysomycin A was successfully cloned and elucidated, which afforded novel biosynthetic tools. Chrysomycin monooxygenases were found to catalyze identical roles to their gilvocarcin counterparts. Cloning of deoxysugar constructs (plasmids) which could direct biosynthesis of ketosugars, NDP-D-virenose, and NDP-D-fucofuranose in foreign pathways was undertaken in specific aim 2. Finally, these "sugar" plasmids were introduced into producer organisms of elloramycin and mithramycin pathways in specific aims 3 and 4 to interrogate the endogenous glycosyltransferases in order to alter their glycosylation patterns. These experiments resulted in the successful generation of a newly glycosylated tetracenomycin, as well as premithramycin, and mithramycin analogues. In specific aim 4, a new mithramycin analogue with an altered sugar pattern rationally designed and improved structural features was generated and structurally elucidated.

KEYWORDS: Polyketides, Combinatorial Biosynthesis, Gene Cluster, Glycosyltransferases, Glycodiversification

Eric Nybo
Student's Signature

9-27-2011
Date

ISOLATION AND ELUCIDATION OF THE CHRYSOMYCIN BIOSYNTHETIC GENE CLUSTER AND ALTERING THE GLYCOSYLATION PATTERNS OF TETRACENOMYCINS AND MITHRAMYCIN-PATHWAY MOLECULES

By

Stephen Eric Nybo

Dr. Jurgen Rohr
Director of Dissertation

Dr. Jim Pauly
Director of Graduate Studies

9-27-2011

Dedicated to Minji Sohn and my family

DEDICATIONS

Human beings will be happier - not when they cure cancer or get to Mars or eliminate racial prejudice or flush Lake Erie but when they find ways to inhabit primitive communities again. That's my utopia. - Kurt Vonnegut

Heavy Horses, move the land under me/ Behind the plough gliding --- slipping and sliding free/ Now you're down to the few/ And there's no work to do/ The tractor's on its way…A Heavy Horse and a tumbling sky/ Brewing heavy weather. –Jethro Tull, "Heavy Horses"

This dissertation is composed of five years of intensive singular effort and study, but its composition would have been doubtful without the tremendous contributions of several extraordinary individuals. First, my Dissertation Chair, Dr. Jurgen Rohr deserves the highest thanks and praise for his support, his optimism and encouragement, and certainly for the high level of scientific training and deductive reasoning he employed in evaluating and critiquing my work. His mentoring is directly responsible for the scientific maturation I have today. Next, I would like to thank my Dissertation Committee for their time and their helpful suggestions, and the outside examiner, respectively: Dr. Kyung-bo Kim, Dr. Chris Schardl, Dr. Steven van Lanen, Dr. Janice Buss, and Dr. David Watt. Their suggestions and expertise were essential to developing the theoretical aspects of this project.

In addition to the mentoring and expertise of my committee members, I would like to thank my girlfriend, Minji, for her unconditional love and support throughout my doctoral process. I could not ask for a more desirable companion and her patience through my working long hours.

Without my colleagues, I simply would not have had the disposition or scholarly counseling on a day to day basis necessary to survive this process. Dr. Madan Kharel, my senior and molecular biology mentor, essentially trained me from the ground up with regards to molecular cloning, biosynthetic pathways, and *Streptomyces* manipulations. I am very greatful for the training he provided me in my time in the Rohr lab. Dr. Miranda Beam helped me to understand that it was "OK" to not be so high-strung in the laboratory. Mike Smith's sarcasm and light-hearted outlook made for a very pleasant work environment. Dr. Mohammed Abdelfattah and Dr. Irfan Baig always encouraged me in my first two years and instructed me in basic extraction techniques. Dr. Pallab Pahari was always quick with a joke, and was gracious in taking many NMR measurements for me. Micah Shepherd's off-the-wall humor always mirrored my own, and he served as an inspiration for hard work and organization. Dr. Mary Bosserman always challenged me to become a better scientist, and her questioning approach to science has assuredly benefited my work. Dr. Guojun Wang always helped when I had a *Streptomyces* quandary, and I owe a huge debt of gratitude to Dr. Khaled Shaaban for helping transform me into a better experimental chemist with regards to chromatography and structure elucidation. To Theresa Downey, it is a long process but you will eventually reach the culmination of your Ph.D., too. Keep your strong work ethic and your sense of humor. They will propel you through periods of tough experimentation.

My family remains my stronghold, and I am lucky to have two loving and world-class parents. My dad would always offer a kind word and advice when I needed a dad's perspective. My mother's selflessness is the reason for my success as an individual; her life lessons that she instilled in me at an early age, her trips to Lexington to go grocery shopping and do laundry, and the countless times she has been there for me must simply be praised. My grandparents (of whom I am fortunate to have with me in my graduate career) have always afforded their love and kindness, as well as the sharpness of their perception and charming wit. My uncle and aunt have frequently gone above and beyond the call of duty with regards to spoiling their nephew; my uncle's penchant for gambling and never growing up have served as tremendous inspiration for me. My sister's support and love and zeal for life and happiness encouraged me to leave the lab and find a life of my own. While an individual effort, this work was made possible by the support of a cast of extraordinary human beings, indelible in character and invaluable in terms of contributions.

ACKNOWLEDGEMENTS

Dr. Madan Kharel and Micah Shepherd are thanked for the initial work on the *Streptomyces albaduncus* cosmid library. Drs. Carsten Fischer and Lili Zhu are acknowledged for their work generating the *gilL* and *gilN*-deleted cosG9B3 cosmids. Dr. Jose Salas and co-workers are acknowledged for the numerous contributions to *in vivo* deoxysugar biosynthesis and generation of several parent plasmids that formed the platform from which much of this present work proceeded. Dr. Khaled Shaaban is acknowledged for his assistance in collecting spectroscopic data and in natural product isolation techniques.

TABLE OF CONTENTS

LIST OF TABLES

LIST OF FIGURES

LIST OF ABBREVIATIONS

ACAT	Acetyl-Coenzyme A acetyltransferase
ACP	acyl carrier protein
APCI	atmosphere pressure chemical ionization
AT	acyl transferase
ATP	adenosine triphosphate
BLAST	Basic-Localized Alignment Search Tool
bp	(nucleotide) base pair
CLF	chain length factor
CoA	co-enzyme A
chry	chrysomycin gene cluster
COSY	correlation spectroscopy
CV	chrysomycin V
DEBS	6-deoxyerythronolide B synthase
DH	4,6-dehydratase/ dehydratase
DNA	deoxyribonucleic acid
DMSO	dimethylsulfoxide
E. coli	*Escherichia coli*
ESI	electrospray ionization
FAD	flavin adenine dinucleotide
FLP	flippase
FRT	FLP recombinase recognition target
GT	glycosyltransferase
GV	gilvocarcin V
HMBC	heteronuclear multiple bond correlation
HPLC	high performance liquid chromatography
KSα	ketoacyl synthase
KSβ	chain length factor (CLF)
LB	lysogeny broth (also Luria-Bertani broth)
MCAT	malonyl-CoA acyl carrier protein transacylase
MT	methyltransferase

MTM	mithramycin (*mtm*= mithramycin gene cluster)
SDK	mithramycin shortened diketone
SK	mithramycin shortened ketone
NAD	nicotinamide adenine dinucleotide (oxidized)
NAD(P)H	nicotinamide adenine dinucleotide phosphate (reduced)
NMR	nuclear magnetic resonance
ORF	open reading frame
PCR	polymerase chain reaction
PEG	polyethylene glycol
PKS	polyketide synthase
PV	polycarcin V
R_t	HPLC retention time (relative)
RV	ravidomycin V
TCMC	tetracenomycin C
TE	thioesterase
TLC	thin layer chromatography
UV	ultraviolet
UV-VIS	ultraviolet visible spectrum

CHAPTER 1: BACKGROUND AND INTRODUCTION

INTRODUCTION

General Overview and Pharmaceutical Relevance of Polyketides

Since the earliest development of scientific thought, natural products have occupied a central role as pharmaceutical agents in the treatment of human disease. The etymology for pharmaceutic stems from the Greek word, *pharmakon*, meaning "a remedy or poison." This distinction keenly demonstrates that the earliest Hippocratic physicians understood drugs to have beneficial or harmful effects on human physiology. With the advent of modern pharmacognosy, natural products have served an integral role as first-resort therapeutic agents, models for elucidating biosynthetic pathways, and as targets for chemical total synthesis (*1*).

Within the greater context of natural products, polyketides are a family of bacterial- and fungi-derived natural products that serve in many pharmaceutically relevant capacities (*2*). Polyketides are produced by polyketide synthases (PKS) through a series of linear condensation steps between a starter unit (e.g. acetyl-CoA, propionyl-CoA) and several extender units (e.g. malonyl-CoA) to yield in type II PKS systems an enzyme-tethered poly-β-ketoester. Many polyketides are biosynthesized by gram positive, soil-dwelling bacteria of the *Actinomycetes* family, with most of these compounds being produced by the genus *Streptomyces* (*3*).

Polyketide-derived molecules are unmatched in structural diversity and many of them possess anticancer and other biological activities (**Figure 1**) (*4*). These activities include immunosuppressant, antimicrobial, antineoplastic, and cholesterol-reducing drugs, to name a few; the sales of polyketide-derived pharmaceutics are in excess of fifteen billion dollars per annum (*2*). So far, three types of polyketide synthases have been described with respect to the nature of their biosynthesis: type I, type II, and type III. As such, these families of polyketide synthases are capable of generating very diverse chemical structures. Resveratrol (**1**) is a type III stilbene-type compound that has received considerable interest for its anti-inflammatory and cancer-preventive activities, while tetrangulol (**2**) is the first such characterized type II PKS-derived angucycline antibiotic (*5*). Methymycin (**3**) and especially erythromycin A (**7**) are 12-membered and

14-membered macrolides, respectively, studied for their antimicrobial activities (*6*-*7*). Amphotericin B (**4**) is a clinically important type I PKS-derived antifungal agent (*8*). Lovastatin (**6**) is a highly reduced iterative type I PKS-derived product that possesses nanomolar inhibition of HMG-CoA reductase, and as such, is representative of the blockbuster statin drugs (*9*-*10*). Oxytetracycline (**5**) is a type II PKS-derived antibiotic, whereas tetracenomycin C (**8**) was important in initial studies for aromatization and cyclization of nascent polyketide intermediates in context with type-2 PKSs (*11*).

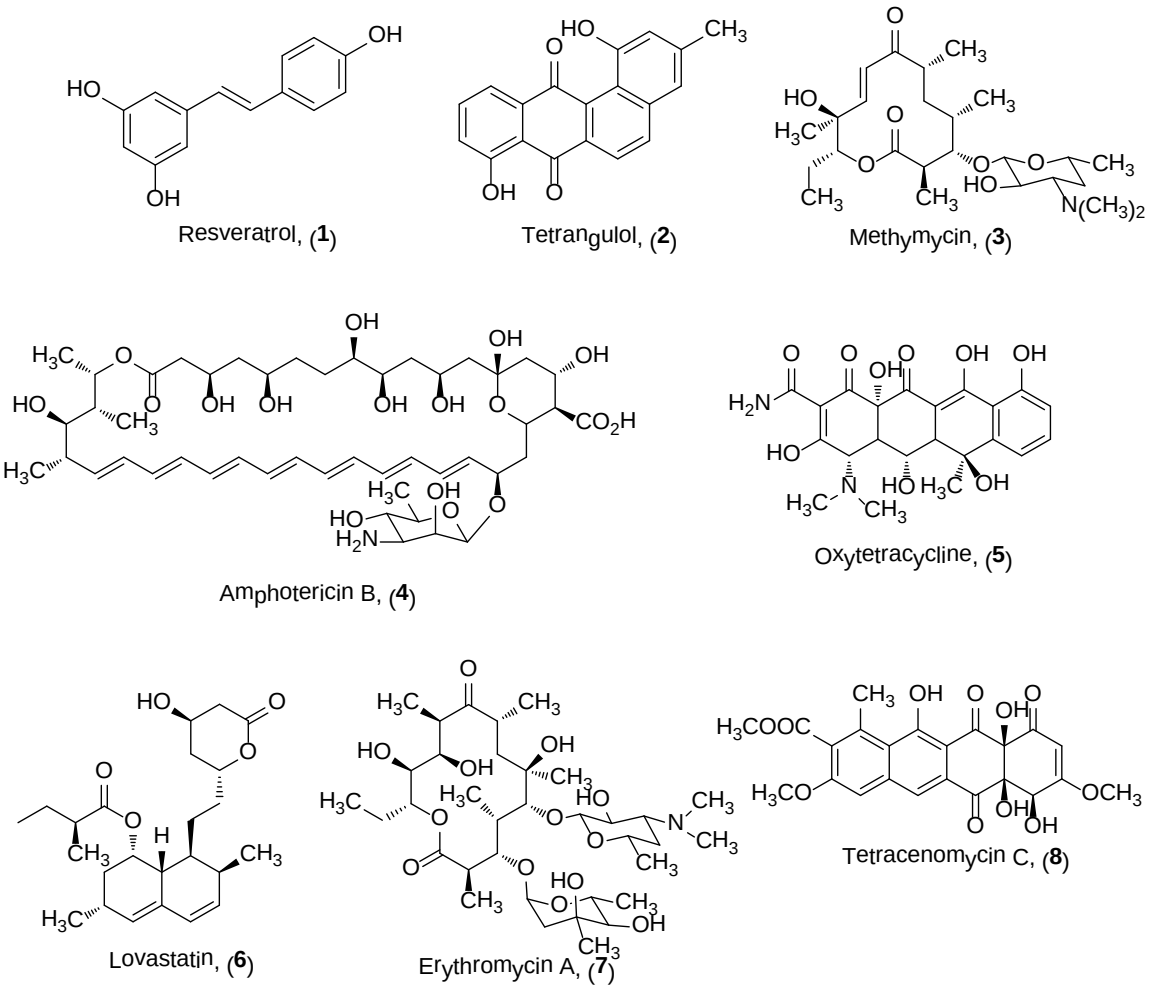

Figure 1 Representative examples of clinically-relevant type I, type II, and type III-derived polyketides.

The pharmaceutical importance of polyketide-derived molecules has generated tremendous interest in elucidating the biosynthetic machinery responsible for generating their chemical diversity (*4*). The advent of molecular biology has allowed for cloning of

entire biosynthetic loci of polyketide-type compounds. Ever since the cloning and heterologous expression of the entire actinorhodin biosynthetic locus (*12*), recombinant techniques have become indispensable for understanding the role of individual enzymes (e.g. gene inactivation) or groups of enzymes (e.g. heterologous expression of minimal polyketide synthase) in generation of polyketide scaffolds. As a result, these preliminary studies can allow for manipulation of these pathways to generate novel derivatives with more advantageous pharmaceutical properties.

Type I Polyketide Synthase-Derived (PKS) Molecules

The Type I polyketide synthases are "megasynthases" composed of many modules, which are roughly analogous to the fatty acid synthase from primary metabolism (*13*). As such, both the highly functionalized type I "megasynthase" domains and fatty acid synthases share similar biosynthetic routes (**Figure 2**), with two major differences: 1) type I polyketide synthases utilize more diverse extender units and starter units than simply malonyl-CoA and acetyl-CoA, respectively (e.g. methylmalonyl-CoA for extender units, propionyl-CoA starter unit, etc.), and 2) type I polyketide synthases often have incomplete reduction cycles (*13*). Type I polyketide synthases are unlike their fatty acid counterparts that produce exclusively a saturated chain, and type I PKSes require subsequent desaturases to introduce double bonds. In fatty acid biosynthesis, priming of acetyl-CoA onto the acyl carrier protein (ACP) by ACAT is followed by its binding to a sulfhydryl group on a nearby enzymatic site. Malonyl-CoA is loaded onto the ACP *via* MCAT, then malonyl -ACP undergoes decarboxylation, and then the resulting carbanion condenses with acetyl-S-Enz. The β-ketone is then stepwise reduced to a fully saturated sp^3 bond. Subsequent elongations give a fully reduced fatty acid. In the type I PKS, the reduction cycle is abrogated at one of several steps, often the result of missing or inactivated modules along the megasynthase, which functionalizes the resulting C_2 extender units with ketone, hydroxyl, olefinic, or fully saturated moieties (*6-7, 14*).

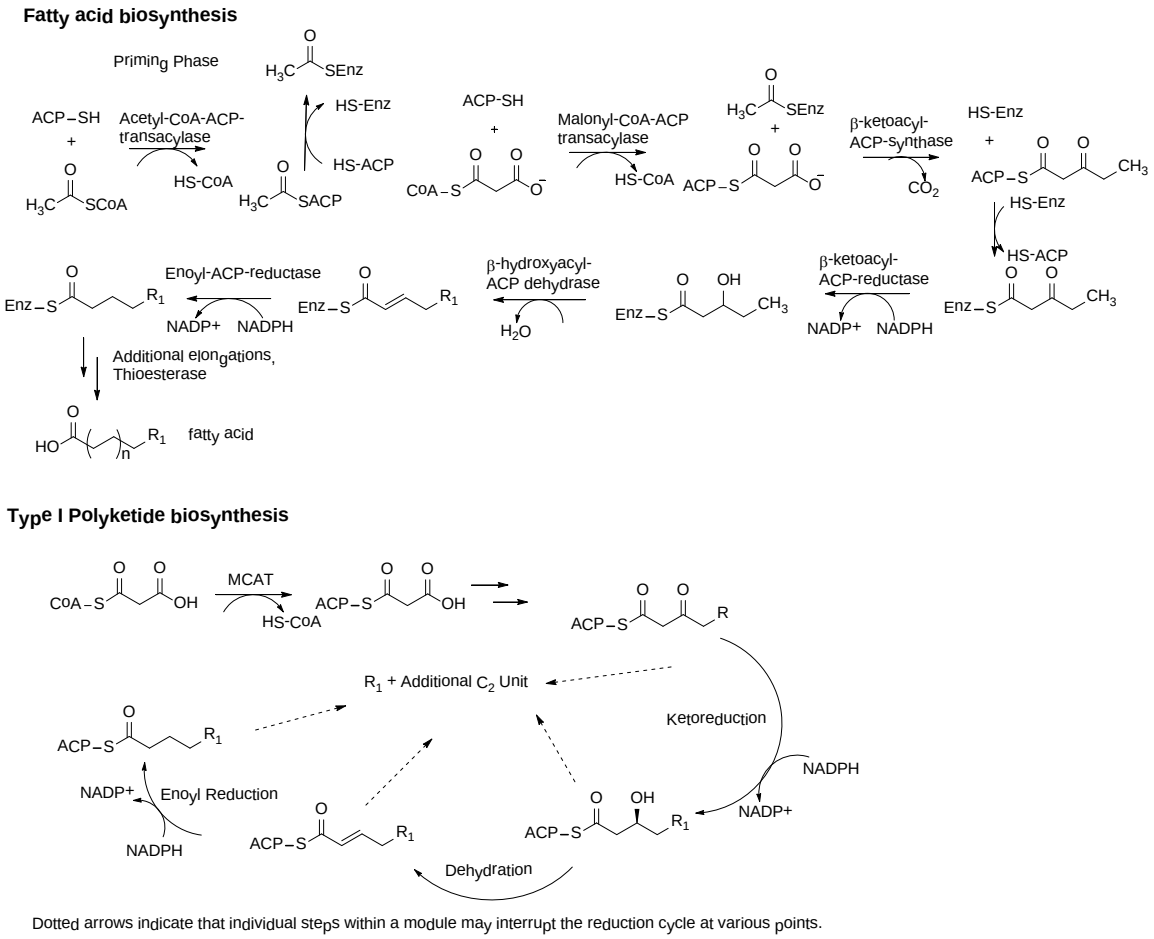

Figure 2 Comparison of fatty acid biosynthesis with the incomplete reduction cycle of a prototypical type I PKS.

The products of type I PKS megasynthases polyketides are 12-, 14-, and 16-membered macrolides, polyenes, and polyethers (*14*). The loading domains may consist of solely an ACP (e.g. in the case of avermectin and erythromycin type I PKS) or may also contain a ketoacyl synthase domain with a glutamine substitution for cysteine (*14*). These synthases are subdivided into modules consisting of acyltransferase (AT), acyl carrier protein (ACP), ketoreductase (KR), dehydratase (DH), enoyl reductase (ER), ketosynthase (KS). The last module possesses an additional thioesterase domain (TE) for hydrolysis and lactonization of the linear polyketide chain (**Figure 3**). The type I PKS has a co-linearity between its modules, and as such, a nascent polyketide chain is passed along from the sulfhydryl group of the ACP of one domain to the next ACP until the TE domain hydrolyzes it (*14*).

In the early 1990's, the sequence and linearity of erythromycin A biosynthesis was firmly established as representative of type I PKS molecules with the cloning of the entire 6-deoxyerythronolide B (6-dEBS) PKS cluster (*7*). The PKS region (*eryA*) is coded on three ORFs spanning ~35kb of chromosomal DNA, and its enzymatic domains are encoded within 6 PKS modules (*7*) (**Figure 3**).

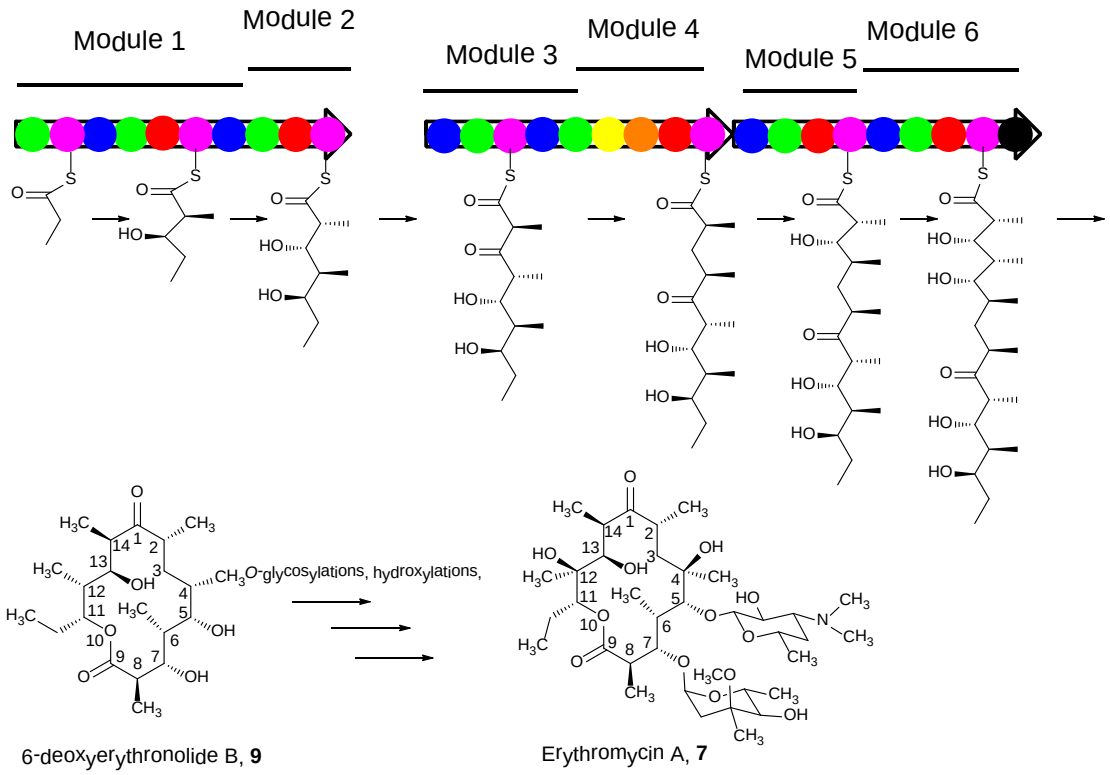

Figure 3 Elucidation of the EryA polyketide megasynthase.
Domains are color-coded by function. AT=Green, ACP=Pink, KS=Blue, KR=Red, DH=Yellow, ER=Orange, TE=**Black**.

The elucidation of the linear organization of EryA suggested possible domain functions in which inactivation of specific domains could result in predictable structures. Indeed, inactivation of the ketoreductase in module five resulted in a corresponding 5,6-deoxy-3-α –L-mycarosyl-5-oxoerythronolide B compound (not shown), lacking the desosamine residue due to the establishment of a 5-keto group instead of the alcohol, to which the sugar could have been attached (*14*). The use of genetic data to predict domain function, and consequently, to hypothesize about structures resulting from inactivation of specific domains was somewhat successfully employed also for other type I PKS systems (*14*).

Type II Polyketide Synthase (PKS) Molecules

Type II polyketides consist primarily of the polyaromatic/cyclized classes of polyketide-derived molecules (*13, 15*). The poly-β-ketothioester is installed iteratively by a type-II PKS, also called the "minimal PKS" (*16*), consisting of β-ketoacyl synthase (KSα), chain length determinant enzyme (CLF/KSβ) (KSα and KSβ form a close heterodimer), and an acyl carrier protein (ACP) for successive transfer of malonate to the growing polyketide chain, in addition to the necessary enzymes for chain initiation (*4*). This "minimal" polyketide synthase has the minimal number of enzymes necessary to produce the first visualized intermediates in type II pathways. MCAT transfers malonyl-CoA to the ACP as in other PKS pathways for use as the extender units; however, different starting units can also be utilized in type II PKS pathways (e.g. malonamyl-CoA, propionyl-CoA, crotonyl-CoA, butyryl-CoA). Specialized enzymes have been evolved to biosynthesize and load these starter units (*17-19*). Chain initiation begins when the starter unit is loaded onto the KSα-KSβ. Malonyl-ACP is decarboxylated in β-ketoacyl synthase and is condensed with the starter unit, and the extended polyketide chain is transferred to the β-KS to release the ACP, which is now free to accept another malonyl-CoA (*4, 20*). X-ray crystallography studies on the actinorhodin KSα-KSβ complex revealed its heterodimeric nature; as a rule, these two enzymes are almost always translationally coupled (*16*). A tunnel in the heterodimer allows for expansion of the growing nascent (and highly reactive) poly-β-ketothioester, thereby shielding it from nucleophilic water molecules (*16*). In the actinorhodin KSα- KSβ heterodimer, cysteine 169 is the catalytic amino acid residue required for formation of the thioester, and phenylalanine 116 a gating residue, which prevents further condensations of acetate units beyond a heptaketide (*16*).

The cyclization strategies employed in type II polyketide pathways give rise to the structural diversity observed among the anthracycline, angucycline, tetracycline, and tetracenomycin-type molecules (**Figure 4a**) (*4*). The poly-β-ketothioester is highly reactive, and therefore every type II PKS cluster has a functional set of closely-associated cyclases/aromatases/oxoacyl-ketoreductases necessary to steer the cyclization(s) of the polyketide core towards a certain skeletal framework (*4*).

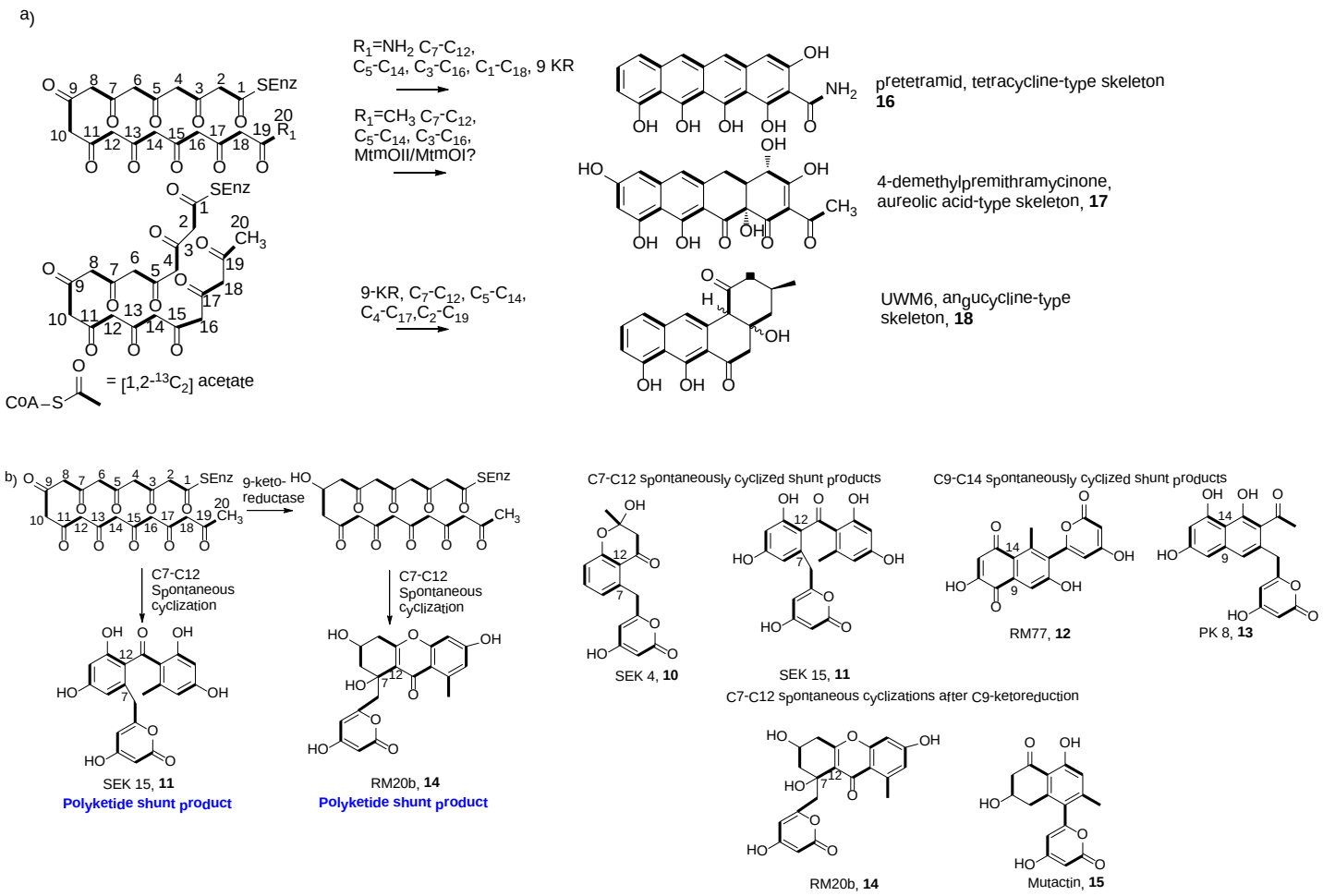

Figure 4 Spontaneous cyclization of polyketides.
a) Cyclization events yielding skeletal frameworks for families of type II polyketides. b) Example of spontaneous cyclization event in the absence of cyclase enzyme and examples of spontaneously cyclized shunt products.

The minimal PKS directs the folding pattern to the nascent polyketide chain, and the cyclases and aromatase enzymes are responsible for "locking-in" the skeleton, or in the case of angucycline polyketides, installing the angular shape by initiating C4-C17 cyclization (*4*, *14*). In the case of tetracycline and aureolic acid polyketide cyclization, C7-C12 are linked in the first ring cyclization, followed by C5-C14 linking in the second ring cyclization, C3-C16 linking in the third ring cyclization, and finally C1-C19 linking in the fourth ring cyclization in the case of the tetracyclines (**16**) (*21-22*) (**Figure 4a**). In the case of premithramycin type molecules (e.g. **17**), it is possible that tandem oxygenations by MtmOI (?)/MtmOII act on a tricyclic intermediate, which establishes an

epoxide. The epoxide is reductively opened, thereby allowing fourth ring cyclization (*23-24*). These four ring cyclizations yield a linear molecule. In the case of the angucyclines, the first two ring cyclizations are similar to the tetracycline/aureolic acid cyclizations, C7-C12 and C5-C14, but a specialized C4-C17 third ring cyclase is responsible for creating the angular appearance of these molecules, followed by C2-C19 fourth ring cyclization, resulting in intermediate UWM6 (**18**) (**Figure 4a**).

In the absence of the polyketide-associated ketoreductase or cyclase/aromatase enzymes, spontaneous cyclization processes occur involving the highly reactive poly-β-ketothioester. These aberrant cyclizations result in "shunt products," which are polyketide metabolites that accumulate in the pathway that are not intermediates for downstream pathway enzymes. In general, shunt products are biosynthetically unproductive but they reveal some information about the preceding biosynthesis (**Figure 4b**).

Type III PKS Molecules

Type III PKS molecules are produced predominantly in plants, but some are also biosynthesized in bacteria. Type III polyketides are biosynthesized by a single β-ketoacyl synthase enzyme without the assistance of an ACP (*25*), and the enzyme makes use of a variety of starter units (e.g. coumaroyl-CoA, etc.). Resveratrol, **1**, is an example of a stilbene-type polyketide from this pathway.

Post-PKS Tailoring steps

After the core skeleton has been assembled, the post-PKS tailoring steps functionalize the molecule, thereby supplying it with the chemical moieties that contribute to its biological activity (*26*). The oxygenations, methylation, glycosylations, aminotransfer reactions, halogenations, reductions that tailor these polyketide skeletons are catalyzed by highly specialized sets of enzymes (*26*). Post-PKS tailoring enzymes have evolved to bind restrictively to a particular substrate and many have stringent cofactor requirements for catalysis. The genetic and biochemical characterization of specific tailoring enzymes and their substrates is often the first objective for combinatorial biosynthesis (*27*). Combinatorial biosynthesis, the modification and

recombining of heterologous genes in a biosynthetic pathway to achieve novel natural products, is practically often concerned with the characterization and interchange of these post-PKS tailoring enzymes (*27*). As such, an introduction to some of these post-PKS enzymes is merited.

Oxygenases

Oxygenases are some of the most common and diverse enzymes employed in secondary metabolic pathways (*27*). In general, oxygenases install oxygen moieties as aldehydes, ketones, or hydroxyl groups. These oxygen moieties are handles for important chemical transformations and can serve as mediators of biological activity. For example, the installation of a hydroxyl or a ketone moiety creates an additional hydrogen bond donor or acceptor. Ketones reduce the pK_a of α-hydrogens, which allows for more facile abstraction by a base. In addition, oxygenases mediate carbon-carbon bond cleavage, and some oxygenases may install highly reactive epoxides, for example (*27*). Oxidoreductases also add or remove hydrogens (dehydrogenases, ketoreductases) and oxidize C-O bonds (e.g. oxidases, secondary alcohol to ketone), and dehydratases catalyze the elimination of water to install double bonds.

Oxygenases are easily characterized by their cofactor requirements, conserved amino acid moieties, and the number of oxygens that are installed on a substrate. Cofactor free monooxygenases have no cofactor involved in their mechanism; rather, the substrate assists in the installation of molecular diatomic oxygen. These oxygenases are also referred to as anthrone oxygenases or also "internal monooxygenases" (*27*). The HypC anthrone oxygenase from *Aspergillus parasiticus* was overexpressed in *E. coli* and purified for *in vitro* conversion of norsolorinic acid anthrone to norsolorinic acid (**Figure 5**). HypC possesses two catalytic domains that are conserved across emodinanthrone oxygenases- QLXXQWSRIFY and RXLXXPL (the active site residues are underlined) (*28*). Tryptophan 43, tyrosine 48, and arginine 140 are involved in coordinating an enzyme-stabilized zwitterion of norsolorinic acid anthrone (**19**) that allows for molecular oxygen to attack para to the anthrone oxygen (**Figure 5**). Glutamine 38 stabilizes the reaction product by hydrogen bonding with the newly-formed quinone oxygen in norsolorinic acid (**20**) (*28*).

Flavin-dependent monooxygenases possess an *N*-terminal domain (GXGXXG) which is involved in binding of FAD (*27*). These oxygenases also bind NAD(P)H for reduction of FAD to $FADH_2$, which then binds diatomic oxygen to form the key peroxyflavin intermediate (*27*). A nucleophile present on the substrate then attacks the peroxide, thereby forming a new bond with oxygen and forming water (*27*). Cytochrome P-450 oxygenases possess a prosthetic heme group, which coordinates a Fe^{3+} cation. These CYP-450 oxygenases often require an accessory ferredoxin protein to regenerate NADPH (*27*). One FAD- and NADPH-dependent oxygenase (DnrF) and a P450 monooxygenase from the doxorubicin biosynthetic pathway (DoxA) are depicted with cofactor requirements in **Figure 5.**

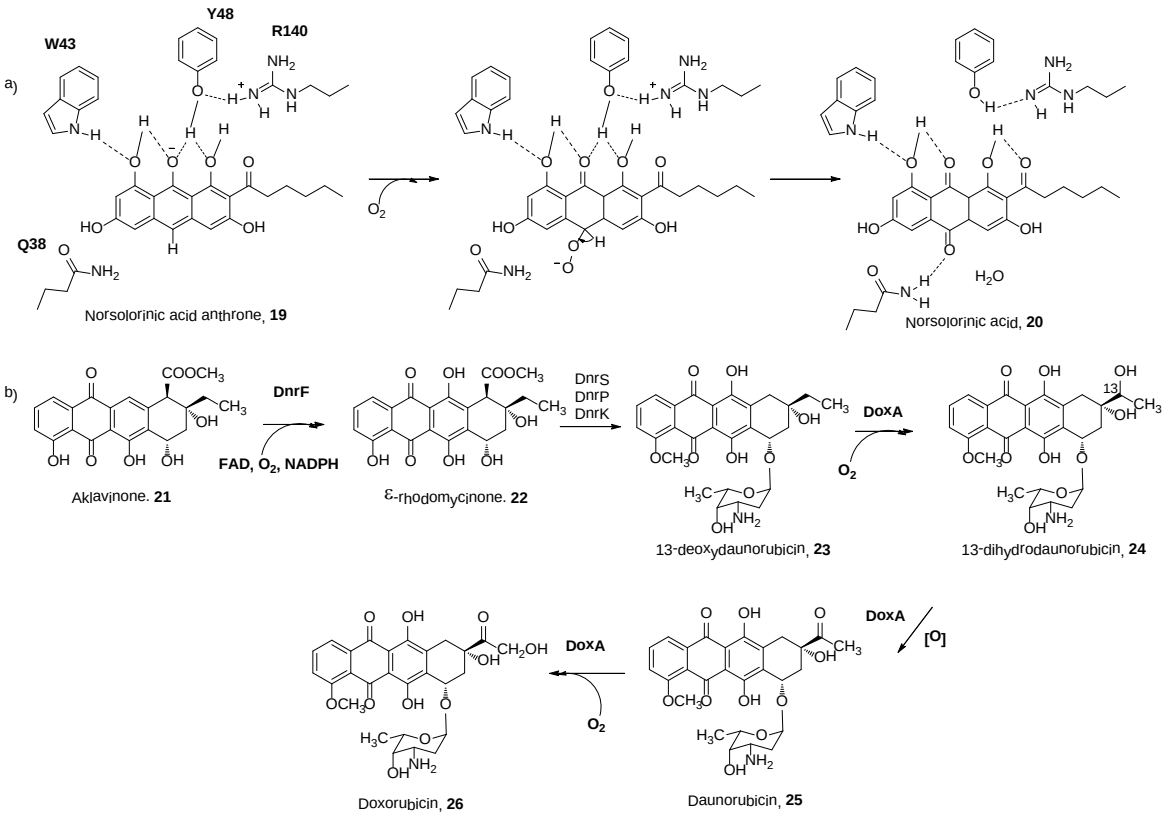

Figure 5 Mechanisms of cofactorless and FAD-dependent monooxygenases.
a) Mechanism of cofactor-free oxygenase HypC. b) FAD- and NADPH- dependent monooxygenase DnrF and P450 oxygenase DoxA from doxorubicin pathway.

DnrF is involved in 11-hydroxylation of aklavinone to afford ε-rhodomycinone in an FAD and NADPH-dependent manner, whereas DoxA is a CYP-450 that catalyzes both 13-hydroxylation and hydroxymethyl formation at C-14 (*27, 29*).

Methyltransferases, Aminotransferases, and glycosyltransferases

Methyltransferases and aminotransferases are important enzyme classes for post-PKS decoration. These enzymes modify the reactivity and lipophilicity/ hydrophilicity of natural products through the addition of methyl groups and amino functionalities, respectively. Methyltransferases add an additional C_1 unit by means of a nucleophilic attack by an electron-rich donor moiety on *S*-adenosyl methionine to afford *S*-adenosyl homocysteine and a methylated compound. One pertinent example of *O*-methylation is catalyzed by MtmMI from the mithramycin biosynthetic pathway of *Streptomyces argillaceus* (*23*). MtmMI catalyzes the removal of a proton from the 4-OH group, and the resulting oxygen nucleophile attacks the methyl group of *S*-adenosyl methionine that is positioned in the methyltransferase active site to give premithramycinone (**27**) (**Figure 6**) (*30*). *N*-methylation or *O*-methylation increases the hydrophobicity of a compound by removing a hydrogen bond donor (*27*). *N*-methylations can form tertiary amines, which give very important pharmaceutical properties to a drug (*27*). *C*-methylations are employed biosynthetically to introduce a "branch" into a deoxysugar or onto a polyketide skeleton.

Aminotransferases catalyze the transfer of an amine group to a corresponding carbonyl. The amino group donor is usually pyridoxamine phosphate (PMP), which forms an imine with the carbonyl carbon, which is then hydrolyzed to yield the newly transaminated substrate and pyridoxal phosphate (PLP) (*31*). Aminotransfer reactions require a carbonyl handle. The transformation of a carbonyl into an amine converts a hydrogen bond acceptor into a hydrogen bond donor, which is often important for biological activity. As such, this greatly enhances the hydrophilicity of a compound. In the oxytetracycline pathway, the PMP-dependent aminotransferase OxyQ is used to transaminate the 4-keto position of 4-ketoanhydrotetracycline (**28**), a very unstable pathway intermediate, to afford 4-aminoanhydrotetracycline (**29**) (**Figure 6**). OxyQ

tailors one of the canonical tetracycline reactions (amine group at 4 position), and effectively "captures" the labile **28** (*21*, *31*).

Glycosyltransferases (GTs) are among the most numerous and utilitarian enzymes in all of nature. As such, glycosylations are invaluable to the biological activity of polyketides. Indeed, many polyketides are inactive without their appended sugars (*32*). Glycosylation increases biological activity and hydrophilicity of a compound by virtue of installing several –OH hydrogen bond donors present on a sugar. Glycosyltransferases require a pool of "donor substrates," nucleotide diphosphate-bound (NDP) sugars that often are deoxygenated at one or more positions, and an "acceptor substrate," which in most cases is an aglycone or suitable polyketide core that will receive the sugar donor (*33*). Glycosyltransferases have evolved into two predominant families characterized by the nature of their Rossman folds, GT-A and GT-B superfamilies (*34*). Most polyketide glycosyltransferases are members of the GT-B superfamily of glycosyltransferases, and they possess two domains with an α/β Rossman fold involved in the binding of the sugar donor substrate in the *C*-terminus and the acceptor substrate in the *N*-terminus (*34*-*35*). Glycosyltransferases can either catalyze glycosylation with inversion or retention of configuration; in most cases with the GT-B superfamily of glycosyltransferases, glycosylation involves inversion of configuration, which is the underlying reason for the earliest discovery of Klyne's Rule (*36*) (**Figure 6**).

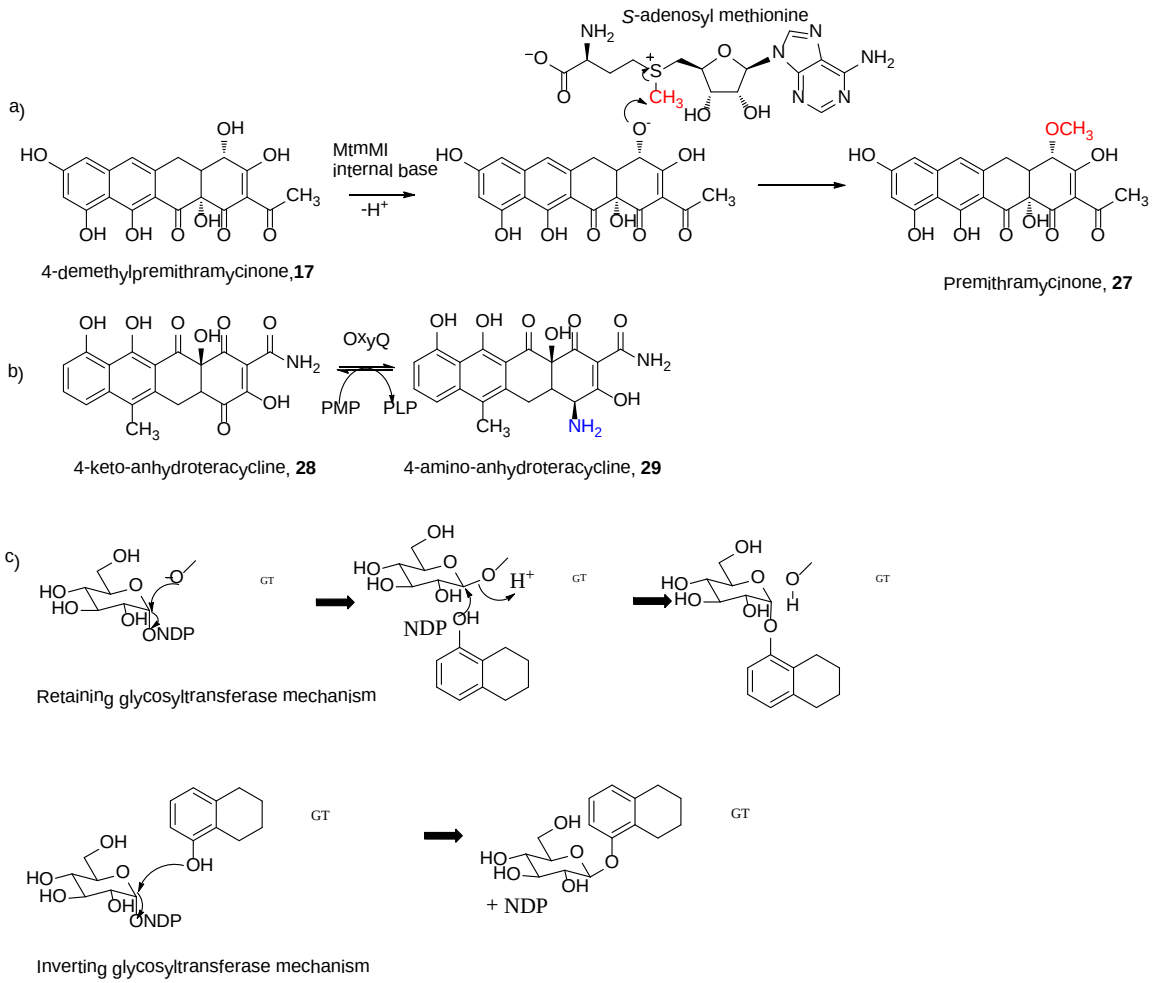

Figure 6 Depictions of methyltransfer, aminotransfer, and glycosyltransfer reactions. a) 17 is methylated at 4-OH by MtmMI to give 27. b) aminotransfer reaction catalyzed by OxyQ. c) Depictions of both retaining and inverting glycosyltransfer reactions.

In addition to glycosyltransferases, nature has evolved many different deoxysugar tailoring enzymes involved in the modificiation of sugar donors (*37*). These deoxysugar pathways begin with D-glucose-6-phosphate, which is interconverted to D-glucose-1-phosphate (**30**) by phosphoglucomutase (**Figure 7**). D-glucose-1-phosphate (**30**) is captured by NDP-glucose synthase, a specialized enzyme that catalyzes the coupling of NMP from a corresponding NTP with the phosphate group of **30**. A second enzyme that is usually clustered near NDP-glucose synthase is NDP-D-glucose-4,6-oxidoreductase (*38*) (or simply NDP-4,6-dehydratase). This enzyme catalyzes the NAD-dependent removal of two electrons and two protons from C-4 and 4-OH, and dehydrates across the 5,6 bond of **31** to afford a double bond, which is then reduced by 4,6 dehydratase to generate NDP-4-keto-6-deoxy-D-glucose (**32**) (**Figure 7)** (*32*).

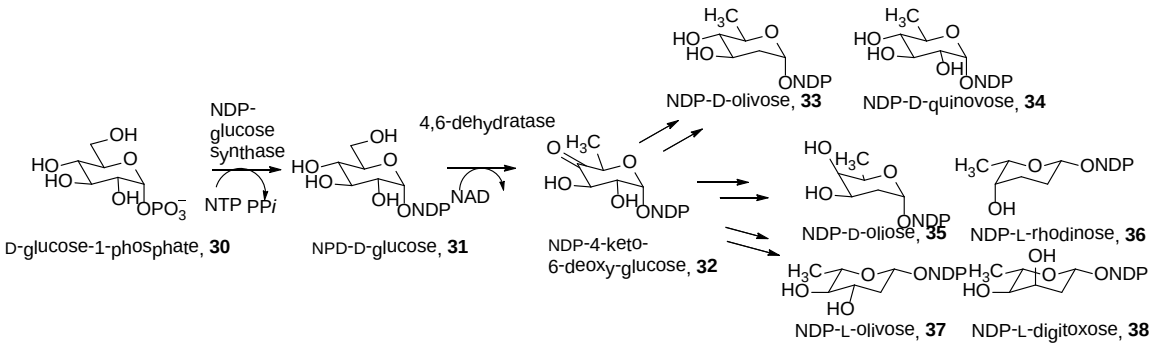

Figure 7 Deoxysugar biosynthesis from D-glucose-1-phosphate (30). D-glucose-1-phosphate (**30**) coupled with NMP *via* NDP-glucose synthase to give NDP-D-glucose (**31**) in an NTP-dependent manner. **31** is dehydrated and reduced across the 5, 6 bond and oxidized at C-4 to afford NDP-4-keto-6-deoxy-D-glucose (**32**), which is a universal intermediate for downstream deoxysugar tailoring enzymes, which can generate tremendous chemical diversity as witnessed in sugars **33-38.**

A series of downstream tailoring enzymes can catalyze further deoxygenations, epimerizations, and other reactions to generate chemical diversity in sugar donors. The cloning of these deoxysugar pathways and their subsequent heterologous introduction into foreign hosts has become a very important strategy for altering the glycosylation pattern of polyketides (*39*).

Introduction to Gilvocarcin (GV) Biosynthesis

Gilvocarcin V (GV) (**39**) (toromycin A, anandimycin A) is the most important representative compound of the benzo[*d*]naphtho[1,2-*b*]pyran-6-one *C*-glycoside antibiotics (*40*). It was first isolated in 1981 in Japan from a fermentation of *Streptomyces gilvotanereus* (NRRL 11382) along with its congeners gilvocarcin M (**40**) and gilvocarcin E (**41**) (from *S. anandii*), and the antibiotic gets its name from the grayish yellow color of this strain after it has aged (*40*) (**Figure 8**). It was also isolated from fermentations of *Streptomyces arenae, Streptomyces anandii*, and *Streptomyces griseoflavus* Gö 3592 (*41-42*). Gilvocarcin V was determined to have excellent biological activity against *Staphylococcus aureus* and *Bacillus subtilis*, and weak activity against gram negative bacteria. However, it demonstrated remarkable antitumor activity against sarcoma 180 solid tumors and Ehrlich ascites carcinoma in murine cell lines (Increased Life Span of 126%) (*40, 43*). Interestingly, **39** maintained a very low *in vivo* cytotoxicity profile despite its considerable antitumoral effects (*43*). Experiments by

Elespuru *et al*. confirmed that treatment of **39** with visible light photoactivated a [2+2] cycloaddition of **39** with thymine residues of DNA. This contrasts with the mostly inactive gilvocarcin M (**40**), which possesses an 8-methyl side chain. Gilvocarcin M lacks the photosensitizing effect exhibited by gilvocarcin V, most likely because it lacks the 8-vinyl sidechain (*44*). Further studies confirmed that **39** binds to histone H3 and cross-links DNA, which the *C*-glycosidically-linked D-fucofuranose may play an essential role in its binding to the histone H3 protein (*45-47*).

Additional *C*-glycosidically linked gilvocarcin-type analogues, the chrysomycins (**42-44**) and the ravidomycins (**45-48**) were soon isolated from fermentations of *S. albaduncus* AD0819 and *S. ravidus* (*48-50*) (**Figure 8**). Chrysomycin was originally isolated in 1955 by Strelitz *et al*., however, the structure elucidation of these compounds was not conducted until the 1980s (*51*). Structure elucidation using ^{1}H-NMR and ^{13}C-NMR experiments revealed that **42** and **43** shared the same benzo[*d*]naphtho[1,2-*b*]pyran-6-one chromophore as **39**, yet differed with respect to the 8-side chain (vinyl in the case of chrysomycin A and methyl in the case of chrysomycin B) (*50*). Furthermore, the chrysomycins possess a *C*-glycosidically-linked branched sugar called D-virenose (named for virenomycin, which was the name given to these compounds by the Russian group who elucidated the structure of the sugar moiety of **42-44**) (*52*). The ravidomycins were elucidated to possess the same chromophore. However, they possessed an aminosugar, D-ravidosamine, *C*-glycosidically linked at 4-position, with 4'-*O*-acetyl groups present in some of the isolated compounds (*48*, *53*). Ravidomycin V (RV, **45**) and chrysomycin A (CV, **42**) demonstrated promising antitumor activities, with RV (**45**) and 4'-*O*-desacetyl RV demonstrating the most potent biological activities against cancer cell lines (*48*) (**47**).

The isolation of other related natural products: L-rhamnosylated *O*-glycosides BE-12406A and B (not shown), polycarcin V (**53**), and *C*-glycosidically-linked ketopyranose and ketofuranose compounds (Mer- 1020 dA-dD, **49-52**, respectively) greatly expanded the library of known gilvocarcin-type compounds (*54-57*) (**Figure 8**).

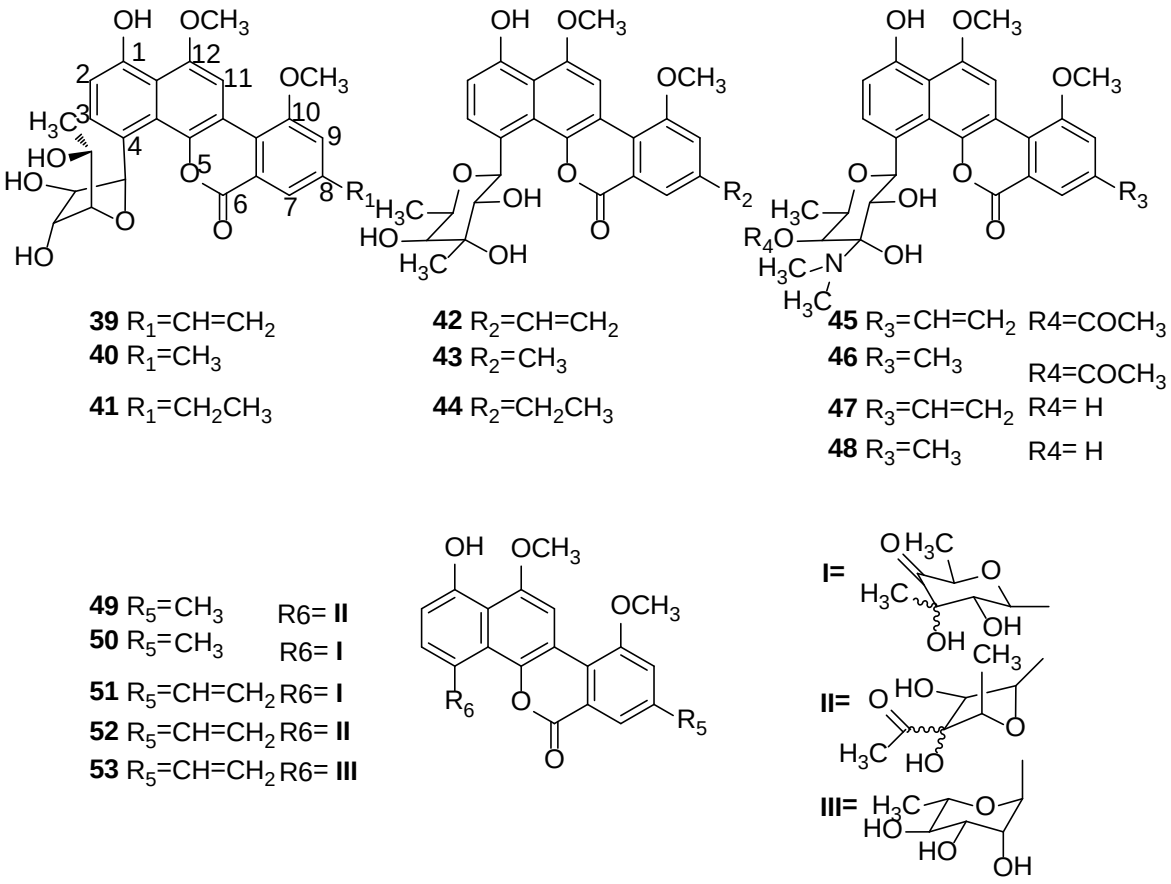

Figure 8 Structures of gilvocarcin-class antitumor antibiotics.
Structures of the gilvocarcins (**39-41**), the chrysomycins (**42-44**), the ravidomycins (**45-48**), and other gilvocarcin-type *C*-glycosides (**49-53**).

Feeding experiments of gilvocarcin V and chrysomycin A with [1-^{13}C] and [2-^{13}C]acetate by Takahashi *et al*.(*58*) and Carter *et al*.(*59*) revealed that 9 aromatic carbons were enriched, and feeding with [3-^{13}C] and [2-^{13}C]-labeled propionate revealed that the vinyl side chain of gilvocarcin V was the result of incorporation of a propionate starter unit. Labeling with [1,2-$^{13}C_2$]acetate produced the labeling pattern seen in (**Figure 9**). Feeding with [1-^{13}C, $^{18}O_2$]-labeled acetate by Liu *et al*. demonstrated that the oxygens at C-1, C-10, and C-12 derived from acetate units (**Figure 9**) (*60*). The labeling of C-6 with one carbon from labeled acetate presupposes a C-C bond cleavage at carbons C-5 and C-6 of an angucycline intermediate, in addition to the oxygens at 5 and 6 positions that must derive from atmospheric oxygen (*60*).

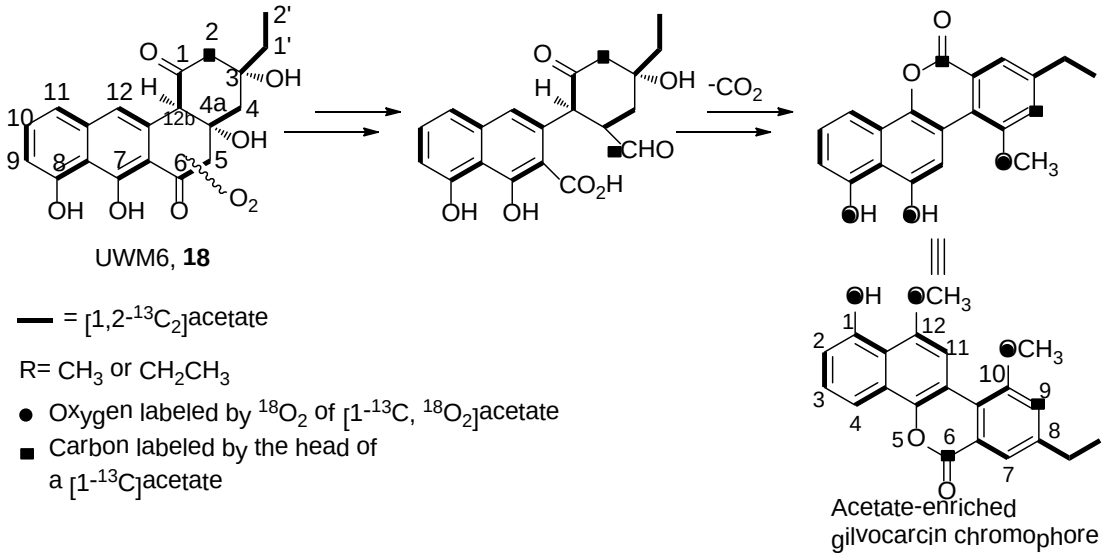

Figure 9 Gilvocarcin labeling pattern, after incorporation experiments using [1,2-$^{13}C_2$] acetate and [1-^{13}C, $^{18}O_2$]-acetate of gilvocarcin, respectively.

Subsequently, the entire gilvocarcin biosynthetic gene cluster was cloned from genomic DNA of gilvocarcin-producing *Streptomyces griseoflavus* Gö 3592 onto a single pOJ446-derived *E. coli-Streptomyces* shuttle cosmid, named cosG9B3 (*61*). When cosG9B3 was heterologously expressed in host *Streptomyces lividans* TK 24, **39** and **40** were produced with yields comparable to wildtype *S. griseoflavus* Gö 3592 (*61*). With the entire gilvocarcin gene cluster in hand, gene inactivation experiments of the gilvocarcin oxygenases, glycosyltransferase, oxidoreductases, and methyltransferases shed considerable light on the order of biosynthetic events for **39** (*60, 62-64*). Of considerable interest in this biosynthetic pathway are the enzymatic steps necessary to generate the oxidative cleavage of the 5,6 bond, the genes encoding NDP-D-fucofuranose biosynthesis and attachment, and the enzymes responsible for the installation of the 8-vinyl side chain (*60, 62-64*).

The biosynthetic pathway of **39** was laid out through bioinformatic analysis of the *gil* gene cluster and inactivation experiments. GilP and GilQ were identified as functional malonyl-CoA and propionyl-CoA acyltransferases for the transfer of starter units to the minimal PKS, which consists of GilABC (**Figure 10**) (*65*). Oxoacyl ketoreductase GilF presumably reduces the resulting C-9 carbonyl, which is then dehydrated to aromatize ring D, then cyclases GilG and GilK aromatize ring C and

cyclize rings A and B to afford the first postulated angucycline intermediate of this pathway, homo-UWM6 (**18**) (*66*). GilOIV and GilOI were found to encode dual-function FAD-dependent monooxygenases/dehydratases, presumably involved in the oxygenation cascade (*60*, *63*).

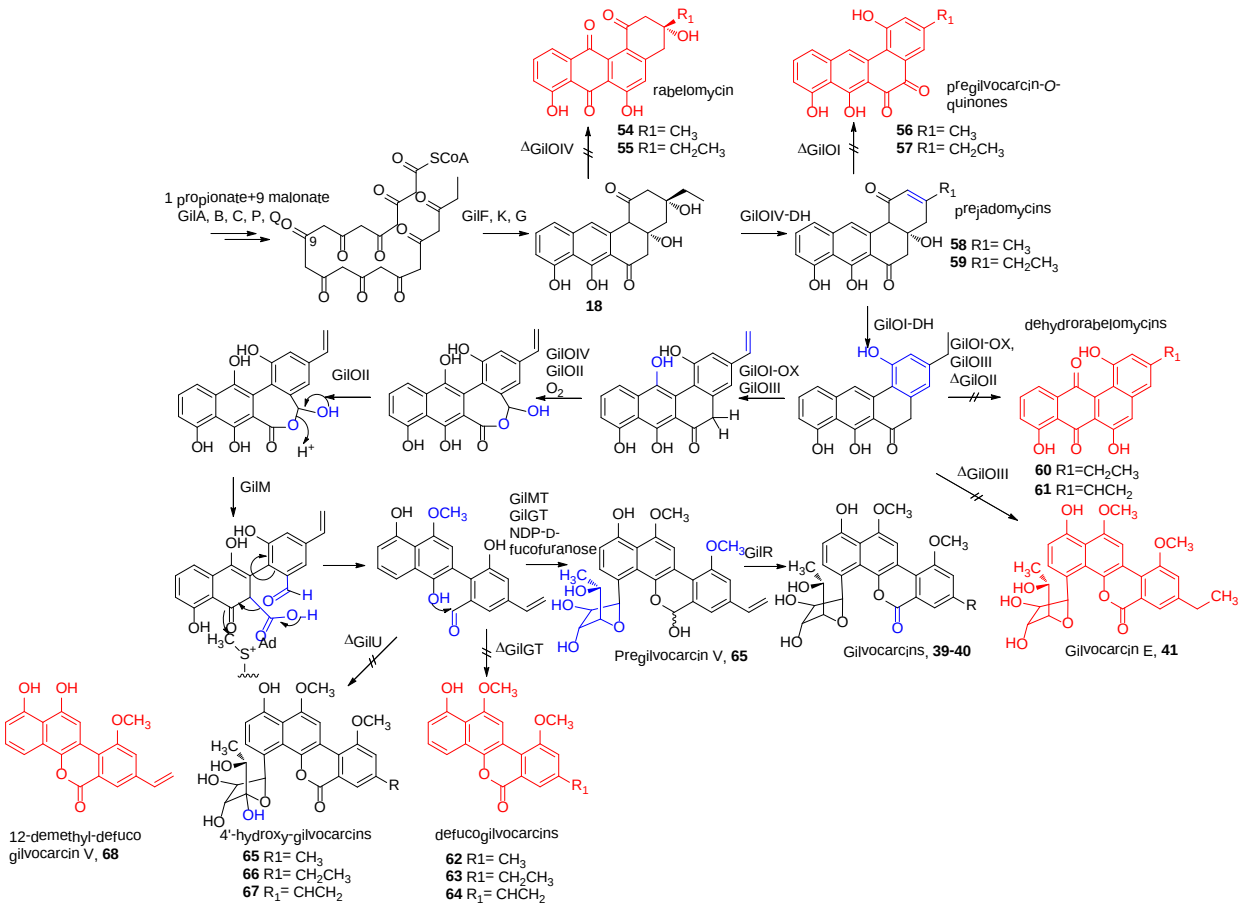

Figure 10 Hypothesis for GV (**39**) biosynthetic pathway.
Enzymatic transformations are indicated in blue. Shunt products accumulated in indicated G9B3 gene-deletion mutants are depicted in red.

Inactivation of *gilOIV* in G9B3 resulted in accumulation of rabelomycin (**54**) and homorabelomycin (**55**) as shunt products, which are not capable of being processed by downstream oxygenases (**Figure 10**). Rabelomycin (**54**) and homorabelomycin (**55**) are likely spontaneously oxidized at C-12 to afford the quinone (*66*). Inactivation of *gilOI* yielded intermediates **58** and **59**, prejadomycins, which are dehydrated across C-2 and C-3. This demonstrated that GilOIV likely acts first, dehydrating across the 2-3 bond, followed by dehydration by GilOI across the 4a-12b bond to aromatize ring A.

Shunt products **56** and **57** suggest a C-5 oxygenation by GilOIV or GilOII, but the exact order of oxygenation events is not well understood. Inactivation of the jadomycin A FAD-monooxygenase/dehydratases JadF (GilOIV homologue) and JadH (GilOI homologue) gave similar results as the respective GV oxygenase inactivations (*63, 67*) (**Figure 10**). JadH was found to complement the cosG9B3-gilOI$^-$ strain, and JadF was found to complement the cosG9B3-gilOIV$^-$ strain to reconstitute **39** production (*68*). These experiments demonstrated that GilOI/GilOIV/GilOII act in a co-dependent, multi-oxygenase complex as do the jadomycin counterparts JadF/JadH/JadG. Further evidence of JadH/GilOI function was recently provided by Yang *et al*. to demonstrate that JadH is an FAD, NADPH-dependent dehydratase/ oxygenase that dehydrates C-4a, C-12b of **58**, then acts as a C-12 oxygenase to afford the C-3 methyl homologue of **60** as a shunt product (*69*). Therefore, it is proposed that GilOI dehydrates C-4a, C-12b **59**, then oxygenates C-12 to yield the hydroquinone. Shortly after the first ring is aromatized, it is likely that GilOIII hydroxylates at the benzylic position of the 3-propionyl side chain, which resultantly undergoes dehydration to afford the vinyl moiety (this is evinced in the shunt product vinyl-dehydrorabelomycin, **61**) (*70*). Subsequent oxygenations by GilOIV and/or GilOII result in a Baeyer-Villiger intermediate, which subsequently cleaves the 5,6 C-C bond, affording an acid and an aldehyde intermediate (as determined by pregilvocarcin V, a hemiacetal isolated from the GilR-deleted cosG9B3 strain) (*71*). It should be noted that an analogous ring-cleaved intermediate is also hypothesized to be an intermediate of the jadomycin pathway just before L-isoleucine incorporation (**Figure 11**). In the gilvocarcin pathway, GilM theoretically captures this intermediate and methylates at the 7-hydroxyl, effectively steering this pathway away from an angucycline-framework towards the gilvocarcin chromophore (Unpublished Results, Madan Kharel, Tao Liu). Further 10-*O*-methylation by GilMT, *C*-glycosylation using NDP-D-fucofuranose at C-4 by GilGT, and dehydrogenation of the 6-OH by GilR to afford the lactone completes biosynthesis of **39** (*70-71*).

Gene disruption experiments of the gilvocarcin biosynthetic pathway have been important not only for shedding some light into the sequence of enzymatic steps, but they have also resulted in generation of novel gilvocarcin analogues (*70-72*). Disruption of *gilGT* led

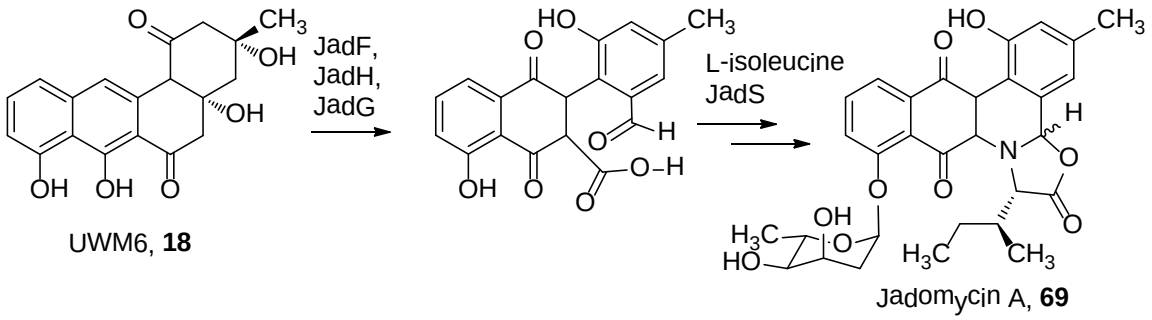

Figure 11 Depiction of oxygenase cascade between UWM6 (**18**) and Jadomycin A (**69**).

to the accumulation of defucogilvocarcins E and M (**62** and **63**), which clearly revealed GilGT's role in *C*-4 glycosylation with the structurally distinct D-fucofuranose (*70*). Furthermore, the *S. lividans* (cosG9B3-GilGT$^-$) is an important strain for combinatorial biosynthesis involving heterologously expressed *C*-glycosyltransferases from related pathways, such as the chrysomycin pathway. Also, disruption of 4-ketoreductase GilU from NDP-D-fucofuranose biosynthesis resulted in 4'-hydroxy-gilvocarcins, with improved bioactivity against cancer cell lines as compared to **39**, as well as improved solubility due to the additional 4'-OH group (*72*). Such a finding reveals unexpected substrate flexibility by the sugar ring contraction enzyme and by GilGT towards an unnatural NDP-furanose donor substrate. As a result, the elucidation of biosynthetic gene clusters of related gilvocarcin-type antibiotics, e.g. chrysomycin and ravidomycin, is not only an important exercise for understanding the role of uncharacterized *gil* genes (*gilLMN*), but it can yield valuable tools for recombining genes to generate novel gilvocarcins.

Introduction to Mithramycin (MTM) Biosynthesis

Mithramycin (MTM) (**70**) is a representative member of the aureolic acid family of antineoplastic antibiotics (**Figure 12**). It is accumulated in strains of *Streptomyces plicatus* and *Streptomyces argillaceus*. Aureolic acid antibiotics are named after their yellow color (Latin, *aurum*= gold), and they are distinguished by their many saccharidal chains *O*-glycosidically linked at 2-position and 6-position, as well as the highly oxidized pentyl side chain at 3-position (**Figure 12**) (*73-74*). The other representative members, chromomycin A_3, UCH9, durhamycin A, olivomycin A all possess the highly oxidized 3-aliphatic side chain, but differ with respect to the nature of the sugars, the nature of their

linkage, and the degree of *O*-methylation or *O*-acetylation of the various sugar residues, or in the case of durhamycin A, *C*-acylation at C-7 position (*75*-*77*).

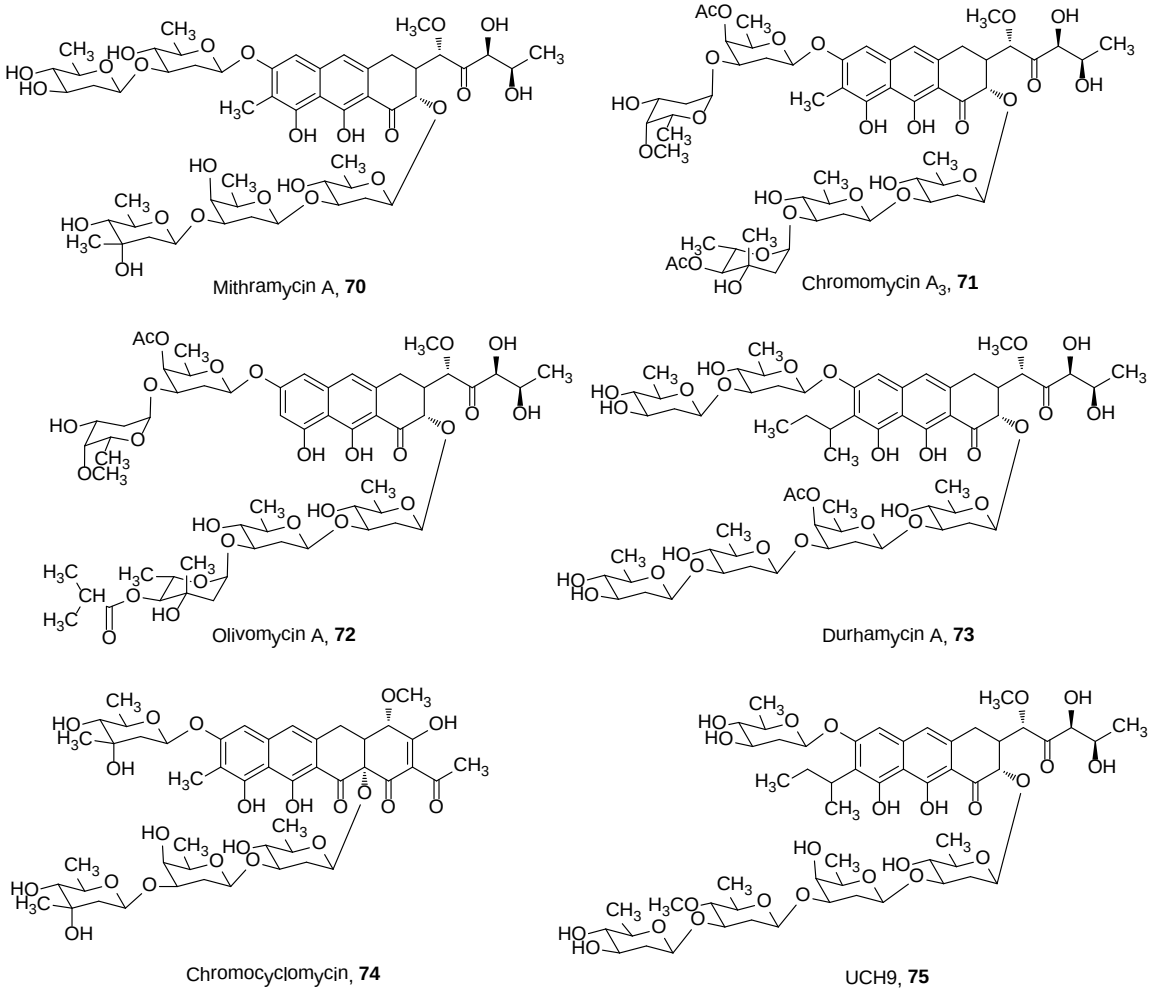

Figure 12 Mithramycin A (**70**) and structures of related aureolic acid antibiotics (**71**-**75**).

Mithramycin was discovered by Grundy *et al*. in 1953, and its structure was subsequently revised several times with regard to the linkage of the trisaccharide chain and the stereochemistry of the sugars; ultimately, Rohr *et al*. confirmed the structure as being **70** using 2D NMR spectroscopic methods (*78*). Mithramycin has been employed in the treatment of Paget's bone disease, testicular carcinomas, and hypercalcemia (*79*-*85*). Mithramycin's mode of action is that it binds to the GC-rich minor groove of protooncogenic regions, such as *c*-*myc*, *c*-*src*, and other Sp1-dependent pathways in a homodimer, coordinated head to tail with another molecule of **70** by an Mg^{2+} cation (*86*-*88*). However, despite its promising activity, prolonged mithramycin treatment is not

well-tolerated. It has major cytotoxic side effects, including bone marrow, hepatic, and kidney cytotoxicities (*89*). Additional biological activities for the aureolic acid family include nanomolar HIV Tat protein inhibition by durhamycin A, and mithramycin has potential Sp1-dependent therapeutic value in treating Alzheimer's disease and Huntington's disease (*90-94*).

The biosynthesis of mithramycin (**70**) has been studied extensively by the Salas and Rohr groups during the 2000s, and the functions of most of the candidate enzymes were identified through gene disruption experiments (*23-24, 89, 95-108*) (**Figure 13**). Inactivation of the *mtmPKS* genes led to a nonproducing mithramycin mutant, and inactivation of monooxygenase MtmOII lead to an improperly cyclized shunt product, premithramycinone G (**87**, **Figure 14**) (*24, 106, 108*). This latter observation caused re-envisioning of the early mithramycin cyclization steps as going through a putative tricyclic intermediate, which would be oxygenated by MtmOI and/or MtmOII, then cyclized to yield the first tetracyclic premithramycin compound in the pathway, 4-demethylpremithramycinone (**17**) (*23-24, 101*). Subsequent 4-*O*-methylation by MtmMI leads to premithramycinone (**27**), which was accumulated by the *S. argillaceus* (MtmGIV$^-$) (*100*). Subsequent glycosylation of the first D-olivose by MtmGIV (premithramycin A1, **76**), and the second sugar of the trisaccharide D-oliose by MtmGIII (premithramycin A2, **77**) were revealed through inactivation of both *mtmGIV* and *mtmGIII* in *S. argillaceus*, respectively (*100*). However, as there are five deoxysugars in biosynthesis of **70**, and only four glycosyltransferases, either MtmGIV or MtmGIII were anticipated to be responsible for transfer of the third sugar of the trisaccharide chain, D-mycarose, with MtmGIV being the preferred candidate for this dual action (*100*). Individual inactivation experiments of *mtmGI* and *mtmGII* , and cross-feeding of **79** into both the *S. argillaceus* (MtmGI$^-$) and *S. argillaceus* (MtmGII$^-$) revealed that MtmGI is responsible for attaching the first D-olivose to the 6-*O* position and then MtmGII *O*-glycosidically links the last D-olivose to the 3A-*O* position of **79** to yield the fully-glycosylated premithramycin B **80** (*96, 105*). Premithramycin B was determined to be the substrate for a novel Baeyer-Villiger monooxygenase, MtmOIV, and this enzyme has been crystallized and modeled to identify the active site residues necessary for catalyzing ring cleavage of **80** to **81** (*95, 103, 109-110*) . This is perhaps the single most important

unifying step for this biosynthesis, because MtmOIV acts as a "gatekeeper" that necessarily allows for generation of active mithramycin molecules (tricyclic with highly functionalized aliphatic side chain branching from C-3) from inactive premithramycin molecules (tetracyclic) (*95*). Finally, MtmW captures the labile mithramycin β-diketone intermediate, and reduces the 4'-ketone to afford **70**.

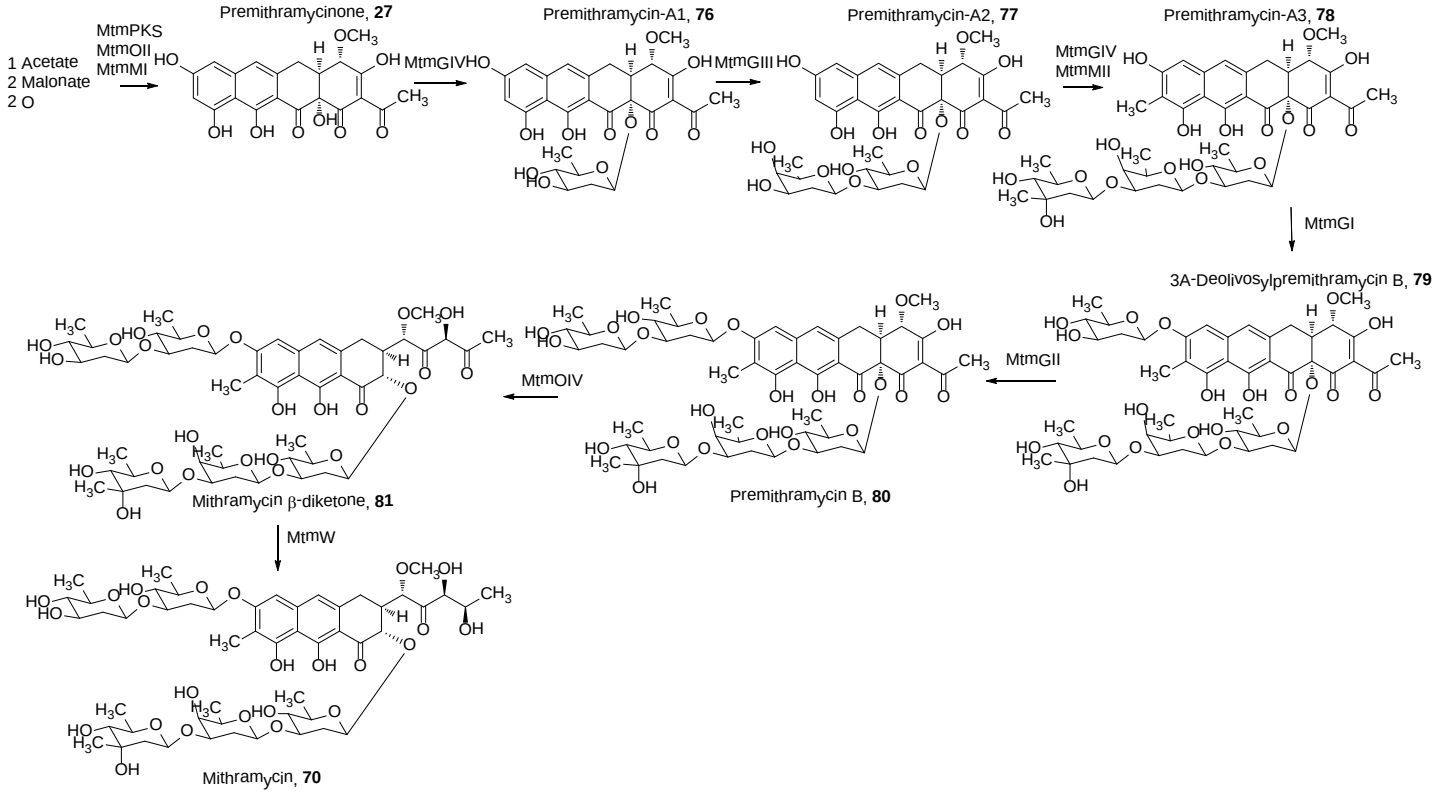

Figure 13 Biosynthetic pathway of Mithramycin (**70**).
Highlights include individual glycosylation steps catalyzed by MtmGI, MtmGII, MtmGIII, and MtmGIV, and Baeyer-Villiger-oxidative cleavage by MtmOIV, and final reduction by associated ketoreductase MtmW.

Combinatorial biosynthesis of the mithramycin pathway has been an invaluable tool for generating novel premithramycin and mithramycin analogues shown in **Figure 14** (*23*, *89*, *96-98*, *100*, *103*, *105*, *109*, *111-113*). Inactivation experiments of the various glycosyltransferases have generated premithramycins with different lengths of saccharidal chains (**76-80**). Inactivation experiments of the various methyltransferase genes (*mtmMII*, *mtmMI*, *mtmC*) have resulted in a 7-demethylmithramycin analogue (**82**), 4-demethylpremithramycinone (**17**), and inactivation of the *mtmC* and *mtmTIII* genes has resulted in isolation and characterization of novel ketopremithramycins and

ketomithramycins (**83-86**), respectively. Recombination with glycosyltransferase *urdGT2* and *lanGT4* from the urdamycin and landomycin pathways, respectively, resulted in novel premithramycin 7-*C*-glycosides (**88-92**) (*113*). Furthermore, recombination with deoxysugar biosynthetic genes from heterologous hosts has resulted in many novel mithramycin-type molecules with altered saccharidal moieties (e.g. **93**) (*111-112*) (**Figure 14**). Therefore, combinatorial biosynthesis remains the best methodology for generating novel mithramycins. Synthetic approaches towards total synthesis of aureolic acids have proven to be step-intensive and difficult with respect to maintaining stereochemical control. For example, Roush *et al*. have synthesized the tetrasaccharide and the chromophore of durhamycin A, the latter being composed of >13 synthetic steps (*77, 114*). In contrast, the problems of stereochemical control and poor step economy are more readily overcome with combinatorial biosynthesis.

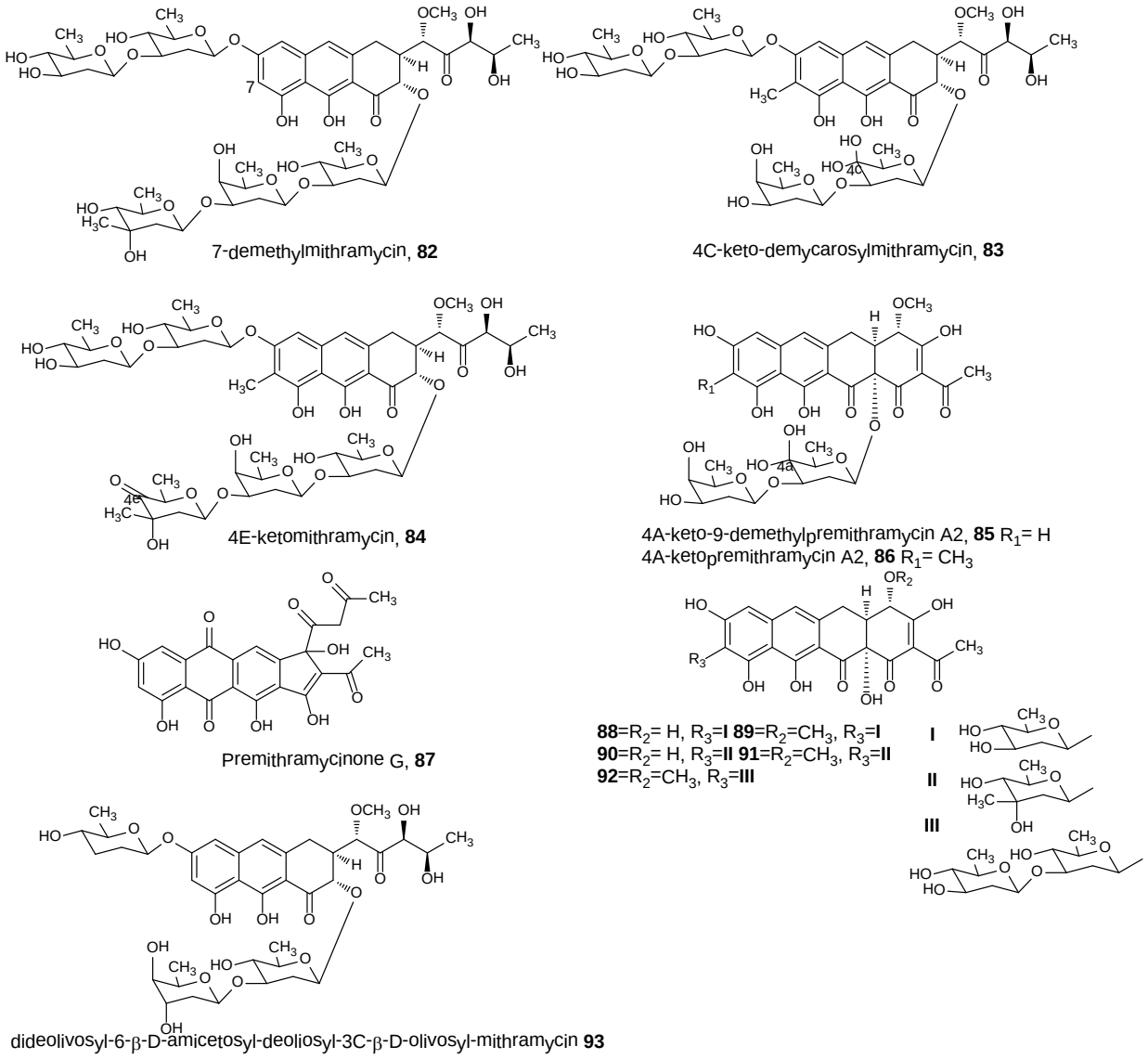

Figure 14 Premithramycins and mithramycins previously generated by combinatorial biosynthesis.

SPECIFIC AIMS

Combinatorial biosynthesis has emerged as a key strategy for generating novel derivatives of complex natural products, particularly with regards to modification of post-polyketide tailoring steps. Over the last few years, significant illumination into the biosynthesis of the gilvocarcins and jadomycins has been accomplished through the cloning and genetic investigation of these pathways, yet some enzymes of these pathways remain enigmatic. In the spirit of furthering knowledge about the biosynthesis of these

clinically promising molecules, this present research is conducted to clone the gene cluster for the related benzo[*d*]naphtho[1,2-*b*]pyran-6-one *C*-glycoside antibiotic chrysomycin A. Furthermore, characterization of this gene cluster is conducted with an emphasis on the monooxygenase enzymes and the deoxysugar tailoring enzymes for generation of NDP-D-virenose. Another purpose of this work is to generate novel tetracenomycin and aureolic acid derivatives with altered glycosylation patterns using combinatorial biosynthesis. For this, cloning of novel deoxysugar-biosynthesizing cassettes and introduction of these plasmids into producing strains was conducted. Resulting metabolites were isolated, and their structures were determined in order to draw conclusions about the substrate flexibility of the endogenous glycosyltransferases.

Specific Aim 1: To clone and analyze the entire chrysomycin A biosynthetic gene cluster. To prove its functional role in chrysomycin biosynthesis experiments by cross-complementing chrysomycin monooxygenases in gilvocarcin-oxygenase deficient mutants.

The cloning of entire *Streptomyces* sp. biosynthetic gene clusters was possible using cosmid vectors, which can often contain 30-40kb of genomic DNA. Using the cloning of the gilvocarcin biosynthetic gene cluster as a template for this study, the complete chrysomycin gene cluster was cloned on one or more cosmids, probed, and sequenced. The sequencing of this cluster gave valuable information about the shared enzymes between these pathways and their shared roles in **39** and **42-43** biosynthesis. Furthermore, the identification of novel enzymes responsible for biosynthesis and attachment of NDP-D-virenose will be useful for heterologous expression of these enzymatic components in other producing organisms. Cross-complementation of the oxygenases from this cluster into the respective blocked mutants of the gilvocarcin pathway can prove the role of this biosynthetic locus in production of chrysomycin. This aim will be discussed in chapter 2.

Specific Aim 2: To investigate the potential role of enzymes in D-fucofuranose ring contraction in biosynthesis of gilvocarcin V. Structure elucidation of the metabolites

accumulated in this strain will give valuable analysis about its role. Furthermore, this information will be used to clone constructs for the biosynthesis of NDP-D-virenose and NDP-D-fucofuranose *in vivo*.

Recombination of deoxysugar biosynthetic genes is one effective means of exploiting endogenous glycosyltransferase donor substrate flexibility. Inactivation of the putative glycosyltransferase GilN proved that it plays no role in NDP-D-fucofuranose biosynthesis. This finding was an important step towards identifying the enzyme responsible for furanose ring contraction. Furthermore, plasmids directing the biosynthesis of NDP-D-virenose and NDP-D-fucofuranose and their biosynthetic intermediates were cloned for heterologous expression and interrogation of endogenous glycosyltransferases from other pathways. These aims will be discussed in chapter 3.

Specific Aim 3: To interrogate the substrate flexibility of the glycosyltransferase, ElmGT, towards a variety of deoxysugar donor substrates. Various constructs directing the biosynthesis of novel deoxysugars will be transformed into a recombinant strain harboring the genes for 8-demethyl-tetracenomycin C biosynthesis and the sugar donor flexible glycosyltransferase, ElmGT.

The substrate flexibility of glycosyltransferases is one important factor in generating novel derivatives with altered glycosylation patterns. Another factor is the introduction of recombinant plasmids that direct biosynthesis of novel deoxysugars, which are not present in a producing organism. For this, a recombinant strain, namely *S. lividans* (cos16F4), which harbors the biosynthetic genes for the production of 8-demethyl-tetracenomycin C and the sugar flexible glycosyltransferase, ElmGT, will be used as an expression host. Glycodiversification studies will further clarify the substrate flexibility of ElmGT and the role of these cassettes in biosynthesizing various NDP-deoxysugars. These aims will be discussed in Chapter 4.

Specific Aim 4: To generate novel mithramycin derivatives with altered glyosylation patterns.

The mithramycin biosynthetic pathway of *Streptomyces argillaceus* has five glycosyltransfer steps and four glycosyltransferases, which presents an excellent system for glycodiversification experiments involving novel deoxysugar plasmids. For this, plasmids directing the biosynthesis of various deoxysugar cassettes will be heterologously introduced into *Streptomyces argillaceus* and several blocked mutants using protoplast transformation. Any accumulated novel mithramycin derivatives were structurally elucidated to yield important compounds for biological testing. These objectives will be discussed in Chapter 5.

CHAPTER 2: ISOLATION AND ELUCIDATION OF THE CHRYSOMYCIN BIOSYNTHETIC GENE CLUSTER

INTRODUCTION

Previous isolation of benzo[d]naphtho[1,2-b]pyran-6-one C*-glycoside antibiotics*

The chrysomycins (**42** and **43**) were historically the first gilvocarcin-type *C*-glycosides isolated, by Strelitz and Flonne in 1955 (*51*), though their structures were not determined, and only published in the 1980s by Weiss *et al*. (*50*). The initial structure determination of the sugar moiety of **42** and **43** by Weiss *et al*. was suggested to have a $^1C_4$ configuration. However, their assignments were based on relative stereochemistry assigned by coupling constants. Brazhnikova *et al*. isolated the sugar component of **42** and **43** (their group had referred to it as virenomycin) through methanolysis and 1D- and 2D-NMR analysis of the sugar moiety identified it to be methyl-β-D-virenoside, thereby disproving the $^1C_4$ configuration suggested by Weiss *et al*. (*52*)

Biological activity of chrysomycin A

The antitumor activity of chrysomycin A was established in a murine P 388 lymphocytic leukemia cell line (*50*). Chrysomycin A protected the mice with an increased lifespan of 54% compared to control mice. As such, the antitumor activity of chrysomycin A was established as being very similar to gilvocarcin V in this cell line (57% increased life span and LD_{50} at doses greater than 1 g/kg), while exhibiting no lethal effects at the dose administered (*50*). Photoactivation studies confirmed the role of the 8-vinyl side-chain of **42** DNA-binding using a [2+2] cycloaddition to thymine residues (*115-116*). Studies on the crosslinking of histone H3(*116*) suggest an important role for the binding of the *C*-glycoside moiety to this densely positively-charged protein (*117*). Matson *et al*. reached the same conclusions about the activity of chrysomycin A, while suggesting that another factor of its binding, other than photoactivation of the 8-vinyl side, was responsible for the binding of chrysomycin A to DNA (*118*). Structure-activity relationships by the Mercian company on the 4-keto-D-virenose derivative **51** showed that this derivative has improved activity in solid tumor cell lines over **42**, an observation only attributable to the presence of a ketosugar.

Rationale for cloning chrysomycin A biosynthetic gene cluster

Previous work on the gilvocarcin biosynthetic gene cluster was paramount for development of a coherent biosynthetic pathway and for generation of novel derivatives through inactivation experiments and glycodiversification experiments (*72*, *119*). Therefore, cloning of the chrysomycin A gene cluster will be important for expanding the combinatorial biosynthetic toolbox with NDP-D-virenose biosynthetic genes. Furthermore, because chrysomycin A possesses a pyranose *C*-glycosidic moiety compared to the furanose moiety of gilvocarcin, the *C*-glycosyltransferase responsible for attachment of NDP-D-virenose to the polyketide acceptor substrate is valuable for interrogation of other pyranose substrates. As it is anticipated that **39** and **42** share identical biosynthetic steps towards the generation of the gilvocarcin-type chromophore, the *chry* cluster should possess a homologous set of genes to the characterized *gil* gene cluster. Additionally, direct comparison of the genes present in the chrysomycin A gene cluster with those that are present in the gilvocarcin gene cluster as well as the gene cluster of the ravidomycins, will possibly illuminate the roles of some still unknown gilvocarcin biosynthetic enzymes, among these are *gilLMNV*.

RESULTS AND DISCUSSION

Construction of cosmid library for S. albaduncus AD819

A library screening approach was envisioned for the isolation and sequencing of cosmid DNA pertinent to the biosynthesis of chrysomycin. Cosmid vector pOJ446 was selected as the cosmid cloning vector for this (previously used for cloning of the gilvocarcin gene cluster) (*61*). The vector pOJ446 possesses several useful features: its *cos* sites allow for packaging 35-40 kilobase pair fragments of genomic DNA; it possesses origins of replication for cloning in both *E. coli* and *Streptomyces* sp. (SCP2*). It also has an *oriT* site for conjugal transfer into *Streptomyces* sp. hosts. For this, a cosmid library of *Streptomyces albaduncus* AD819 was generated by ligating partially-digested *Sau*3AI fragments of genomic DNA into pOJ446, prepared with *Hpa*I/*Bam*HI (*3*). The evaluation of the amount of the genome that is covered in the cosmid library

can be modeled using a mathematical equation. This equation factors the average size of genomic DNA inserted into a single plasmid, the number of *E. coli* colonies transformed with cosmids harboring genomic DNA, and the size of the genome. To calculate the total coverage of the cosmid library, the following equation was used:

$$N = \log(1-f_c) / \log(1-L/G)$$

Where N= the total number of clones, f_c is the fractional coverage of the genome, L is the length of genomic DNA present in each cosmid clone, and G is equal to the total length of the genome (*3*). G for the total genomic length of *Streptomyces albaduncus* is approximated by comparing the lengths of the characterized *Streptomyces lividans* TK 66 (NCBI data) (8,318,010 bp) and *Streptomyces coelicolor* A3(2) (8,667,507 bp) genomes, or about 8,500,000 bp (*120*). F_c is usually calculated to be >95% coverage of a genome, and L was determined by restriction analysis of ten random cosmids from the titering reaction (**Figure 15**). This analysis indicated that an average insert size of ~38 kb was present in the cosmids so digested. Therefore, approximately 670 unique colonies from a titering reaction would be required for >95% coverage. The resulting number of colonies from titering was 2300 colonies, which is roughly ~4x the theoretical coverage of the entire *S. albaduncus* genome.

Positive hybridization of probes of NDP-glucose-4,6-dehydratase, 3-oxoacyl-acyl carrier protein-reductase (chryF), and Ketoacyl synthase (KSα) cosmid DNA

For the isolation of cosmids pertinent to chrysomycin biosynthesis, two DNA fragments were designed for probing the genomic library corresponding to genes that were theorized to be a part of the gene cluster of **42**. Two degenerate fragments corresponding to conserved regions of β-ketoacyl synthase (KSα) and NDP-4,6-dehydratase were synthesized (*38, 61, 121*). KSα is an essential component of the "minimal polyketide synthase" responsible for polymerizing additional acetate units to a growing poly-β-ketothioester (**Figure 10**). NDP-4,6-dehydratase is an essential early-acting deoxysugar enzyme (**Figure 7**). Such an approach of using two probes increases the chances of finding clusters that are pertinent to chrysomycin biosynthesis, because deoxysugar biosynthetic genes and polyketide synthase genes were expected to be clustered together. Furthermore, polyketide gene clusters are fairly ubiquitous among

streptomycetes, and screening with a single KSα probe may uncover multiple polyketide gene clusters from *S. albaduncus*. For example, in the chartreusin biosynthetic pathway, cosmids positively hybridizing to PKS probes were isolated from at least 3 different PKS-encoding pathways (*122*).

It was necessary to design a second NDP-4,6-dehydratase probe than the one used by Bechthold *et al*. upon discovering a conserved downstream region (e.g. reverse primer synthesized from BEWLHVDDHC region) that is absolutely conserved among 4,6-dehydratases. Colony hybridization with the two digoxigenin (DIG)- labeled probes (~650 basepair KSα probe and ~600 basepair 4,6 dehyratase probe) resulted in colonies that hybridized with both the KSα and the NDP-4,6-dehydratase probe (**Figure 15**). One of these cosmids, namely cosChry1-1, was chosen for Southern Blot analysis and shotgun sequencing.

After sequencing revealed that cosChry1-1 was lacking a polyketide-associated ketoreductase, a "*gilF*" candidate gene essential for biosynthesis of the polyketide, a third DIG-labeled-probe based on conserved amino acid residues for 3-oxoacyl-ACP-reductases was generated. A second round of colony hybridization resulted in 3 more colonies that positively hybridized to the *chryF* probe. The cosmids isolated from these colonies were called cosChryF1, cosChryF2, and cosChryF3, because they each harbored the putative *chryF* gene.

Southern blot studies of cosChry1-1, cosChryF1, cosChryF2, cosChryF3

CosChry1-1 was digested with *Bam*HI and was hybridized with both DIG-labeled KSα and NDP-4,6-dehydratase probes (**Figure 16**). The Southern Blot of *Bam*HI-digested cosChry1-1 indicated positive binding of the KSα probe to a 7.0 kilobase pair region, and the NDP-4,6-dehydratase probe was confirmed to bind to a ~7.8 kilobase pair fragment. Therefore, cosChry1-1 was confirmed to contain both the putative KSα and 4,6-dehydratase genes necessary for chrysomycin biosynthesis clustered together on the same cosmid. As a result, cosChry1-1 was used for further "shotgun" sequencing experiments.

It was necessary to confirm the presence of *chryF* in each of the three cosmids identified by colony hybridization. Therefore, each of the three cosmids were digested

with *Bam*HI and were hybridized with the DIG-labeled *chryF* probe (**Figure 16**). In all three cases, *chryF* was found to strongly hybridize with a ~4 kilobase pair region on the cosmids. An additional PCR experiment using the KSα primers amplified the expected KSα fragment from each cosmid, confirming that the *chryF* and the putative β-ketoacyl synthase genes were clustered together on each of cosChryF1, cosChryF2, cosChryF3.

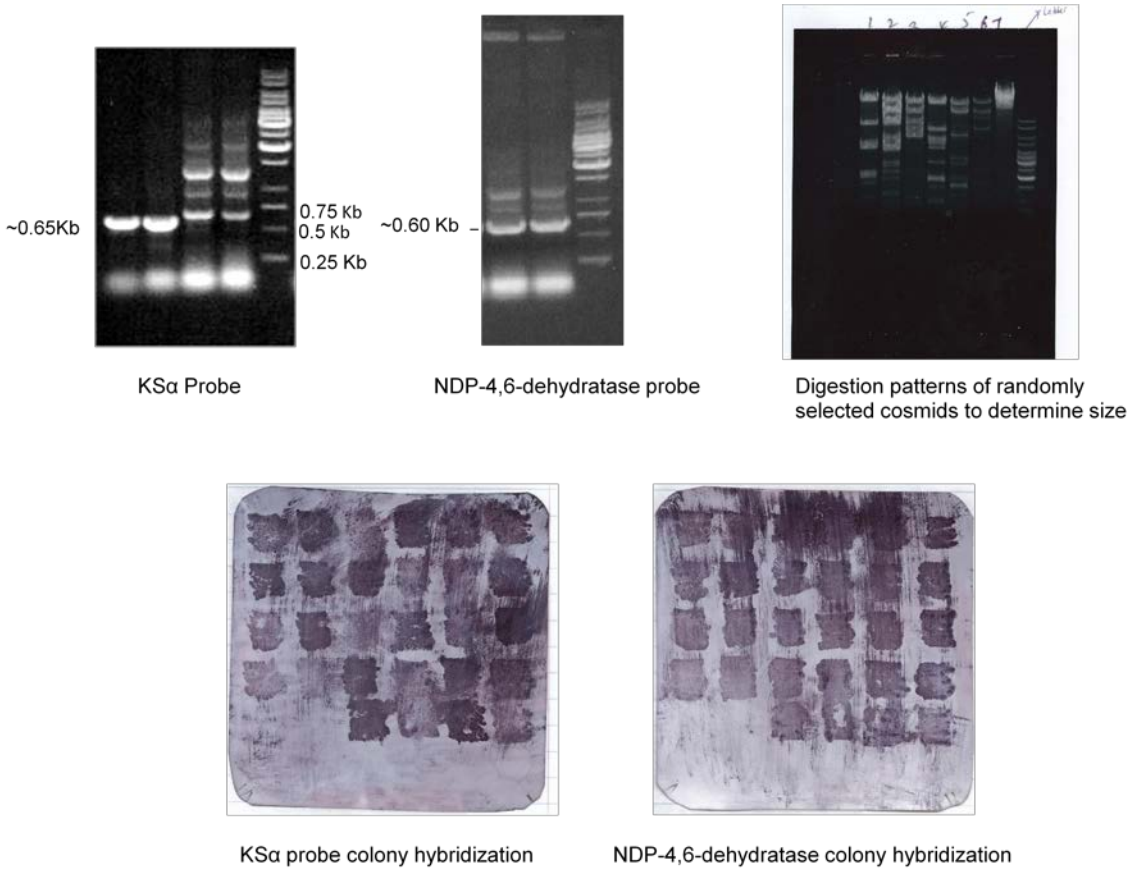

Figure 15 Amplification of probes and colony hybridization.
(Upper Left) 0.7% agarose gel of KSα probe and NDP-4,6-dehydratase probe (Upper Middle). (Upper Right) *Bam*HI digest of 7 randomly selected cosmids to determine size of inserts from restriction analysis. (Bottom) Plaques from colony hybridizations with DIG-labeled KSα and 4,6-dehydratase probes. Darkest colonies are clones that are positively hybridizing.

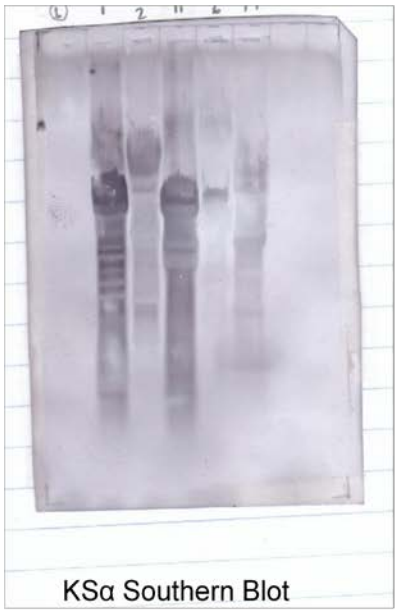

KSα Southern Blot

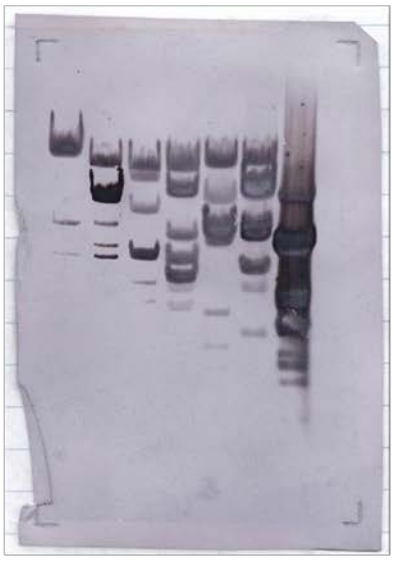

4,6 Dehydratase Southern Blot

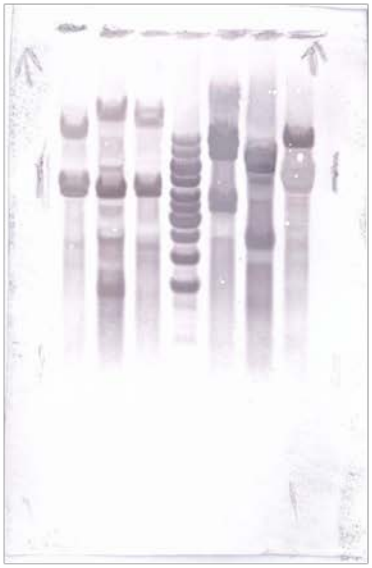

ChryF Southern Blot

~0.65 kb

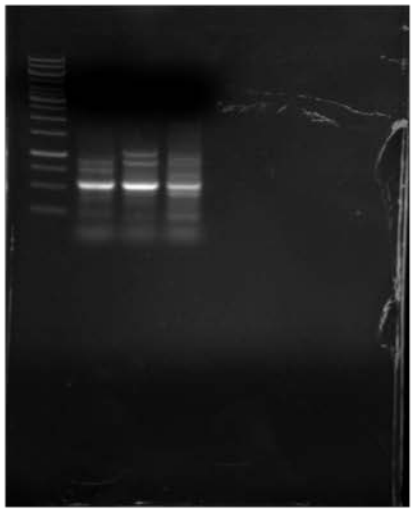

PCR amplification of *chryA* from cosChryF1-F3

Figure 16 Southern blot studies of *chry* cosmids.
(Upper Row) Southern blots of selected *Bam*HI digested cosmids with DIG-labeled KSα and NDP-4,6-dehydratase probes, respectively. (Lower Left) Southern blot of DIG-labeled chryF with BamHI-digested cosChryF1, cosChryF2, cosChryF3 on left and cosChryF1, cosChryF2, cosChryF3 digested with PstI on the right. (Lower Right) Amplification of *chryA* (0.65 kb) from cosChryF1, cosChryF2, cosChryF3.

Shotgun sequencing of cosChry1-1, primer walking of cosChryF1-cosChryF3, subcloning of chryF *fragment*

CosChry1-1 was shotgun sequenced using a Mu transposon-based insert to allow for generation of short (800 bp-1000 bp) reads by a sequencer (HyperMu Transposase, Materials and Methods) (*123-124*). The resulting short reads were combined by the Phred/Phraps/Consed software package, which was used to generate **contig**uous sequence reads (contigs). From this sequencing, three contiguous regions of ~8 kilobases, ~12 kilobases, and ~13 kilobases were generated. To sequence the overlapping regions of these contigs, subcloning experiments of cosChry1-1 were undertaken. CosChry1-1 was digested with *Bam*HI, and two resulting fragments of ~7.8 kilobases and 3 kilobases were rescued and cloned into the same sites of pBluescript II K/S+, and these resulting constructs (pBS7PQ and pBS3U, respectively) were used for primer walking. An 80 basepair overlap of pBS7PQ between *chryQ* and *chryX1* revealed one connection, and the other came from sequencing pBS3U from the 5'-end of *chryU* to the 3'-end of *chryRM*.

To sequence *chryF*, a ~4kb *Bam*HI fragment was subcloned into the same restriction sites of pBluescript II K/S+ to give pBS4F, which was primer walked outward from the center of *chryF* (this sequence being provided by sequencing the *chryF* probe in a pGEM-T vector) until arriving at known sequence from cosChry1-1. A combination of primer walking and subcloning revealed the upstream *chryF*-containing region and connected it with known *chryOI* ORF from the cosChry1-1 shotgun sequencing experiments. The sequencing of the upstream region was stopped when all genes necessary for biosynthesis of **42** were determined (based on direct comparison with the GV gene cluster). A further sequencing of 1000 base pairs revealed ORFs whose encoded proteins seemed to be irrelevant for biosynthesis of **42**, and were likely involved in primary metabolism, which effectively bounded the upstream region of the cluster.

Bioinformatics analysis of DNA

The resulting sequence reads were analyzed *via* the FramePlot and NCBI BLAST databases for the determination of discrete open reading frames (ORFs) and assignment of putative functions to *chry* genes from similarity searches (Materials and Methods). ORFs were also judged to possess a relatively high percentage of GC bases in the wobble

base position of their codons. *Streptomyces* sp. genes are characterized by a relatively high percentage of guanines and cytosines (high GC %) residing in the third base pair, or wobble base pair, of codons. As a result, analysis of the 34,654 nucleotide sequence resulted in 35 open reading frames that were identified for genes putatively responsible for biosynthesis of **42**, self-defense from chrysomycin, regulation of the pathway, or constituted genes whose encoded protein products were of unknown function (*chryLV*). Prospective gene candidates were named according to their *gil* cluster homologues. Therefore, the nomenclature of the *chry* cluster reflects the precedence of the gilvocarcin gene cluster and the similarities between their biosynthetic components. A table of ORFs and proposed functions of encoded enzymes is included in **Figure 20**. The complete *chry* cluster nucleotide sequence is assigned the NCBI Accession No. **FN565166**.

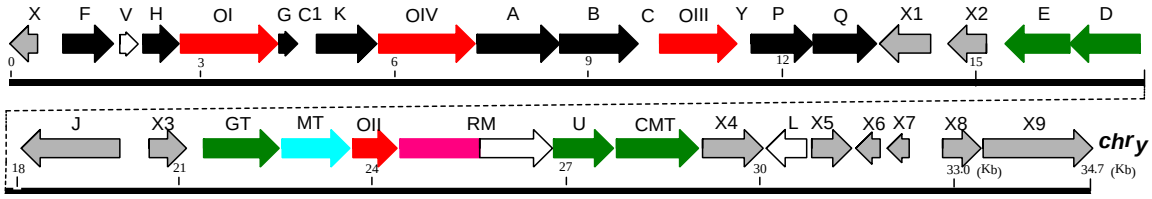

Figure 17 Map of the chry cluster using arrows to indicate direction of candidate ORFs. Polyketide biosynthesis enzymes depicted in **Black**, deoxysugar biosynthetic and glycosyltransferase enzymes are **Green**, monooxygenases are **Red,** enzymes involved in regulation or export of CV are **Grey,** polyketide *O*-methyltransferase in **Light Blue**, and putative ORFs encoding proteins of unknown function are White.

Minimal 'PKS' genes and genes implicated in polyketide cyclization, ketoreduction, aromatization

The minimal polyketide synthase, consisting of *chryABC*, is clustered towards the upstream region of the *chry* cluster, near the polyketide cyclases *chryGK* and the PKS-associated ketoreductase, *chryF* (**Figure 17**). *ChryABC* are translationally-coupled with one another, which is a common feature of type-II polyketide synthase genes. *ChryA* encodes the ketoacyl synthase for chrysomycin biosynthesis; its protein product consists of 422 amino acids, and demonstrates strong sequence identity and similarity to other known ketoacyl synthases (KSα). It particularly exhibits strong sequence similarity to the *Streptomyces ravidus* RavA KSα protein (423 amino acids, 90% identity/94% similarity) and the *S. fradiae* UrdA KSα protein (426 aa, 80% identity, 88% similarity).

It has a KAS type I-II domain, a FabF domain, a putative dimer interface for interaction with ChryB, and a putative conserved catalytic cysteine residue, C169 (*16*). *ChryB*, the chain length determinant-encoding gene (KSβ), encodes a 402 amino acid chain length determinant, which forms a heteromeric complex with ChryA. *ChryB* demonstrates similarity to known type II KSβ proteins (71%/83% with UrdB, 51%/67% GilB, 77%/85% RavB). *ChryC* encodes the PKS-associated acyl carrier protein (ACP) of the "minimal" PKS. The 87 amino acid product bears similarity to the ACPs of the jadomycin and ravidomycin pathways (JadC 61%/71%, RavC 79/84%).

Amazingly, the *chry* cluster possesses another ACP homologue, namely *chryC1*, which is transcribed in the same direction as and is between the cyclases *chryGK*. ChryC1 possesses strongest sequence similarity with acyl carrier proteins RavC1 (71%/81%) and SimA3 from *S. antibioticus* (59%/72%). It is unclear what role a second ACP has in the *chry* cluster, however, it may be used for extending the polyketide chain with either the malonate or propionate starter unit selectively. Because chrysomycin biosynthesis involves both malonate and propionate starter units, the presence of two ACPs might help steer the pathway towards production of either **42** or **43**. However, Shepherd *et al*. have shown that sister protein RavC1 loads both propionyl-CoA and malonyl-CoA comparably (*65*). The *chry* and *rav* gene clusters represent an anomaly in type II polyketide biosynthesis encoding two functional acyl carrier proteins in the same gene cluster (*65*). Only in a couple other type II PKS gene clusters have two encoded ACPs been found clustered together- the frenolicin and R1128 clusters (*65*). Therefore, it is possible that ChryC1 is an ancillary ACP that assists in extending the growing polyketide chain along with ChryC. *ChryP* (protein product is 322 amino acids) and *chryQ* (protein product is 327 amino acids) encode a malonyl-CoA acyltransferase (MCAT) and a propionyl-CoA acyltransferase, respectively. The *gil* biosynthetic machinery also possesses a homologous pair of MCAT and propionyl-CoA acyltransferase enzymes, GilP and GilQ, respectively, however, MCATs can also be recruited from the fatty acid biosynthesis (*18*). A BLAST database search of ChryP reveals sequence similarity to MCATs from other type II PKS pathways (PgaH 50%/64%). ChryQ resembles the closely related RavQ propionyl-CoA acyltransferase from the *rav* gene cluster (65%/72%).

ChryF encodes the putative polyketide-associated ketoreductase (261 aa) necessary for ketoreduction at the C-9 carbonyl of the polyketide chain (**Figure 18**). It has significant similarity to known oxoacyl-ACP-ketoreductases RavF (86%/92%) and Orf7 from *S. echinatus* (72%/84%). Interestingly, *chryF* is in stand alone at the beginning of the *chry* cluster (**Figure 17**), whereas in the *gil* cluster *gilF* is transcribed directly after the gilvocarcin minimal polyketide synthase, *gilABC*, reflecting the intimate nature of its interaction with GilABC. However, clustering of *chryF* with the minimal PKS genes is not an absolute requirement. The cyclases-encoding genes *chryGK* are immediately upstream of *chryOIV* and *chryABC* (**Figure 17**). *ChryG* (109 aa) and *chryK* (314 aa) encode the cyclases responsible for installing the angucycline framework of CV. ChryG (OvmC- 71%/84%, UrdF 74%/84%) exhibits strong similarity to other angucycline-type C4-C17 cyclases, and ChryK exhibits similarity to bifunctional dehydratases/cyclases (RavK 72%/81%, SaqL 61%/72%). In theory, ChryK acts first, dehydrating the C-9 position, which results in spontaneous aromatization of the first ring and cyclization of the second ring, and cyclase ChryG acts next, cyclizing the third ring and performing C4-C17 angular cyclization of ring A of homo-UWM6 (**18**) (**Figure 18**).

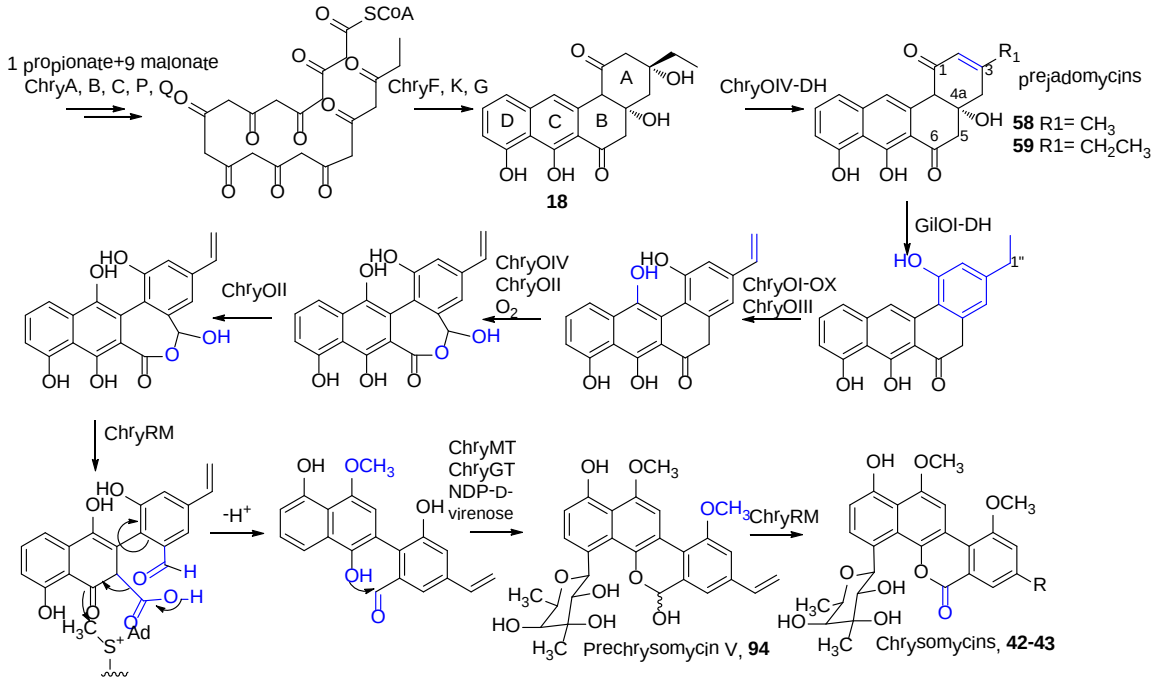

Figure 18 Proposed biosynthetic pathway to chrysomycin A and B (**42** and **43**). Transformations catalyzed by *chry* enzymes are indicated in blue.

Oxygenases, oxidoreductase, and methyltransferase genes

The oxygenases of the *chry* cluster are integral for the transformations that result in **18** being rearranged into the distinctive gilvocarcin-chromophore (**Figure 18**). Four oxygenase encoding genes were identified in the *chry* cluster, which is in agreement with a complement of four oxygenases being required for biosynthesis of GV (**Figure 10)** (*60, 62, 68-69*). *ChryOI*, *chryOII*, *chryOIII*, and *chryOIV* encode the four monooxygenase homologues so identified in this gene cluster. *ChryOIV* and *chryOI* encode putative FAD-dependent oxygenases. Furthermore, their products ChryOIV (491 aa) and ChryOI (513 aa) demonstrate sequence similarity with one another (46%/55%), which is also the case with FAD-dependent monooxygenase pairs JadF/H and GilOIV/OI from the jadomycin and gilvocarcin pathways, respectively. The product of *chryOIV* demonstrates sequence similarity to GilOIV (36%/48%) and JadF (55%/63%), which are known to catalyze the 2,3-dehydration step of homo-UWM6 (**Figure 18**). ChryOIV is also believed to play a vital role in the installation of a 5-OH, which in a presently unclear and perhaps concerted manner with ChryOII, undergoes a Baeyer-Villiger oxidative cleavage of a hypothetical intermediate to afford a ring-opened acid/aldehyde compound (**Figure 18**). The encoded product of *chryOI* demonstrates sequence similarity to JadH (60%/69%) and GilOI (43%/55%), which has been shown to catalyze the 4a, 12b-dehydration of 2,3-dehydro-homo-UWM6 (**59**). Furthermore, it is proposed that ChryOI installs a 12-hydroxyl moiety to afford a hydroquinone, which Chen *et al*. refer to as CR1 (*69*). However, this compound rapidly oxidizes to the dehydrorabelomycins (**60** and **61, Figure 10**).

ChryOIII encodes a P450 monooxygenase responsible for installation of the 8-vinyl side chain of **42**. The encoded product (394 aa) has considerable sequence similarity to P450 monooxygenases from other pathways, including GilOIII (72%/81%). It is believed that as soon as the A ring is fully aromatized and either just before or after 12-hydroxylation that ChryOIII acts as to install the 3-vinyl side chain (**Figure 18**). *ChryY* encodes a ferredoxin accessory protein just downstream of *chryOIII*: P450 monooxygenases utilize either their own ferredoxin accessory protein, or recruit ferredoxin from the electron transport chain. It is unclear by what mechanism the 3-vinyl side chain is installed. However, by employing chemical logic, ChryOIII could install a

hydroxyl group on the 1" benzylic position of the 3-ethyl group. This hydroxyl group could be potentially installed *via* a radical mechanism, for example. Once the hydroxyl moiety has been installed, a facile dehydration would afford the vinyl side chain that serves as the warhead for chrysomycin's biological activity.

ChryOII encodes a putative anthrone monooxygenase that initially was hypothesized to catalyze 12-hydroxylation. It demonstrates similarity to other putative anthrone monooxygenases (JadG 53%/71%, GilOII 65%/76%). However, JadH has been shown to catalyze this 12-hydroxylation, and furthermore, the absence of 12-hydroxylated shunt products in the GilOI- and JadH-deleted strains indicate that ChryOI probably catalyzes a similar step in the biosynthesis of **42** (*60*, *69*). However, C-12 hydroxylation could also occur spontaneously as a shunt process, as in the case of rabelomycin. This assignment is purely suppositional, and the assignment of GilOII-type cofactorless monooxygenases as anthrone monooxygenases may just reflect that little is known about this intriguing class of oxygenases. It is more likely that C-12 hydroxylation occurs during an oxygenase cascade in a concerted and mechanistically-controlled fashion after ring A aromatization, thereby affording a hydroquinone intermediate (**Figure 18**). Therefore, ChryOII might be responsible for the C5-C6 carbon-carbon bond cleavage reaction, perhaps as a novel Baeyer-Villiger (BVMO) type reaction (**Figure 19**). It may act in a concerted fashion with ChryOIV to generate the acid-aldehyde ring-opened intermediate. Furthermore, BLAST analysis suggests that ChryOII has a conserved histidine, H185 that is in common with the larger antibiotic monooxygenase superfamily. It is possible that this residue may be involved in the ring cleavage reaction; this H185 is absolutely conserved in JadG/GilOII/RavOII as well. To prove this hypothesis, in theory a simple mutagenesis experiment of ChryOII H185 to alanine could confirm this catalytic role. For example, the vancomycin dioxygenase DpgC involves conversion of 3,5-dihydroxyphenylacetyl coenzyme A to 3,5-dihydroxyphenylglyoxylate using a single-electron transfer mechanism from the substrate to one oxygen of diatomic oxygen (*125*). Therefore, it could be proposed that H185 serves as a conserved base in ChryOII for abstraction of a proton from C5, which allows for subsequent attack of the substrate onto diatomic oxygen (**Figure 19**). The following mechanism can either follow a BVMO route (**A**) or proceed *via* a dioxetane route (**B**)

(**Figure 19**), as was suggested by the DpgC crystal structure (*125*). The BVMO route (**A**) proposes oxygenation at C5 by ChryOII, reduction catalyzed by an unknown enzyme, and oxygenation by ChryOIV. One of the mechanistic limitations of this route is the requirement for another reduction event. The dioxetane route (**B**), however, generates a dioxetane intermediate and subsequent rearrangement affords the acid and aldehyde. However, one limitation of this route (**B**) is that ChryOIV only serves as the 2,3-dehydratase in this pathway and has no oxygenase function. This route may be supported by inactivation experiments, however, because in the *S. lividans* (cosG9B3-GilOIV$^-$) mutant production spectrum, a small amount of gilvocarcin M is produced along with the major products of rabelomycin and homorabelomycin (Madan Kharel, unpublished results), only using GilOI and GilOII. Therefore, in the absence of GilOIV, GilOI may possess slight flexibility towards UWM6 (**18**) enough to catalyze both the 2,3-dehydrations and 4a-12b dehydrations, which then allows for GilOII to perform the dioxygenase reaction in the absence of GilOIV, resulting in the accumulation of small amounts of GM. Additionally, it is interesting to note that upon feeding dehydrorabelomycin (3-methyl congener of **60**) to a PKS-deficient mutant strain of *S. venezuelae* that both CR1 and dehydrorabelomycin were both fully-converted to jadomycin A, whereas feeding of **60** to the *S. lividans* (cosG9B3-*gilOIV*$^-$) strain did not result in conversion to **39** (*68*). Cross-complementation of the *jadG* gene into the GilOII-deleted mutant failed to complement the pathway and restore production of **39**. As a result, GilOII/ChryOII and JadG may bind different pathway molecules, in the case of the gilvocarcins and chrysomycins, a hydroquinone.

ChryMT encodes a putative 340 amino acid protein that serves in *O*-methylation of the chromophore of chrysomycin (**Figure 18**). ChryMT exhibits strong sequence similarity to *O*-methyltransferases from other pathways (e.g. MetLA1 50%/64%). ChryMT is hypothesized to be a SAM-dependent *O*-methyltransferase that *O*-methylates either the 12-hydroxyl or 10-hydroxyl moieties. ChryMT is proposed to *O*-methylate the 10-hydroxyl position due to the suspected involvement of ChryRM in catalyzing an unusual methylation immediately after the C5-C6 cleavage step, which becomes 12-*O*-methyl. The substrates for these reactions are completely unknown, however. Furthermore, it is uncertain if 10-*O*-methylation occurs before or after glycosylation with

D-virenose. It seems plausible that the presence of the 4-*C*-virenoside moiety is not an essential requirement for ChryMT methylation, as defucogilvocarcins (**62-64**), which are *O*-methylated at 10- and 12-positions, are accumulated in the *S. lividans* (cosG9B3-*gilGT*-) strain and other producing organisms.

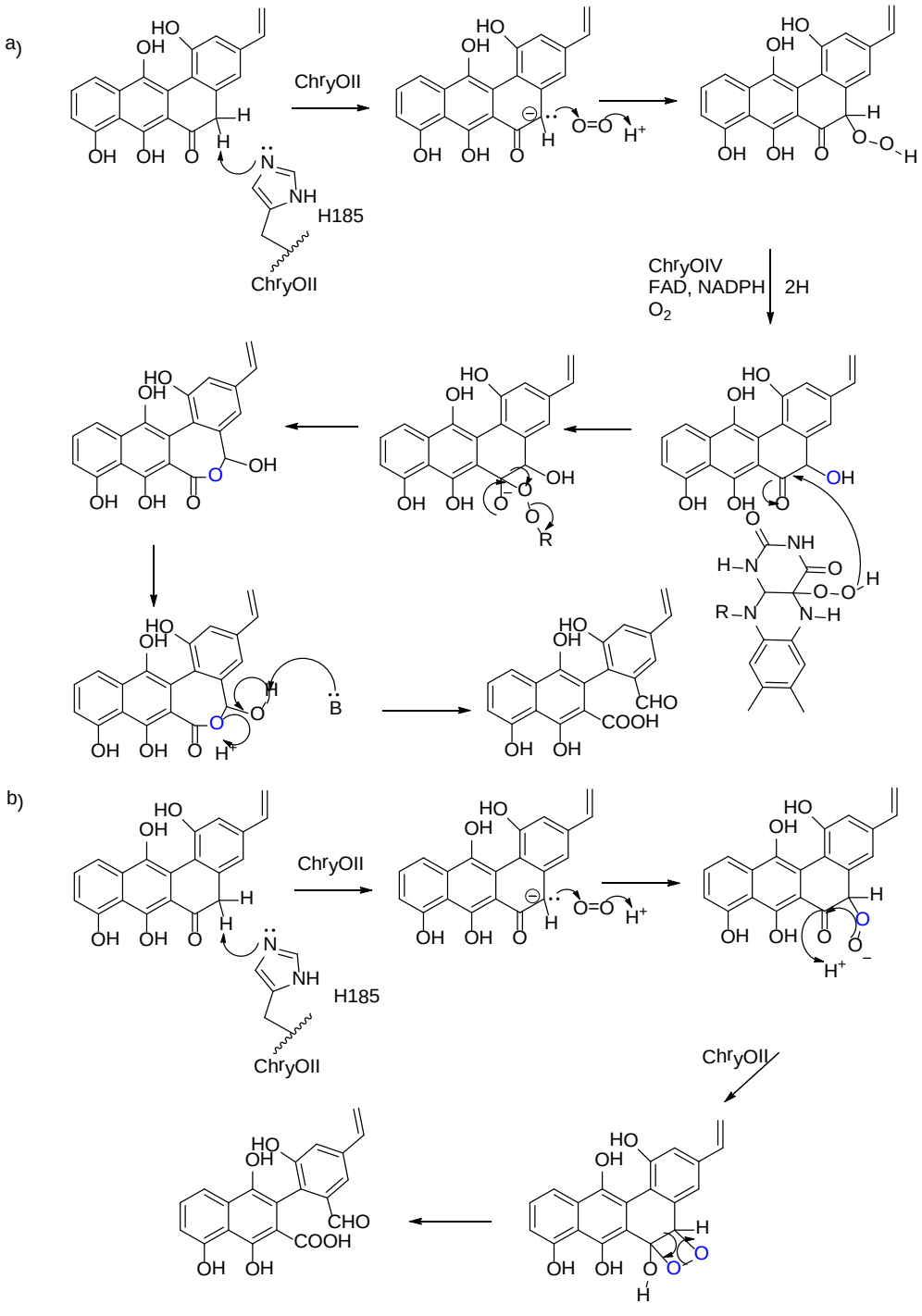

Figure 19 Theoretical routes to C5-C6 carbon carbon bond cleavage of the chrysomycins.

H185 of ChryOII is portrayed as a predicted catalytic base. A) Baeyer Villiger-catalyzed route towards the ring-cleaved acid/aldehyde intermediate. B) Dioxygenase and dioxetane formation by ChryOII route to acid/aldehyde intermediate.

ChryRM encodes a putative two-domain protein that involves both a GilM-type methylation step and a GilR-type dehydrogenation step of prechrysomycin V (**96)**. ChryRM (*N*-terminal domain=518 aa, *C*-terminal=243 aa) demonstrates sequence similarity to GilM (41%/58%) and GilR (50%/63%). Initially, the putative *chryR* was suspected to be sequenced wrong, in that an extra nucleotide insertion appeared to have happened in the initial sequencing file. Upon re-sequencing and confirmation that the *chryR* sequence was indeed correct, it was determined that *chryRM* composed a single ORF whose product would be a dual domain protein, ChryRM. Sequence comparison with *ravRM* confirmed that both the *rav* and *chry* clusters encode such a predicted two domain protein. The 761 aa predicted ChryRM could potentially have important ramifications for elucidation of the late-acting chrysomycin biosynthetic steps from the ring-cleaved acid-aldehyde intermediate to the final dehydrogenation step of prechrysomycin V **94** to chrysomycin V **42**. It is interesting that in the case of the ravidomycin and chrysomycin clusters, these two proteins are fused versus in the gilvocarcin cluster where GilM and GilR are separate entities. The *rav* and *chry* clusters very likely share a common ancestor, given that their genetic organization is almost identical, and this may account for the presence of a fused protein. This protein very likely was originally fused in an ancestor, and then over time genetic mutation may have caused the *chryRM*/*ravRM* to become two functional ORFs *gilR* and *gilM* in the *gil* cluster. However, both the *rav* and *chry* clusters encode deoxyhexose tailoring enzymes, in essence the only major difference between these clusters, and the presence of a deoxyhexose of the prechrysomycin/preravidomycin intermediates may require a very specialized RavR or ChryR domain to catalyze dehydrogenation of the hemiacetal to the lactone (as compared to the fucofuranose-containing pregilvocarcin). Kharel *et al*. demonstrated that GilR catalyzes the turnover of pregilvocarcin V (k_{cat} =2.29±0.03 min^{-1}), but also the unglycosylated predefucogilvocarcin V less effectively (k_{cat}=0.65±0.086 min^{-1}). Interestingly, prechrysomycin V (**94**) turned over poorly by GilR (*71*). This observation clearly demonstrates the preference and substrate specificity for these

dehydrogenases towards a very particular type of glycosylated molecule, a deoxyfuranose for GilR, and deoxypyranoses for RavRM and ChryRM. Therefore, ChryRM is unusual in that it is anticipated to accept two separate substrates- the acid/aldehyde intermediate, and a fully-glycosylated prechrysomycin compound (**94**). Its overexpression would be useful in studies aimed at determining the nature of collaboration between the R and M enzyme-activities. This could be used to interrogate turnover of various pyranosyl pregilvocarcins that could be generated with "sugar plasmid" recombination experiments *in vivo*.

ChryH encodes a putative NAD(P)H-dependent FAD reductase with significant sequence similarity to other similar reductases (e.g. Kfla_5747, 64%/75%). It is thought that ChryH binds NAD(P)H and provides reduced $FADH_2$ to the FAD-dependent oxygenases ChryOIV/ChryOI. Disruption of GilH did not abrogate biosynthesis of **39**, and heterologously-expressed GilH evinced a yellow color indicative of FAD binding, thereby confirming its role as an accessory protein (*64*).

Genes involved in self-defense, regulation, and other functions

The *chry* cluster has several ORFs which are predicted to encode proteins essential for regulation and export of chrysomycin. *ChryX* demonstrates sequence similarity to spore-associated protein precursors (SapA, 73%/84%), which may have some role in regulating sporulation of *S. albaduncus*. Upstream of *chryX* is an ORF encoding a Zinc-finger SWIM protein >700 bp long, therefore this region demarcates one boundary of the cluster with genes whose encoded functions are not necessary for biosynthesis of chrysomycin. *ChryX1* and *chryX2* encode an apparent two-component response regulation system that is also encoded by ORFs *ravJ* (54%/70%) and *ravX5* (67%/82%) that are likely involved in regulating expression of *chry* biosynthetic genes. *ChryX3, X5, X6, X7,X8* represent various regulators putatively involved in chrysomycin biosynthesis, with *chryX3* encoding a putative MarR type regulator, and *chryX5, X7,* and *X8* pertaining to putative TetR family regulators. *ChryJ* encodes a drug efflux permease, and would be similar in this respect to *gilJ*. It is believed that ChryJ is essential for export and self-defense for *S. albaduncus* from chrysomycin. *ChryX9* encodes a putative Acyl-CoA dehydrogenase (SSDG_02680, 84%/89%), which is an enzyme from fatty acid

β-oxidation from primary metabolism. *ChryX4* putatively encodes hexokinase (Tfu_1012 61%/75%), which catalyzes the transfer of a phosphate to the 6-position of D-glucose in the first step of glycolysis. Interestingly, *chryL* (GilL, 37%/50%) is also present, and it encodes a putative NAD-dependent epimerase/dehydratase, but its role in the biosynthesis of **42** can only be speculated about. This gene demonstrates similarity to *gilL*, an ORF encoding a protein of unknown function in gilvocarcin biosynthesis. *ChryV* is another gene of unknown function related to *gilV*; BLAST analysis indicates that ChryV has a domain that is related to the chlorite dismutase family of enzymes. Enzymes of this family are largely hypothetical proteins, however, chlorite dismutase is responsible for dissociation of chlorite into its composite chlorine and oxygen species.

Genes involved in biosynthesis and attachment of NDP-D-virenose

NDP-D-virenose is a key structural feature of **42**, and the genes involved in deoxysugar biosynthesis are a unique feature of the *chry* cluster. *ChryDE* are translationally-coupled and encode an NDP-glucose synthase (ChryD, 355 aa, SSEG_09374, 78%/90%) and an NDP-4,6-dehydratase (ChryE, 328 aa; SSDG_01263 77%/84%), respectively. It is believed that these two enzymes are responsible for the first two transformation steps from D-glucose-1-phosphate (**30**) to NDP-D-glucose (**31**) to NDP-4-keto-6-deoxy-D-glucose (**32**) (**Figure 20**). Very often, the genes encoding these two enzymes are translationally coupled; however, in some clusters, these genes are located in another chromosomal locus, far-removed from the antibiotic biosynthetic genes. For example, the elloramycin producer *Streptomyces olivaceus* clusters the 8-demethyl tetracenomycin C antibiotic genes in a separate chromosomal locus from the *rhaABCD* genes necessary to supply NDP-L-rhamnose (*126*). *ChryCMT* (411 aa, PCZA361 61%/72%) and *chryU* (Acel_0416 46%/55%) are clustered together and encode a putative *C*-methyltransferase and a truncated 4-ketoreductase, respectively. ChryCMT is predicted to use a SAM cofactor, and ChryU could be an NAD(P)H-dependent ketoreductase enzyme. ChryCMT and ChryU could potentially catalyze the last two transformations of **32** to a 3-*C*-methylated ketosugar, **95**, and ChryU could potentially reduce **95** to an axial 4-OH, to yield NDP-D-virenose. The assignments of the

enzyme functions encoded by these genes and their cloning into overexpression vectors will be covered in **Chapter 3**.

ChryGT (379 aa, GilGT, 44%/62%) encodes the only candidate glycosyltransferase in the *chry* cluster. It is hypothesized to use **96** as the donor substrate to transfer D-virenose the polyketide acceptor substrate, which at this point remains a hypothesized intermediate. The mechanism for direct *C*-glycosylation of the chrysomycin chromophore is anticipated to involve the phenolic 1-OH group, but an additional Fries-like rearrangement has also been postulated (*56*). However, *chryGT* potentially encodes a valuable C-GT for pathway engineering. For example, *chryGT* could be placed under the strong *ermE** promotion and subsequently integrated into the chromosome of the *S. lividans* (cosG9B3-gilGT$^-$) genome for interrogation with foreign deoxysugar donor substrates. These could easily be supplied as plasmid-borne sugar "cassettes" over-expressing deoxysugar biosynthetic enzymes from exogenous hosts.

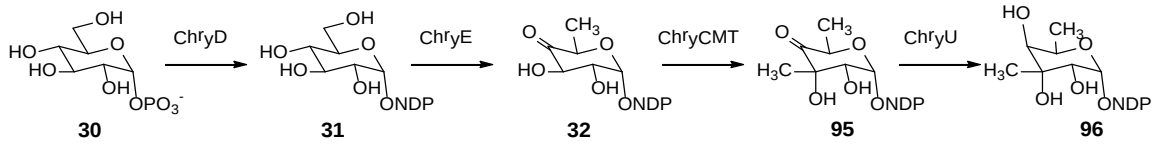

Figure 20 Hypothesized biosynthetic route to NDP-D-virenose (**96**).
ChryD catalyzes 1-phosphonucleotide transfer to D-glucose-1-phosphate (**30**). ChryE catalyzes 4-oxidation and 6-reduction of NDP-D-glucose (**31**) to afford NDP-4-keto-6-deoxy-D-glucose (**32**). ChryCMT catalyzes 3-*C*-methyltransfer to **32** to afford NDP-4-keto-D-virenose (**95**), and ChryU catalyzes 4-ketoreduction of **95** to afford NDP-D-virenose (**96**).

ORFs	Size[a]	ID/SM (%)[b]	Origin	Nucleotide accession no.	Proposed function
chryX	149	84/89	*S. griseoflavus* Tu 4000	ZP_05536903	Spore-associated protein precursor
chryF	261	71/83	fabG, *S. echinatus*	ABL09955	Ketoreductase
chryV	110	31/52	GilV, *S. griseoflavus*	ABE03981	Hypothetical Protein
chryH	189	62/73	*Kribbella flavida* DSM 17836	ZP_03859638	Oxidoreductase/NADH-dependent FMN Reductase
chryOI	513	59/70	PgaE, *Streptomyces sp*. PGA64	2QA1_A	FAD-Dependent Monooxygenase
chryG	109	70/83	OvmC, *S. antibioticus*	CAG14964	Cyclase
chryC1	83	58/71	SimA3, *S. antibioticus*	AAL15582	Acyl Carrier Protein
chryK	314	61/71	Tfu_1222, *Thermobifida fusca* YX	YP_289283	Bifunctional Cyclase/Dehydratase
chryOIV	491	55/63	OvmOII, *S. antibioticus*	CAG14970	FAD-Dependent Monooxygenase
chryA	422	79/87	Pd2A, *Streptomyces sp*. WP 4669	AAO65362	Ketoacyl Synthase (KSα)
chryB	402	70/82	UrdB, *S. fradiae*	CAA60570	Chain Length Factor (KSβ)
chryC	120	60/70	Acp, *S. venezuelae*	AAB36564	Acyl Carrier Protein
chryOIII	394	71/80	GilOIII, *S. griseoflavus*	AAP69584	Cytochrome P-450 Monooxygenase
chryY	62	44/62	FdxD, *Mycobacterium tuberculosis* H37rv	NP_218020	Ferredoxin
chryP	322	49/63	PgaH, *Streptomyces sp*. PGA64	AAK57533	Malonyl-CoA Carrier Protein Transacylase
chryQ	327	49/58	AknF, *S. galileus*	AAF70110	Propionyl-CoA Carrier Protein Transacylase
chryX1	265	38/50	AurIO, *S. aureofaciens*	AAK59995	Regulator
chryX2	201	56/72	Gra-orf10, S. *violaceoruber*	CAA09631	Two-Component Response Regulator
chryE	328	77/84	SSDG_01263, S. *pristinaespiralis* ATCC 25486	YP_002200633	TDP-glucose-4,6-dehydratase
chryD	355	78/90	SSEG_09374, *S. sviceus* ATCC 29083	YP_002205669	Glucose-1-phosphate thymidylyltransferase

chryJ	623	78/87	SGR_4823, *S. griseus* subsp. *griseus* NBRC 13350	YP_001826335	Major facilitator superfamily permease
chryX3	293	71/82	*SGR*_4824, *S. griseus* subsp. *griseus* NBRC 13350	YP_001826336	MarR family transcriptional regulator
chryGT	379	44/62	GilGT, *S. griseoflavus*	AAP69578	*C*-glycosyltransferase
chryMT	340	49/63	MetLA1, *S. tubercidicus*	AAT45282	*O*-methyltransferase
chryOII	236	65/76	GilOII, S. *griseoflavus*	AAP69583	Anthrone Monooxygenase
chryRM	761	52/67; 41/58	ORF 22, *S. echinatus*/GilM, *S. griseoflavus*	ABL09969/ AAP69591	Oxidoreductase/ Methyltransferase
chryU	302	46/55	Acel_0416, *Acidothermus cellulolyticus* 11B	YP_872176	TDP-4-dehydrorhamnose ketoreductase
chryCMT	411	61/72	PCZA361, *Amycolatopsis orientalis*	CAA11777	*C*-methyltransferase
chryHK	309	61/75	Tfu_1012, *Thermobifida fusca* YX	YP_289073	Hexokinase
chryL	210	37/50	GilL, *S. Griseoflavus*	AAP69590	NAD-dependent epimerase/dehydratase
chryX4	135	70/82	SGR_2879, *S. griseus* subsp. *griseus* NBRC 13350	YP_001824391	TetR Family transcriptional regulator
chryX5	120	61/74	SC2H2.18, *S. coelicolor* A3(2)	NP_631661	Hypothetical Protein
chryX6	202	78/83	SGR_429, *S. griseus* subsp. *griseus* NBRC 13350	YP_001821941	TetR Family transcriptional regulator
chryX7	545	83/89	SSDG_02680, *S. pristinaespiralis* ATCC 25486	YP_002198950	Acyl-CoA Dehydrogenase
chryX8	129	61/68	SCD31.02c, *S. coelicolor* A3(2)	NP_628836	Regulatory Protein
chryX9	155	62/79	Caul_2306, *Caulobacter* sp. K31	YP_001683931	TetR Family transcriptional regulator

[a]: number of amino acids; [b]: identity/similarity

Figure 21 Table of proposed chrysomycin ORFs, predicted functions of their producers, and identity/similarity scores among closest homologues.

Attempts at heterologous expression and inactivation of chrysomycin biosynthetic genes

In order to prove the role of the *chry* cluster in production of chrysomycin, heterologous expression experiments of the various cosmids encoding chrysomycin biosynthetic genes were undertaken. Chry1-1 and CosChryF2 were chosen for heterologous expression in *Streptomyces lividans*, because they contained the greatest portion of the *chry* cluster genes as determined by restriction analysis. *Streptomyces lividans* TK 24 is a preferred transformation host because of its genetic pliability, and because under normal conditions it fails to express antibiotic biosynthetic genes, making it effectively "background neutral" (*3*). The cosmids were transformed into *S. lividans* TK 24 by a well-characterized conjugation protocol between a special *E. coli* host and *Streptomyces lividans* (See Materials and Methods) (*3*). Exconjugants were fermented for 4-5 days, and methanolic extracts were chromatographed *via* HPLC/MS to evaluate the production of chrysomycin-related metabolites (See Materials and Methods). Expression of cosChry1-1 or cosChryF2 in *S. lividans* failed to result in the production of metabolites with the characteristic chromophore of angucycline or gilvocarcin-related compounds when compared to extracts of *S. lividans* (pOJ446) as a negative control. Because *chryABCFGKP* were present on cosChryF2, at least rabelomycin or UWM6 should have been accumulated in the *S. lividans* (cosChryF2) strain. The lack of accumulated metabolites likely resulted from poor cosmid expression or missing/dysfunctional regulators necessary for chrysomycin biosynthesis.

As an alternative, classical inactivation experiments were envisioned for disruption of the *chryA* and *chryCMT* genes. Inactivation of *chryA* would result in a non-producing mutant and inactivation of *chryCMT* was anticipated to disrupt NDP-D-virenose biosynthesis, and depending on the substrate flexibility of ChryGT, would result in a novel gilvocarcin with a *C*-glycosidically linked pyranose moiety. *ChryA* and *chryCMT* were cloned into pKC1139, which is an RK2-derived vector that is used for gene deletion experiments in *Streptomyces*. pKC1139 features a temperature-sensitive replicon that prevents it from replicating autonomously, so any surviving Apr^R transformants must be single-crossover mutants (*3*). A thiostrepton resistance cassette was cloned and inserted into unique restriction sites in the middle of *chryA* and *chryCMT*

(*Xma*I for *chryA* and *Bgl*II in *chryCMT*) (See Materials and Methods). The resulting constructs, pKC1139-*chryCMT* and pKC1139-*chryA*, were unable to be transformed into *S. albaduncus via* protoplast transformation, electroporation, and conjugation procedures. *S. albaduncus* may simply be recalcitrant to genetic manipulation due to a severe restriction system.

Cross complementations using chrysomycin oxygenases

In order to prove the chrysomycin biosynthetic gene cluster was responsible for biosynthesis of **42**, when inactivation experiments and heterologous expression of the chrysomycin cluster were not feasible, *in vivo* cross-complementation experiments were envisioned using *chry* biosynthetic genes and gilvocarcin blocked mutants. For this, the four *chry* monooxygenases were selected for overexpression, because they are crucial for the 12-position hydroxylation, C5-C6 bond cleavage, and installation of the 8-vinyl side chain, steps that are unmistakably characteristic for the biosynthesis of the chrysomycin chromophore. *ChryOI*, *chryOII*, *chryOIII*, and *chryOIV* were cloned into pEM4 under the strong, constitutive *ermE** promoter (see Materials and Methods). The resulting constructs, pChryOI, pChryOII, pChryOIII, pChryOIV were transformed into gilvocarcin mutants deficient in the oxygenases GilOI, GilOII, GilOIII, and GilOIV respectively.

When pChryOI was transformed into *S. lividans* TK 24 (cosG9B3/GilOI$^-$), for unexplained reasons, the resulting transformant neither produced gilvocarcin (**39)**, as expected, nor even prejadomycins (**58**) or (**59**), as are typically accumulated in the *gilOI*-deleted strain. This is likely explained by poor host utilization of the cosG9B3-GilOI$^-$ cosmid. The *S. lividans* TK 24 (cosG9B3/GilOIV$^-$)/pChryOIV strain successfully restored production of gilvocarcin biosynthesis, producing **39** and **40** (see **Figure 22**). Because *chryOIV* and *chryOI* both encode FAD-dependent monooxygenases and are quite similar to each other, it could be possible that ChryOIV might actually be the GilOI-homologue, or it may be able to catalyze both 2,3-dehydration and 4a,12b-dehydration steps. Therefore, pChryOIV was cross-complemented into the *S. lividans* TK 24 (cosG9B3/GilOI$^-$) mutant. The resulting transformant failed to recapitulate gilvocarcin biosynthesis, indicating that ChryOIV is responsible for 2,3-dehydration in chrysomycin biosynthesis (see **Figure 22**).

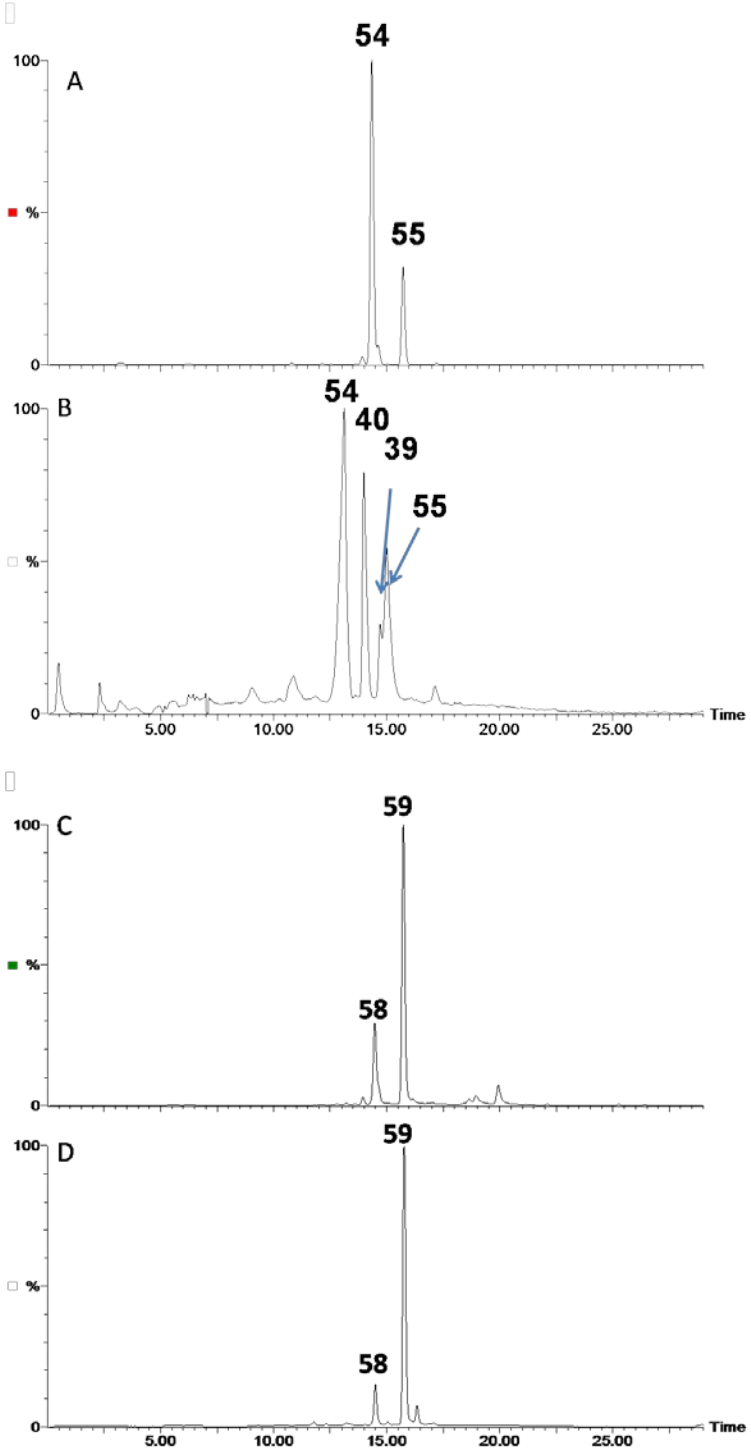

Figure 22 HPLC chromatograms of pChryOIV complementations
A) *S. lividans* (cosG9B3-GilOIV$^-$) extract- rabelomycin (**54)** (R_t=13.0 min^{-1}) and homorabelomycin (**55)** (R_t=14.9 min^{-1}). **B)** *S. lividans* (cosG9B3-GilOIV$^-$)/pChryOIV extract- gilvocarcin M (**40)** (R_t=14.2 min^{-1}) and gilvocarcin V (**39**) (R_t=14.7 min^{-1}). **C)** *S. lividans* (cosG9B3-GilOI$^-$) extract-prejadomycin (**58**) (R_t=14.5 min^{-1}) and homo-prejadomycin (R_t=15.8 min^{-1})**D)** *S. lividans* (cosG9B3-GilOI$^-$)/pChryOIV extract.

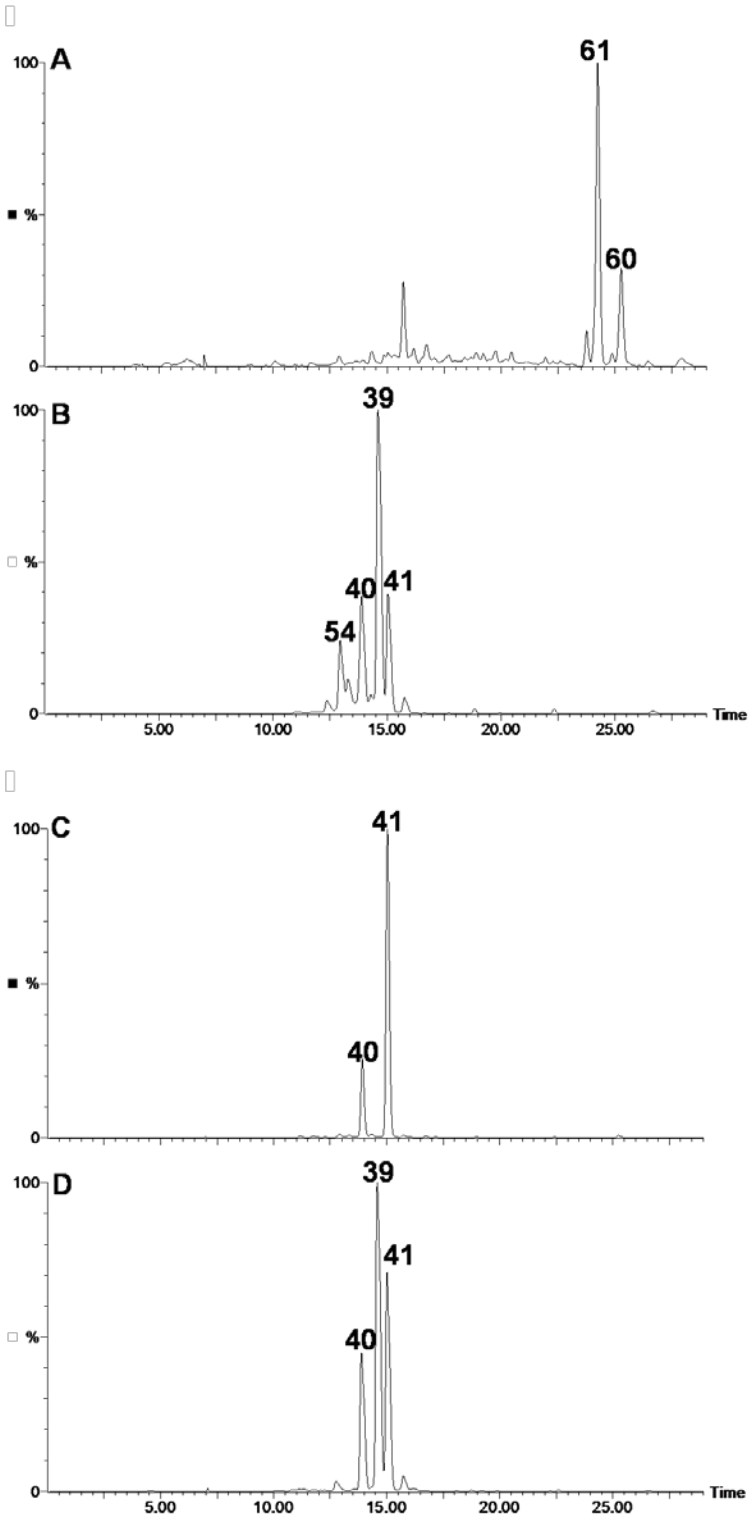

Figure 23 HPLC chromatograms of pChryOII and pChryOIII chromatograms. **A)** *S. lividans* (cosG9B3-GilOII$^-$) extract-dehydrorabelomycin V **(61)** (R_t=24.3 min^{-1}) and dehydrorabelomycin E **(60)** (R_t= 25.3 min^{-1}). **B)** *S. lividans* (cosG9B3-GilOII$^-$)/pChryOII extract- gilvocarcin M (**40)** (R_t=14.2 min^{-1}), gilvocarcin V (**39**) (R_t=14.7 min^{-1}), gilvocarcin E (**41**) (R_t= 15.0 min.$^{-1}$), rabelomycin (**54**) (R_t=13.0 min^{-1}) **C)** *S. lividans*

(cosG9B3-GilOIII$^-$) extract- gilvocarcin M (**40)** (R_t=14.2 min^{-1}) gilvocarcin E (**41**) (R_t= 15.0 min.$^{-1}$) **D)** *S. lividans* (cosG9B3-GilOIII$^-$)/pChryOIII extract- gilvocarcin M (**40)** (R_t=14.2 min^{-1}), gilvocarcin V (**39**) (R_t=14.7 min^{-1}), and gilvocarcin E (**41**) (R_t= 15.0 min.$^{-1}$) .

The failure of pChryOIV to completely restore gilvocarcin production probably indicates that ChryOIV is not a perfect fit with GilOI and/or GilOII in the hypothetical multi-oxygenase complex, and therefore, some of the pathway continues towards unproductive accumulation of shunt rabelomycins.

Both pChryOIII and pChryOII completely restored production of **39** and **40** **(Figure 23)**, which indicates that ChryOIII is responsible for installation of the 8-vinyl side chain, likely through hydroxylation and spontaneous dehydration at 1"-position of the ethyl side chain of a still undetermined pathway intermediate. Simultaneously, this experiment also indicates that ChryOII is capable of functioning in a surrogate capacity when GilOII is not present in the oxygenase cascade. However, the presence of rabelomycin indicates that some UWM6 is incompletely converted in this complementation strain. Furthermore, the presence of gilvocarcin E, **41**, may be explained by an incomplete activity of GilOIII in this strain. In the GilOII-deleted strain, both dehydrorabelomycin E and V are accumulated, which may indicate that GilOIII acts on a hydroquinone intermediate. This result suggests that ChryOII is involved in the C5-C6 carbon-carbon bond cleavage reaction, however, the mechanism by which it acts is elusive.

SUMMARY

The chrysomycin biosynthetic gene cluster was cloned successfully onto four cosmids that spanned 34,654 nucleotides and possessed 35 open reading frames pertinent to biosynthesis of chrysomycin A. The involvement of the chrysomycin biosynthetic gene cluster in biosynthesis of chrysomycin was successfully demonstrated by heterologous complementation of the GilOII-, GilOIII-, and GilOIV-deleted mutants of the gilvocarcin pathway by expression constructs pChryOII, pChryOIII, and pChryOIV in these pathways. As a result, the *chry* cluster affords novel genes for expression in other pathways, such as *chryGT*, which is likely responsible for the 4-*C*-glycosylation of

the chrysomycin chromophore. Furthermore, the identification of NDP-D-virenose biosynthetic genes is intriguing for further heterologous expression experiments to characterize the encoded products of *chryD*, *chryE*, *chryCMT*, *chryU*, and possibly *chryL*.

EXPERIMENTAL

DNA Isolation, Subcloning, and cloning of plasmids

For general cloning conditions, the protocols in Sambrook and Russel were followed with regards to introduction of DNA into *E. coli*. For isolation of plasmid DNA, the Fermentas GeneJET MiniPrep spin columns were used as per the manufacturer's protocol. For isolation of DNA fragments from electrophoresis gels, the QIA QG buffer (Qiagen, California) was used for extracting DNA from gel fragments. High fidelity *pfu* DNA polymerase was used to generate PCR fragments *via* the following program (Hot start, 1 cycle @ 96 °C for 3 minutes, 30 cycles- 94 °C for 30 seconds, lowest Tm-5 °C for 1 minute, 72 °C @ 1 min/1kb amplified DNA, 1 cycle 3 minutes @ 72 °C). PCR fragments were ligated into PCR-Blunt-IITOPO vector (Invitrogen). For cloning pChryOI, pChryOII, pChryOIII, pChryOIV the corresponding oxygenase genes *chryOI*, *chryOII*, *chryOIII*, and *chryOIV* were amplified from cosChry1-1 cosmid DNA, cloned into TOPO vector, then cut with *Xba*I/*Eco*RI and ligated into the exact sites of pEM4 to give the expression vectors. For cloning pKC1139-*chryA* and pKC1139-*chryCMT*, a ~3kb *chryA* or *chryCMT* fragment was ligated into the *Eco*RI/*Hind*III sites of pKC1139 vector. A thiostrepton resistance gene, *tsr*, was amplified from pEM4 and ligated into into a unique restriction marker in the middle of the target gene for inactivation (*chryA*- *Xma*I, *chryCMT*- *Bgl*II). Plasmids used in this study are summarized in Table 2.1. Primers used in this study are summarized in Table 2.3.

Table 1 Plasmids used in Chapter 2

Plasmid Name	**Relevant Characteristics**	**Reference**
pOJ446	*Streptomyces-E. coli* shuttle vector for cosmid library generation	(*127*)
cosChry1-1	Partial chrysomycin cluster cloned into pOJ446	This work
cosChryF1	Partial chrysomycin cluster cloned into pOJ446	This work
cosChryF2	Partial chrysomycin cluster cloned into pOJ446	This work
cosChryF3	Partial chrysomycin cluster cloned into pOJ446	This work
pEM4	*E. coli-Streptomyces* shuttle plasmid that contains *ermE** for the expression of genes in *Streptomyces*	(*128*)
pChryOI	*chryOI* cloned into pEM4	This work
pChryOII	*chryOII* cloned into pEM4	This work
pChryOIII	*chryOIII* cloned into pEM4	This work
pChryOIV	*chryOIV* cloned into pEM4	This work
PCR-Blunt-TOPO-II	Clone blunt PCR products	Invitrogen

Bacterial strains and culture conditions

Streptomyces albaduncus AD819 and *Streptomyces lividans* TK 24, and *S. lividans* TK 24 (cosG9B3) and derivative strains were routinely cultivated and maintained on M2 agarose plates (1.5% agar, 0.4% glucose, 1% malt extract, 0.4% yeast extract, and 0.1% $CaCO_3$). For production of spores, *S. lividans* TK 24 was grown on M2 agar for 5-6 days until the production of white-grey spores was visible on top of the mycelia, which were harvested by scraping with a toothpick then deposited in a sterile 1.5 mL Eppendorf-style tube, which were then immediately used for conjugation (see Introduction of *chry* cosmids into *Streptomyces lividans via* Conjugation). For production of metabolites, *S. albaduncus* or recombinant *S. lividans* (cosG9B3) and derivative strains were grown in liquid SG medium (See Production and Isolation of Gilvocarcin-related metabolites).

For growth in liquid medium to prepare protoplasts or for genomic DNA, *S. albaduncus* or *S. lividans* TK 24 were grown in 100 mL YEME media (0.3% yeast extract, 0.5% bacto-peptone, 0.3% malt extract, 1% glucose, 10.3% sucrose, 1L) for 3-4 days at 28 °C in an orbital shaker (250 RPM). For protoplasts, 200μL $MgCl_2$ (2.5M) and 2.5 mL Glycine (20%) were added to each 100 mL flask. Protoplasts were regenerated on R2YE agar (10.3% sucrose, K_2SO_4 0.25 g/L, $MgCl_2$ 10.12 g/L, Glucose 1%, Casaminoacids 0.1 g/L, Yeast extract 5 g/L, agar 15 g) (added to the solution after autoclaving: KH_2PO_4 10 mL (0.5%), $CaCl_2$ 80 mL (3.68%), L-proline 15 mL (20%), TES Buffer 100 mL (5.73%, adjusted to pH 7.2), Trace elements 2 mL, NaOH 5 mL (1N)). All solutions were sterilized by autoclaving before usage.

Escherichia coli XL1 blue MRF cells (Stratagene) were used for routine cloning procedures and propagation of plasmids and cosmid DNA. *E. coli* strains were grown in lysogeny broth (LB) or LB agar containing appropriate antibiotics to select for recombinant plasmids: (kanamycin 50 μg/mL; chloramphenicol 25 μg/mL; apramycin 50 μg/mL, and ampicillin 100 μg/mL) whenever necessary at 37 °C (in an orbital shaker, 250 RPM for liquid cultures). *E. coli* ET12567/pUZ8002 was used as a demethylating strain for conjugation with *Streptomyces sp*.. *S. albaduncus* was used as a source of genomic DNA. Strains generated and used in this study are summarized in Table 2.2.

Table 2 Bacterial strains used in Chapter 2

Strain Name	**Relevant Characteristics**	**Reference**
E. coli XL1-Blue-MRF	Host for routine cloning work and genomic library construction	Stratagene
E. coli ET12567/pUZ8002	Host for conjugal transfer of plasmids into *Streptomyces*	(*129*)
Streptomyces albaduncus	Chrysomycin wildtype producer	(*59*)
Streptomyces lividans TK 24	Streptomyces host	(*3*)
S. lividans (cosG9B3-GilOI-)	Produces **56-59**. *S. lividans* with cosG9B3-GilOI deleted cosmid.	(*130*)
S. lividans (cosG9B3-	Produces **56-59**. pChryOIV	This work

GilOI-)/pChryOIV	transformed into previous strain	
S. lividans (cosG9B3-GilOII-)	Produces **60, 61**. *S. lividans* with cosG9B3-GilOII deleted cosmid.	(*68*)
S. lividans (cosG9B3-GilOII-)/pChryOII	Produces **39-41, 55**. pChryOII transformed into previous strain.	This work
S. lividans (cosG9B3-GilOIII-)	Produces **39, 41**. *S. lividans* with cosG9B3-GilOIII-deleted cosmid.	(*70*)
S. lividans (cosG9B3-GilOIII-)/pChryOIII	Produces **39, 40**. pChryOIII transformed into previous strain.	This work
S. lividans (cosG9B3-GilOIV-)	Produces **54**, **55**. *S. lividans* with cosG9B3-GilOIV-deleted cosmid.	**(*130*)**
S. lividans (cosG9B3-GilOIV-)/pChryOIV	Produces **39, 40**. pChryOIV transformed into previous strain.	This work.

Table 3 Oligonucleotide Primers used in Chapter 2

Primer Name	**Oligonucleotide Sequence**
chryOI_for	5’- CTGGTCTCTAGAGCTGGAGCCGGTCCGCCG AGGAGGGCG -3’
chryOI_rev	5’- ATGTGCGAATTCGTCGGCCGGGACCGCACG-3’
chryOII_for	5’-ATTCTAGACCACCCGTACCGAGCCAC-3’
chryOII_rev	5’-ATGAATTCCCCGTCGTCCGCCGCGCG-3’
chryOIII_for	5’-ATTCTAGAGACCCGTTCCCGCAGCTC-3’
chryOIII_rev	5’-ATGAATTCGAACACGAAGGCTGTCGT-3’
chryOIV_for	5’-GCGGTTCTAGACCGCGCGCACCGGCTGCCCGGG-3’
chryOIV_rev	5’-CCGGTGAATTCACAGGAATCCGATGGCGGT-3’
chryA_ina_for	5’-CGCGAATTCCGACGCCGTACGGGAGCTGCT-3’
chryA_ina_rev	5’-CCAAAGCTTCCGTCCCGGCCGCCGGCCTGC -3’
chryCMT_in_for	5’-CGGAAGCTTTCGTCAACGCCGCCGT-3’
chryCMT_in_rev	5’-GGCGCGAATTCGGGCGGCGAGGTC-3’
Tsr_for	5’- CAGCCCGGGAGATCTTGATAAGGCGAATACTT CATATG -3’
Tsr_rev	5’- TCGCCCGGGAGATCTGTGATCATCACTGACGAA TCGAGGTCGAGGAAC -3’
chryF_probe_for	5’-GCCCTVGTSACSGGNGGNACCAGY-3’
chryF_probe_rev	5’-GTTGCCVAGNCCGCCGCASACGTT-3’
KS_probe_for	5’-GTSTCSACSGGSTGYACSTCSGGS-3’

KS_probe_rev	5’-SCCGATSGCSCCSAGSGARTGSCC-3’
DH_probe_for	5’-CSGGSGSSGCSGGSTTCATSGG-3’
DH_probe_rev	5’-CAGTGGTCSACGTGSAGCCACTCSCG-3’

Construction and Screening of *S. albaduncus* Genomic Library

Genomic DNA of *S. albaduncus* was isolated following standard protocol (*3*). The genomic DNA was partially digested with *Sau*3AI, dephosphorylated with calf intestinal phosphatase (CIP) and ligated to pOJ446 vector digested with *Bam*HI and *Hpa*I. The ligation sample was transduced into *E. coli* XL1-Blue MRF using Gigapack III XL packaging extract (Stratagene). A titering of 2300 colonies was obtained for the library. Two sets of degenerate primers (a standard KS-probe-for and KS-probe-rev, and a newly designed DH-probe-for and DH-probe-rev) were used to amplify the internal nucleotide sequences of ketoacyl synthase (KSα) and NDP-D-glucose-4,6-dehydratase from the genomic DNA of *S. albaduncus*. The amplified KSα fragment was labeled with DIG and used to screen positive colonies. The positive colonies were further screened with the NDP-D-glucose-4,6-dehydratase probe. Colony hybridization and southern blot analyses revealed three cosmid clones for *S. albaduncus* genomic libraries. A probe suited to detect a type II PKS-associated ketoreductase gene (gilF homologue) was also constructed (chryF_probe_for and chryF_probe_rev) to probe for cosmids that contained chryF. Three positively hybridizing colonies yielded cosmids cosChryF1, cosChryF2, and cosChryF3. CosChryF2 demonstrated the most overlap with cosChry1–1 according to the restriction analysis map. Thus, cosmids cosChry1–1 and cosChryF2 were selected for sequencing.

Sequencing and annotation of the *chry* cluster

Sequencing of the cosmids was carried out involving a standard shotgun approach using the HyperMu™ MuA Transposase kit (Epicentre) following the reported protocol used by the sequencing facilities of the Advanced Genetic Technologies Center (AGTC) located in the College of Agricultural Sciences of the University of Kentucky (http://www.uky.edu/Centers/AGTC/). Phred/Phrap/Consed software package (http://www.phrap.org.) was used to process and assemble raw sequence data into larger

contigs. The small gaps between contigs were filled by primer walking. Frame plot (http://www.nih.go.jp/~jun/cgi-bin/frameplot.pl) and ORF finder (http://www.ncbi.nlm.nih.gov/projects/gorf/) were used to assign the open reading frames. Functional assignments of ORFs were performed through database comparison using BLASTX and BLASTN search tools on the server of the National Center for Biotechnology Information, Bethesda, Maryland, USA (http://www.ncbi.nlm.nih.gov).

Introduction of *chry* cosmids into *Streptomyces lividans via* Conjugation

Cosmid DNA was introduced into *S. lividans* TK 24 *via* conjugation with *E. coli* ET12567/pUZ8002 containing cosmids cosChry1-1and cosChryF2. The *E. coli* donor was grown overnight supplemented with kanamycin 50 μg/mL; chloramphenicol 25 μg/mL; apramycin 50 μg/mL in a 7 mL culture tube. The cells were centrifuged, washed twice with sterile LB, and resuspended in 500 μL of 2 x YT broth (1.6% tryptone, 1% yeast extract, and 0.5% NaCl (pH 7.0)). *S. lividans* TK 24 spores were taken from a 5-6 day old M2 agar plate, scraped into 500 μL 2 x YT broth, heat shocked at 50 °C, placed on ice for 5 minutes, and finally mixed with the *E. coli* donor cells. 200 μL aliquots were plated on MS agar plates (mannitol 20 g/L, soya flour 20g/L, agar 20g/L, 10mM final conc. $MgCl_2$) and incubated at 28 °C for 24 hours before being overlaid with apramycin (50 μg/mL) and nalidixic acid (100 μg/mL). Exconjugants were picked after 3-5 days of incubation at 28 °C.

Production and Isolation of Gilvocarcin-related metabolites

For production of gilvocarcin-related metabolites, a small chunk of spores from a 3-5 day old M2 agar plate of *S. albaduncus* or *S. lividans* TK 24 (cosG9B3)-derived strains was grown in 100 mL of Soytone-Glucose medium (Glucose 20 g/L, soy peptone 10g/L, $CaCO_3$ 2 g/L, $CoCl_2$ 1 mg/L) in a 250 mL baffled flask at 28 °C in an orbital shaker (250 RPM) . This culture was supplemented with apramycin (50 μg/mL) and/or thiostrepton (25 μg/mL) when appropriate. After 4-5 days, 25 mL of the culture was collected in a 50 mL Falcon-style centrifuge tube, extracted with 25 mL ethyl acetate, and centrifuged for 5 minutes at 3000 RPM. The EtOAc layer was pipetted off and collected in a round bottom flask (RBF) and the organic solvent was dried *in vacuo* under reduced

pressure conditions. The remaining yellow oil was dissolved in a small amount of methanol, filtered through a 0.2 μm syringe-driven filter, and subjected to HPLC/MS and UV-analyses. A linear gradient of acetonitrile and acidified water (solvent A = 0.1% formic acid in H_2O; solvent B = acetonitrile; 0–15 min 25% B to 100% B; 16–24 min 100% B; 25–26 min 100% to 25% B; 27–29 min 25% B) was used to separate compounds. A Symmetry C_{18} (4.6 250 mm, 5 μm) column was used for analytical scale separations. A flow rate of 0.5 mL/min was used for analytical scale separations. Micromass ZQ 2000 (Waters) equipped with HPLC (Waters alliance 2695 model) and photodiode array detector (Waters 2996) were used to analyze the compounds. Atmospheric pressure chemical ionization (APCI) and Electrospray ionization (ESI) probes were used to detect molecular ions.

CHAPTER 3: *IN VIVO* STUDIES AND CLONING OF DEOXYSUGAR CASSETTES DIRECTING BIOSYNTHESIS OF NDP-D-FUCOFURANOSE AND NDP-D-VIRENOSE

INTRODUCTION

NDP-D-fucofuranose and NDP-D-virenose serve as integral structural moieties in the activity of both gilvocarcin V (**39**) and chrysomycin A (**42**), respectively. Both are characterized by being 6-deoxygenated sugars distinctive tailoring steps: ring contraction to a furanose for NDP-D-fucofuranose and *C*-methylation for NDP-D-virenose (see **Figure 28**). These sugars are relatively scarce in nature: NDP-D-fucofuranose is a requisite component of *E. coli* O52 antigen, and NDP-D-virenose is present as a residue of *Coxiella burnetii* phase I lipopolysaccharide (*131-133*). As such, both NDP-D-virenose and NDP-D-fucofuranose both enhance the biological activity of these antigenic polysaccharides through their interactions with host immune systems. Beyond this, the L-configurated fucofuranose is a key component of hygromycin B, and the structure elucidation gilvocarcin V was the first example of a D-configurated fucofuranose (**Figure 24**). NDP-D-virenose is fairly unique among branched sugars, as most are 2'-deoxygenated, e.g. NDP-L-mycarose, NDP-D-mycarose, NDP-L-axenose, and NDP-L-chromose B (*134-136*) (**Figure 24**).

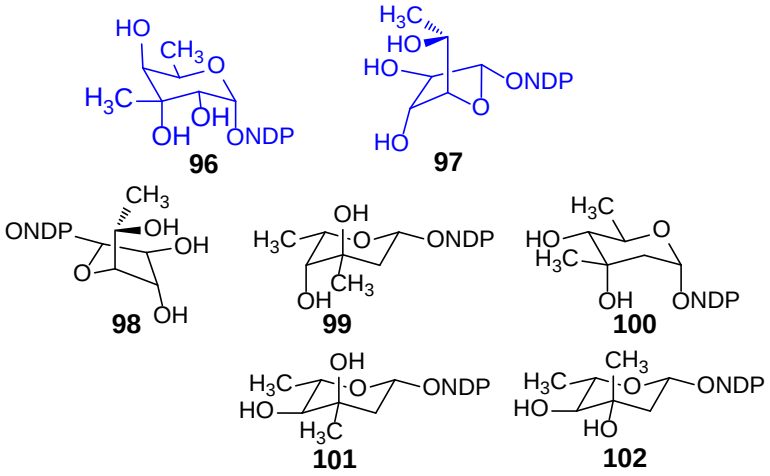

Figure 24 Structures of NDP-D-fucofuranose (**97**) and NDP-D-virenose (**96**). Compared to NDP-activated furanose (NDP-L-fucofuranose **98**) and branched pyranose (NDP-L-axenose (**99**), NDP-D-mycarose (**100**), NDP-L-mycarose (**101**), and NDP-L-chromose B (**102**)) sugars.

Common examples of branched sugar biosynthesis

The biosynthesis of branched-chain sugars involves specialized enzymes that attach one or two carbon unit extensions using *S*-adenosyl methionine or pyruvate as cofactors (*137*). Deoxysugars with single carbon extensions use *C*-methyltransferases that catalyze nucleophilic attack of a corresponding NDP-activated deoxysugar enolate to a $^{+}CH_3$ moiety of an enzymatically-bound *S*-adenosyl methionine cofactor (**Figure 25**). This *S*-adenosyl methionine can be positioned above or below the NDP-4'-keto species (*si*-face or *re*-face) which imparts the stereochemistry of the methyl group (**Figure 25**) (*137*). An example of *C*-methylation catalyzed by the product of *chryCMT* is indicated in **Figure 25.**

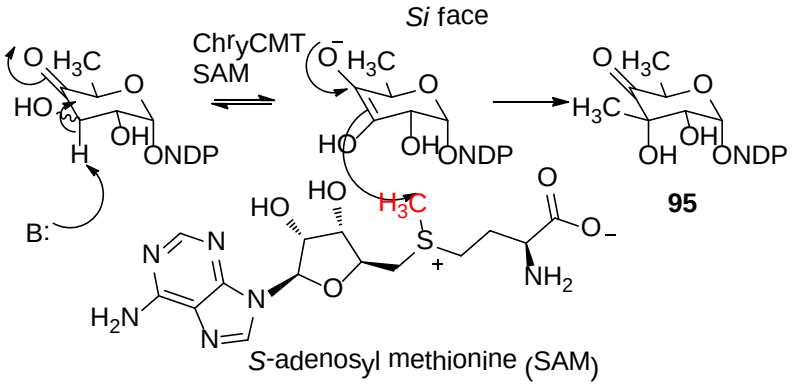

Figure 25 SAM-dependent *C*-methylation by ChryCMT of NDP-4-keto-6-deoxy-D-glucose to afford **95**.

Nature's strategies for catalyzing pyranose-furanose transformations

Furanoses are scarce in polyketide pathways, but along with pyranoses, the furanose conformation is energetically favored (*64*). The *C*-glycosidically linked D-fucofuranose of gilvocarcin V possesses all of the stereocenters of gilvocarcin, and it is believed to be essential for binding to histone H3 (*46, 64*). As such, identification of the enzymatic strategies that nature uses to contract pyranoses to furanose sugars, such as D-fucofuranose, merits some discussion. Primarily, most of the enzymes that are known to catalyze furanose ring contraction are mutases, such as UDP-galactose mutase. This enzyme catalyzes pyranose to furanose ring contraction of UDP-D-galactose in an FAD-dependent manner. (The crystal structure of *K. pneumoniae* UDP-galactose mutase was

crystallized with 2.25 Å resolution and bound flavin (FAD) by Beis *et al.*) (*138*) **(Figure 26)**. The UDP-galactose mutase from *Deinococcus radiodurans* was crystallized to 2.36 Å resolution with bound UDP-D-galactose by Partha *et al.* (*139*). The UDP-D-galactose substrate is stabilized through interactions of the FAD 4-position oxygen with the C4-hydroxyl of UDP-D-galactose, and several water molecules bond with conserved active site residues to correctly position the sugar substrate: His88, Arg364, Tyr371, Asn372, and His109 (*139*) (**Figure 26**).

These mutases are very similar with the recently characterized Fcf2, which catalyzes the identical pyranose to furanose ring contraction for NDP-D-fucopyranose to **97** (*131*). Fcf2, unlike the UDP-galactose mutase enzymes, catalyzes ring contraction in a cofactor-free manner (*131*). Furthermore, the 4-*C*-D-fucofuranose moiety of gilvocarcin has been shown to rearrange from a furanose to pyranose ring in an acid-catalyzed manner, without the presence of a specific enzyme (*140*). However, this results in a mixture of β- and α-connected fucopyranose moieties. The D-fucofuranose moiety of For *Streptomyces griseoflavus*, it might be plausible that the NDP-D-fucose to NDP-D-fucofuranose ring contraction might occur in an enzymatically controlled fashion. For the analogous reaction in *Escherichia coli*, it can be theorized that an internal basic amino acid in Fcf2 performs the same catalytic role that the enzymatically-bound FADH- plays in the galactose mutases. An amino acid residue could attack the anomeric carbon of NDP-D-fucose, thereby causing opening of the ring oxygen. An internal base could catalyze removal of the proton of 4-OH, therby allowing for a facile intramolecular attack of the 4-alkoxide onto the enzymatically bound anomeric center, affording **97** (**Figure 27**).

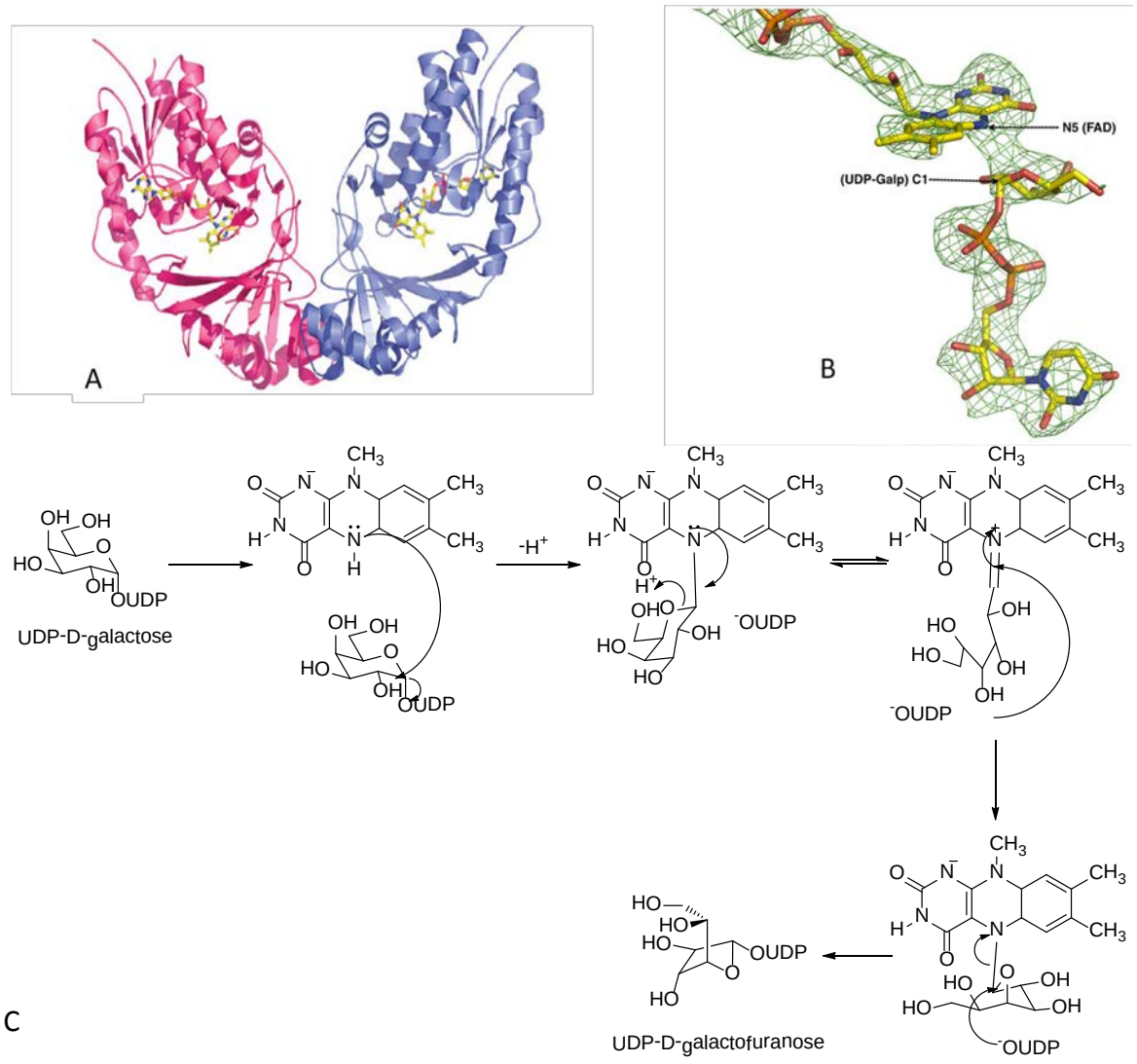

Figure 26 Crystal structures of pyranose-furanose contraction enzymes.
A) Crystal structure of UDP-galactose mutase from *K. pneumoniae* with bound FAD by Beis *et al*(*138*). . **B)** Crystal structure of UDP-galactose-mutase from *D. radiodurans* with bound UDP-galactose by Partha *et al*.(*139*). **C)** $FADH^-$ -dependent catalysis of UDP-D-galactose ring contraction mechanism.

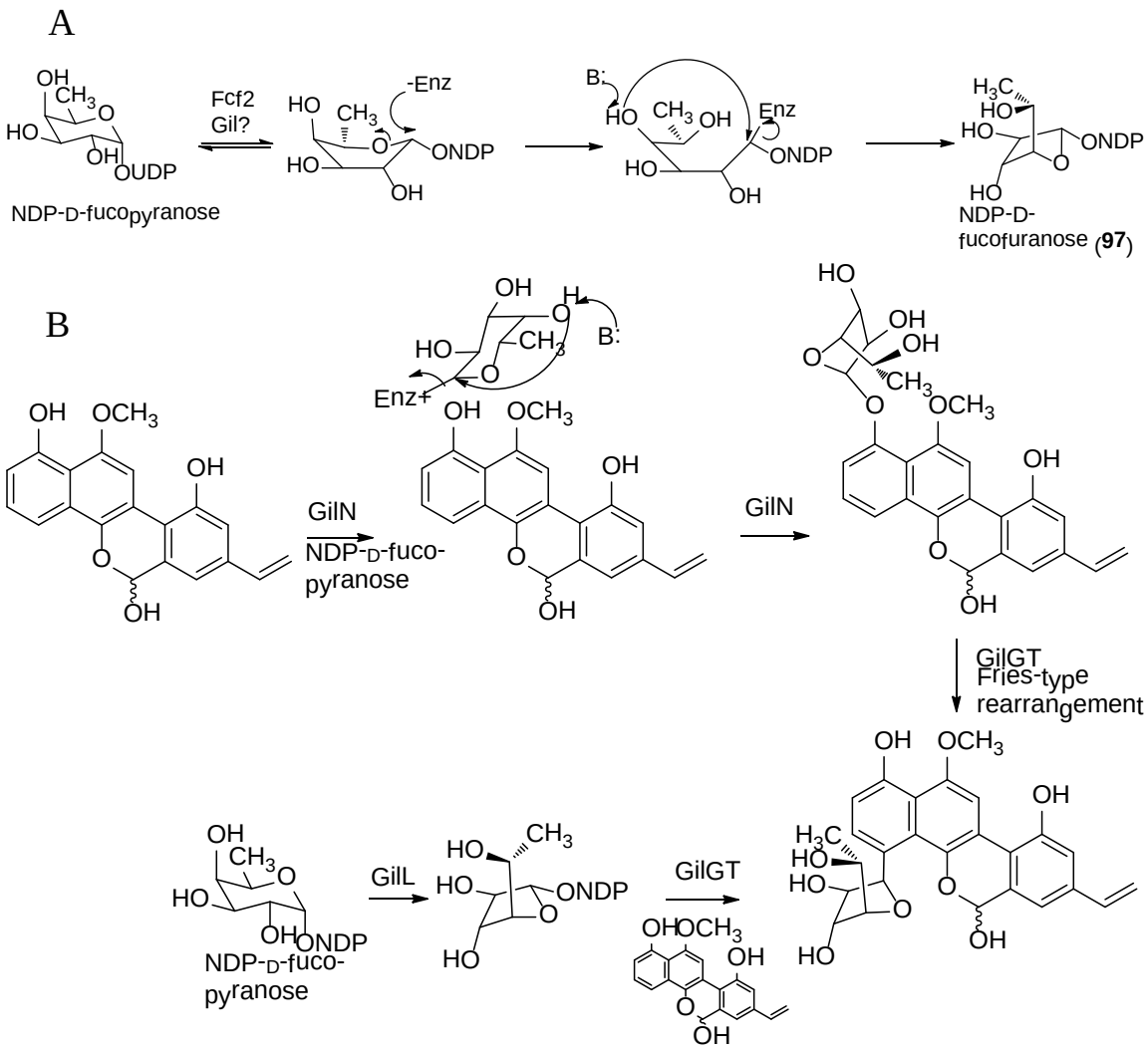

Figure 27 Routes to NDP-D-fucofuranose ring contraction.
A) Cofactor free catalysis of NDP-D-fucose ring contraction to NDP-D-fucofuranose (**97**) catalyzed by Fcf2 and unknown Gil enzyme. **B)** Suggested routes to NDP-D-fucofuranose ring contraction, as GilN- (glycosyltransferase) or GilL- (NAD-dependent epimerase/dehydratase)-mediated routes.

RESULTS AND DISCUSSION

Identification of gilL *and* gilN *candidate genes for NDP-D-fucofuranose biosynthesis*

In the gilvocarcin pathway, several candidate enzymes for biosynthesis of **97** were previously identified through bioinformatics analyses and inactivation experiments. *GilD* and *gilE* were identified as encoding the enzymes NDP-glucose synthase and NDP-4,6-dehydratase to catalyze transformation from D-glucose-1-phosphate (**30**) to NDP-D-glucose (**31**) and NDP-4-keto-6-deoxy-D-glucose (**32**), respectively (see **Figure 28**). GilU was demonstrated to be a truncated ketoreductase involved in 4'-ketoreduction of **32** to afford NDP-D-fucose **103** (See **Figure 28**). *GilU* was previously inactivated in cosG9B3 by Liu *et al.*, and heterologous expression of the mutagenized cosmid resulted in accumulation of 4'-hydroxygilvocarcins and defucogilvocarcins (*72*). Hydration of NDP-4-keto-6-deoxy-D-glucose (**32**) resulted in a substrate that closely resembled the putative NDP-D-fucose substrate of the ring contraction enzyme, and amazingly, both the ring contraction and the glycosyltransfer of the surrogate NDP-4-hydroxy-D-fucose sugar are carried out *in vivo*. The *gilU*-deleted mutant strain, *S. lividans* (cosG9B3-GilU$^-$), evinced important considerations about the deoxysugar biosynthesis of the D-fucofuranose moiety. The ring contraction enzyme and GilGT both demonstrate some substrate flexibility towards a foreign donor substrate. However, disruption of *gilU* caused detrimental downstream effects, in that unglycosylated defucogilvocarcins were predominantly accumulated in this strain. Also, this strain was successfully used by Shepherd, Liu *et al*. as a transformation host for flooding of the gilvocarcin pathway with foreign deoxysugars, effectively resulting in polycarcin (**53**) and 4-*C*-β-D-olivosyl gilvocarcin analogues (*119*).

The identity of the enzyme involved in ring contraction is currently unknown. The *gil* cluster does not contain any Fcf2/UDP-galactose mutase-type candidates for the contraction of NDP-D-fucose (**98**) to NDP-D-fucofuranose (**97**) (*131*). However, *gilL* and *gilN* are two candidate ORFs whose encoded products could potentially be involved in ring contraction of the sugar. **Figure 27** illustrates that *gilN* encodes a hypothetical 297 amino acid glycosyltransferase that could catalyze ring contraction of the sugar in the enzymatic pocket, then attach it to the 1-OH of the acceptor substrate. A subsequent

Fries-like rearrangement by GilGT might result in the anticipated C-4 glycosylation. Or, alternatively, the product of *gilL*, a putative 212 amino acid NAD-dependent epimerase/dehydratase (similar BLAST description to *gilU*), may represent a novel sugar ring-contraction enzyme. To clarify this question, both *gilN* and *gilL* had been previously inactivated, but the resulting cosmids cosG9B3-GilN$^-$ and cosG9B3-GilL$^-$ have not been successfully characterized through heterologous expression.

*Generation of a G9B3-*gilN- *and G9B3-*gilL- *deletion cosmids and heterologous expression*

Previous work by Carsten Fischer and Lili Zhu had resulted in cosG9B3-derived cosmids in which individual *gil* genes had been deleted *via* the PCR Redirect technology (see Materials and Methods, Chapter 3). The resulting cosmids cosG9B3-GilN$^-$ and cosG9B3-GilL$^-$ were introduced into *Streptomyces lividans via* a conjugation procedure between *S. lividans* and *E. coli* ET12567/pUZ8002 (see Materials and Methods, Chapter 2). Despite screening several

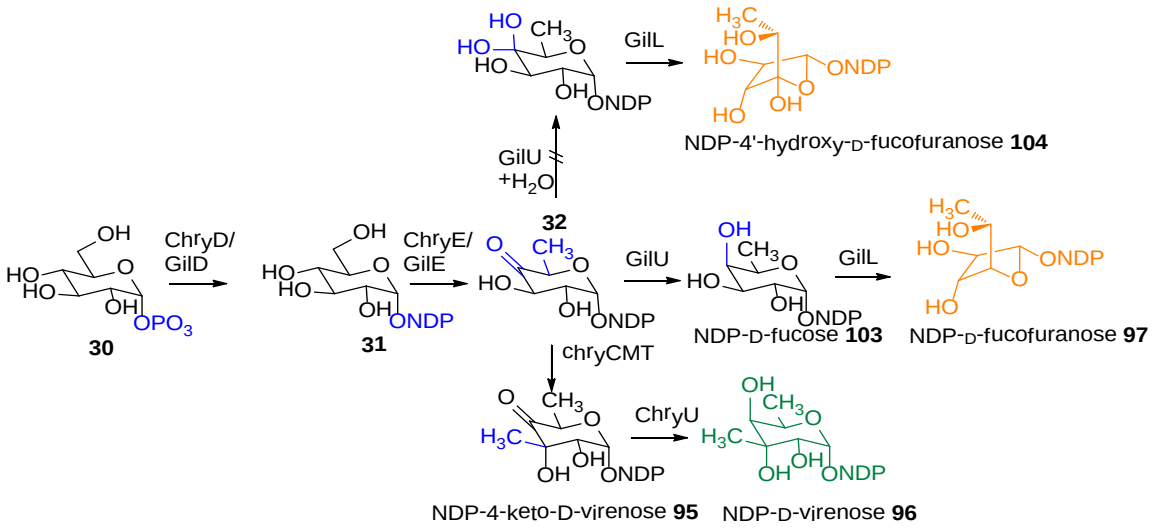

Figure 28 Biosynthetic pathways to NDP-D-fucofuranose and NDP-D-virenose.

transformants, *S. lividans* TK 24 (cosG9B3-GilL$^-$) exconjugants were fermented in SG media after 4-5 days and the methanolic extracts were chromatographed *via* HPLC/MS, there was no difference in the production spectrum as compared to extracts of control strain *S. lividans* TK 24 (pOJ446) with empty plasmid (See Materials and Methods, Chapter 2). Conjugation was repeated with *S. albus*, which has been noted to be an

optimal strain for heterologous production of antibiotic gene clusters as compared to *S. lividans*, so the conjugation protocol was repeated using *S. albus* as transformation host. Still, no heterologous expression of cosG9B3-GilL$^-$ could be achieved, likely owing to poor cosmid utilization by the *Streptomyces* spp. hosts.

S. lividans TK 24 (cosG9B3-GilN$^-$) was confirmed to lack a complete *gilN* gene by amplification of the ~200 base pair FLP scar *via* colony PCR (**Figure 29**). Exconjugants were fermented in 100 mL SG medium for 4-5 days, and methanolic extracts were chromatographed *via* HPLC/MS to visualize the production pattern. This strain was determined to be producing metabolites with a gilvocarcin chromophore. As a result, this strain was cultured in 5 liters of SG media to isolate enough of the metabolites for structural elucidation.

Structure determination of metabolites accumulated by S. lividans *TK 24 (cosG9B3-gilN-) strain*

Culturing of the *gilN*-deleted disruption strain encoding a putative glycosyltransferase revealed metabolites with gilvocarcin chromophores (See Materials and Methods, Chapter 3). Two metabolites with a gilvocarcin-type chromophore were identified at R_t= 14.65 min^{-1} and R_t= 15.30 min^{-1}, respectively. Low resolution ESI/MS revealed a peak of 481 *amu* (-)ESI-MS mode for the metabolite with R_t= 14.65 min^{-1} and a peak of 493 *amu* (-)ESI-MS mode for the metabolite with R_t= 15.30 min^{-1}. A minor product was identified with R_t=16.18 min^{-1}, and it was identified as homorabelomycin (**55**) *via* UV, mass, and identical retention time upon co-injection with standard homorabelomycin. The identities of these metabolites were assigned *via* mass, UV, and ^{1}H-NMR spectral analysis. Because the anticipated metabolites of the *gilN*-deleted mutant could have been structural isomers of **38** and **39** with *C*-glycosidically-linked pyranose sugars instead of D-fucofuranose, it was necessary to isolate enough of the compounds for structural elucidation.

The major compound was identified to be gilvocarcin V (**39**) based on identical retention time to **39** as determined by co-injection with standard gilovcarcin V, identical low resolution mass (493 *amu* [M-H] (-ve) mode), and analysis of the ^{1}H NMR-coupling constants of the sugar moiety (**Figure 30** and **Table 3.2**). The 1'-H signal appeared as a

doublet at δ 6.19 with *J*=5.5 Hz. The 2'-H (δ 4.67) and 3'-H (δ 3.86) both indicated an integration of one proton and a multiplet splitting pattern. This resembles the *trans*-axial splitting of the 2'-H and 3'-H signals of D-fucofuranose. Furthermore, the 4'-H appeared at δ 3.51 as a doublet of doublets with *J*= 4.2, 5.9 Hz, and 5'-H was at δ 3.86 with a multiplet splitting pattern. The 6'-CH_3 was at δ 1.24 as a doublet with *J*= 6.5 Hz. Because furanoses have a compact, "envelope" conformation, the coupling constants between their protons are less than 7 Hz. The rest of the ^{1}H-NMR signals corresponded to the chromophore of gilvocarcin V when compared to published spectral data. Furthermore, the yield of this metabolite was comparable to that of wildtype *S. griseoflavus* and *S. lividans* (cosG9B3) (yield ~11.0 mg/L), therefore GilN appears to be not involved in GV biosynthesis. Therefore, by process of elimination, it seems possible that *gilL* could encode a novel NAD-dependent epimerase/dehydratase enzyme involved in ring contraction of **103** to yield **97.**

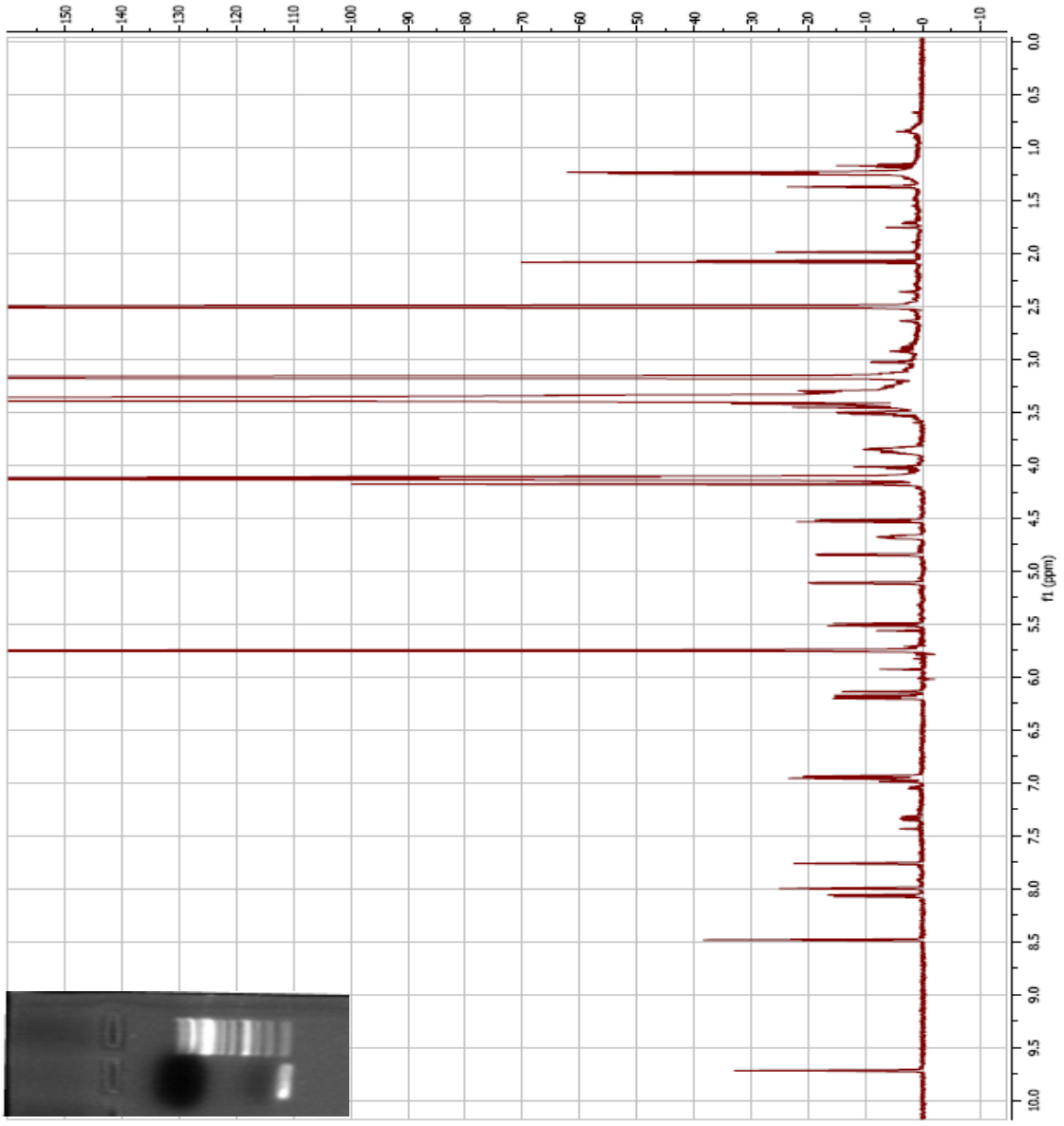

Figure 29 ^{1}H-NMR spectrum of gilvocarcin V isolated from S. lividans (cosG9B3-*gilN*-) (500 MHz).
Electrophoresis gel detailing colony PCR of ~200 base pair FLP scar from the *gilN*-mutant.

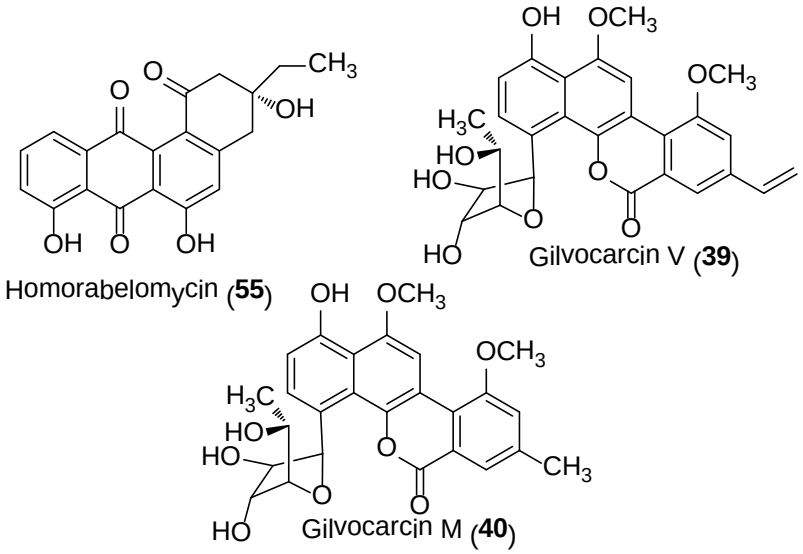

Figure 30 Structures of metabolites isolated from *S. lividans* (cosG9B3-*gilN*-).

The presence of *chryL* in the *chry* cluster might be more clear upon this hypothesis that *gilL* might encode a putative ring contraction enzyme. Obviously, *S. albaduncus* does not produce a *C*-glycosidically-linked furanose, but the Mercian strain that produces furanose compounds, Mer-1020 dA (**49**) and Mer-1020 dD (**52**), may employ a GilL/ChryL-like enzyme to ring contract the 4-keto-D-virenose moiety of the Mer-1020 dC and Mer-1020 dB compounds. Or, possibly, this occurs nonenzymatically and spontaneously.

Construction of NDP-D-fucofuranose and NDP-D-virenose and intermediate-synthesizing cassettes for in vivo interrogation of GTs

Previously, Salas *et al*. have demonstrated the ubiquity of cloning entire deoxysugar operons onto single plasmids for *in vivo* overexpression experiments (*39*). This approach has resulted in generation of novel tetracenomycins and steffimycins with altered glycosylation patterns (*141*). However, this approach has mostly focused on 2,6-dideoxygenated and 2,3,6-trideoxysugars, while only one construct exists with a 2'-hydroxysugar encoding L-rhamnose (pRHAM) (*39*). Therefore, constructs which can direct biosynthesis of NDP-D-virenose and NDP-D-fucofuranose might be useful for *in vivo* glycodiversification. To investigate the role of the various NDP-D-virenose biosynthetic genes in encoding biosynthesis of **96**, and to evaluate the role of *gilL* in ring

contraction of **97**, constructs were generated directing the biosynthesis of these sugars and their intermediates. For this, pUWL201PW and pEM4 were used for expression of entire or combinations of the deoxysugar biosynthetic pathways. Both pEM4 and pUWL201PW are *Streptomyces* spp. expression vectors that use the constitutive, strong *ermE** promoter to overexpress cloned genes (*128, 142*). For this, *chryCMT* was amplified upstream of its putative ribosomal binding site and cloned into pEM4, to yield pEN1. *ChryGT* was cloned into pEN1 to yield pEN2, and both of these constructs were introduced into the *S. lividans* TK 24 (cosG9B3-GilU$^-$) and *S. lividans* TK 24 (cosG9B3-GilGT$^-$) *via* protoplast transformation. The resulting transformants were screened for their production of novel gilvocarcin-related compounds, however, unfortunately no new metabolites were accumulated in these strains. This can be explained by the failure of GilGT to accept a branched sugar donor, or the failure of the pEN1 construct to encode a functional *C*-methyltransferase. Simultaneously, the failure of pEN2 may account for ChryGT's inability to accept five-membered sugar donors.

ChryGT was replaced by *chryU* in pEN2 to afford pEN3 for heterologous expression in other pathways with NDP-glucose synthase and NDP-4,6-dehydratase. Furthermore, a series of pUWL201PW constructs were prepared with an entire NDP-D-virenose pathway. pUWL201PW affords a couple advantages: several unique cloning sites for introduction of genes or combinations of genes, the aforementioned *ermE** promoter, and an optimized ribosomal binding site. First, *ravDE* were cloned into pUWL201PW in the *Pst*I/*Bam*HI sites to provide NDP-glucose synthase and NDP-4,6-dehydratase (construct pUWL-DE). *RavDE* have been proven to be functional through *in vivo* heterologous expression of the ravidomycin gene cluster and through *in vitro* characterization of their ability to produce NDP-4-keto-6-deoxy-D-glucose (*30, 143*). Cloning of *chryCMT* afforded pKVIR and addition of *chryU* afforded pVIR*II. pKVIR is intended to biosynthesize NDP-4-keto-D-virenose (**95**), while pVIR*II is intended to biosynthesize NDP-D-virenose (**96**).

A series of constructs intended to encode NDP-D-fucofuranose biosynthetic genes were prepared. *GilU* was cloned into a unique site of pUWL-DE to afford pFUCO, which should biosynthesize NDP-D-fucose (**103**) *in vivo*. *GilL* was cloned into this construct to afford pFUCOII, which should encode NDP-D-fucofuranose biosynthesis

(**97**). All together, these constructs potentially biosynthesize rather unique 2-hydroxy-6-deoxysugars that are not encoded in many biosynthetic pathways. Furthermore, they might prove useful in interrogating the substrate flexibility of glycosyltransferases in other polyketide-producing organisms.

SUMMARY

In this chapter, *gilL* and *gilN* were both studied as potential candidates for the ring contraction step of D-fucofuranose, *gilL* encoding an NAD-dependent epimerase/dehydratase and *gilN* encoding a putative glycosyltransferase. Subsequent inactivation of *gilN* in cosG9B3, and expression of this deleted cosmid, resulted in production of gilvocarcin V and M, which were verified by co-injection with standard **39** and **40**, mass, UV, and 1H-NMR spectral characterization. Furthermore, production of gilvocarcin V in this strain was close to wildtype yields (~11.0 mg/L), which indicates that *gilN* plays no role in gilvocarcin biosynthesis. *GilL*, then, appears to be a likely candidate for ring contraction. Like *gilU*, *gilL* demonstrates similarity to NADH-dependent epimerases/dehydratases, and its similarity to *chryL* might indicate a common ring contraction enzyme in both *S. griseoflavus* and the Mercian strain. As heterologous expression of cosG9B3-*gilL*$^{-}$ was not possible, A number of different constructs were prepared with genes implicated in biosynthesis of NDP-D-fucofuranose and NDP-D-virenose.

EXPERIMENTAL

Table 4 Bacterial strains and plasmids used in Chapter 3

Strain/Plasmid Name	**Relevant Characteristics**	**Reference**
Strains		
S. lividans TK 24 (cosG9B3-GilN^{-})	Produces **39** and **40**. *S. lividans* with cosG9B3-GilN^{-}deleted cosmid.	This work.
Plasmids		
pET-28a(+)	Km^{R}. *E. coli* protein expression vector. Used for subcloning.	Novagen.
pUC19	Amp^{R}. *E. coli* cloning vector.	Stratagene.

pUWL201PW	Amp^R, Tsr^R. *E. coli-Streptomyces* shuttle vector. Used to overexpress genes under *ermE** promotion.	(*144*)
pEM4	Amp^R, Tsr^R. *E. coli-Streptomyces* shuttle vector. Used to overexpress genes under *ermE** promotion.	(*145*)
pEN1	Amp^R, Tsr^R. *chryCMT* cloned under *ermE** in pEM4. Intended to produce NDP-4-keto-D-virenose in strain with endogenous NDP-glucose synthase & 4,6-DH.	This work.
pEN2	Amp^R, Tsr^R. *chryCMT* and *chryGT* cloned under *ermE** in pEM4. Intended to produce NDP-4-keto-D-virenose and ChryGT in strain with endogenous NDP-glucose synthase & 4,6-DH.	This work.
pEN3	Amp^R, Tsr^R. *chryCMT* and *chryU* cloned under *ermE** in pEM4. Intended to produce NDP-D-virenose in strain with endogenous NDP-glucose synthase & 4,6-DH.	This work.
pFUCO	Amp^R, Tsr^R. *gilU*, *ravDE* cloned under *ermE** in pUWL201PW. Intended to produce NDP-D-fucose.	This work.
pFUCOII	Amp^R, Tsr^R. *gilLU*, *ravDE*, cloned under *ermE** in pUWL201PW. Intended to produce NDP-D-fucofuranose.	This work.
pKVIR	Amp^R, Tsr^R. *chryCMT*, *chryDE* cloned under *ermE** in pUWL201PW. Intended to produce NDP-4-keto-D-virenose.	This work.
pVIR*II	Amp^R, Tsr^R. *chryCMT*, *chryU, ravDE* cloned under	This work.

	*ermE** in pUWL201PW. Intended to produce NDP-D-virenose.	

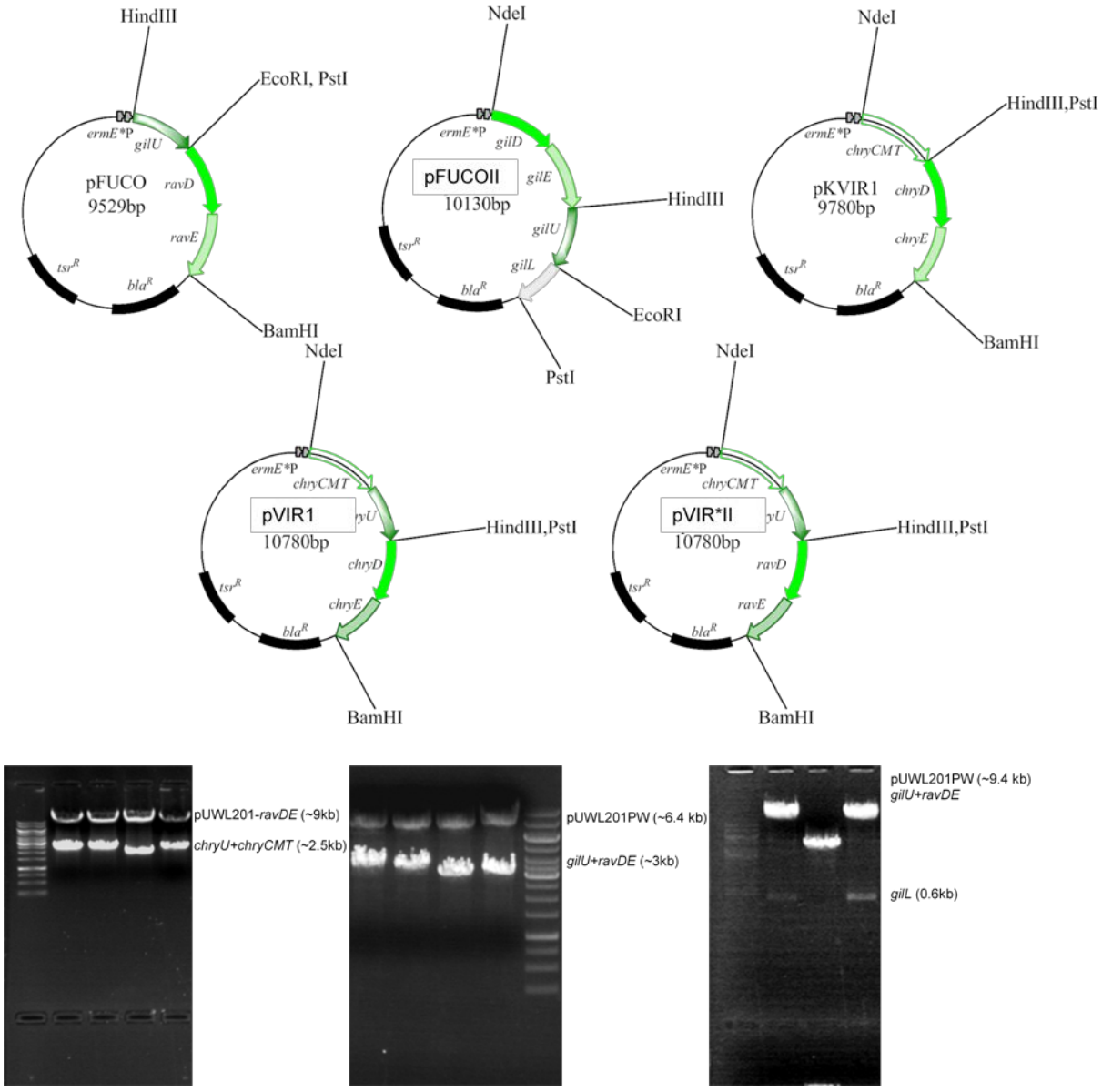

Figure 31 DNA electrophoresis gels of D-fucofuranose and D-virenose constructs.

(Upper) Plasmid maps of pFUCO, pFUCOII, pVIR*II. (Lower Left) *Nde*I/*Hind*III digest of pVIR*II. (Lower Middle) *Hind*III/*Bam*HI digest of pFUCO. (Lower Right) *Nde*I/*Hind*III digest of pFUCOII.

Table 5 Physico-chemical characterization of metabolites of *S. lividans* (cosG9B3-GilN$^-$) strain

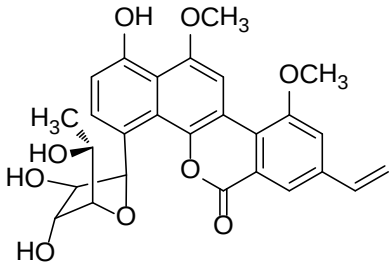

Gilvocarcin V (39)

R_{rel}= 15.30 min^{-1}; Yield: 11.0 mg/L

MW= 494 g/mol ($C_{27}H_{28}O_9$)

Negative mode APCI-MS: m/z=493 [M-H] (low res)

UV maxima (from HPLC-diode array): 250 (90%), 287 (100%), 398 (35%)

Position	Gilvocarcin V (**39**)
	δ_H (500 MHz)
1-OH	9.71 (1H, s)
2-H	6.95 (1H, d, *J*=8.5)
3-H	8.06 (1H, d, *J*=8.5)
7-H	7.99 (1H, d, *J*=2.0)
9-H	7.76 (1H, s)
10-OCH_3	4.19 (1H, s)
11-H	8.48 (1H, s)
12-OCH_3	4.12 (1H, s)
1′-H	6.19 (1H, d, *J*=5.5)
2′-H	4.67 (1H, m)
3′-H	3.86 (1H, m)
4′-H	3.51 (1H, dd, *J*=4.2, 5.9)
5′-H	3.86 (1H, m)
6′-CH_3	1.24 (1H, d, *J*=6.5)
1”-H	6.94 (1H, dd, *J*=18.0, 11.0)
2”-H_e	5.50 (1H, d, *J*=11.0)
2”-H_z	6.14 (1H, d, *J*=18.0)

[a)] Dimethyl sulfoxide-d_6, *J* in Hz

Table 6 Oligonucleotides used in Chapter 3

Primer Name	**Oligonucleotide Sequence**
chryCMT_XbaI_for	5’- ATTTCTAGACCTTCCCGACGCCCCGTG-3’
chryCMT_NdeI_for	5’- ATTCATATGCCTTCCCGACGCCCCGTG-3’
chryCMT_SpeIEcoRI_rev	5’- ATTGAATTCTACTAGTGCGGCGGCG GGGTGC-3’
chryU_SpeI_for	5’-ATACTAGTCGGAATGCCGACAACT-3’
chryU_EcoRI_rev	5’-GTCGAATTCGAGGTCTCCTCGGATCG-3’
chryGT_SpeI_for	5’- ATACTAGTGCTAGCACGGCGGCGCCG TTTCC-3’
chryGT_EcoRI_rev	5’-ATGAATTCAGGCGGGAGCAGGCGGG -3’
chryDE_PstI_for	5’-ATCTGCAGTTTGTCCACGCTGTTGTTT-3’
chryDE_BamHI_rev	5’-TTCGGATCCAATGCCCTATGCGAT-3’
gilU_HindIII_for	5’- ATAAGCTTGCAGTGAGGCACTC CTGTCGTC -3’
gilU_EcoRI_rev	5’-ATGAATTCCGGCCTGGGTCTTTTGT CGTTC -3
ravDE_PstI_for	5’-GTTCTGCAGTCC GCAGTGAATTCC CGG -3’
ravDE_BamHI_rev	5’-TTA AGGATCCGAGATGAGTGCGCACCCA-3’
gilL_NdeI_for	5’- ACCATATGAAAGTAGCAGTGCTCGGT-3’
gilL_HindIII_rev	5’- ACAAGCTTGACACACGTGTCCCTGGT-3’
gilN_FRT_for	5’- CGTCAGCGGAGCAGCCGGGTGGAGTGGGGTGAGGGCATG ATTCCGGGGATCCGTCGACC -3’
gilN_FRT_rev	5’- CCTCGTTCTCTTCTGCCGCCGCGTTCGCCCTTCGGGTCATG TAGGCTGGAGCTGCTTC -3’
gilN_ctrl_for	5’-CTGTTCGTGTGGGGCGGG-3’
gilN_ctrl_rev	5’-TCGCCGCCGCGGCCCGGTCCGCA -3’

Isolation of metabolites from *S. lividans* TK 24 (cosG9B3-GilN$^-$)

For the isolation of substantive amounts of the major metabolite from *S. lividans* TK 24 (cosG9B3-GilN$^-$), a 5 liter fermentation of the organism in SG media was carried out in a two stage fermentation process. In brief, a glycerol stock of *S. lividans* TK 24 (cosG9B3-GilN$^-$) was thawed and 100 µL of the revived strain was plated on an M2 agar plate supplemented with 50 µg/mL apramycin and incubated at 28 °C for 5 days. In a

first stage growth phase, spores of this organism were inoculated into a 100 mL flask of sterilized SG media in a 250 mL baffled flask, and this flask was incubated in an orbital shaker for 3 days (250 RPMs, 28 °C). For the production phase, five liters of sterilized SG media was apportioned in 500 mL amounts in 10 baffled 2 liter Erlenmeyer flasks. This media was supplemented with 50 μg/mL apramycin and 5% (v/v) of the culture from the growth phase flask was inoculated into each of the production phase flasks. This fermentation was carried out for five days. The culture was collected, filtered with celite (50 g/L fermentation), and the resulting mycelial cake was extracted twice with acetone, dried *in vacuo* under reduced pressure, and the rest of the aqueous phase was dried by lyophilization. The culture filtrate was passed over a 5 × 10 cm C_{18} reverse phase silica column, washed with water, and the retained material was eluted in a gradient of 20%, 40%, 60%, 80%, and finally 100% MeOH:H_2O. The major metabolites were mostly eluted in the 80% and 100% gradients of MeOH. The fractions containing gilvocarcins were compiled, the solvent was dried *in vacuo*, and the water was removed by lyophilization on a freeze drier.

The individual peaks were resolved *via* semi-preparative high-performance liquid chromatography (HPLC) on a Sun-Fire semi-prep C18 column (19×150 mm, 5 μm) on a Waters 1525 EF platform with a Waters 2487 dual absorbance detector UV lamp. A gradient of 0.2% formic acid in double distilled water and acetonitrile was used (Solvent A= 0.2% formic acid in water, solvent B=acetonitrile; 0–15 min 25% B to 100% B; 16–24 min 100% B; 25–26 min 100% to 25% B; 27–32 min 25% B, flow rate 2.5 mL/min). The eluted material under each peak was collected, dried *in vacuo*, and finally lyophilized. Sample purity was verified *via* HPLC/MS analysis to assure the presence of a single peak. The sample was further dried under nitrogen gas for 2-3 hours, and finally, dissolved in DMSO-d_6 for ^{1}H-NMR measurements. NMR was recorded on a Varian VNMR 500 MHz spectrometer.

PCR Redirect inactivation of *gilN* and conjugal transfer of cosG9B3-*gilN*⁻

The disruption cassette for inactivation of *gilN* was amplified using a chloramphenicol resistance template and 59-nucleotide long primers gilN_FRT_for and gilN_FRT_rev (see **Table 3.3**). The boxed-in regions of the primers indicate genetic

regions of 39 base pairs directly upstream and downstream of the *gilN* ATG start codon (gilN_FRT_for) and the *gilN* TGA stop codon (gilN_FRT_rev), respectively, and the 20 nucleotides that are not boxed-in bind to the chloramphenicol resistance cassette. The cassette was introduced into *E. coli* BW25113/pKD20, containing cosmid G9B3 (Apr-resistant), which encodes all of the genes for gilvocarcin biosynthesis in *Streptomyces* sp. The disrupted cosmid (cosG9B3-CHL-*gilN*$^-$), containing the chloramphenicol resistance cassette, was introduced into *E. coli* XL-Blue MRF'/pcp20. This *E. coli* strain harbors an FLP-recombinase gene that recognizes genetic sites on both sides of the *gilN*-CHL genetic locus of cosG9B3-CHL-*gilN*$^-$, and it excises this genetic locus resulting in an in-frame 81 base pair scar. Apr^R, Chl^S sensitive colonies were identified by replica plating and verified by PCR analysis using a pair of control primers that amplify a region~100 base pairs upstream and downstream of *gilN*, gilN_ctrl_for and gilN_ctrl_rev (see **Table 3.3**). While the original *gilN* PCR products from cosG9B3 showed products of 966 base pairs, after FLP-mediated excision of the disruption cassette, a PCR product of ~250 bp was obtained (**Table 3.3**). CosG9B3-*gilL*$^-$ was generated in a similar fashion. The mutated cosmids cosG9B3-*gilL*$^-$ and cosG9B3-*gilN*$^-$ were introduced into *Streptomyces lividans* TK24 by conjugation from *E. coli* ET12567 carrying the non-transmissible helper plasmid pUZ8002 as described by Kieser *et al.* (*3*)

Cloning of 6-deoxy-2'-hydroxy-hexose biosynthesizing plasmids

For the generation of plasmids that could direct the biosynthesis of NDP-D-fucofuranose and NDP-D-virenose, the various genetic components of their biosyntheses were amplified *via* polymerase chain reaction using cosChry1-1 and cosG9B3 as templates (**Figure 30**). *Pfu* polymerase was used to amplify genes from template DNA as described in chapter 2, except for *gilU*, which was cloned with Taq polymerase, blunt ended, then cloned into TOPO vector. All PCR products were ligated into TOPO cloning vector following the manufacturer's protocols. *ChryCMT* was amplified from cosChry1-1 with two sets of forward primers and reverse primers, one pair for incorporating *Xba*I/*Eco*RI restriction sites and one pair for incorporating *Nde*I/*Hind*III restriction sites, for pEM4-based and pUWL201PW-based cloning, respectively. TOPO-*chryCMT* was digested with *Xba*I/*Eco*RI and ligated into the same sites of pEM4 downstream of the

*ermE** promoter to give pEN1. This resulting construct was digested with *Spe*I/*Eco*RI for ligation of *chryGT* to yield pEN2. For pEN3, *chryGT* was digested out with *Spe*I/*Eco*RI and *chryU* was ligated into the same restriction sites. For vectors with an enhanced ribosomal binding site and for expressing entire NDP-D-fucofuranose and NDP-D-virenose biosynthetic pathways, pUWL201PW was chosen. *RavDE* and *chryDE* were amplified independently, cloned into TOPO vector, and digested with *Pst*I/*Bam*HI and ligated into a unique restriction site downstream of the *ermE** promoter of pUWL201PW to give pUWL(*chryDE*) or pUWL(*ravDE*). TOPO-*chryCMT*(*Nde*I) was digested with *Nde*I/*Eco*RI and ligated into the same sites of pET-28a(+) to give pET-28a(+)-(*chryCMT*). *ChryU* was ligated into the *Spe*I/*Eco*RI site of this vector, to yield pET-28a(+)-(*chryCMT+chryU*), which was then digested with *Nde*I/*Hind*III to give a ~2.4 kb *chryCMT-U* band, which was then rescued and ligated into the *Nde*I/*Hind*III sites of pUWL(*ravDE*) to afford pVIR*II. *ChryCMT* from pET-28a(+)-(*chryCMT*) was digested out and ligated into the *Nde*I/*Hind*III sites of pUWL(*chryDE*) to give pKVIR. Digestion of *gilU* with *Hind*III/*Eco*RI from TOPO-*gilU* and subsequent ligation of it into pUWL(*ravDE*) afforded pFUCO. pFUCOII was generated by ligation of *gilL* cut with *Nde*I/*Eco*RI into pFUCO in the same sites.

CHAPTER 4: ALTERING THE GLYCOSYLATION PATTERN OF TETRACENOMYCINS

INTRODUCTION

Tetracenomycin C (**8**) and elloramycin (**106**) are anthracycline-like polyketides produced by *Streptomyces glaucescens* and *Streptomyces olivaceus* Tü 2353. Tetracenomycin C was discovered by Weber *et al*. in 1979, and elloramycin was discovered and its structure solved by Rohr *et al*. in 1985 (*146-147*). The cloning of the biosynthetic gene loci for **8** and **106** by Hutchinson *et al*. paved the way for further characterization of the enzymatic components for these compounds, and polyketides as a whole (*148-149*) The biosynthesis of these molecules was fundamental for understanding the role individual enzymes in polyketide synthesis and establishing minimal gene sets for cyclization/aromatization (*150-153*). The biosynthesis of **8** and **106** was found to have tetracenomycin B_3 as a branching point between them, in the case of elloramycin having 8-*O*-rhamnosylation by ElmGT and in the case of tetracenomycin C 8-*O*-methylation by TcmN (**Figure 32**) (*154*).

The minimal PKS consisting of ElmKLM installs the poly-β-ketothioester, which is cyclized by ElmNI, J, and I to afford tetracenomycin F1 (**Figure 32)**. ElmH installs the quinone oxygen, and ElmG is a novel monooxygenase-dioxygenase that catalyzes the triple hydroxylation of tetracenomycin A2 to afford tetracenomycin C (**8**) (*155*). The 4- and 12a- oxygens are installed stepwise from molecular diatomic oxygen, while the 4a-oxygen is installed from attack of water onto the oxirane. In the process, the aromaticity of the D ring of tetracenomycin is broken, thereby resulting in a hypsochromic shift in the UV spectrum from ~450 nm (e.g. red anthraquinones TCM B3 and D3) to ~412 nm (e.g. yellow 8-DMTC, **105**). In the biosynthesis of elloramycin, ElmGT glycosylates 8-*O* position of **105** with L-rhamnose, and subsequent *O*-methylations of the 2', 3', and 4'-OH positions of the L-rhamnose moiety by ElmMI, ElmMII, ElmMIII, and *O*-methylation of the 4a-OH by ElmD (**Figure 32**)(*126, 156*).

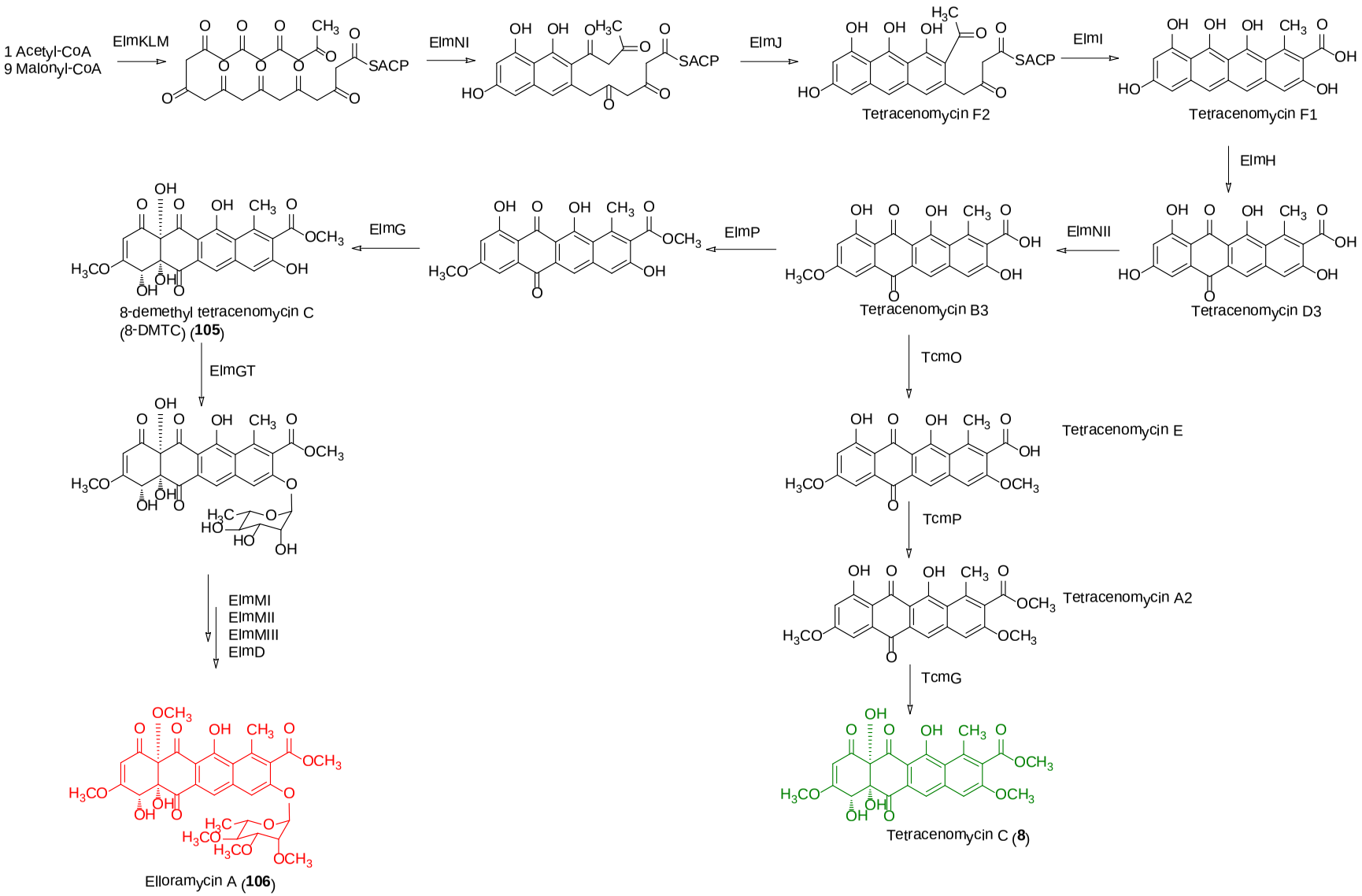

Figure 32 Biosynthetic routes to elloramycin (**106**) and tetracenomycin C (**8**).

ElmGT is one of the most flexible glycosyltransferases in secondary metabolism

Cos16F4 was hypothesized to harbor a sugar flexible glycosyltransferase after it was heterologously expressed in the mithramycin producer, *S. argillaceus*, and the urdamycin producer, *S. fradiae* (*157*). When expressed in PKS-deletion mutants of both producing strains, D-olivosyl (**107**), L-rhodinosyl (**116**), D-mycarosyl (**108**), and D-olivosyl-1,3-D-olivosyl (**109**) tetracenomycin analogues were accumulated in the fermentations of these recombinant organisms (**Figure 33**) (*157-158*). Furthermore, these derivatives were produced in a *S. argillaceus* mutant in which all four glycosyltransferases were inactivated, thereby indicating that the glycosyltransferase responsible for the sugar transfer was encoded on cos16F4 (*157*). The identification of the 1149 nucleotide sequence for *elmGT* enabled new experimentations regarding deoxysugar biosynthesis.

Salas *et al*. expounded upon the cosmid expression experiments of Rohr *et al*. by cloning accessory plasmids that encoded deoxysugar biosynthetic genes into a single combinatorial operon. By cloning genes from the oleandomycin biosynthetic pathway, L-oleandrose biosynthetic genes were sequentially cloned into plasmid "pLN2" and successfully co-expressed with cos16F4 to afford L-olivosyl tetracenomycin C (**113**) and several congeners (e.g. **114,Figure 33**) that were *O*-methylated by the ElmMI, ElmMII, and ElmMIII *O*-methyltransferases (**Figure 32**) (*39, 159*). By deleting the *oleV* (2,3-dehydratase) and *oleW* (3-ketoreductase) genes from this construct resulted in pLN2Δ or pRHAM plasmids (e.g. NDP-L-rhamnose biosynthesis) that when co-expressed with cos16F4 in *S. lividans* restored production of elloramycin A (**106**) (*39*). These initial experiments revealed remarkable flexibility of the deoxysugar biosynthetic genes *oleL* (3,5-epimerase) and *oleU* (4-ketoreductase) in accepting both NDP-4-keto-2,6-deoxyhexose and NDP-4-keto-6-deoxyhexose intermediates. Furthermore, it proved that deoxysugar biosynthetic genes could be cloned into a single operon for heterologous overexpression in a foreign host. These experiments demonstrated that ElmGT had unprecedented substrate flexibility towards foreign D- and L-configurated deoxysugar donor substrates. Furthermore, substrate flexibility on behalf of the deoxysugar biosynthetic enzymes revealed that it would be possible to exploit the "plug and play" construction of pLN2 to incorporate other genes that would alter the stereochemistry of

deoxysugars produced *in vivo*. Taken together, these results yielded a platform in which the substrate flexibility of ElmGT could be interrogated and different deoxysugar constructs could be assayed for their ability to produce novel glycosylated tetracenomycins.

This proof of concept yielded many other deoxysugar constructs that produced novel tetracenomycin derivatives (**107**-**120**), which were able to be characterized *via* mass, UV, and various ^{1}H, ^{13}C, and 2D NMR spectroscopic analyses (**Figure 32**) (*39, 160-163*). Unfortunately, the antitumoral activity of many of these compounds was worse than **106**, with the exception of **118**, which exhibited GI_{50} values in several breast (MDA-MB-231), NSCL (A549), and colon (HT-29) cancer cell lines of below 10^{-5} molar concentrations in the sulforhodamine B cytotoxicity assay (*162*). Very likely, the presence of a *C*-3'-methyl branch on the α-L-mycarose moiety is partly responsible for the slightly improved cytotoxicity of this derivative.

Surprisingly, accumulation of **113** in the culture broth of *S. lividans* (cos16F4)/pRHAM indicated that ElmGT could accept NDP-D-glucose (**30**) as a donor substrate (*163*). This was surprising because many glycosyltransferases involved in polyketide biosynthesis discriminate against nondeoxygenated sugars, such as NDP-D-glucose (**30**). Instead, 6-deoxygenation appears to be a structural pre-requisite before many glycosyltransferases will bind a sugar donor substrate, even though NDP-D-glucose is present as an intermediate in many biosynthetic pathways. Interestingly, NDP-D-oliose (**35**) was never transferred by ElmGT, neither when a sugar plasmid directing its biosynthesis was introduced, nor when cos16F4 was heterologously expressed in *S. argillaceus*, which produces NDP-D-oliose endogenously (*158, 160*). As such, **111** is the only example in which a D-configurated sugar with an axial 4-OH has been transferred by ElmGT; the axial 3-OH may force it to have a slight conformational change in the active site that allows it to bind. One other "limitation" of ElmGT appeared to be its apparent inability to transfer ketosugars; one plasmid, pRHAMΔU, which directs NDP-4-keto-L-rhamnose biosynthesis, did not result in any glycosylated tetracenomycins when it was co-expressed with cos16F4. Recently, mutation of active site residues of ElmGT has been shown to modulate transfer of specific deoxysugars (*164*).

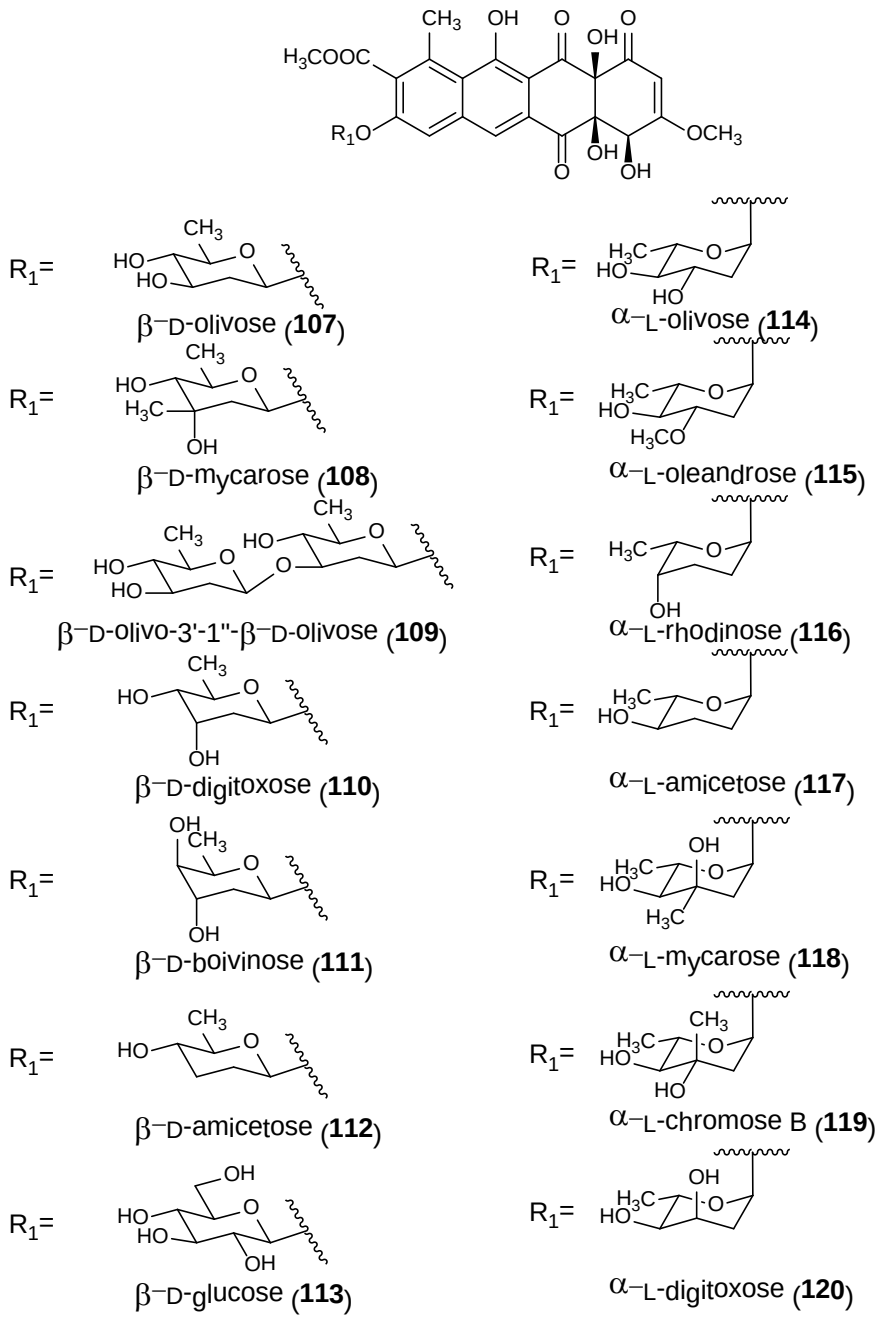

Figure 33 Elloramycin analogues generated by combinatorial biosynthesis. Previously reported differentially glycosylated derivatives of 8-demethyl tetracenomycin C (**105**). ElmGT demonstrates remarkable substrate flexibility to a variety of L- and D-configurated NDP-deoxysugar donors (**107-120**).

Aminosugars: their importance for glycodiversification, bioactivity, and solubility

Incorporation of aminosugars into a glycosylated antibiotic is one important strategy for altering its bioactivity through glycodiversification. Aminosugars are

important for the bioactivity of many antibiotic compounds. Among the foremost of these are the aminoglycosides, such as kanamycin and neomycin, which are broad spectrum antibiotic agents that bind to the 30S subunit of the ribosome of bacteria. The biosynthesis of these important antibiotics features generation of a diversity of aminosugars and specialized glycosyltransferases that catalyze their attachment. Being that these compounds are purely carbohydrate derived, they are highly soluble in water and can be packaged as a salt.

Macrolides, such as methymycin (**3**) and erythromycin A (**7**), employ an aminosugar, NDP-D-desosamine, which enables binding to the 30S subunit of the ribosome as a mechanism of action (*165*). NDP-D-desosamine is a particularly intriguing aminosugar, from the standpoint that it is 4-deoxygenated. The desosamine biosynthetic pathway has been studied extensively by the Hung-wen Liu group, and it was demonstrated that NDP-4-keto-6-deoxy-D-glucose (**32**) is the substrate for a novel PLP-dependent 4-aminotransferase, DesI, which generates TDP-4-amino-4,6-dideoxy-D-glucose (**121**), which is then oxidatively deaminated by DesII to afford TDP-3-keto-4,6-dideoxy-D-glucose (**122**), which undergoes PLP-dependent 3-amination by DesV to afford TDP-3-N,N-didemethyl-D-desosamine (**123**) (**Figure 34**) (*166-170*).

Medermycin is a member of the benzoisochromanequinone family of polyketides, and its only distinguishing characteristic is the *C*-glycosidically linked aminosugar D-angolosamine. It has activity against gram positive bacteria, and like **123**, possesses a dimethylamino functionality at 3-position, in the case of **123** 3,4,6-trideoxygenation and in the case of **124** 2, 3, 6-trideoxygenation (**Figure 34**). The dimethylamino functionality is important for converting the amine functionality into a tertiary amine, which is potentially useful for the formation of a quaternary ammonium cation in solution. In the biosyntheses of both **123** and **124**, a keto group is the handle for transamination: for **123**, the 3-keto group from 2,3 dehydration by Med16, and in the case of **124**, the 4-keto group of NDP-4-keto-6-deoxy-D-glucose and the resulting 3-keto group from DesII deamination of **121 (Figure 34)**.

Daunorubicin (**25**) and doxorubicin (**26**) are canonical polyketide anticancer drugs. Central to their activity is the α-glycosidically linked L-daunosamine residue (**126**, **Figure 34**), that is responsible for positioning these drugs within the minor groove of

DNA (*171*). The L-acosamine sugar (**125**) of 4'-epidoxorubicin (epirubicin) affords this drug with faster clearance, and as a result, it evinces lessened cardiotoxicity as compared to **26**. Hutchinson *et al*. were able to genetically engineer a 4'-epirubicin-producing strain of *S. peucetius* 29050 by inactivating the host 4-ketoreductase, *dnmV*, and integrating a copy of the equatorial-reducing 4-ketoreductase, *avrE*, into the chromosome (*171*) (**Figure 34**). This experiment demonstrated the ubiquity of inactivating/recombining deoxysugar biosynthetic genes to steer flexible glycosyltransferases towards accepting alternate sugar donors.

As a result, constructs pertaining to the biosynthesis of **121-127** were previously cloned by Madan Kharel and Tao Liu, yet the functionality of these plasmids to encode successful aminosugar synthesizing pathways had not successfully been addressed. One of the aims of this present work is to individually transform each of these aminosugar plasmids into *S. lividans* (cos16F4) in an effort to interrogate ElmGT's ability to transfer sugar donor intermediates that may be accumulated in these recombinant strains (**Chapter 4 Experimental**).

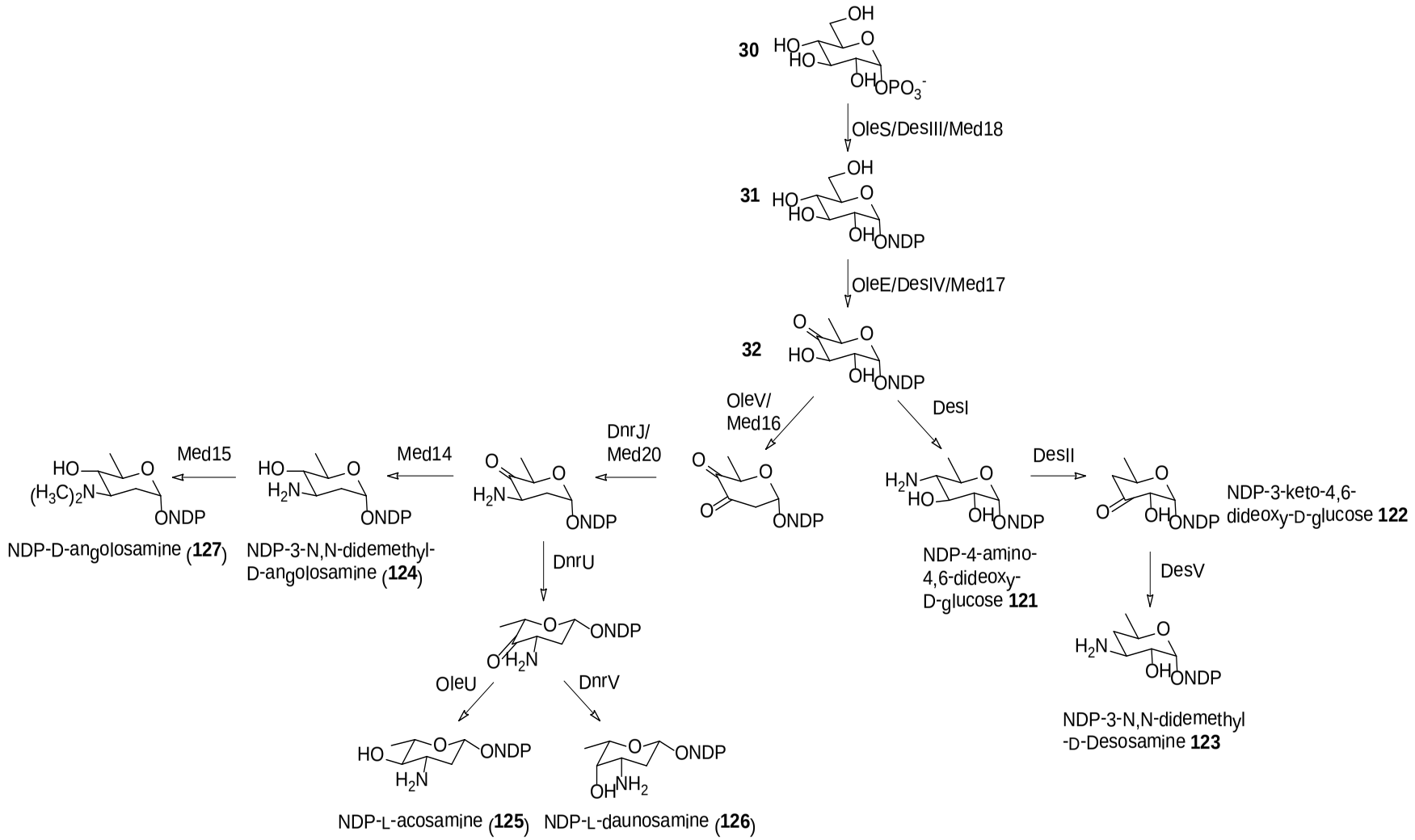

Figure 34 Biosynthetic pathways of aminosugars encoded by plasmids.

RESULTS AND DISCUSSION

Reconstitution of cos16F4 8-demethyl tetracenomycin C heterologous production

Previously in the Rohr lab, *S. argillaceus* (MtmPKS$^-$)/cos16F4 and *S. fradiae* (UrdA$^-$)/cos16F4 strains were generated by heterologously expressing cos16F4 *in vivo(172).* However, no glycerol stock for the *S. lividans* (cos16F4) strain used by Salas *et al*. for co-expression of "sugar plasmids" along with *elm* biosynthetic machinery was available. Moreover, it was necessary to re-establish a producing strain for co-expression experiments. The advantage of using *S. lividans* as a host strain for heterologous expression of cos16F4 is that it possesses no overt deoxysugar biosynthesis of its own, therefore, expression of cos16F4 in *S. lividans* results in accumulation of the aglycone, 8-demethyl tetracenomycin C. Therefore, it was envisioned that cos16F4 could be transformed efficiently *via* either protoplast transformation or electroporation. Because cos16F4 is a pKC505-derived vector, it lacks the necessary *oriT* for conjugation with *E. coli* ET12567/pUZ8002, as was used to transform the cosmids in **Chapter 1** (Materials and Methods). Therefore, protoplasts of *S. lividans* TK 24 were prepared and transformed with cos16F4 DNA. Several days later, thirteen colonies expressing the Apr^R were selected and plated on an M2 agar plate supplemented with apramycin. One colony exhibited excellent growth and a dark red-orange pigmentation, and this colony was fermented in 100 mL SG media supplemented with apramycin. After four days, this strain was extracted with EtOAc, and the extract had a characteristic red-orange hue. To this end, 20 μL of this methanolic extract was analyzed by HPLC/MS and a single peak eluting at R_t=12.0 min^{-1}, with a characteristic UV absorption of the tetracenomycins (UV (MeOH) λ_{max} at 212, 289, 412 nm) (**Figure 35**). The compound demonstrated a parent fragmentation of 459 *amu* [M-H] (ESI-MS (*–ve*) mode, **Figure 35**) which was consistent with the reported mass/UV spectra for 8-demethyl tetracenomycin C. Furthermore, the extract exhibited strong blue fluorescence when exposed 360 nm UV light. This strain, *S. lividans* (cos16F4) was saved for further transformation experiments with deoxysugar cassettes.

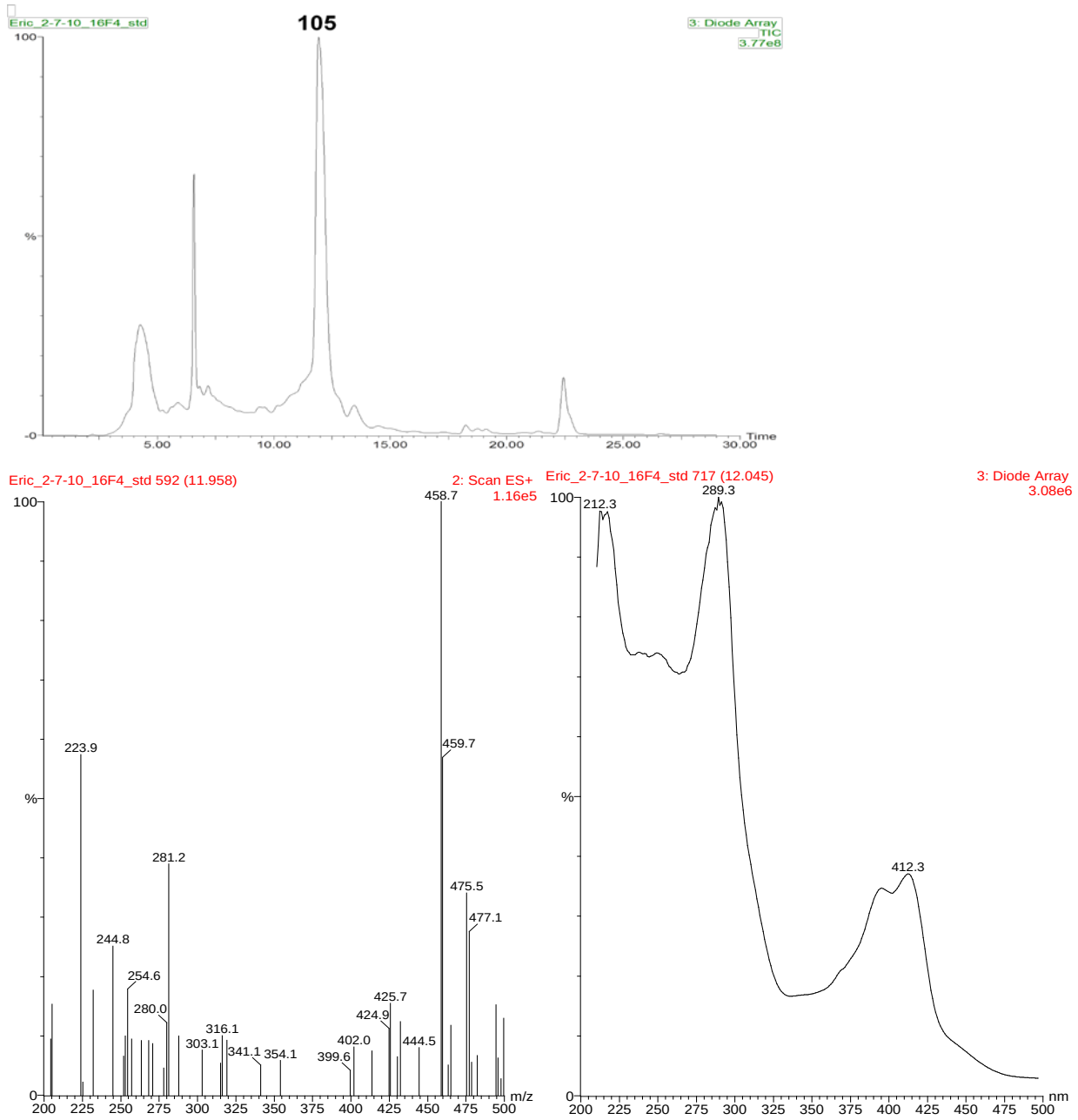

Figure 35 (Upper) HPLC Chromatogram trace of S. lividans (cos16F4) methanolic extract, 8-demethyl tetracenomycin C (**105**) R_t=12.0 min^{-1}. (Lower) ESI-MS (low res) [459 *amu*, M-H] (–ve) mode of **105**. Characteristic UV-vis of 8-demethyl tetracenomycin C (**105**).

Heterologous expression of aminosugar and 2'-hydroxysugar synthesizing cassettes

Previously, constructs directing the biosynthesis of NDP-D-angolosamine and NDP-3-*N,N*-didemethyl-D-desosamine were cloned using the strong constitutive *ermE** promoter of pEM4 (**Chapter 2**, **Table 2.1; Chapter 4, Table 4.1**). The desosamine biosynthetic genes were cloned sequentially into pEM4 by Dr. Kharel, synthesizing three cassettes that would biosynthesize **121-123** (Dr. Kharel, Unpublished Results). pDesI contains *desIII*, *desIV*, and *desI* and should biosynthesize aminosugar **121**; pDesII contains *desIII*, *desIV*, *desI*, and *desII* and should biosynthesize 3-ketosugar **122**; pDesIII contains *desIII*, *desIV*, *desI*, *desII*, and *desV* and should synthesize didemethyl NDP-D-desosamine. pDmnI was made by replacing the *oleW* 3-ketoreductase gene of pLN2 with the daunosamine 3-aminotransferase, *dnrJ*, and it was anticipated to encode biosynthesis for **125.** For biosynthesis of **126**, NDP-L-daunosamine, a gene complement of *dnrJUV* was substituted for the *oleWLU* 3-ketoreductase, 3,5-epimerase, and 4-ketoreductase genes of pLN2. The incorporation of these genes should afford 3-transamination, 3,5 epimerization, and axial 4-ketorduction to yield **126**.

Upon transforming each of these constructs independently into the *S. lividans* (cos16F4) strain, and analyzing methanolic extracts of the transformants, most of these strains failed to accumulate glycosylated tetracenomycins. Most likely, ElmGT is incapable of transferring aminosugars. As an alternative explanation, the aminosugar plasmids may not synthesize the intended aminosugars *in vivo.* Surprisingly, in extracts of *S. lividans* (cos16F4)/pDmnI, an additional peak with R_t= 15.7 minutes was accumulated, in addition to **105 (Figure 36)**. This peak demonstrated a parent fragmentation of 659 *amu* in (-ve) ESI-MS mode, which corresponds to the mass of elloramycin A (**106**). No other glycosylated tetracenomycins could be identified in these extracts when investigating the UV spectrum at 385 nm wavelength. This finding can be explained because pDmnI also contains *oleSELU*, which are the gene complement of the pRHAM plasmid that is known to produce NDP-L-rhamnose *in vivo* (*39*). *OleLU* demonstrate flexibility towards both NDP-6-deoxyhexoses and NDP-2,6-deoxyhexoses. The deletion of *oleLU* and replacement of these genes with *dnrJUV* in pDmnII effectively eliminated this NDP-L-rhamnose pathway, as **106** was not accumulated in that

strain. The failure to accumulate tetracenomycins with appended aminosugars is not unusual, as there are virtually no examples of glycosyltransferases in secondary metabolism that show flexibility towards aminosugar donors that do not already bind an aminosugar donor as a natural substrate. Recently, in the *S. venezuelae* pikromycin biosynthetic pathway, the DesVII desosaminyltransferase responsible for transferring NDP-D-desosamine to its macrolide aglygones was found to require the co-expression of DesVIII in order to form a catalytically active glycosyltransferase (*173*). Without DesVIII, DesVII was catalytically inactive, however, when co-expressed with DesVIII then separated, DesVII was catalytically active. The erythromycin, doxorubicin, and tylosin biosynthetic pathways all possess candidate ORFs for such aminosugar glycosyltransferase auxillary proteins: EryCII, DnrQ, and TylM3 (*173*). Very likely aminosugar glycosyltransferases require these chaperone proteins for proper folding; the one glycosyltransferase where this does not appear to be the case is RavGT, which can transfer both NDP-D-fucofuranose and NDP-D-ravidosamine without an apparent chaperone (*30*). To prove the functionality of these constructs, very likely they will need to be expressed in blocked pathways from which they were expressed (e.g. pDmnI or pDmnII in daunosamine disruption mutants of *S. peucetius*; pDesI, pDesII, pDesIII in desosamine disruption mutants of *S. venezuelae*).

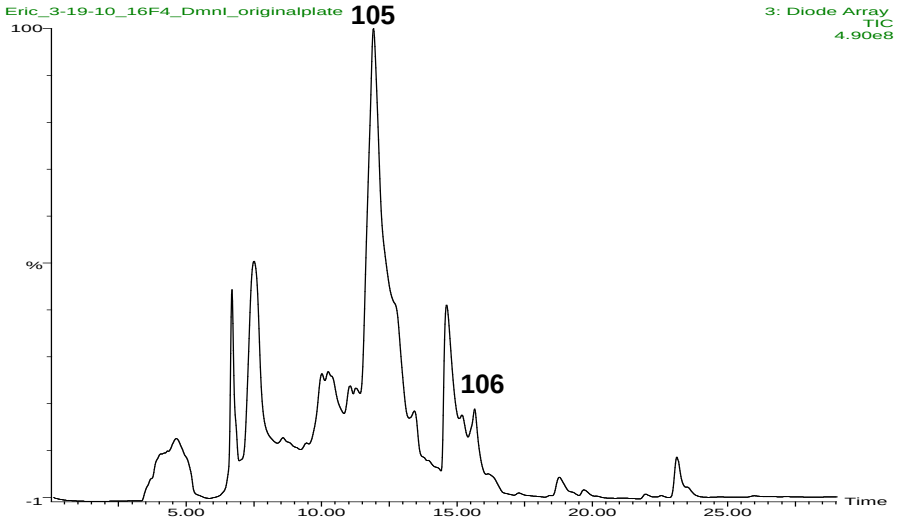

Figure 36 HPLC chromatogram of S. lividans (cos16F4)/pDmnI extract.

Heterologous expression of 2-hydroxysugar plasmids and ketosugar plasmids

pFUCO, pFUCOII, pVIR*II, and pKVIR were all introduced into *S. lividans* (cos16F4) *via* protoplast transformation. Fucosylated and virenosylated tetracenomycins were expected to be accumulated in the recombinant strains. Unfortunately, methanolic extracts failed to reveal the presence of glycosylated tetracenomycins. Again, either the constructs failed to synthesize the intended deoxysugars *in vivo*, or ElmGT was unable to successfully accept the donor substrate. There is some evidence to support this latter finding, because in at least two separate cases, ElmGT was unable to accept a D-configurated sugar that has an axially positioned 4'-OH (*158, 160*). When cos16F4 was heterologously expressed in the mithramycin producer *S. argillaceus*, and when cos16F4 was co-expressed with a plasmid directing biosynthesis of NDP-D-oliose (**35**), no D-oliosyl tetracenomycin C was isolated and described (*158, 160*). This indicates that ElmGT has poor tolerance for D-configurated sugar donors with axially configurated 4-OH groups, which applies to sugars **96** and **103**. However, these constructs may not also be functioning *in vivo*.

Additionally, ketosugar constructs were generated by deletion of 4-ketoreductases from pFL942 and pLN2-derived constructs (*39*) (**Figure 37**). pKOL was generated by deleting *oleU* from pLN2 and re-ligating the plasmid, and it should direct biosynthesis of NDP-4-keto-L-olivose (**Figure 37** and **Figure 38**) pFL952 (e.g. NDP-4-keto-L-mycarose, **Figure 37**) was constructed by deleting *eryBIV* from pFL942 and re-ligating, and *cmmUII* and *oleY* were removed from pMP1*UII to afford pDKOL (e.g. NDP-4-keto-D-olivose) (**Figure 37**).

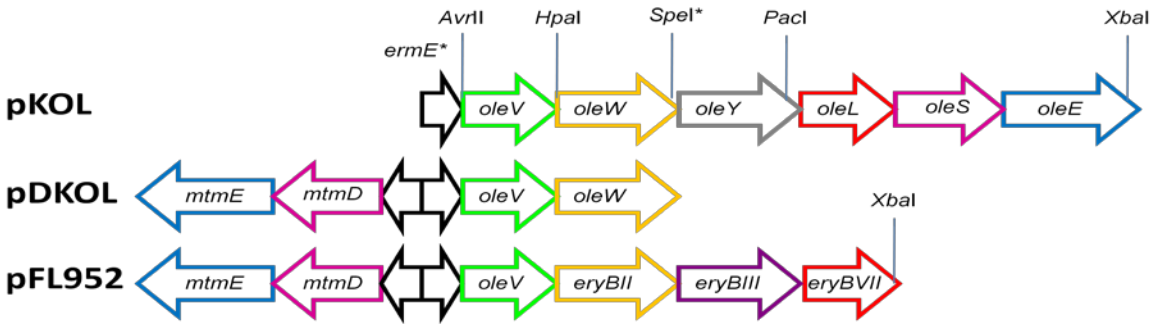

Figure 37 Ketosugar plasmid maps generated for this work.
Genes are color-coded according to function: Pink (NDP-glucose-synthase); Blue (4,6 dehydratase); Green (2, 3-dehydratase); Yellow (3-ketoreductase); Grey (*O*-methyltransferase not functioning in this construct), Purple (3-*C*-methyltransferase); Red

(3,5 epimerase (*oleL*)) or 5-epimerase (*eryBVII*)); Appropriate restriction sites used for cloning are indicated.

In these latter two constructs, *mtmD* and *mtmE* are under the control of one divergent *ermE** promoter, and the other sugar genes are under the control of another divergent *ermE** promoter. Plasmid maps for all of these constructs are depicted in **Figure 37**.

The activities of OleS (NDP-glucose-synthase), OleE (NDP-glucose-4, 6-dehydratase), OleV (2, 3-dehydratase), OleL (3, 5-epimerase), and OleW (3-ketoreductase) catalyze the conversion of NDP-D-glucose to NDP-4-keto-2, 6-dideoxy-D-glucose during the biosynthesis of NDP-L-olivose (**Figure 38**). The 4-ketoreduction step catalyzed by OleU represents the last step of the NDP-L-olivose biosynthetic pathway.

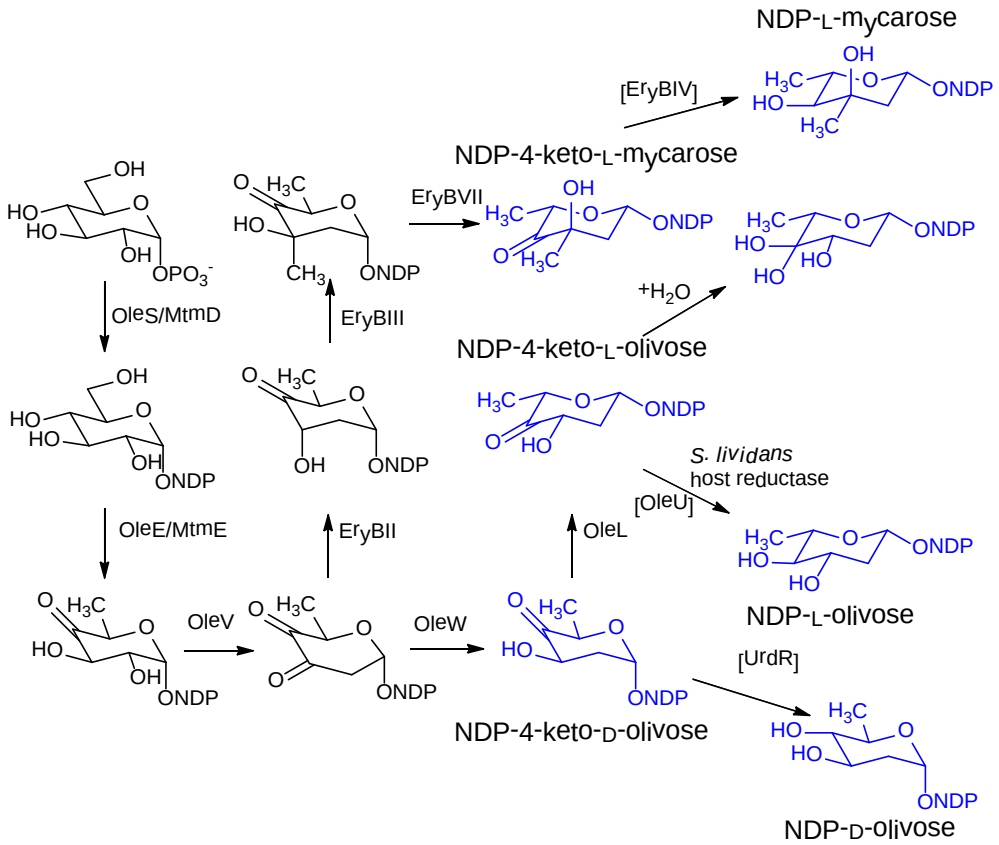

Figure 38 Deoxysugar biosynthesis for ketosugars encoded by pKOL, pDKOL, and pFL952.
Blue sugars are encoded final products of these pathways. Enzyme names in brackets indicate genes that were deleted from these constructs.

Thus, the absence of *oleU* from pLN2 in pKOL would lead to the accumulation of NDP-4-keto-L-olivose, which could be utilized by ElmGT as an alternative donor substrate when the natural substrate (TDP-L-rhamnose) is not available. To test this hypothesis, the pKOL plasmid was expressed in the *S. lividans* (cos16F4) strain.

Interestingly, expression of pKOL in *S. lividans* (cos16F4) resulted in the accumulation of two major peaks with R_t (10.76 and 11.26 min., respectively), in addition to 8-DMTC, when ethyl acetate extracts were analyzed by HPLC/MS (**Figure 39**). Both peaks showed UV absorption typical for a tetracenomycin-type compound. Low resolution ESI/MS revealed a peak of 585 *amu* (-ve mode) pertaining to the molecular ion of the compound and a pseudomolecular ion of the hydrated species at 603 *amu* (-ve mode), indicating the addition of water to the molecule. These data suggested that this compound could be a new tetracenomycin analogue with an attached NDP-4-keto-2, 6-dideoxy ketosugar. Under aqueous condition, ketosugars can easily interconvert from the keto form to a hydrate form. The second peak possessed an *m/z* value of 587 in (-) ESI mode. These mass data suggested the presence of a glycosylated tetracenomycin in which the sugar was fully reduced. Both peaks possessed a fragmentation ion corresponding to the 8-DMTC aglycone (*m/z* 457, $M\text{-}H^-$). This strain was fermented in a large scale fermentation (7.2 L) for isolation and spectroscopic characterization of the metabolites. Unfortunately, expression of pFL952 and pDKOL failed to accumulate appreciable amounts of glycosylated metabolites. Very likely, the encoded donor sugar substrates are not recognized by ElmGT.

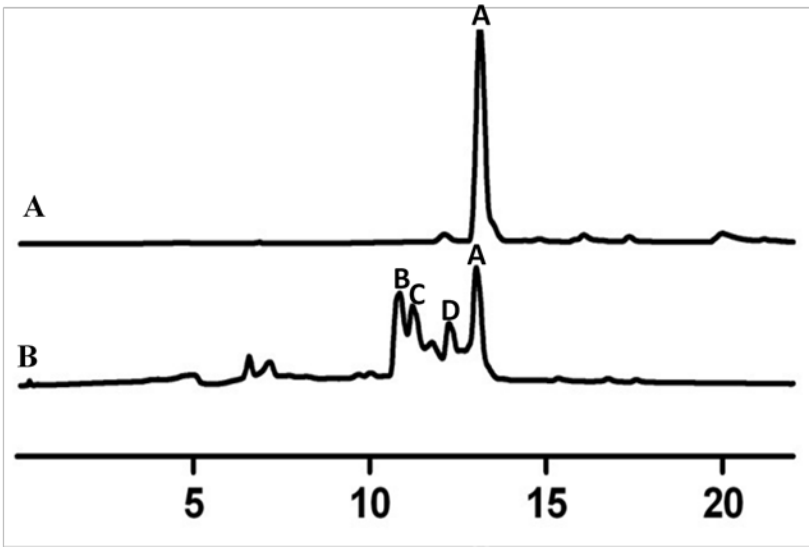

Figure 39 HPLC analyses of the metabolites:
trace A, 8-demethyl-tetracenomycin C (**A**) (Rt. 12.98 min.) isolated from *S. lividans* (cos16F4); trace B, metabolites isolated from the *S. lividans* (cos16F4)/pKOL mutant, 8-demethyl-(4'-keto)-α -L-olivosyl-tetracenomycin C (**B** (Rt. 10.76 min.) and **D** (Rt. 12.26 min.) denote hydrated and keto forms, respectively) and 8-demethyl-α -L-olivosyl-tetracenomycin C (**C)** (Rt. 11.26 min.)

Structural Elucidation of Metabolites Accumulated by the S. lividans (cos16F4)/ pKOL strain

The structure of 8-demethyl-8-(4′-keto)-α-L-olivosyl-tetracenomycin C (**127, Figure 40**) was solved through NMR and mass spectral analyses. The (-) HR-ESI MS of 3 showed two peaks at 585.1267 *amu* and 603.1363 *amu*, which corresponded to the molecular formula of its keto form ($C_{28}H_{26}O_{14}$, calcd. molecular weight 585.1317 [M-H$^-$]) and its hydrate from ($C_{28}H_{26}O_{14}$, calcd. molecular weight 603.1423 amu [M-H$^-$]), respectively. ^{1}H NMR data of **127** revealed 2 singlets for two aromatic protons (δ 7.94 and δ 7.66) and two methoxy signals corresponding to the 3-OCH_3 (δ 3.81) and 9-OCH_3 (δ 3.97) of 8-DMTC, respectively (^{1}H and ^{13}CNMR table in **Table 4.3**). The anomeric proton of the sugar appeared as a broad singlet (δ 6.16) which suggested its α configuration. A pair of protons at δ 2.13 and δ 2.24 corresponded to the C-2′ methylene protons. A 4′-H signal was not observed, indicating the presence of keto/hydrated-keto group. The splitting of the 3′-H (dd, J= 12.0, 6.5 Hz) at δ 4.68 indicated a large diaxial coupling with 2′-H_a and an axial-equatorial coupling with 2′-H_e. The 5′-H appeared as a quartet (J= 6.5 Hz) at δ 4.39, which indicated coupling with 6′-CH_3. The ^{1}H, ^{1}H-COSY

exhibited two spin systems for the sugar moiety, one stretching from 1′-H to 3′-H, and the other stretching from 5′-H to 6′-CH_3, which strongly indicates the presence of a ketone/hydrated ketone at C-4′ (**Figure 40**). The ^{13}C showed a carbonyl signal at δ 207.4, which indicates that **127** is present predominantly in the ketosugar form when measured in Methanol-d_4. The HMBC demonstrated correlations between 6'-CH_3 protons and both 5'-C and 4'-carbonyl, which indicated that the ketone was present at 4'-position (**Figure 40**). These data suggested the structure of **127** as 8-demethyl-8-(4′-keto)-α-L-olivosyl-tetracenomycin C.

Compound **114** was eluted at the identical retention time when co-injected with standard 8-demethyl-8-α-L-olivosyl-tetracenomycin. The identity of **114** as 8-demethyl-8-α-L-olivosyl-tetracenomycin was further confirmed through the comparison of ^1H NMR data with published ^1H NMR data.

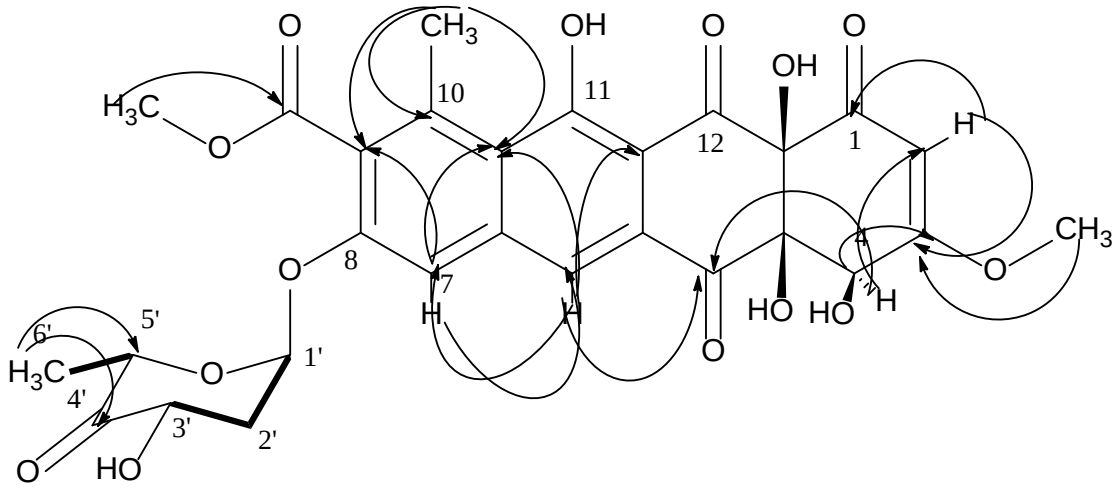

Figure 40 Selected 2D-NMR for **127**.
^1H-^1H-COSY (▬), and selected HMBC (→) correlations of 8-Demethyl-8-(4'-keto)-α-L-olivosyl-tetracenomycin C (**127**).

The presence of **127** was quite interesting, because ElmGT has never been shown to carry a ketosugar before. As such, isolation and characterization of **127** represents the first successful attempt to overcome ElmGT's inflexibility towards a ketosugar. As a result, it seems plausible that ElmGT demonstrates at least some substrate flexibility to this L-configurated ketosugar, because of its close stereoelectronic similarity to NDP-L-rhamnose. It is possible that ElmGT binds the hydrated form of NDP-4-keto-L-olivose,

which would present three hydroxyl groups to ElmGT, much like NDP-L-rhamnose also possesses three hydroxyl groups that may be recognized. However, it is also surprising that ElmGT was unable to accept the NDP-4-keto-D-olivose, NDP-4-keto-L-rhamnose, and NDP-4-keto-L-mycarose sugars (*39*). NDP-L-mycarose was previously shown to be a poor substrate for ElmGT (only ~10% of all tetracenomycins in the *S. lividans* (cos16F4)/pFL942 strain were L-mycarosylated tetracenomycins) (*162*).

Production of **114** along with **127** by *S. lividans* (cos16F4)/pKOL was surprising. It is speculated that a pathway-independent ketoreductase of *S. lividans* TK 24 might be responsible for the conversion of NDP-4-keto-L-olivose to NDP-L-olivose, and the latter is probably utilized by ElmGT as an alternate substrate to yield **114**. Pathway independent reductions have been reported previously in the literature. Earlier in the pikromycin biosynthetic pathway, a D-quinovosyl macrolide was accumulated instead of the anticipated 4-keto-6-deoxy-D-glucosyl analogue when *desI* was inactivated in *Streptomyces venezuelae* (*168*). To search for possible sugar ketoreductases in *Streptomyces lividans* TK 24 that could be responsible for reduction of NDP-4-keto-L-olivose, thus possibly explaining the presence of **114**, the amino acid sequence for OleU was compared to encoded proteins in the *Streptomyces lividans* genome using the protein BLAST public database. One such candidate was indicated in the search, SSPG_00655 (30% sequence identity/42% sequence similarity). This candidate has a domain that shows similarity to RfbD, which is a 4-ketohexulose reductase responsible for equatorial 4-ketoreduction of NDP-4'-keto-L-rhamnose in the NDP-L-rhamnose pathway. This enzyme may be responsible for the 4-ketoreduction witnessed in **114**.

*Biological activity of **127** towards Streptomyces prasinus*

To evaluate the biological activity of **127**, 1 mg mL^{-1} methanolic solutions of **127** and **106** were prepared. **106** was included as a positive control. *Streptomyces prasinus* NRRL B-2712 was chosen as a test organism, because it was the most sensitive gram positive organism tested against **106** (*146*). Disc diffusion assays were performed in triplicate as previously described (*146*), and both **106** and **127** demonstrated activity against *S. prasinus*. However, **127** (mean zone of inhibition 12±2 mm diameter) demonstrated less antibacterial activity than **106** (mean zone of inhibition 24±2 mm

diameter). This is not surprising, as many tetracenomycin derivatives with substitutions in the 8-*O*-glycoside moiety exhibit lower antibacterial activity and antitumoral activity than **106**, which demonstrates that the 8-*O*-permethylated L-rhamnose moiety is important for the biological activity of elloramycin.

Glycosyltransfer of ketosugars is a rare phenomenon; expanding the catalogue of known substrates for ElmGT

ElmGT represents one of the most flexible glycosyltransferases with respect to its ability to accommodate a large number of sugar donor substrates as compared to glycosyltransferases in other secondary metabolite biosynthetic pathways. ElmGT reportedly utilizes various NDP-D-sugars: D-olivose, D-mycarose, D-diolivose, D-amicetose, D-boivinose, D-digitoxose, and D-glucose. ElmGT also accepts a number of NDP-L-sugars: L-rhamnose, L-rhodinose, L-digitoxose, L-olivose, L-amicetose, L-mycarose and 4-deacetyl-L-chromose B. However, ElmGT has not been previously shown to accommodate NDP-ketosugars. In this context, production of **127** through the expression of pKOL in *S. lividans* (cos16F4) was interesting, especially, as earlier efforts to glycosylate 8-DMTC with NDP-4-keto-L-rhamnose were unsuccessful (Rodriguez, *et al.*, 2000).

Despite the many glycosyltransferases discovered, those which can attach ketosugars to their acceptor co-substrates are relatively scarce. MtmGIV (and possibly MtmGIII) from the mithramycin pathway has/have been shown to handle NDP-4-keto-D-olivose and NDP-4-keto-D-mycarose to generate novel premithramycin and mithramycin analogues in *Streptomyces argillaceus* strains in which *mtmC* (3-*C*-methyltransferase) and *mtmTIII* (4-ketoreductase) genes were disrupted (Remsing, *et al.*, 2002). EryBV from the erythromycin pathway has been shown to accommodate NDP-4-keto-L-mycarose (Salah-Bey, *et al.*, 1998). Similarly, BgtfA from the balhimycin pathway is capable of utilizing NDP-4-keto-L-vancosamine as a natural sugar donor substrate (Pelzer S - Sussmuth, *et al.*). The unprecedented flexibility of ElmGT towards NDP-4-keto-L-olivose reported in this communication is particularly encouraging for further studies towards understanding the structural role of ElmGT in binding deoxysugar substrates.

SUMMARY

In summary, cos16F4 was used to heterologously express 8-demethyltetracenomycin C and the glycosyltransferase ElmGT. Various "sugar plasmids" were co-expressed with resulted in recombinant strains, and co-expression of plasmid pKOL, which biosynthesizes NDP-4-keto-L-olivose resulted in accumulation of the new tetracenomycin analogue 8-demethyl-8-(4'-keto)-*α*-L-olivosyl-tetracenomycin C. This analogue was structurally elucidated through HR-ESI mass, ^{1}H-NMR, ^{13}C-NMR, ^{1}H,^{1}H-COSY, and HMBC NMR spectroscopy. It was determined to have roughly 50% of the antimicrobial activity of elloramycin A towards *Streptomyces prasinus*.

EXPERIMENTAL

Bacterial Strains and Culture Conditions

Escherichia coli XL1 blue (Invitrogen) was used as a host for routine cloning experiments and was grown on LB agar or in LB broth at 37 °C. *S. lividans* TK24 and derivative strains were grown on M2 agar or in YEME liquid medium at 28 °C for 3 days for preparation of protoplasts following the previously reported protocol (*3*). When antibiotic selection of recombinant strains was required, 25 μg/mL apramycin, 25 μg/mL thiostrepton, or 100 μg/mL of ampicillin were used. Protoplast transformation was carried out to introduce the cosmid cos16F4 into *Streptomyces lividans* TK 24 following the standard protocol (*3*, *174*). An apramycin resistant colony was selected for the production of 8-demethyl-tetracenomycin and was used as host for the expression of a newly generated deoxysugar biosynthetic construct(s).

Bioactivity conditions against *Streptomyces prasinus* NRRL B-2712 were carried out as previously described (*146*). In brief, spores of *Streptomyces prasinus* were grown on plates (0.4% yeast extract, 1.0% malt extract, 0.4% glucose, 2.0% agar). The strain was grown for 50 hours until the plate was well-sporulated, then the spores were collected, diluted in sterile water, and adjusted to OD 1.3 (560 nm). 0.5 mL of the spore suspension was plated on each of 3 plates, and methanolic test solutions were prepared at a concentration of 1 mg/mL. 6 mm filter discs were prepared from Wattman filter paper using a hole punch, were sterilized in a 50 mL centrifuge tube, soaked in the antibiotic

solution, allowed to dry in a laminar flow hood for 30 minutes, then grown in the presence of *S. prasinus*. Zones of inhibition were measured in triplicate and averaged.

Generation of plasmids directing the biosynthesis of ketosugars, aminosugars, and 2-hydroxysugars

The 4-ketoreductase gene (oleU) was removed from plasmid pLN2 (Rodriguez, *et al*., 2002). *Nhe*I and *Spe*I were used to digest pLN2, thereby releasing the *oleU* fragment. DNA gel electrophoresis was carried out to remove the *oleU* gene and the resulting fragment (~14kb) was rescued and re-ligated to generate pKOL. In this construct, all of the sugar genes are under strong *ermE** promotion. The plasmid map for this construct is depicted in **Figure 37**. This plasmid was introduced into the *S. lividans* (cos16F4) strain through protoplast transformation. Plasmid pFL952 was prepared as described previously (*134*). In brief, plasmid pFL942 (directs biosynthesis of NDP-L-mycarose), was digested with *Spe*I/*Nhe*I, thus releasing the *eryBIV* 4-ketoreductase. The ~14kb plasmid was rescued, self-ligated using T4 DNA Ligase, and then transformed into XLI Blue *E. coli* for amplification of the construct.

Plasmids pVIR*II, pFUCOII, pFUCO, and pKVIR were prepared as discussed in **Chapter 2**, Materials and Methods. Plasmids pRavI, pDmnI, pDmnII, pDesI, pDesII, and pDesIII were prepared by Dr. Madan Kharel (Personal Communication). Plasmid pTLAG was cloned by Dr. Tao Liu (Dissertation).

Table 7 Plasmids used in Chapter 4

Plasmid Name	**Relevant Characteristics**	**Reference**
Cos16F4	Apr^R. Directs biosynthesis of 8-DMTC (**105**) in *Streptomyces*. Encodes ElmGT, pKC505-derived cosmid.	(*149*)
pLN2	Amp^R, Tsr^R. *OleVWSELUY* under *ermE** promotion. NDP-L-olivose.	(*135*)
pFL942	Amp^R, Tsr^R. *OleV, MtmDE, EryBII, BIII, BIV, BVII* under divergent	(*134*)

	*ermE** promotion. NDP-L-mycarose.	
pMP*UII	Amp^R, Tsr^R. *OleVW, cmmUII, OleY, MtmDE,* under divergent *ermE** promotion. NDP-L-mycarose.	(*160*)
pRavI	Amp^R, Tsr^R. *RavDE*, *NMT*, *AMT*, *IM* under *ermE** promotion. NDP-D-ravidosamine	Madan Kharel, Personal Communication
pDmnI	Amp^R, Tsr^R. *OleSEVLU DnrJ* under *ermE** promotion. NDP-L-acosamine	Madan Kharel, Personal Communication
pDmnII	Amp^R, Tsr^R. *OleSEV, DnrJUV* under *ermE** promotion. NDP-L-daunosamine	Madan Kharel, Personal Communication
pDesI	Amp^R, Tsr^R. *DesIII*, *DesIV*, *DesI* under *ermE** promotion. NDP-4-amino-6-deoxy-D-glucose (**121**)	Madan Kharel, Personal Communication
pDesII	Amp^R, Tsr^R. *DesIII*, *DesIV*, *DesI*, *DesII* under *ermE** promotion. NDP-3-keto-4,6-dideoxy-D-glucose (**122**).	Madan Kharel, Personal Communication
pDesIII	Amp^R, Tsr^R. *DesIII*, *DesIV*, *DesI*, *DesII*, *DesV* under *ermE** promotion. NDP-3-N,N-didemethyl-D-desosamine (**123**).	Madan Kharel, Personal Communication.
pTLAG2	Amp^R, Tsr^R. *Med20, 18, 17, 16, 15, 14* under *ermE** promotion. NDP-D-angolosamine	Tau Liu, Dissertation.
pKOL	Amp^R, Tsr^R. *OleVWSELY* under *ermE** promotion. NDP-4-keto-L-olivose.	This work.
pFL952	Amp^R, Tsr^R. *OleV, MtmDE, EryBII, BIII, BIV, BVII* under divergent *ermE** promotion. NDP-4-keto-L-mycarose.	(*134*)
pFUCO	Amp^R, Tsr^R. *gilU, ravDE*	This work.

	cloned under *ermE** in pUWL201PW. Intended to produce NDP-D-fucose.	
pFUCOII	Amp^R, Tsr^R. *gilLU*, *ravDE*, cloned under *ermE** in pUWL201PW. Intended to produce NDP-D-fucofuranose.	This work.
pKVIR	Amp^R, Tsr^R. *chryCMT*, *chryDE* cloned under *ermE** in pUWL201PW. Intended to produce NDP-4-keto-D-virenose.	This work.
pVIR*II	Amp^R, Tsr^R. *chryCMT*, *chryU*, *ravDE* cloned under *ermE** in pUWL201PW. Intended to produce NDP-D-virenose.	This work.

Table 8 Bacterial strains used in Chapter 4

Strain Name	**Relevant Characteristics**	**Reference**
S. lividans TK24 (cos16F4) §	Harbors cos16F4. Produces **105.**	**(*149*)**
S. lividans (cos16F4)/pRav1	§ co-expressed with pRavI. Produces **105**.	This work.
S. lividans (cos16F4)/pDmnI	§ co-expressed with pDmnI. Produces **105** and **106**.	This work.
S. lividans (cos16F4)/pDmnII	§ co-expressed with pDmnI. Produces **105.**	This work.
S. lividans (cos16F4)/pDesI	§ co-expressed with pDesI. Produces **105.**	This work.
S. lividans (cos16F4)/pDesII	§ co-expressed with pDesII. Produces **105.**	This work.
S. lividans (cos16F4)/pDesIII	§ co-expressed with pDesIII. Produces **105.**	This work.
S. lividans (cos16F4)/pTLAG2	§ co-expressed with pTLAG2. Produces **105.**	This work.
S. lividans (cos16F4)/pFUCO	§ co-expressed with pFUCO. Produces **105.**	This work.
S. lividans (cos16F4)/pFUCOII	§ co-expressed with pFUCOII. Produces **105.**	This work.
S. lividans (cos16F4)/pVIR*II	§ co-expressed with pVIR*II. Produces **105.**	This work.

S. lividans (cos16F4)/pKVIR	§ co-expressed with pKVIR. Produces **105.**	This work.
S. lividans (cos16F4)/pKOL	§ co-expressed with pKOL. Produces **105**, **114**, **127**.	This work.
S. lividans (cos16F4)/pDKOL	§ co-expressed with pDKOL. Produces **105.**	This work.
S. lividans (cos16F4)/pFL952	§ co-expressed with pFL952. Produces **105.**	This work.

Table 9 Physicochemical characterization and NMR data of 8-Demethyl-8-(4'-keto)-α-L-olivosyl-tetracenomycin C (**127**).

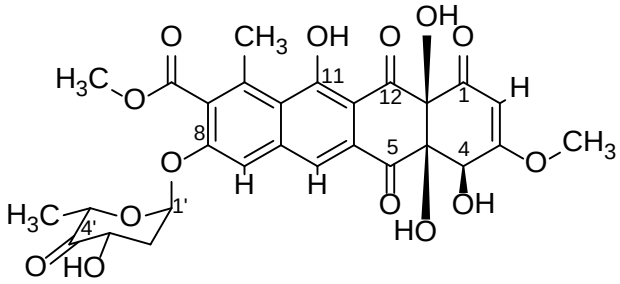

R_{rel}= 10.76 min^{-1}; Yield: 2.0 mg/L

MW= 586 g/mol ($C_{28}H_{26}O_{14}$)

Negative mode APCI-MS: m/z=585 [M-H] (low res), m/z=603 (hydrate); (-) HR-ESI MS (keto form calc. 585.1317 *amu*, found 585.1267 *amu* [M-H^-]; hydrate form calc. 603.1423, found 603.1363 *amu* [M+18])

UV maxima (from HPLC-diode array): 210 (60%), 286 (100%), 409 (20%)
NMR Data (d_4-methanol)

Position	8-Demethyl-8-(4'-keto)-α-L-olivosyl-tetracenomycin C (**127**)[a]	
	δ_C (125 MHz)	δ_H (500 MHz)
1	193.0	-
2	100.8	5.62 (s)
3	176.1	-
3-OCH_3	57.8	3.81 (s)
4	70.7	4.88 (d, 1.5)
4-OH	-	-
4a	85.9	-
4a-OH	-	-
5	194.8	-
5a	141.5	-
6	122.1	7.91 (s)
6a	129.6	-
7	112.4	7.55 (s)
8	155.4	-

9	130.9	-
9-OCH_3	53.4	3.97 (s)
9-CO	169.5	-
10	139.5	-
10-CH_3	21.3	2.79 (s)
10a	122.6	-
11	167.8	-
11-OH	-	-
11a	110.6	-
12	198.2	-
12a	84.6	-
12a-OH	-	-
1′	96.4	6.16 (s)
2′	37.3	2.24 (ddd, 15.0, 12.0, 3.0, H_a), 2.13 (dd, 15.0, 6.5, H_e)
3′	70.6	4.68 (dd, 12.0, 6.5)
3′-OH	-	-
4′	207.4	-
4′-OH	-	-
5′	72.5	4.39 (q, 6.5)
6′	14.3	1.12 (keto, d, 6.5) 1.16 (hydrate, d, 6.5)

Isolation of tetracenomycins from recombinant *S. lividans* (cos16F4) strains

S. lividans (cos16F4)/pKOL was grown on M2 agar medium at 28 °C supplemented with thiostrepton and apramycin for 5 days. For small scale production of tetracenomycins, an agar chunk of bacterial spores was inoculated in 250 mL Erlenmeyer flasks containing 100 mL of Soytone-Glucose (SG) medium supplemented with antibiotics for 4-5 days. 25 mL of the culture was extracted with ethyl acetate and the organic layer was dried *in vacuo*. Extracts were then redissolved in methanol and were subjected to HPLC/MS analyses on a MicroMass ZQ 2000 (Waters) instrument equipped with HPLC (Waters alliance 2695 model) and photodiode array detector (Waters 2996). A Sun-Fire semi-prepC_{18} column (19 × 250 mm, 5 μm) and Symmetry C_{18} (4.6 x 250 mm, 5 μm) analytical column were used for semi-preparative and analytical scale separations, respectively. A gradient of acetonitrile and 0.1% formic acid in water was used to separate compounds as reported previously (See **Chapter 3,** Materials and Methods).

For larger scale production of glycosylated tetracenomycins, 7.2 L of SG medium and allocated into 800 mL portions in 9 baffled 2 L Erlenmeyer flasks. The production media was supplemented with antibiotics and inoculated with freshly prepared spores

from M2 agar plates of the recombinant strains. Fermentation was carried out for 5 days at 28 °C in an orbital shaker. The culture was harvested, mixed with celite (50 g/L fermentation broth), and then filtered. The mycelial cake was discarded, and the culture broth was passed through Amberlite® XAD16 resin (column dimensions 80 cm x 4 cm). The column was washed with 100% distilled water, and crude tetracenomycins were obtained by elution with 2 L of methanol. The solvent was dried *in vacuo*. This extract was separated *via* silica gel column chromatography using 200 mL gradients of dichloromethane and methanol from 0-100% of methanol, increasing in 5% each step. Fractions containing tetracenomycins were pooled, dried *in vacuo*, and further purified using semi-preparative HPLC as described previously (**Chapter 3**, Materials and Methods). Using this protocol, 14.4 mg and 12.2 mg of compounds **127** and **114** were isolated, respectively. (-) High resolution ESI spectra of pure compounds were recorded at the University of Wisconsin Biotechnology Center. NMR spectra were recorded on a Varian VNMR 500 MHz spectrometer using deuterated methanol as solvent.

CHAPTER 5: ALTERING THE GLYCOSYLATION PATTERN OF MITHRAMYCINS

INTRODUCTION

Biological activity of mithramycin

The aureolic acid antibiotic mithramycin (**70**) has been well-studied by various groups for the tremendous potential it exhibits as an antineoplastic, Alzheimer's, and Parkinson's drug (*79, 83-84, 86, 90-91, 93*). As an anticancer agent, it has been used to treat Paget's bone disease, bone-related malignancies, and testicular carcinoma (*88*). It binds to the minor groove of GC-rich DNA, especially in proto-oncogenes *c-src* and *c-myc*, and as such, it is a *de facto* inhibitor of Sp1-dependent pathways (*87, 89, 91, 94*). Overexpression of Sp1 has been implicated in Alzheimer's disease and colon, breast, and pancreatic cancers. Mithramycin binds as a homodimer in head to tail fashion, that is coordinated by a Mg^{2+} cation (*87*). Structurally, mithramycin consists of a tricyclic core and possesses a dihydroxy-methoxy-oxo-pentyl side chain at 3-position, which is responsible for interaction with the phosphate backbone (*86*). The disaccharide consisting of D-olivose, D-olivose is important for binding to DNA, perhaps by stacking on top of the dimer aromatic core (*86*). The trisaccharide is also essential, because the D-mycarose moiety is positioned in the floor of the minor groove of DNA, and it provides stabilization of the MTM-Mg^{2+}dimer complex by virtue of hydrogen bonding with both strands of DNA(*98*). Mithramycin, however, is contraindicated due to severe hepatic, renal, and gastrointestinal cytotoxicities (*86*).

Mithramycin has also found use as part of a multi-drug therapy with bevacizumab in down-regulating VEGF (vascular epithelial growth factor) (*111*). Mithramycin itself has been independently confirmed to decrease *c-myc/c-src* expression in cancer cell lines, inhibiting Sp1 from binding to these promoters (**70** inhibits *c-src* promotion in a luciferase-reporter assay to about 30% of the expression of a control sample not treated with **70**) (*86*). As such, mithramycin has been increasingly employed in multi-drug therapies to target cancers that are refractory to treatment with a single chemotherapeutic. Mithramycin's Sp1-dependent inhibition effectively blocks all downstream cell signaling pathways that depend on Sp1-promoted upregulation, and this may work in tandem with other compounds that target some other aspect of cancer cell/Alzheimer's proliferation,

for example VEGF or beta amyloid precursor protein, for example (*86-87, 90-91, 93, 111*).

Despite its tremendous potential as a cancer therapeutic, mithramycin and the other first generation aureolic acids suffer from severe drawbacks. Because these molecules are biosynthesized naturally, they have not been optimized for binding to mammalian targets, such as protooncogenes, and as such, these drugs exhibit detrimental effects in healthy somatic cells and cancer cells alike. Due to the severe cytotoxic side effects of **70**, combinatorial biosynthetic methods have been employed in the Rohr and Salas labs to generate novel mithramycin analogues with better drug properties: lessened cytotoxicity or higher potency (e.g. IC_{50}). These alterations have focused on derivatizing the polyketide aglycone and substitutions in the saccharide pattern. These "second generation" combinatorial mithramycin/premithramycin analogues have revealed tremendous insights into the biosynthesis and of **70.** Furthermore, the isolation of several analogues has revealed unanticipated substrate flexibility displayed by the enzymatic machinery, and some of these analogues possess enhanced potency and reduced cytotoxicity as compared to mithramycin.

Pathway engineering studies to alter the mithramycin/premithramycin polyketide skeleton

The Rohr and Salas labs have previously conducted several inactivations of genes responsible for modification of the polyketide. Inactivations of *mtmMI* and *mtmMII* revealed the functions of these encoded proteins as the 4-*O*-methyltransferase that installs the methoxy group onto 4-demethylpremithramycinone (**27**), and the 7-*C*-methyltransferase responsible for installing the 7-*C*-methyl sidechain of **70** (*23*). The accumulation of 7-demethylmithramycin (**82**) in the *S. argillaceus* (*mtmMII*-) strain revealed that all of the downstream biosynthetic enzymes could process the 7-desmethyl substrates, however, this compound failed to exhibit any *in vivo* cytotoxicity, indicating the importance of the 7-*C*-methyl group for binding to DNA (**Figure 41**) (*86*)**.** Disruption of *mtmOI* and *mtmOIII* did not result in disruption of mithramycin biosynthesis, however, disruption of *mtmOII* led to production of premithramycinone G (**87**, **Figure 41**) (*24*). This improperly cyclized molecule reveals important implications for MtmOII's role in early mithramycin biosynthesis, either by installing a ketone to

allow for fourth ring cyclization and/or installation of the 2-oxygen of **70**. Inactivation of *mtmOIV* resulted in the accumulation of premithramycin B (**80**), a tetracyclic premithramycin that features the intact trisaccharide (D-olivose, D-oliose, D-mycarose) at 2-position and the disaccharide at 6-position (D-olivose, D-olivose) (**Figure 41**) (*95*, *103*). Elucidation of the structure of **80** lead to the elaboration of MtmOIV being a highly specific Baeyer-Villiger monooxygenase (BVMO) responsible for oxidative cleavage of the fourth ring to afford the canonical tricyclic mithramycin scaffold (*95, 103, 109, 175*).

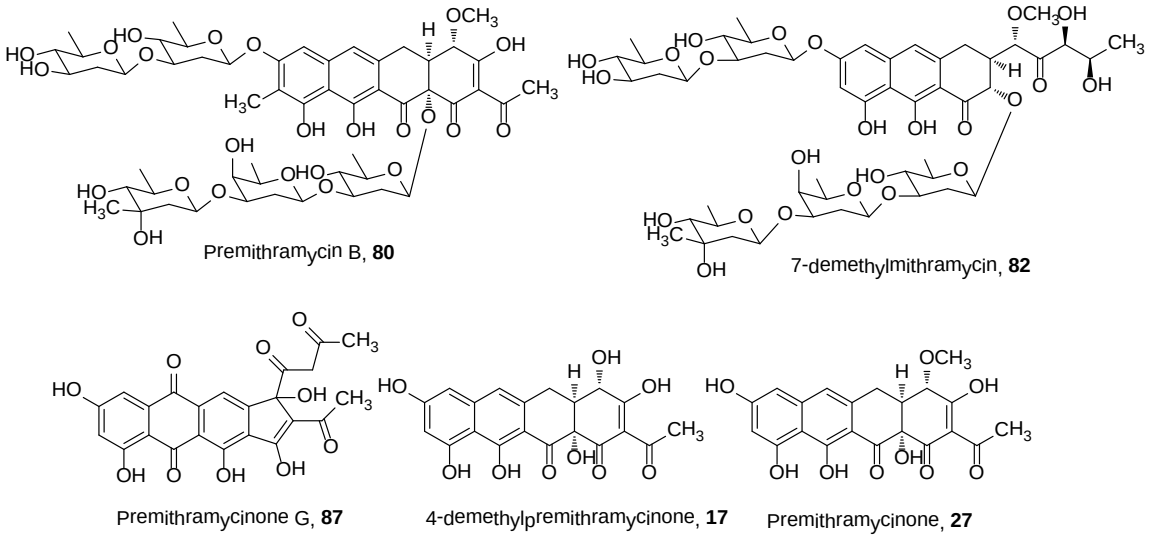

Figure 41 Premithramycin and mithramycin-type compounds from inactivating genes responsible for altering the polyketide-derived portion of mithramycin.

MtmOIV is unique in that it is a BVMO for which the substrate is known. The fact that MtmOIV only recognizes a fully glycosylated premithramycin B molecule indicates that this rigid structural specificity is an intrinsic means by which the *mtm* pathway avoids wasteful and promiscuous generation of less active mithramycins with fewer sugars (*95, 103, 109, 175*). However, this same rigidity also prevents MtmOIV from turning over novel premithramycin substrates that may bear unusual or foreign deoxysugars.

The inactivation of the *mtmW* gene resulted in novel mithramycins with unexpectedly shorter side chains, thereby revealing its role in the 3-sidechain ketoreduction step of the β-diketone intermediate (**Figure 13**). The accumulated products were called mithramycin SK (for shortened ketone) (**128**), demycarosyl-mithramycin SK, mithramycin SDK (shortened diketone) (**129**) , and mithramycin SA (**130**) (shortened

acid) (**Figure 42)** (*89, 97*). The anticipated product was the mithramycin β-diketone compound (**81**), however, because this possesses a highly reactive β-diketone motif, subsequent carbon migration rearrangements occur. If water attacks the 2"-ketone, a hydrate can form. A retro-aldol reaction results in subsequent deprotonation of one of the hydroxyl protons that can restore the ketone, and result in severance of the 2"-3" carbon-carbon bond, which affords mithramycin SA (**130**). Or, if water abstracts a proton from the 3"-hydroxy, carbon migration can result in shifting of the 4"-acyl group to the 2"-position (**Figure 42**). From this species, water either attacks the aldehyde directly, resulting in elimination of formic acid, which affords mithramycin SK (**128**), or water abstracts a proton from 2"-hydroxyl, which results in elimination of formaldehyde, and formation of mithramycin SDK (**129**) (**Figure 42**). Feeding experiments with [1-^{13}C]-acetate and [1,2-$^{13}C_2$]-acetate confirmed that the 3"-carbon is excised during this rearrangement (*97*).

The antitumoral activities of **128**-**130** were evaluated in 60 cell line panel by using the NCI sulforhodamine B cytotoxicity assay. Mithramycin SA **130** demonstrated very weak binding to Salmon testes DNA and exhibited weak *in vivo* cytotoxicity, due in large part to the fact that its 3-side chain is much too short to interact specifically with the phosphate backbone of DNA (*86-87*). Mithramycin SK **128**, however, demonstrated 1500-fold less cytotoxicity than mithramycin, and furthermore, it demonstrated up to 90 times higher activity than mithramycin in squamous, melanoma, leukemia, and CNS cancer lines (*86-88*). Furthermore, mithramycin SK was able to inhibit polyploidy in actively dividing cancer cells (*112*). Mithramycin SDK **129**, however, severely inhibits Sp1-

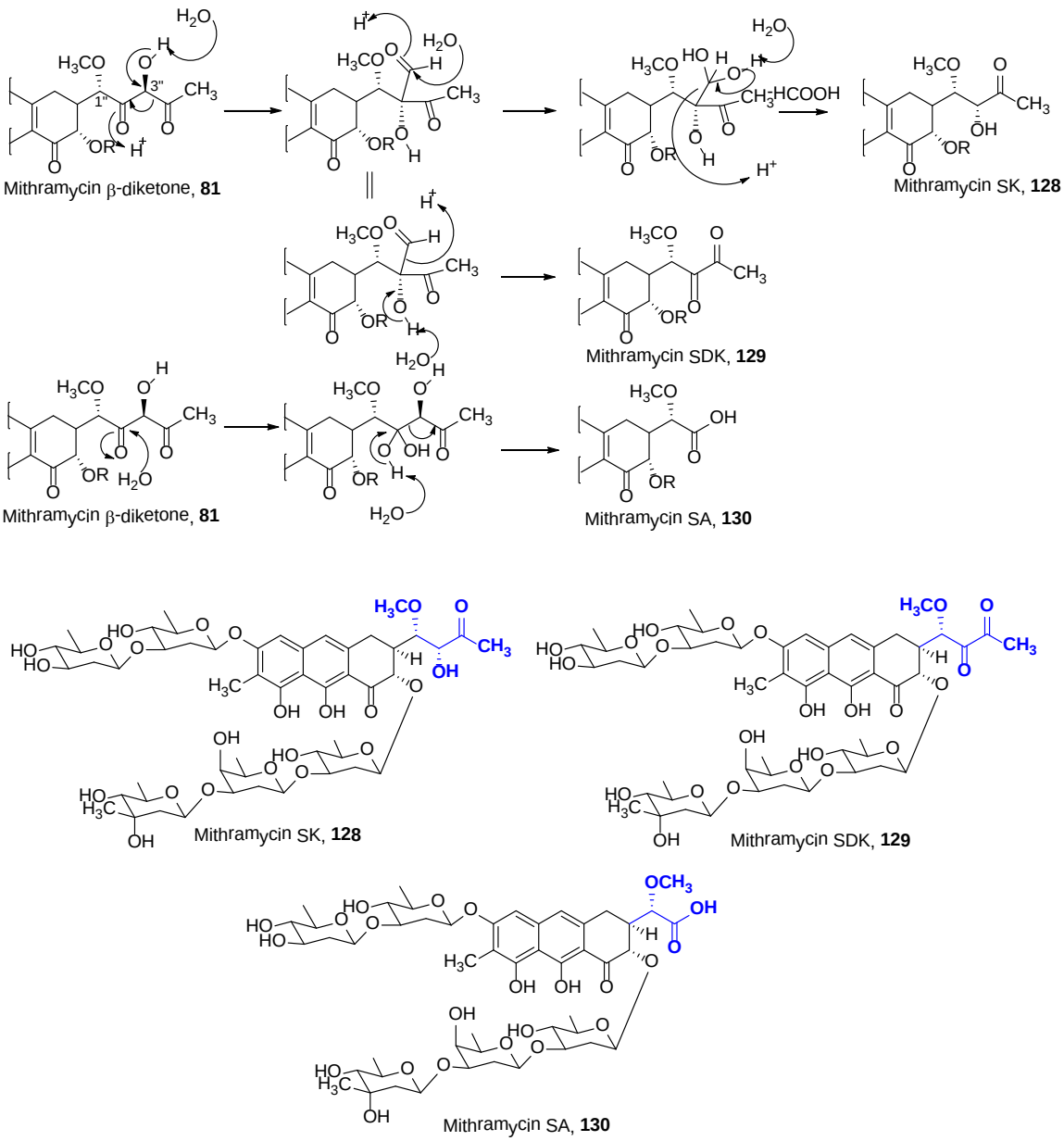

Figure 42 Spontaneous rearrangements of Mithramycin SK (**128**), mithramycin SDK (**129**) and mithramycin SA (**130**).
Mechanisms for rearrangements of 3-pentyl side chain of mithramycin β-diketone to form mithramycin SK (**128**), mithramycin SDK (**129**), and mithramycin SA (**130**)**.** Structures of metabolites from *mtmW*-disrupted strain *S. argillaceus* M7W1 with shortened side chains in blue.

dependent pathway transcription, up to 90% at a 100 nM concentration in a luciferase-based reporter assay (as compared to 40% for **70** and 60% for **128**) (*89*). The IC_{50} for

129 was up to 2-fold lower than for **70** and **128** (*87*). Astonishingly, when orthotopic ovarian tumor xenografts were introduced into a mouse model, then treated with 400 μg/kg/day of **70**, **128**, or **129**, median survival in the **129** treated group was 80 days (as compared to 55 for the control group without mithramycin treatment), yet 4 of the 10 mice treated with **129** survived past 100 days tumor free (*87, 89*). These studies cemented mithramycin SDK as the best-in-class aureolic acid derivative with most potential for further clinical trials.

Altering the glycosylation pattern of premithramycins/mithramycins through "flooding" of the pathway with nucleoside-diphosphate-activated deoxysugars and inactivation experiments

As discussed in Chapter 4, glycodiversification is a powerful strategy for altering the structure and activity of a particular drug. The successful implementation of this strategy requires the accumulaton of nucleoside-diphosphate-activated deoxysugars that are not normally produced in the strain and the successful interrogation of a donor-flexible glycosyltransferase. The Salas group demonstrated the effectiveness of interrogating the substrate-flexible ElmGT with a variety of plasmid-borne NDP-deoxysugars. In Chapter 4, the successful generation and structure elucidation of a new ketosugar-bearing tetracenomycin (**127**) illustrated this approach *in vivo*.

The mithramycin biosynthetic pathway features five glycosyltransfer events and four glycosyltransferases, therefore inactivation experiments of various deoxysugar biosynthetic genes and glycosyltransferases were undertaken (*98-99*). Inactivation of *mtmGI*, *mtmGII*, *mtmGIII*, and *mtmGIV* and feeding of 4A-deolivosyl-premithramycin B to the *mtmGI*-deleted mutant established the unambiguous order of glycosylation events leading to **70** (*96, 100, 105*) (Figure 13). While inactivation of several of the deoxysugar biosynthetic genes (e.g. *mtmV*, *mtmU*, *mtmC*, *mtmDE*) resulted in accumulation of early pathway intermediates premithramycinone or premithramycin A1, inactivation of *mtmTIII* and *mtmC* revealed an unanticipated accumulation of premithramycins and mithramycins with alterations to the saccharidal moieties (*88, 98-99*) (**Figure 43**). These molecules revealed substrate flexibility on the part of MtmGIV and/or MtmGIII towards accepting ketosugars.

As a further extension of their work, the Salas lab envisioned that transformation of *S. argillaceus* with various sugar plasmids could result in mithramycin molecules with substitutions in the saccharide chain.

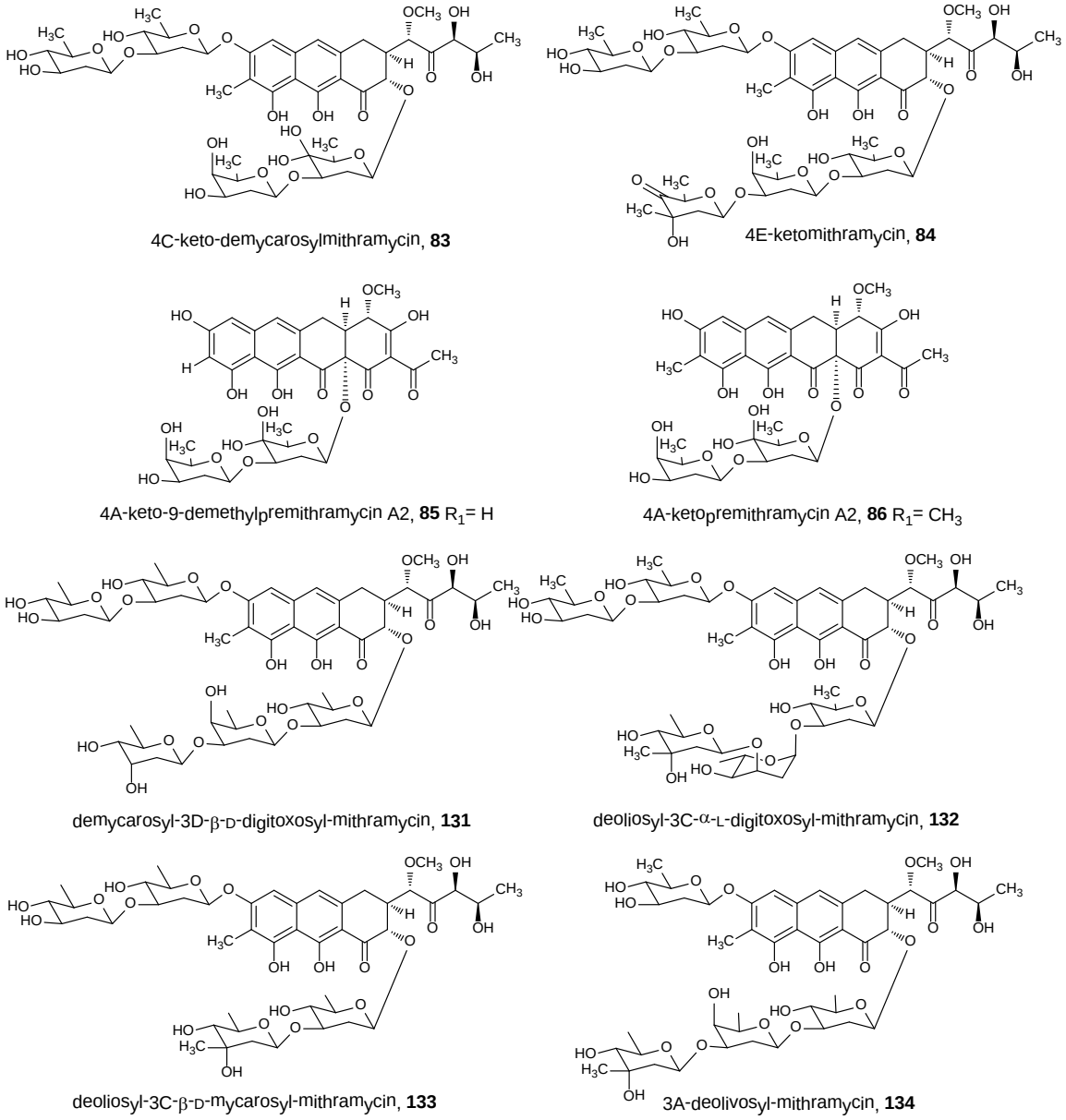

Figure 43 Structures of mithramycin-type compounds resulting from *S. argillaceus mtmTIII*⁻ and *mtmC*⁻ (**83-86**) inactivations.
Mithramycins resulting from overexpression of NDP-L-digitoxose plasmid in *S. argillaceus.*

Overexpression of several of these resulted in novel mithramycins that were active or slightly less active than **70** in the cancer cell lines tested (*111*). When plasmid pLNBIV (encodes NDP-L-digitoxose biosynthesis) was introduced into *S. argillaceus via*

protoplast transformation, four new mithramycins were identified (**131-134**) with substitutions in the saccharide pattern (*112*). Two of these compounds were the result of "jamming" of glycosyltransferases, **133** and **134**. From a biosynthetic perspective, these compounds were interesting and revealed unexpected flexibility by the glycosyltransferases. Very likely, jamming of MtmGIV/MtmGIII results in accumulation of **133** and jamming of MtmGII results in accumulation of **134**. **133** indicated an acceptor flexibility of *mtmGIV* and possibly acceptor/donor flexibility of MtmGIII to transfer NDP-D-mycarose to premithramycin A1. **132** was unique from all mithramycins generated by these experiments, because it was the only compound to feature an L-sugar (NDP-L-digitoxose), yet a simple ring flip to the $^4C_1$ conformer likely accounts for its acceptance by MtmGIII (the $^4C_1$ conformer of NDP-L-digitoxose possesses the same stereochemistry at 3- and 4-position as NDP-D-oliose, the natural substrate of MtmGIII). All compounds exhibited unanticipated substrate specificity on behalf of MtmOIV, but compound **131** demonstrated much improved bioactivity over **70** in many of the cancer cell lines tested by the NCI (*112*). In ER+ MCF-7 breast cancer cells, mithramycin induced 37.8% apoptosis, whereas **131** induced 64.8% apoptosis. In ER- MDA-231 cells, mithramycin only induced 2.6% apoptosis; however, **131** induced an amazing 63.6% apoptosis. **131** is essentially an isostere of mithramycin, possessing the same stereochemistry of the E sugar (NDP-D-digitoxose vs. NDP-D-mycarose), yet it lacks the 3-*C*-methyl branch. Because the D-mycarose moiety sits in the floor of GC-rich minor grooves and forms hydrogen bonds with both strands of DNA, the methyl group may cause steric interference (*98*). Apparently, the D-digitoxose substitution greatly enhances the activity of **131** as compared to mithramycin, yet, in both ER+ and ER- breast cell cancer lines, it possessed the highest level of biological activity compared to the other glycorandomized mithramycins produced in these studies. ER- breast cell cancer desparately requires novel treatments to overcome its considerable chemoresistance (*112*). This validates the approach of glycodiversification towards optimizing the ligand binding of mithramycin-type compounds.

MtmOIV is the Baeyer-Villiger Monooxygenase (BVMO) that catalyzes fourth ring scission in biosynthesis of mithramycin

MtmOIV catalyzes the key oxidative cleavage of mithramycin biosynthesis that results in generation of an active tricyclic compound(*95, 103, 109, 175*). MtmOIV and its sister enzyme from chromomycin A_3 biosynthesis, CmmOIV, have both been crystallized and their active site residues determined through mutagenesis experiments (*176*) (**Figure 44**). Some of these mutants, such as MtmOIV-R204A feature mutations in key residues, such as arginine 204, that are responsible for limiting MtmOIV's tolerance to premithramycin substrates. In this case, arginine 204 is considered to be a key gatekeeper residue that allows for the stabilization of the trisaccharide chain of premithramycin B in the enzymatic active site. Mutation of arginine 204 to alanine achieved a significant reduction of the K_m of MtmOIV-R204A with respect to its affinity for premithramycin B, while retaining a comparable k_{cat} to the wildtype enzyme. As such, MtmOIV reduces bound FAD to FADH *via* NADPH, after which diatomic oxygen binds to form the key peroxyflavin species (**Figure 44**). The peroxyflavin species attacks the 1-position carbonyl, forming the Criegee intermediate, oxygen inserts into the carbon-carbon bond, and the lactone collapses to form mithramycin DK (**81**). Substrate flexible MtmOIV mutants will be useful for future combinatorial generation of mithramycins, and part of the aim of this work is to generate strains and characterize suitable premithramycins for such an approach.

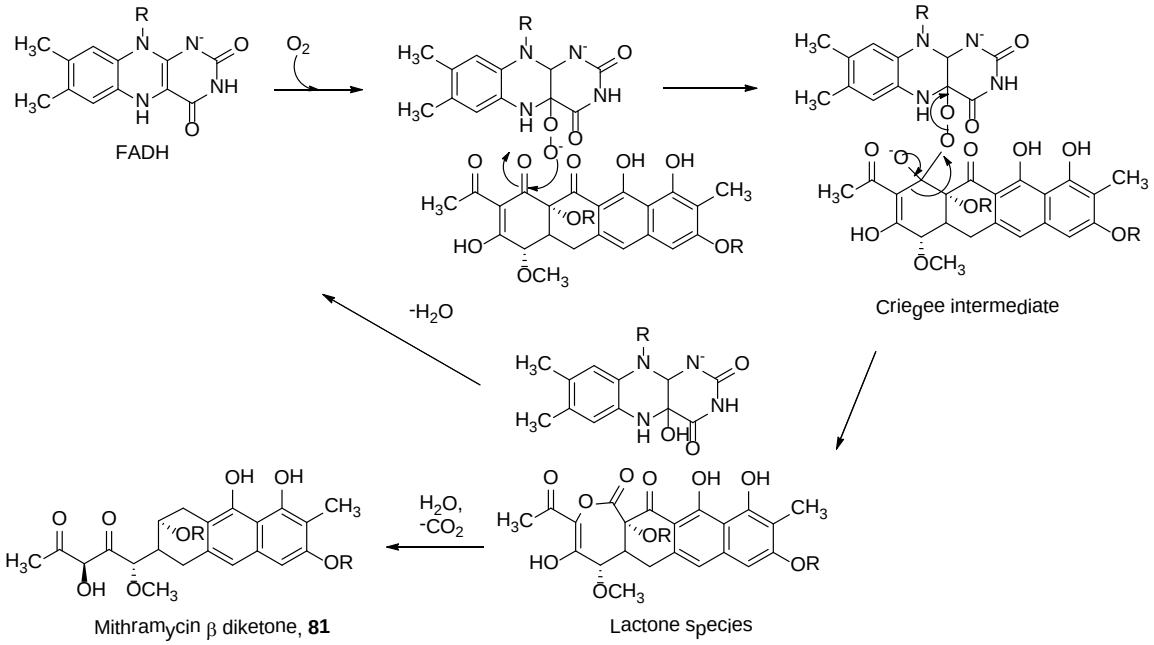

Figure 44 MtmOIV-catalyzed Baeyer-Villiger monooxygenative cleavage of premithramycin B.

RESULTS AND DISCUSSION

Despite the considerable advances that have been made to understand the biosynthesis and generate novel derivatives of mithramycin, new interrogations of biosynthetic machinery involving uninvestigated deoxysugar donor substrates and recombinations of sugar plasmids with restricted mutants of *S. argillaceus* remain to be tested. The work of the Salas group in heterologous expression of NDP-deoxysugar cassettes served as the impetus and inspiration for envisaging new mithramycin scaffolds. Based on what is already known about the substrate flexibility of the *mtm* GTs, several novel strains were prepared and preliminary investigation of the compounds accumulated in these novel strains was undertaken.

In preliminary screening of recombinant strains for the presence of additional mithramycin-type/premithramycin compounds, methanolic extracts of recombinant strains were compared to extacts of the parent wild-type or restricted *S. argillaceus* strain. Additional peaks were visualized *via* a UV photodiode array detector on a Waters HPLC-MS as discussed in **Chapter 3**. Premithramycin-type compounds are clearly distinctive based on their tetracyclic ring system, and as such, they possess a characteristic UV spectrum with absorption maxima at 230 nm, 280 nm, 329 nm, and 424 nm. Mithramycins, with a tricyclic chromophore and 3-aliphatic side chain, were clearly identified with absorption maxima at 230, 278, 317, and 411 nm (*111*). In this case, the hypsochromic shift from 329 nm to 317 nm from the MtmOIV-catalyzed opening of the fourth ring is particularly diagnostic for distinguishing premithramycin and mithramycin-type compounds.

The generation of a novel fermentation method towards demycarosyl-3D-β-D-digitoxosyl mithramycin and generation and structure elucidation of demycarosyl-3D-β-D-digitoxosyl mithramycin SK were achieved using a different methodology different from that of the EntreChem^{TM} biotech company (personal communication, Dr. Rohr), and our lab's methodology is being drafted into a manuscript for submission soon.

Generation of S. argillaceus wildtype *strains overexpressing NDP-activated L-sugars*

Several strains were reported by Salas *et al*. to produce novel premithramycin-type compounds, but were not further investigated. As such, the production spectrum of these strains could serve as a useful point of reference for evaluating the production of other deoxysugar plasmid-containing *Streptomyces argillaceus* strains. *Streptomyces argillaceus* was independently transformed with pLN2 (NDP-L-olivose), pLNBIV (NDP-L-digitoxose), and pRHAM (NDP-L-rhamnose) to afford strains *S. argillaceus* (pLNBIV), *S. argillaceus* (pLN2), and *S. argillaceus* (pRHAM), respectively. As reported previously, extracts of *S. argillaceus* (pRHAM) accumulated only mithramycin, premithramycin A1, and a small amount of an unknown compound (*111*). This compound demonstrated a mass of 557 *amu* in (-)APCI-MS mode [M-H], which could correspond to 14 mass units higher than premithramycin A1. This compound could correspond to a D-mycarose-substituted premithramycin A1, or more likely, premithramycin A1' with the 7-*C*-methyl group. *S. argillaceus* (pLN2) produced mithramycin and two premithramycin type compounds with a mass each of 674 *amu* [M-H] in APCI (-ve) mode. As reported previously, these could correspond to two novel premithramycins with disaccharides corresponding to D-olivose-1,3-L-olivose and L-olivose-1,3-L-olivose (*111*). What is clear from the overexpression of NDP-activated L-sugars in *S. argillaceus* is that they result in "jamming" of the glycosyltransferases, and the accumulation of these premithramycin-type compounds. This is not unexpected, because the *mtm* GTs normally bind D-configurated sugars, and in only a handful of cases have glycosyltransferases from secondary metabolism been shown to accommodate both D- and L-configurated sugars: GilGT (NDP-L-rhamnose, NDP-D-olivose, NDP-D-fucofuranose), ElmGT (many sugars, see **Chapter 4)**, and UrdGT2 (NDP-L-rhodinose and NDP-D-rhodinose) (*177*). Furthermore, much of this jamming seems to occur with regards to MtmGIII.

In extracts of *S. argillaceus* (pLNBIV), ten metabolites in addition to mithramycin (**70**) were accumulated (**Figure 45**). Four of these are known to be mithramycins described previously (**131-134**), and as such, were able to be assigned according to retention time, UV spectrum, and mass analyses. In addition, six premithramycin type compounds were accumulated. Three of these were identified based on identical retention time with standard compounds and mass analyses as

premithramycin A1 (**76**), premithramycin A1', and premithramycinone. However, three of these compounds are unknown and exhibit atypical UV-Vis absorption spectra for premithramycin type compounds. These three compounds exhibit a sharp absorption maximum at 406 nm. From this experiment, it was apparent that mithramycin was still the major metabolite in the production spectrum, and extract from *S. argillaceus* (pLNBIV) was essential to developing a robust HPLC semi-preparative separation program. Also, the three unidentified premithramycins may be good candidates for pathway engineering. This could be achieved by inserting a copy of a mutagenized *mtmOIV* gene (e.g. R204A) into the chromosome of *S. argillaceus* (pLNBIV).

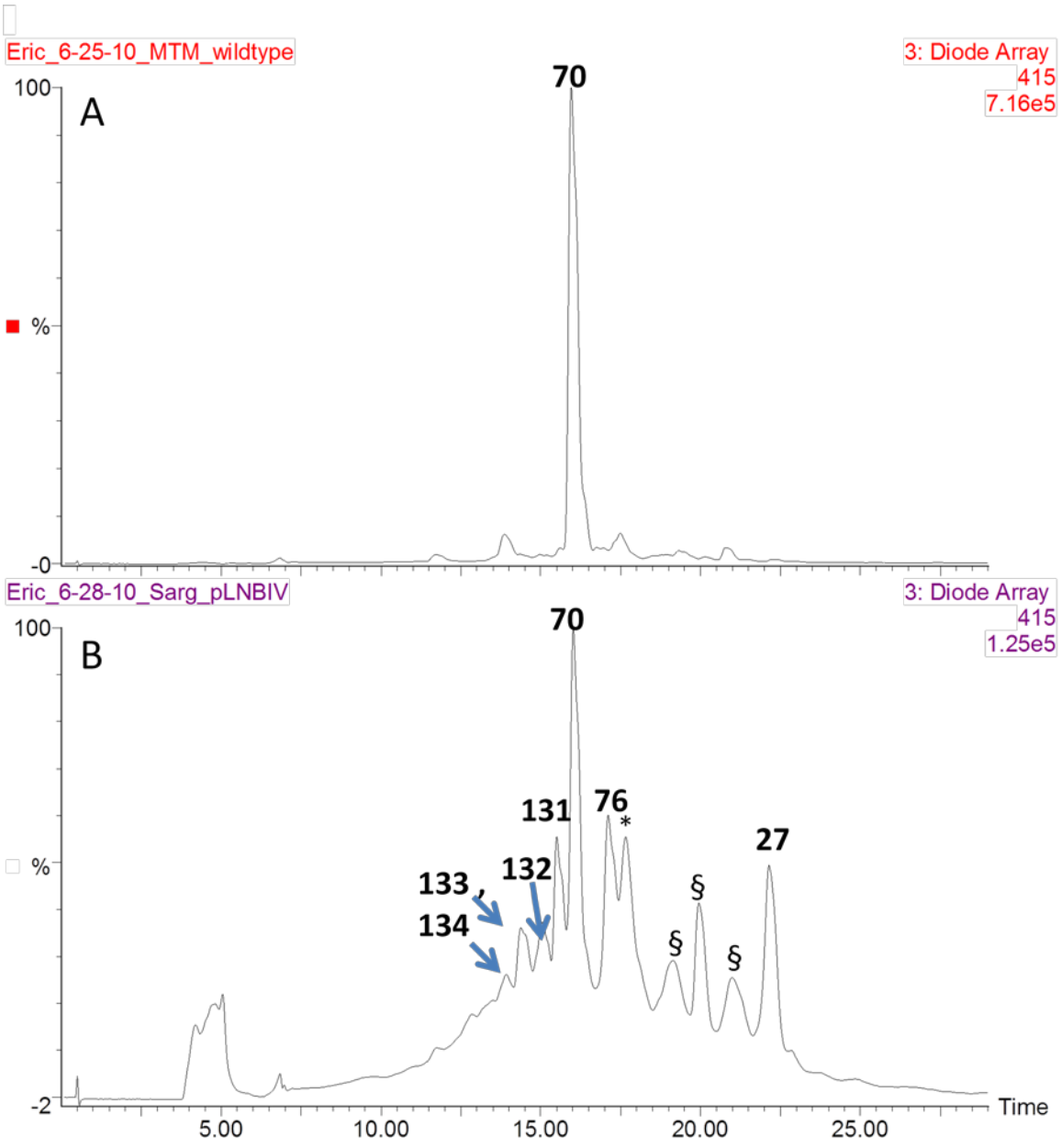

Figure 45 HPLC traces of metabolites of *S. argillaceus* (pLNBIV).
Trace A represents extracts from *S. argillaceus* wildtype, which produces mithramycin (**70**). Trace B represents extracts from *S. argillaceus* (pLNBIV), which produces **70** along with novel mithramycins with substitution in the saccharide chains (**131-134**, **Figure 44**), premithramycin A1 (**76**), * represents the 7-*C*-methyl derivative of **76**, premithramycin A1'. **27** is premithramycinone and § indicates premithramycin-type metabolites with atypical UV (a sharp UV absorption maximum at ~406 nm).

Expression of aminosugar and 2'-hydroxysugar plasmids in S.argillaceus *wildtype*

Deoxysugars directing the biosynthesis of various aminosugars (see **Chapter 4**) were introduced into *S. argillaceus* wildtype. Most of these deoxysugar plasmids failed

to alter mithramycin biosynthesis, however, the *S. argillaceus* (pDesIII) (NDP-N,N-didemethyl-D-desosamine) strain accumulated premithramycin A1 and an additional premithramycin-type compound that was not investigated. Additionally, the *S. argillaceus* (pDmnI) strain accumulated premithramycinone and premithramycin A1, which may result from accumulation of NDP-L-rhamnose jamming MtmGIII, as in the *S. argillaceus* (pRHAM) strain (**Figure 46**). Furthermore, an additional premithramycin was accumulated with R_t=21.3 min^{-1}.

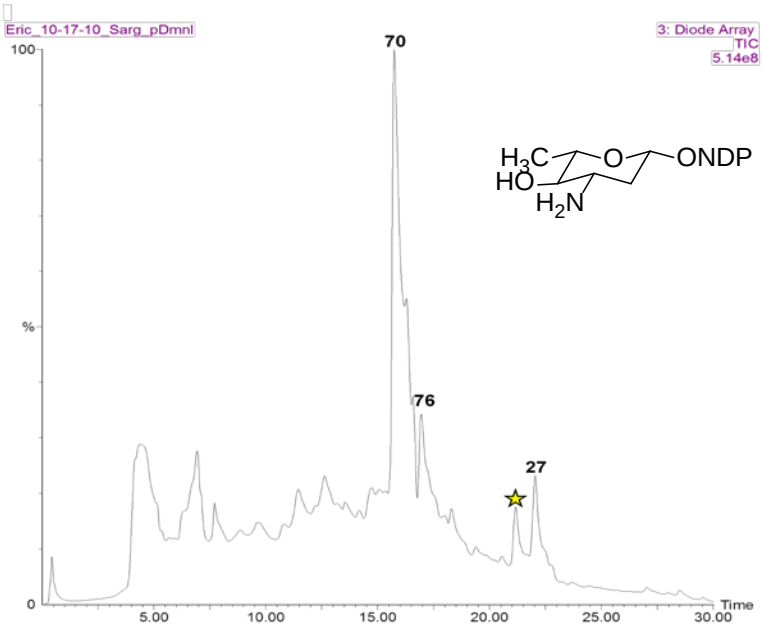

Figure 46 HPLC chromatogram of the metabolites from *S. argillaceus* (pDmnI) strain. This strain accumulates one unknown (yellow star) premithramycin in addition to mithramycin, premithramycin A1, and premithramycinone. The structure of NDP-L-acosamine is indicated as a reference for what the plasmid should biosynthesize.

The 2'-hydroxysugar plasmids pVIR*II, pEN3, pFUCO, and pFUCOII were all introduced into *S. argillaceus* wildtype *via* protoplast transformation. It was envisioned that these plasmids should redirect mithramycin biosynthesis to incorporate 2'-hydroxylated sugars. In the case of pVIR*II or pEN3, it was envisioned that either NDP-4-keto-D-virenose or NDP-D-virenose would be surrogate substrates for MtmGIV and would be incorporated at sugar E position. In the case of pFUCO or pFUCOII, it was envisaged that NDP-D-fucopyranose or NDP-D-fucofuranose would be accumulated in the strain and incorporated into one of the saccharide chains (e.g. perhaps sugar D position, substituting NDP-D-fucose for NDP-D-oliose). Or, alternatively, some collaboration between plasmid-borne enzymes and endogenous sugar tailoring machinery

could result, or perhaps even jamming of the glycosyltransferases, as is witnessed in **133** and **134** in the case of *S. argillaceus* (pLNBIV). Expression of pFUCO and pFUCOII failed to result in new glycosylated mithramycins/premithramycins. However, pVIR*II and pEN3 both successfully generated the same production pattern, indicating that likely the *C*-methyltransferase *chryCMT* at least is functional in these strains, and possibly the virenosyl 4-ketoreductase *chryU*, as well. In these strains, *S. argillaceus* (pEN3) and *S. argillaceus* (pVIR*II), one new mithramycin was accumulated as a minor compound, and 3 premithramycins were accumulated. The premithramycins correspond to premithramycin A1, premithramycinone, and an unknown tetrasaccharidal premithramycin with a mass of 977 *amu* [M-H] in (-) APCI-MS mode, perhaps corresponding to a tetrasaccharidal premithramycin with an NDP-D-virenose moiety in E position (**Figure 47**). The accumulation of premithramycin A1, as seen in other recombinant strains, indicates that NDP-D-virenose or one of its encoded intermediates jams MtmGIII and that perhaps 2'-hydroxysugars are poor substrates for *mtm* pathway GTs. The mithramycin-type compound in these strains evinces a mass of 1099 *amu* in (-) APCI-MS mode, which could be expected for a compound 16 mass units larger than mithramycin. Such an addition could be accounted for by the presence of an additional oxygen substituent, which would be expected if an NDP-D-virenose or its 4'-epimer were incorporated at E position. This plasmid was also introduced into *S. argillaceus* M7W1 strain to generate *S. argillaceus* M7W1 (pVIR*II), which was not further investigated. Both strains are promising for further structure elucidation studies and possibly for structure activity relationship (SAR) studies.

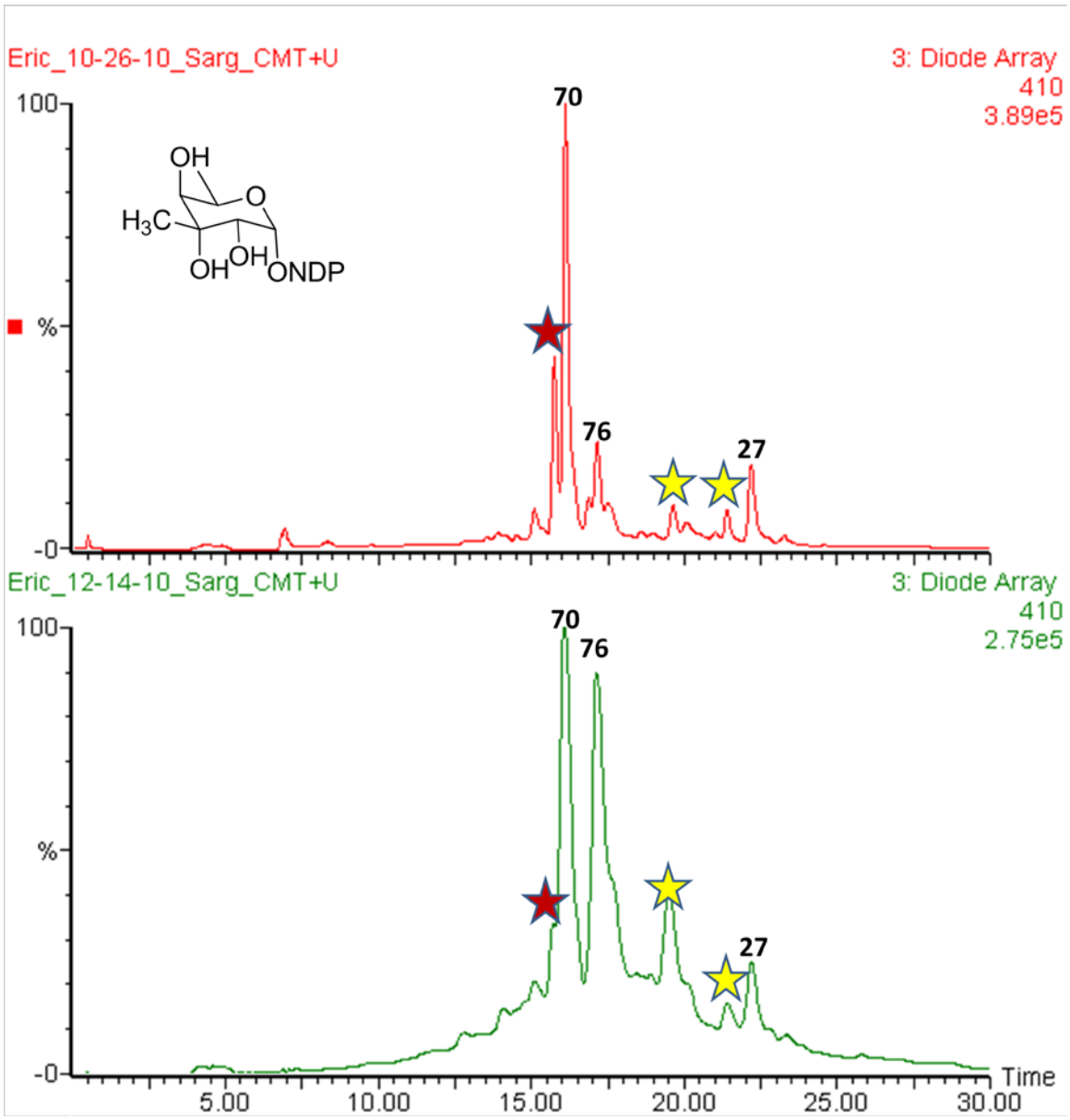

Figure 47 HPLC chromatogram of the metabolites from NDP-D-virenose expressing strains.
(Upper Trace) extracts of *S.argillaceus* (pVIR*II) and (Lower Trace) *S. argillaceus* (CMT+U). Strains both accumulate premithramycin A1, premithramycinone, a mithramycin-type compound R_t= 15.5 min^{-1}(1099 *amu*, [M-H] (-) APCI-MS), and a premithramycin type compound R_t=19.5 min^{-1} (977 *amu*, [M-H] (-) APCI-MS).NDP-D-virenose included as reference. Red stars are mithramycin-type compounds, gold stars are premithramycin-type compounds.

Generation of Streptomyces argillaceus (pKOL)

Given that MtmGIV has a demonstrated capacity for accepting ketosugar donor substrates (*98*), it was envisioned that transformation of *S. argillaceus* wildtype with plasmid pKOL would possibly result in flooding the pathway with NDP-4-keto-L-olivose and its attachment in E position (see **Chapter 4**). Extracts of the resulting strain *S. argillaceus* (pKOL) revealed production of a new mithramycin-type compound with R_t=16.1 min^{-1} as the major product, in addition to a few minor premithramycin-type compounds (**Figure 48**). This mithramycin demonstrated a mass of 1069 *amu* [M-H] in (-) APCI-MS mode, which indicates a loss of 14 mass units from mithramycin. This mass did not correspond with any type of ketosugar-containing compound as was expected, as the anticipated keto/hydrate pseudomolecular ions were not present. Most likely, this 14 *amu* difference corresponds to the difference of a *C*-methyl group. As a result, it appeared as though there was a substitution of the D-mycarose moiety with an unmethylated 2,6-dideoxysugar. Comparison with extract for *S. argillaceus* (pLNBIV) indicated the identical retention time with **131**, and interestingly, the mithramycins from the pLNBIV mutant that resulted from "jamming" of the glycosyltransferases were absent in the pKOL-harboring strain.

Accumulation of **131** in extract of *S. argillaceus* (pKOL) was unexpected, but it can be explained by collaboration of plasmid-borne biosynthetic machinery with endogenous host enzymes. pKOL produces many intermediates that are also used by *mtm* pathway enzymes, which may be accepted by host tailoring genes and the glycosyltransferases. In the normal biosynthesis of mithramycin, the genes are expressed at a rate that maintains a balanced enzymatic flux, which results in the efficient biosynthesis of mithramycin. When pKOL is expressed *in vivo*, this enzymatic flux is imbalanced by the manifestation of foreign enzymes, which presently flood the pathway with NDP-activated deoxysugar donors and may divert it into unforeseen directions. The accumulation of some of these donor sugar substrates may effectively deceive the endogenous glycosyltransferases, which results in the accumulation of side products. With respect to the *in vivo* expression of pKOL, it is remarkable that none of the other mithramycins that "jammed" the glycosyltransferases in the pLNBIV overexpression are present. As such, it can be asserted that the lack of the plasmid-borne 4-ketoreductase is

responsible for removing the bottleneck that jammed the glycosyltransferases in previous experimentation. In the case of pLN2 overexpression, only premithramycins were obtained in addition to **70**, which indicates that the NDP-L-olivose is mostly accumulated in this strain and cannot be processed further than the disaccharide. Furthermore, the 4-ketoreductase gene *eryBIV* in pLNBIV must lead to the predominant accumulation of NDP-L-digitoxose, which can be transferred into the sugar D position by MtmGIII, but only as the $^4C_1$ ring-flipped conformer, which is similar to NDP-D-oliose with regards to stereochemistry (**Figure 49**). The D-digitoxose in E position likely results from accumulation of NDP-4-keto-2,6-dideoxyglucose, which is produced by *oleSEVW* in pKOL, which is then processed by one of two routes: 1) acceptance by MtmGIV and attached in E position, followed by MtmTIII-facilitated tautomerisation of the 3-OH to axial configuration, and finally 4-ketoreduction; or 2) MtmTIII tautomerisation/4-ketoreduction and glycosyltransfer of NDP-D-digitoxose (**Figure 49**).

From a pharmacognosy perspective, the selective accumulation of **131** in a yield of ~5-6 mg per liter as the primary metabolite is a major boon, considering that the D-digitoxose substitution in E position has been shown to have significant antitumoral improvement over mithramycin, especially in ER- breast cancer cell lines. The complex production pattern of *S. argillaceus* (pLNBIV) and the hassle of separation have prohibited the further development of this compound. Therefore, this experiment demonstrates a more effective route towards isolation of **131** *via* an improved fermentation method of a genetically manipulated strain of *Streptomyces argillaceus*.

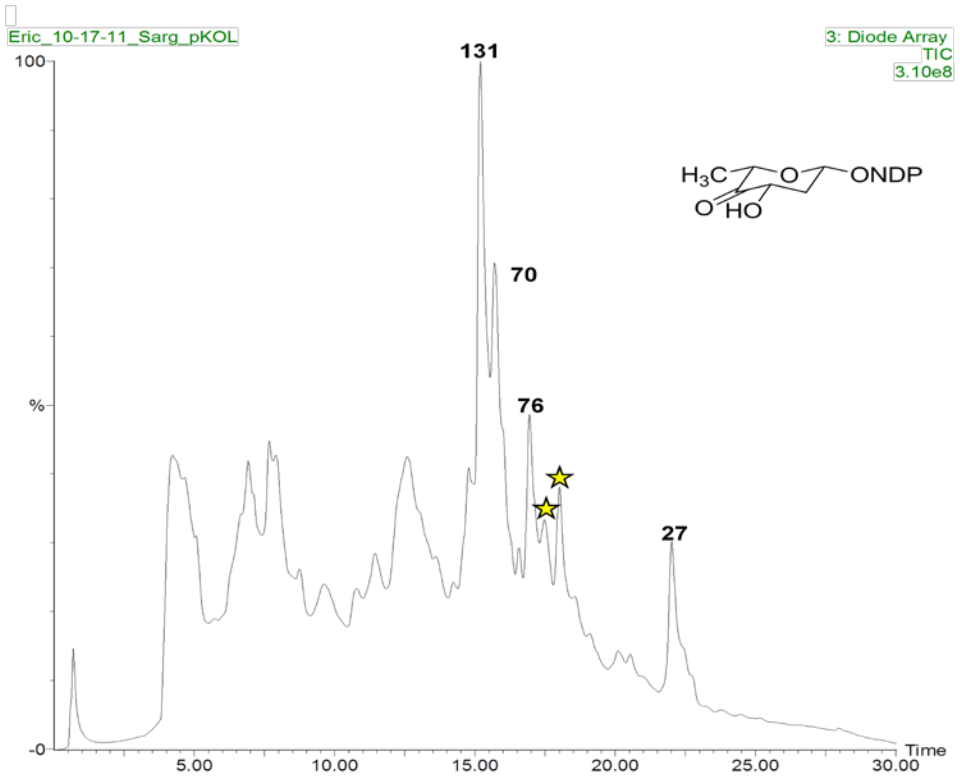

Figure 48 HPLC chromatogram trace of metabolites from S. argillaceus (pKOL) strain. The main compound accumulated is demycarosyl-3D-β-D-digitoxosyl mithramycin (**131**). NDP-4-keto-L-olivose structure indicated as a reference for the sugar that pKOL biosynthesizes.

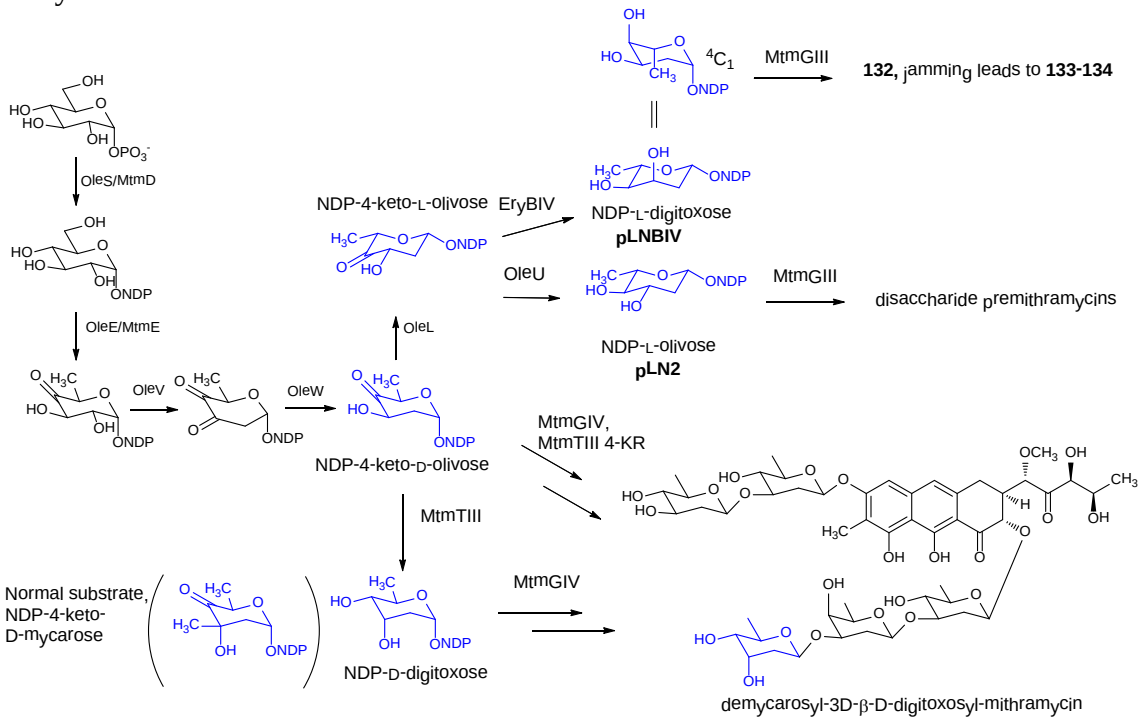

Figure 49 Sugar biosynthesis of deoxysugar plasmids in *S. argillaceus*.

Generation of Streptomyces argillaceus M7W1/pKOL strain and identification of metabolites

Having established an improved fermentation method for the production of **131** in *S. argillaceus* (pKOL), a recombination experiment was envisioned in which a restricted mutant of *S. argillaceus* could be transformed with pKOL to achieve novel mithramycin(s) with a modified polyketide framework and a sugar substitution. For this experiment, *S. argillaceus* M7W1, which features a chromosomal disruption of the *mtmW* gene resulting in mithramycins with shorter aliphatic side chains (**128-130**), was used as a transformation host. The resulting recombinant strain, *S. argillaceus* M7W1/pKOL was fermented for 5 days and methanolic extracts were visualized *via* HPLC/MS. As predicted, several new peaks corresponding to mithramycin-type compounds were visualized (**Figure 50**). Premithramycin A1 and premithramycinone were accumulated. Known metabolites mithramycins SK and SDK were recognized based on their UV-Vis spectrum, comparison of retention time with standard compound (mithramycin SK R_t=17.1 min^{-1} and mithramycin SDK R_t=19.2 min^{-1}), and mass in (-) APCI-MS mode (1053 *amu* for mithramycin SK and 1051 *amu* for mithramycin SDK). One other mithramycin-type compounds was recognized as demycarosyl-mithramycin SK based on its mass in (-) APCI-MS mode (910 *amu*). Two new compounds that were not identified in extracts of *S. argillaceus* M7W1 demonstrated mithramycin-type UV absorption and possessed R_t=Δ-0.6 min^{-1} as compared to the corresponding mithramycin SK and SDK (**Figure 50**). These compounds demonstrated masses that were 14 *amu* less than their mithramycin SK and SDK counterparts, indicating a substitution of an unmethylated 2,6-dideoxysugar at E position (1039 *amu* for **135** and 1037 *amu* for **136**, [M-H] (-) APCI-MS). This indicated that the molecular weight for **135** was 1040 *amu* and for **136** was 1038 *amu*, which suggested that these new compounds might pertain to demycarosyl-3D-β-D-digitoxosyl mithramycin SK (**135**) and SDK (**136**) (**Figure 51**).

135 and **136** combine two of the most advantageous structural features as determined by previous SAR studies of mithramycin analogues (*89, 97, 111-112*). Such heterologous expression experiments using restricted mutants have been performed before, namely transformation of sugar plasmids into a strain blocked in biosynthesis of

NDP-D-oliose (*111*), however, this marks the first successful attempt at combining two beneficial bioisosteres in a single mithramycin molecule: a shortened 3-aliphatic side chain with a sugar substitution.

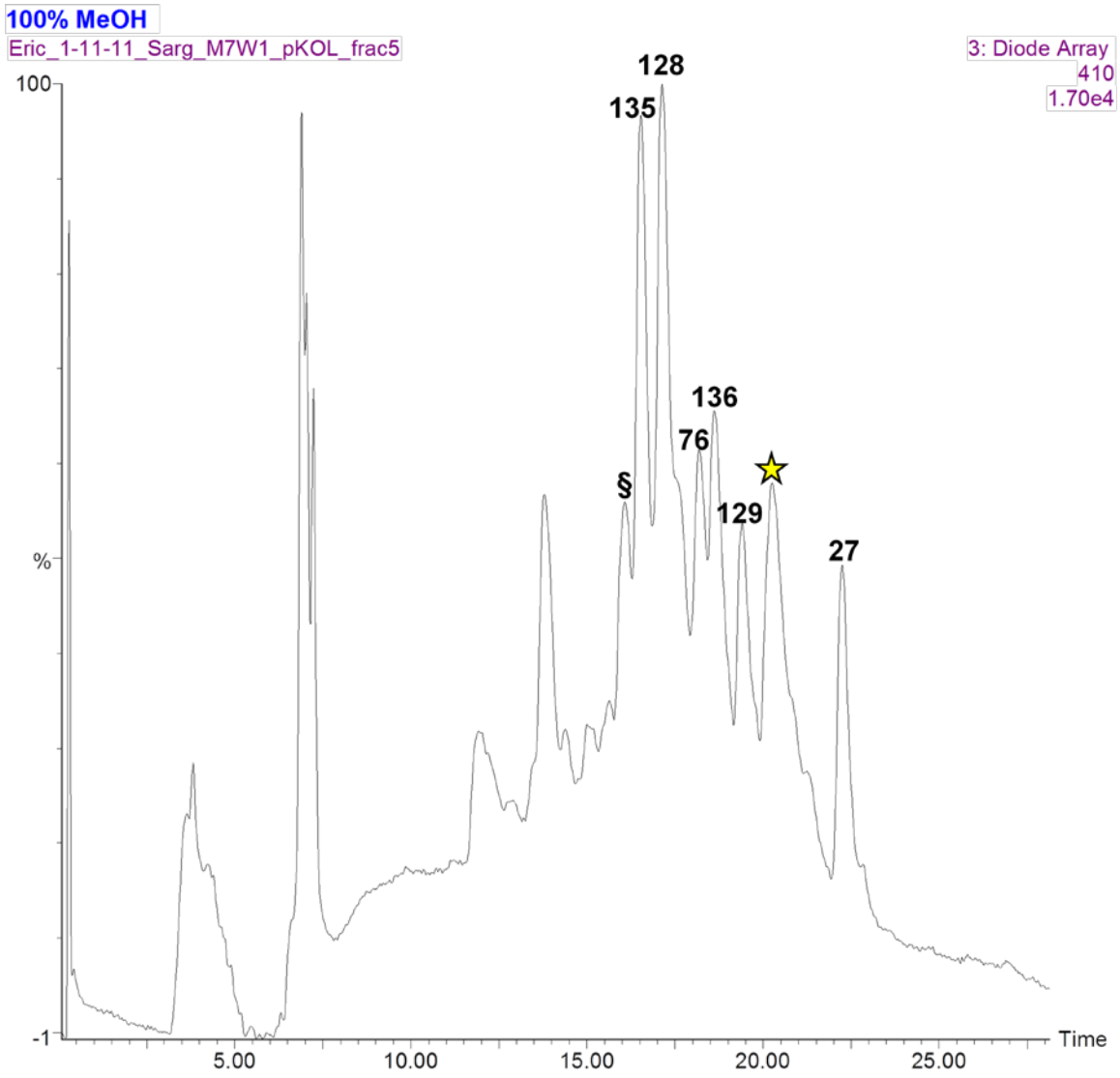

Figure 50 HPLC chromatogram of metabolites from *S. argillaceus* M7W1/pKOL strain. **135** and **136** correspond to new metabolites generated in this strain. § indicates demycarosyl-mithramycin SK normally produced in *S. argillaceus* M7W1.

demycarosyl-3D-β-D-digitoxosyl-mithramycin SK, **135**

demycarosyl-3D-β-D-digitoxosyl-mithramycin SDK, **136**

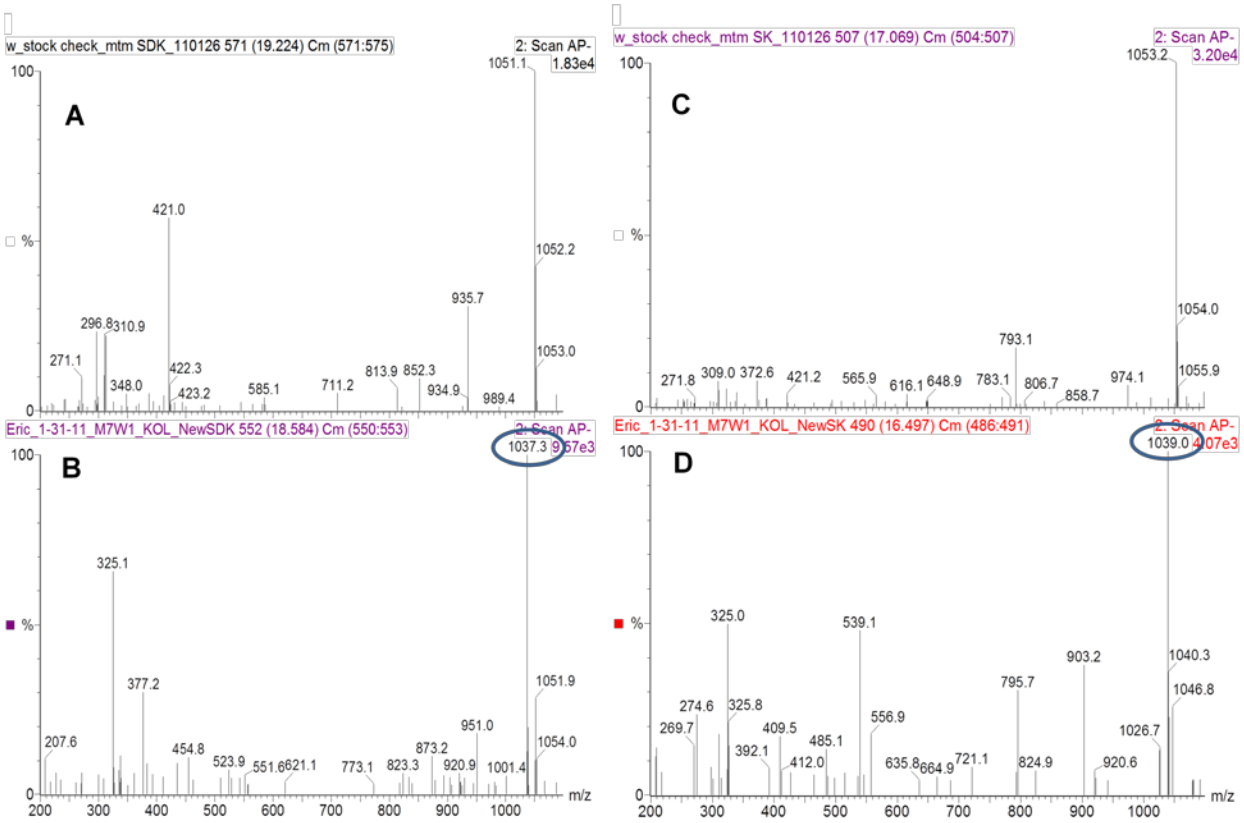

Figure 51 (Upper) Suggested structures of new mithramycin-type compounds isolated from *S. argillaceus* M7W1/pKOL recombinant strain. (Lower) (-) APCI-MS mode mass data corresponding to the [M-H] molecular ion peaks of A) mithramycin SDK, B) **136**, C) mithramycin SK, and D) **135**.

Isolation and structure elucidation of demycarosyl-3D-β-D-digitoxosyl mithramycin SK

A 10.0 liter fermentation of *S. argillaceus* M7W1/pKOL was carried out in a two step process and for five days (See **Experimental** Section). To prevent the accumulation of mithramycin SA-related metabolites, the pH of the production medium (10.0 liters of liquid R5A medium, see **Bacterial Strains and Culture Conditions**) was adjusted to 6.95. After the third day, twenty-five milliliters of sample was extracted with twenty-five milliliters of ethyl acetate acidified with 50 microliters of formic acid, concentrated, and injected for HPLC-MS analysis. The fermentation was allowed to continue for an additional twenty-four hours if premithramycins were present in the production spectrum, likely due to the flooding of the mithramycin pathway with NDP-deoxysugar substrates that had not yet been processed by MTM glycosyltransferases. The fermentation was stopped after five days before the accumulation of mithramycin SA-metabolites.

The culture was acidified to pH 5.5 and extracted three times with an equal volume of ethyl acetate, then was concentrated. The resulting yellow-brown extract was fractionated over a reverse phase C_{18} silica column and the mithramycin compounds were purified via reverse phase HPLC. From this, 22 milligrams of **135** were able to be purified, while the other mithramycin components were produced in insufficient yields or too poorly separated to allow for structural elucidation.

The structure of the new mithramycin analogue was determined through HR-ESI mass spectral and 1D- and 2D-NMR spectroscopic methods, including ^{1}H-NMR, ^{13}C-NMR, ^{1}H-^{1}H-gCOSY, ^{1}H-^{13}C-HSQC, and HMBC methods. Further comparison with published literature concerning the sugar signals of **131**(*112*) was corroborated with the HSQC and HMBC correlations. The low resolution APCI (-ve mode) mass spectral analysis indicated an [M-H] peak of 1039.4 *amu* for **135**, while the APCI (+ mode) indicated a parent peak of 1063.2 *amu* corresponding to [M+Na]. The HR-ESI mass spectral analysis indicated a found mass of 1039.4432 *amu* corresponding to a [M-H] peak and 1063.4337 *amu* corresponding to [M+Na], which established the molecular weight of the new mithramycin to be 1040.4 *amu* and the formula to be $C_{50}H_{72}O_{23}$. This revealed a difference of 14 *amu* between this compound and mithramycin SK, which could correspond to a difference of a single methylene group.

The ^{1}H-NMR and ^{13}C-NMR showed the characteristic signals of the tricyclic mithramycin polyketide skeleton (see NMR table in **Experimental**). Two aromatic protons were observed as singlets (δ_H 6.87 and δ_H 6.69) as 5-H and 10-H, respectively, while the 2-H signal (δ_H 4.89, δ_C 78.0) appeared as a doublet with a large axial splitting shifted downfield due to the neighboring 1-CO moiety. The 4_{ax} and 4_{eq} signals appeared as doublet of doublets (4-H_{ax} at δ_H 3.25 (dd 16, 12 Hz), and 4_{eq} at δ_H 3.00 (dd 16, 3)) with a large germinal splitting and a,a or a,e couplings, respectively, with the 3-H proton (δ_H 3.50 dddd 16, 12, 4, 1; δ_C 41.5). The 7-CH_3 was evident based on a signal at δ_C 9.3 in the ^{13}C spectrum and δ_H 2.47 singlet in the ^{1}H spectrum, indicating it to be the intact aromatic methyl group characteristic of mithramycins. The position of 7-CH_3 was confirmed based on HMBC correlations of the methyl protons with the 6-C and 8-C carbons (**Figure 52**). Nine aromatic signals were detectable in the ^{13}C spectrum, while the 9-C was too small to observe. This essentially left the problem of elucidating the structure of the new mithramycin to alterations in the C-3 side chain and delineating the nature of the saccharidal chains.

The C-3 side chain of the new mithramycin was found to differ considerably from mithramycin due to the ^{1}H and ^{13}C signals. The 1'-OCH_3 was found as a singlet (δ_H3.83, δ_C 59.7), while the 2'-H proton was shifted downfield in the ^{1}H spectrum (δ_H 4.85, δ_C 80.2) as a doublet with a two Hertz coupling. An additional acetoxy methyl singlet was found downfield at δ_H 2.49, which indicated an alpha ketone group. Most importantly, an HMBC correlation between the δ_H 2.49 4'-H methyl protons and the C-3 carbonyl (δ211.0) established the proximity of the 3'-CO and 4'-CH_3 groups. HMBC correlations between the 2'-H and 3-C, 1'-methoxy, and 4'-C carbons further evidenced the presence of a shortened ketone side chain.

The ^{13}C spectrum indicated five anomeric signals (δ97.9, δ99.5, δ98.5, δ100.1, δ101.9) and five deoxysugar methyl groups (δ17.8, δ19.0, δ19.4, δ19.4, δ19.7), while the 3E-CH_3 of D-mycarose was missing. The ^{1}H-^{13}C-HSQC revealed five aliphatic methylene carbons (δ37.9, δ41.6, δ38.5, δ33.3, and δ40.2), the sum total of which identified the characteristic presence of five 2,6-dideoxysugar moieties. The ^{1}H-^{1}H-gCOSY revealed five deoxysugar spin systems stretching from 1H-6H. Furthermore, five anomeric signals presented in the ^{1}H spectrum (δ4.96, δ5.06, δ5.44, δ5.57, δ5.66)

with a large diaxial coupling and an a,e splitting, indicating them to be D-configured 2,6 dideoxysugars as per Klyne's rule (*36*). The ^{13}C and ^{1}H upheld the presence of the 6-*O*-D-olivose-1,3-D-olivose disaccharide, while the C sugar was likewise determined to be a 2-*O*-connected D-olivose based on HMBC correlations between the 1C proton and 2-C and 2-H and 1C anomeric carbon. The HMBC spectrum correlated the 1D anomeric proton to the 3C carbon, while the presence of a characteristic broad doublet δ_H 4.10 (three Hertz coupling) indicated the 4D proton to be equatorial, which confirmed the presence of D-oliose at the D-sugar position. The E sugar was found to be missing the 3E-CH_3 signal from the ^{13}C spectrum and the missing methyl singlet from the ^{1}H spectrum, while the ^{1}H-^{1}H-gCOSY indicated a spin system for this sugar stretching from 1E-6E. It was confirmed to be a β-D-digitoxose sugar, due to the presence of an equatorial 3E proton at δ_H 4.46 (broad d, 3 Hz) and shifted signals for the 2E (δ_C 40.2), 3E (δ_C 69.1), 4E carbons (δ_C 72.1). The couplings of the 2-axial proton (δ_H 2.01 ddd 13, 10, 3 Hz), the 4E proton (δ_H 3.63 dd 9, 3 Hz), and the COSY-correlation between $2E_{eq}$, $2E_{ax}$, and 4E with the 3E proton established the D-digitoxose stereochemistry. Altogether, the structure of **135** was confirmed to correspond to the new compound, demycarosyl-3D-β-D-digitoxosyl mithramycin SK.

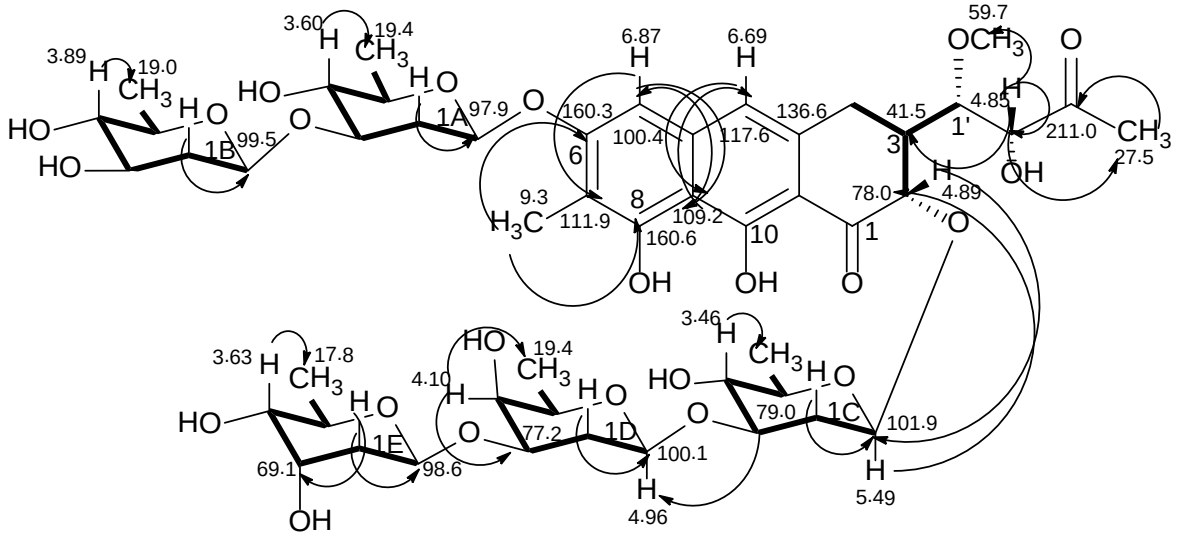

Figure 52 ^{1}H-^{1}H-COSY (▬), and selected HMBC (→) correlations for demycarosyl-3D-β-D-digitoxosyl-mithramycin SK.

Generation of Streptomyces argillaceus *M7W1/pKAM*

As a further extension of the hypothesis that ketosugar plasmids may be potentially useful for producing differentially glycosylated analogues of mithramycin without untoward "jamming" of the glycosyltransferases, an NDP-L-cinerulose biosynthesizing plasmid was constructed from the NDP-L-rhodinose plasmid, pLNRHO, by deleting the 4-ketoreductase gene, *urdZ3*, resulting in plasmid pKAM. It was envisioned that such a plasmid might direct biosynthesis of NDP-4-keto-2,3,6-trideoxy-D-glucose, which might then be reduced by an *mtm* pathway 4-ketoreductase to NDP-D-amicetose, which has then been shown to be transferred by MtmGI very efficiently into A position (**Figure 52**). Previously, Salas *et al*. isolated a novel mithramycin when pFL844 was expressed in *S. argillaceus* wildtype with a D-amicetose replacing the A and B disaccharide (**Figure 52**).

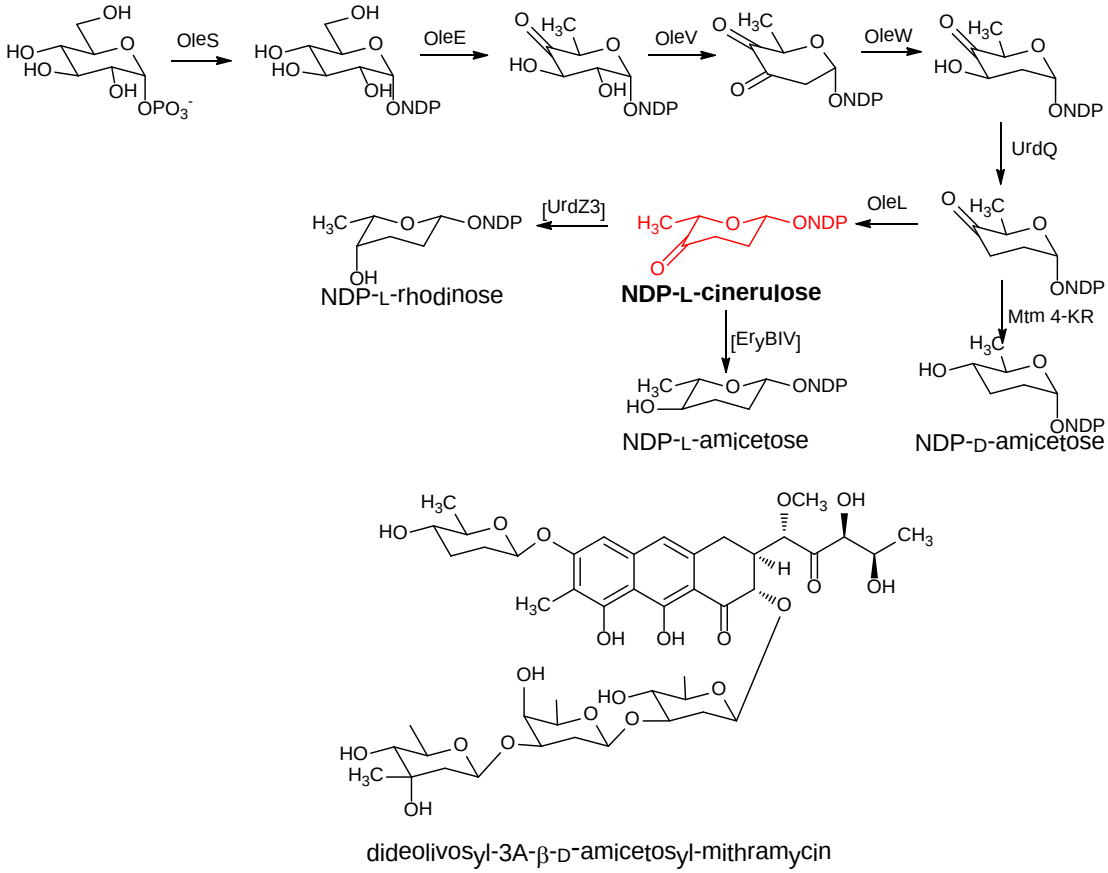

Figure 53 Biosynthetic pathways to trideoxygenated sugars.
NDP-L-cinerulose (pKAM) indicated in red. 4-ketoreductases deleted from pathway (EryBIV/UrdZ3) indicated in brackets. Structure of dideolivosyl-3A-β-D-amicetosyl-mithramycin.

If the endogenous *mtm* sugar ketoreductases can collaborate efficiently with pKAM-borne machinery, then overexpression of pKAM in the *S. argillaceus* M7W1 strain should result in the shortened chain derivatives of dideolivosyl-3A-β-D-amicetosyl-mithramycin. Surprisingly, extracts of *S. argillaceus* M7W1/pKAM contained no new peaks corresponding to mithramycins and only minor amounts of mithramycin SK. Instead, four peaks corresponding to premithramycins in excellent yield were accumulated. Two of these peaks corresponded to premithramycin A1 and premithramycinone, yet two others corresponded to unknown premithramycins with one sugar and four sugars, respectively (**Figure 53**). The monoglycosylated premithramycin evinced a molecular weight of 528 *amu*, as determined by (-) APCI-MS. This corresponds to 16 mass units less than premithramycin A1, which likely indicates a 2,3,6-trideoxygenated sugar at C position. This could correspond either to a D- or L-configurated amicetose sugar, which has never been characterized as being attached at C-position before. From a biosynthetic perspective, such an attachment is unproductive, because this sugar lacks the 3-OH handle which is necessary to establish the next glycosidic bond. The premithramycin with four sugars demonstrated a mass of 928 *amu*, as determined by (-) APCI-MS, which corresponds to a premithramycin with possibly trisaccharide and monosaccharide chains, respectively. The mass suggests that one or possibly two trideoxygenated sugars are incorporated onto this molecule, which given the sugar's lack of a 3-OH, would necessarily restrict their glycosylation to the A and E sugar positions. Given that the amicetosyl-substituted mithramycin is efficiently turned over by MtmOIV, this premithramycin compound likely has a sugar attached in either E or A position that interfere with its turnover by MtmOIV. This compound may be an excellent candidate for interrogating the substrate flexibility mutant MtmOIV oxygenases, given that it possesses a fully intact trisaccharide chain. Furthermore, the production spectrum of this recombinant strain is not complex, and the yield of these compounds appears to be quite reasonable, which are encouraging for further structure elucidation and pathway engineering experiments.

The absence of the dideolivosyl-3A-β-D-amicetosyl-mithramycin derivatives with shortened side chains was surprising. Quite possibly, MtmGI demonstrates flexibility to NDP-L-cinerulose or one of the pKAM-encoded pathway intermediates, and

glycosylation of this sugar at A position results in a molecule which MtmOIV cannot recognize. The presence of a monosaccharidal premithramycin was also surprising, as this sugar has not been reported at C position before; yet, in previous combinatorial biosynthesis experiments involving amicetose sugars, those pathways progressed efficiently towards fully-formed mithramycins. Therefore, this compound may not have been detected in those other strains. Some jamming of glycosyltransferases by NDP-L-cinerulose may be responsible for the accumulation of this latter compound. As a result, it is hypothesized that transformation of pFL844 into *S. argillaceus* M7W1 would very likely result in accumulation of these shortened chain dideolivosyl-3A-β-D-amicetosyl-mithramycin derivatives.

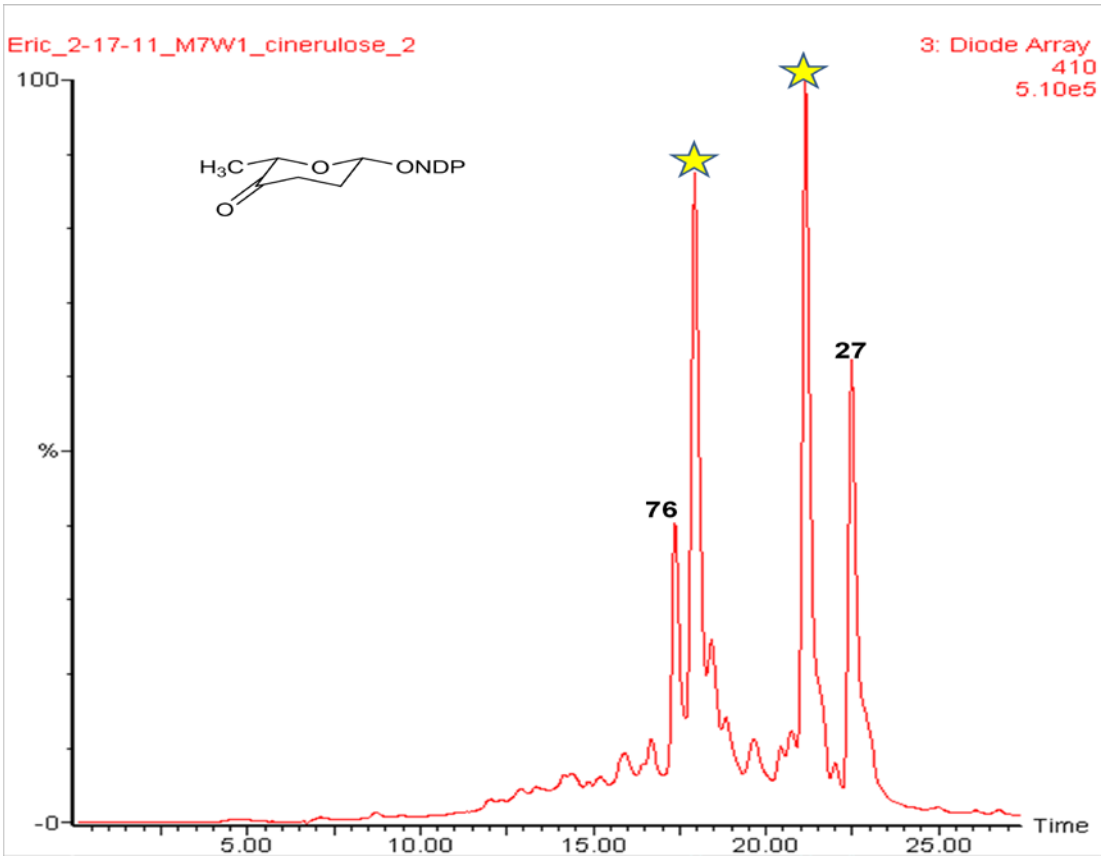

Figure 54 HPLC chromatogram of metabolites from S. argillaceus M7W1/pKAM. This plasmid reprograms the biosynthesis to generate two novel premithramycins with attached trideoxygenated sugars. Monosaccharide premithramycin, 526 *amu* (-)APCI-MS, R_t=21.3 min^{-1}. Premithramycin with four sugars, 928 *amu* (-) APCI-MS, R_t=18.0 min^{-1}.

SUMMARY

In summary, **Chapter 5** has described some preliminary microbiology work towards glycodiversification of the mithramycin scaffold by interrogating the *mtm* pathway glycosyltransferases with "deoxysugar plasmids" that encode novel deoxysugars not previously transformed into *Streptomyces argillaceus*. Through this work, several new recombinant strains with markedly altered production patterns have been produced, and the metabolites from these strains have been preliminarily characterized *via* UV-vis, APCI-MS mass, and retention time analyses. A couple premithramycin compounds with four sugars have been identified, which could be isolated, structurally characterized, then used as substrates for interrogating mutant MtmOIV oxygenases. Or, perhaps, an *in vivo* approach employing an integrative vector, such as pSET152, with a cloned copy of such an MtmOIV (e.g. MtmOIV-R204A) under *ermE** promotion could be integrated into the chromosome of such a strain.

Additionally, the promising antitumoral mithramycin compound **131** was produced selectively in fermentations of *S.argillaceus* (pKOL), which overexpresses the NDP-4-keto-L-olivose pathway. The flooding of this pathway with NDP-activated sugar donors results in accumulation of NDP-4-keto-2,6-dideoxy-D-glucose, which is then transferred to E position as a D-digitoxose. As a further extension of this work, the *mtmW*-disrupted mutant, *S. argillaceus* M7W1, was used as a transformation host for pKOL, which lead to the elaboration of two shortened-chain mithramycins, **135** and **136**. The structure of **135** was confirmed via HR-ESI mass spectral and 1D- and 2D- NMR spectroscopic methods as demycarosyl-3D-β-D-mithramycin SK, which may exhibit exciting new biological activity. The presence of two rationally designed and potentially pharmaceutically advantageous bioisosteres is unprecedented for a mithramycin molecule, and this also reflects on the substantial power of combinatorial biosynthesis to achieve improved analogues of complex natural products.

Furthermore, as Chapters 4 and 5 have demonstrated, the flooding of sugar biosynthetic pathways with ketosugars provides a new approach towards the glycodiversification of polyketide molecules. Because there are so few examples of glycosyltransferases in nature that can transfer a ketosugar, such interrogations are largely serendipitous and unexploited. In Chapter 4, ElmGT was found to have an

unusual capacity to transfer NDP-4-keto-L-olivose to its aglycone, which revealed an unanticipated flexibility towards an NDP-ketosugar. In Chapter 5, by utilizing the same sugar cassette, the *S. argillaceus* mithramycin biosynthetic pathway was interrogated in the same fashion. Although MtmGIV has been demonstrated to attach NDP-D-ketosugars to its acceptor substrate(s), no such ketosugar-decorated polyketide was detected. Instead, the selective accumulation of **131** was achieved, which revealed that by pooling NDP-4-keto-D-olivose and NDP-4-keto-L-olivose, glycosyltransferase jamming was effectively circumvented (as exhibited by the absence of other mithramycin congeners or the appreciable accumulation of premithramycins in the production spectrum.) Just as important, the NDP-4-keto-L-olivose did not appear to serve as a substrate for any of the other glycosyltransferases, and in theory, it may play an important role in inhibiting MtmC to allow for the accumulation of NDP-4-keto-D-digitoxose. Therefore, in *S. argillaceus*, the flooding of the MTM pathway with NDP-4-keto-D-olivose is a necessary pre-requisite to steer the pathway towards production of NDP-4-keto-D-digitoxose, which is likely accepted in the active site of ketoreductase MtmTIII in the absence of its *C*-3 methylated substrate. Furthermore, because the D-digitoxose substitution is sufficiently tolerated by MtmOIV to allow for opening of the fourth ring, this strategy could be repeated in the *S. argillaceus* M7W1 strain to achieve the shortened ketone side chain.

EXPERIMENTAL

Table 10 Plasmids used in Chapter 5

Plasmid Name	**Relevant Characteristics**	**Reference**
pLN2	Amp^R, Tsr^R. *OleVWSELUY* under *ermE** promotion. NDP-L-olivose.	(*135*)
pRHAM	Amp^R, Tsr^R. *OleVWSE* under ermE* promotion. NDP-L-rhamnose.	(*134*)
pMP*UII	Amp^R, Tsr^R. *OleVW, cmmUII, OleY, MtmDE,* under divergent *ermE** promotion. NDP-D-oliose.	(*160*)
pDmnI	Amp^R, Tsr^R. *OleSEVLU*	Madan Kharel, Personal

	DnrJ under *ermE** promotion. NDP-L-acosamine	Communication
pDmnII	Amp^R, Tsr^R. *OleSEV, DnrJUV* under *ermE** promotion. NDP-L-daunosamine	Madan Kharel, Personal Communication
pDesI	Amp^R, Tsr^R. *DesIII*, *DesIV*, *DesI* under *ermE** promotion. NDP-4-amino-6-deoxy-D-glucose (**121**)	Madan Kharel, Personal Communication
pDesII	Amp^R, Tsr^R. *DesIII*, *DesIV*, *DesI*, *DesII* under *ermE** promotion. NDP-3-keto-4,6-dideoxy-D-glucose (**122**).	Madan Kharel, Personal Communication
pDesIII	Amp^R, Tsr^R. *DesIII*, *DesIV*, *DesI*, *DesII*, *DesV* under *ermE** promotion. NDP-3-N,N-didemethyl-D-desosamine (**123**).	Madan Kharel, Personal Communication.
pKOL	Amp^R, Tsr^R. *OleVWSELY* under *ermE** promotion. NDP-4-keto-L-olivose.	This work.
pFUCO	Amp^R, Tsr^R. *gilU*, *ravDE* cloned under *ermE** in pUWL201PW. Intended to produce NDP-D-fucose.	This work.
pFUCOII	Amp^R, Tsr^R. *gilLU*, *ravDE*, cloned under *ermE** in pUWL201PW. Intended to produce NDP-D-fucofuranose.	This work.
pVIR*II	Amp^R, Tsr^R. *chryCMT*, *chryU*, *ravDE* cloned under *ermE** in pUWL201PW. Intended to produce NDP-D-virenose.	This work.
pEN3	Amp^R, Tsr^R. *chryCMT*, *chryU* placed under *ermE** in pEM4. Intended to produce NDP-D-virenose in strain that produces **32**.	This work.
pKAM	Amp^R, Tsr^R. *OleVWSELY* , *urdQ* under *ermE** promotion. Produces NDP-	This work.

	L-cinerulose.	
pLNRHO	Amp^R, Tsr^R. *OleVWSELY* , *urdQ,urdZ3* under *ermE** promotion. Produces NDP-L-rhodinose	This work. (*39*)

Table 11 Bacterial strains used in Chapter 5

Strain Name	**Relevant Characteristics**	**Reference**
Streptomyces argillaceus §	Produces mithramycin (**70**). Wildtype strain.	(*108*)
Streptomyces argillaceus M7W1 †	Produces mithramycins SK/SDK/SA (**128-130**). *mtmW*-disrupted strain.	(*89*, *97*)
Streptomyces argillaceus (pLN2)	§ expressing pLN2. Produces 2 preMTMs and **70**.	(*111*)
Streptomyces argillaceus (pRHAM)	§ expressing pRHAM. Produces **76** and **70**.	(*111*)
Streptomyces argillaceus (pLNBIV)	§ expressing pLNBIV. **131-134**, **76**, **27**, **70**, and 3 unknown pre-MTMs.	(*112*)
Streptomyces argillaceus (pDmnI)	§ expressing pDmnI. Produces **70**, **76**, **27**, and unknown preMTM.	This work.
Streptomyces argillaceus (pDmnII)	§ expressing pDmnII. Produces **70**.	This work.
Streptomyces argillaceus (pDesI)	§ expressing pDesI. Produces **70**.	This work.
Streptomyces argillaceus (pDesIII)	§ expressing pDesIII. Produces **70** and unknown preMTM.	This work.
Streptomyces argillaceus (pFUCO)	§ expressing pDesIII. Produces **70**.	This work.
Streptomyces argillaceus (pFUCOII)	§ expressing pDesIII. Produces **70**.	This work.
Streptomyces argillaceus (pEN3)	§ expressing pEN3. Produces **70**, **76**, **27**. 2 unknown preMTMs and unknown MTM	This work
Streptomyces argillaceus (pVIR*II)	§ expressing pVIR*II. Produces **70**, **76**, **27**. 2 unknown preMTMs and unknown MTM.	This work
Streptomyces argillaceus	† expressing pVIR*II.	This work.

M7W1/(pVIR*II)	Uninvestigated.	
Streptomyces argillaceus (pKOL)	§ expressing pKOL. Produces **70**, **76**, **27**, **131**, and two unknown preMTMs.	This work.
Streptomyces argillaceus M7W1/(pKOL)	† expressing pKOL. Produces **128, 129, 76, 27, 135, 136**.	This work.
Streptomyces argillaceus M7W1/(pKAM)	† expressing pKAM. Produces **76** and **27** and 2 unknown preMTMs	This work.

Table 12 Physicochemical and NMR Data for Demycarosyl-3D-β-D-digitoxosyl mithramycin SK (**135**).

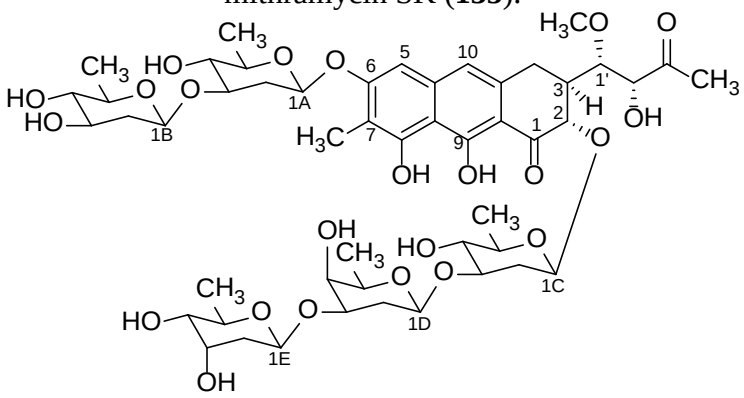

R_{rel}= 16.62 min^{-1}; Yield: 2.2 mg/L

MW= 1040.4 g/mol ($C_{50}H_{72}O_{23}$)

Negative mode APCI-MS: m/z=1039.4 [M-H, 100%]; APCI-MS (+ mode): 1063.2 [M+Na, 40%]. (-) HR-ESI MS ([M-H] calc. 1039.4359 *amu*, found 1039.4432 *amu*. (+) HR-ESI MS [M+Na] calc. 1063.4362 *amu*, found 1063.4337 *amu*.)

UV maxima (from HPLC-diode array): UV (from HPLC-diode array): λ_{max} 211 (85%), 278 (100%), 317 (15%), 332 (13%), 413 (18%)

NMR Data (pyridine- d_5)

Position	Demycarosyl-3D-β-D-digitoxosyl mithramycin SK (**135**)	
	δ_C (125 MHz)	δ_H (500 MHz, *J* in Hz)
1	n.o.*	-
2	78.0	4.89 d (11)
3	41.5	3.50 dddd (16, 12, 4, 1)
4_{ax}	28.3	3.25 dd (16, 12)
4_{eq}		3.00 dd (13, 3)
4a	136.6	-
5	100.4	6.87 s
6	160.3	-
7	111.9	-
7-CH_3	9.3	2.47 s
8	160.6	-
8a	109.2	-
9	n.o.*	-
9a	109.5	-
10	117.6	6.69 s
10a	137.7	-
1’	81.1	4.62 dd (3,2)
1’-OCH_3	59.7	3.83 s
2’	80.2	4.85 d (2)

3’	211.0	-
4’	27.5	2.49 s
5’	-	-
1A	97.9	5.66 dd (10, 2)
$2A_{ax}$	37.9	2.20-2.25 (overlap)
$2A_{eq}$		2.74 td (12, 5)
3A	79.0	3.55 t (9, overlap)
4A	76.1	3.60 m
5A	74.0	4.19 dq (9, 6.5)
6A	19.4	1.69 d (6.5)
1B	99.5	5.06 dd (10, 2)
$2B_{ax}$	41.6	2.20-2.25 (overlap)
$2B_{eq}$		2.65 ddd (12, 5, 4)
3B	73.5	4.17 (overlap)
4B	78.6	3.89 t (10)
5B	73.6	3.63 dq (10, 5)
6B	19.0	1.53 d (6.5)
1C	101.9	5.44 dd (10, 2)
$2C_{ax}$	38.5	2.10-2.15 (overlap)
$2C_{eq}$		2.60-2.65 (overlap)
3C	81.3	3.94 ddd (12, 10, 6)
4C	74.7	3.46 dd (9, 6.5)
5C	72.0	4.26 dq (9, 6.5)
6C	19.7	1.60 d (6.5)
1D	100.1	4.96 dd (10, 2)
$2D_{ax}$	33.3	2.20-2.30 (overlap)
$2D_{eq}$		2.20-2.30 (overlap)
3D	77.2	4.00 ddd (12, 6, 3)
4D	73.3	4.10 br d (3)
5D	73.9	3.75 dq (6.5, 3)
6D	19.4	1.61 d (6.5)
1E	98.6	5.57 dd (10, 2)
$2E_{ax}$	40.2	2.01 ddd (13, 10, 3)
$2E_{eq}$		2.35-2.45 (complex)
3E	69.1	4.46 br d (3)
4E	72.1	3.63 dd (9, 3)
5E	71.1	4.42 dq (9, 6.5)
6E	17.8	1.60 (6.5)

Bacterial Strains and Culture Conditions

Escherichia coli XL1 blue (Invitrogen) was used as a host for routine cloning experiments and was grown on LB agar or in LB broth at 37°C. *Streptomyces argillaceus* or *Streptomyces argillaceus* M7W1 recombinant strains were grown on R5A agar: sucrose, 100 g/liter; K_2SO_4, 0.25 g/liter; $MgCl_2 \cdot 6H_2O$, 10.12 g/liter; glucose, 10 g/liter; Casamino Acids, 0.1 g/liter; yeast extract (Difco), 5 g/liter; and MOPS, 21 g/liter, R5 trace elements, 2 mL/liter. For preparation of protoplasts, spores of *S. argillaceus* or *S. argillaceus* M7W1 were inoculated into 100 mL YEME liquid medium in a 250 mL

baffled Erlenmeyer flask at 28 °C for 3 days for preparation of protoplasts following the previously reported protocol (*3*). When antibiotic selection of recombinant strains was required, 25 μg/mL apramycin, 25 μg/mL thiostrepton, or 100 μg/mL of ampicillin were used. Protoplast transformation was carried out to introduce the various sugar plasmids into *Streptomyces argillaceus* or *Streptomyces argillaceus* M7W1 following the standard protocol (*3, 174*).

Generation of plasmids directing the biosynthesis of ketosugars, aminosugars, and 2-hydroxysugars

The 4-ketoreductase gene (*urdZ3*) was removed from plasmid pLNRHO (*39*). *Nhe*I and *Spe*I were used to digest pLNRHO, thereby releasing the *urdZ3* fragment. DNA gel electrophoresis was carried out to remove the *urdZ3* gene and the resulting fragment (~14kb) was rescued and re-ligated to generate pKAM. In this construct, all of the sugar genes are under strong *ermE** promotion. pKOL was generated in a similar manner (see **Chapter 4, Materials and Methods**).

Plasmids pVIR*II, pFUCOII, pFUCO, and pEN3 were prepared as discussed in **Chapter 2**, Materials and Methods. Plasmids pDmnI, pDmnII, pDesI, pDesII, and pDesIII were prepared by Dr. Madan Kharel (Personal Communication). pLN2, pRHAM, and pLNBIV were all prepared previously by Salas *et al*. (*39*). All plasmids were transformed into *S. argillaceus* or *S. argillaceus* M7W1 *via* protoplast transformation.

Isolation of mithramycins from recombinant *S. argillaceus* M7W1/ (pKOL) strains

One apr^R/tsr^R transformant corresponding to *Streptomyces argillaceus* M7W1/(pKOL) was plated on R5A agar plates supplemented with 25 μg/mL apramycin and thiostrepton at 28 °C for 5 days. For small scale production of mithramycins, an agar chunk of bacterial spores was inoculated in 250 mL Erlenmeyer flasks containing 100 mL of R5A medium supplemented with antibiotics for 4-5 days. 25 mL of the culture was extracted with ethyl acetate and 0.1% formic acid, and the organic layer was dried *in vacuo*. Extracts were then redissolved in methanol and were subjected to HPLC/MS

analyses on a MicroMass ZQ 2000 (Waters) instrument equipped with HPLC (Waters alliance 2695 model) and photodiode array detector (Waters 2996). A Semi-Prep Symmetry C_{18} column (7.8×300 mm, 5 μm) and Symmetry C_{18} (4.6x250 mm, 5 μm) analytical column were used for semi-preparative and analytical scale separations, respectively. A gradient of acetonitrile and 0.1% formic acid in water was used to separate compounds as reported previously (*105*). (Solvent A= 0.1% formic acid in water, solvent B=acetonitrile; 0–20 min 25% B to 70% B; 20-22 min 70%% B to 90% B; 22–24 min 90% to 100% B; 24–26 min 100% B; 26-28 min 100% B to 25% B; 28-30 min 25% B, flow rate 0.5 mL/min).

For larger scale production of glycosylated mithramycins, spores of *Streptomyces argillaceus* M7W1/(pKOL) were grown in eight 100 mL trypticase soy broth (TSB) cultures supplemented with apramycin and thiostreptone at 28 °C for 30 hours. In the production phase, 10.0 L of R5A liquid medium was allocated into 100 mL portions in 100 baffled 250 mL Erlenmeyer flasks and the pH adjusted to 6.95 to promote the generation of mithramycins with SK and SDK side chains. 4% (v/v) of the TSB cultures was used to inoculate each flask, which was supplemented with antibiotics. Fermentation was carried out for 3-5 days at 28°C in an orbital shaker. After the third day, 25 mL of culture was extracted with ethyl acetate, dried, and then checked *via* HPLC/MS analysis to determine the production of mithramycin-type compounds. If premithramycins were detected, fermentation was continued for another 24 hours. As a result of the flooding of the pathway with NDP-deosyxugar intermediates, additional time was required to allow for all glycosyltransfer events and MtmOIV to process premithramycin-type compounds to active mithramycins. After detection of mithramycin-type compounds *via* HPLC/MS, the culture was harvested (to avoid decomposition of metabolites to mithramycin SA), mixed with celite (50 g/L fermentation broth), and then filtered. The mycelial cake was extracted with 400 milliliters of methanol and sonicated for thirty minutes. The culture was acidified to pH 5.5 with concentrated HCl and extracted three times with 2 L of ethyl acetate. The solvent was dried *in vacuo*. The extracts were resuspended in ddH_2O, poured over a reverse phase C_{18} silica column (column dimensions 5.0 cm x 13 cm) under vacuum (1-5 mbar). The column was washed with 1 liter of 10:90 acetonitrile: ddH_2O. Three hundred milliliter fractions were taken, increasing the acetonitrile partition

by 10% each step from 0%-100%. **135** and **136** were found primarily in the 30%, 40%, 50%, and 60% acetonitrile fractions. The 30%, 40%, and 50% acetonitrile fractions were combined, dried *in vacuo*, finally being lyophilized to remove water. This extract was dissolved in methanol, centrifuged, and the supernatant filtered for reverse phase HPLC chromatography. The individual peaks were resolved *via* semi-preparative high-performance liquid chromatography (HPLC) on a Symmetry semi-prep C_{18} column (7.8×300 mm, 5 μm) on a Waters 1525 EF platform with a Waters 2487 dual absorbance detector UV lamp. A gradient of 0.2% formic acid in double distilled water and acetonitrile was used (Solvent A= 0.2% formic acid in water, solvent B=acetonitrile; 0–20 min 25% B to 70% B; 20-22 min 70%% B to 90% B; 22–24 min 90% to 100% B; 24–29 min 100% B; 29-31 min 100% B to 25% B; 31-34.5 min 25% B, flow rate 2.5 mL/min). The eluted material under each peak was collected, dried *in vacuo*, diluted with double distilled water (10 mL), and finally lyophilized. Sample purity was verified *via* HPLC/MS analysis to assure the presence of a single peak. Using this protocol, 22 mg of **135** was isolated. HR-ESI mass spectral analyses were conducted by the Biotech Department at the University of Wisconsin, and NMR measurements were conducted on a 500 MHz Varian VNMR instrument using deuterated pyridine as solvent.

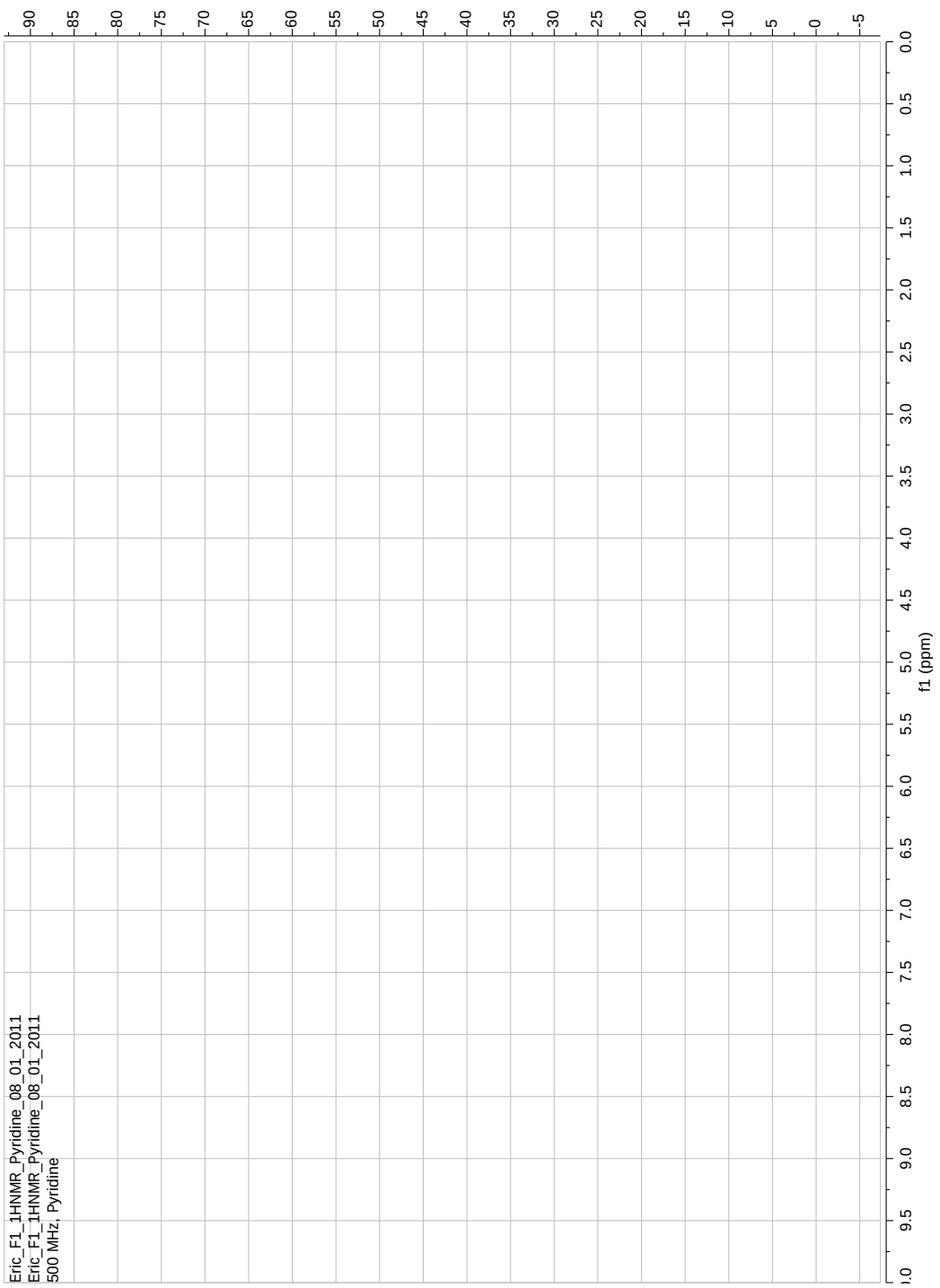

Figure 55 ^{1}H-NMR data for demycarosyl-3D-β-D-digitoxosyl mithramycin SK recorded at 500 MHz.

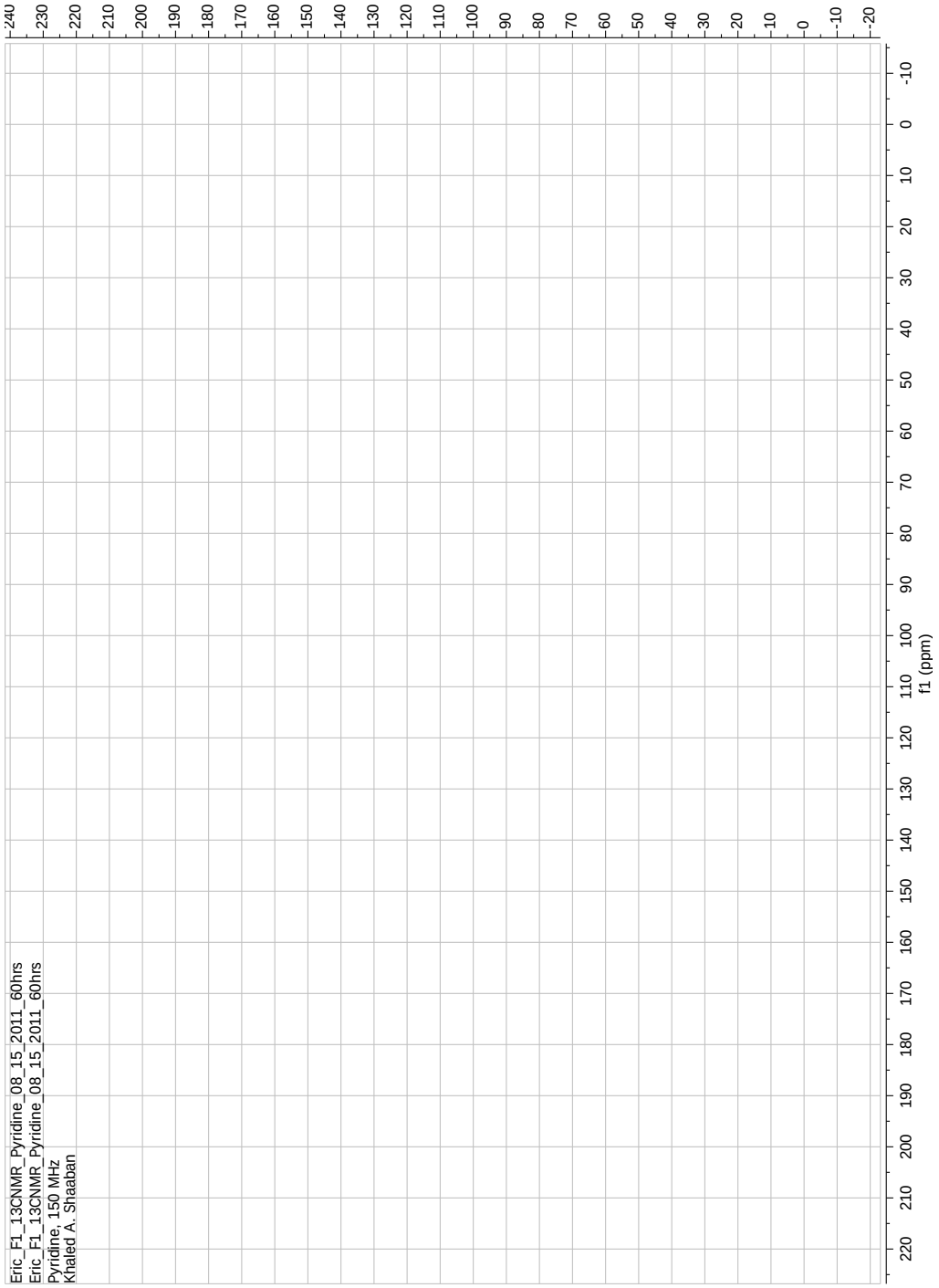

Figure 56 ^{13}C-NMR data for demycarosyl-3D-β-D-digitoxosyl mithramycin SK recorded at 125 MHz.

REFERENCES

1. CLARDY, J., AND WALSH, C. (2004) LESSONS FROM NATURAL MOLECULES, *NATURE 432*, 829-837.
2. ROHR, J. (2000) A NEW ROLE FOR POLYKETIDES, *ANGEW CHEM INT ED ENGL 39*, 2847-2849.
3. KIESER, T., BIBB, M., BUTTNER, M. J., CHATER, K. F., AND HOOPWOOD, D. A. (2000) *PRACTICAL STREPTOMYCES GENETICS THE JOHN INNES FOUNDATION, NORWICH*.
4. ZHOU, H., LI, Y., AND TANG, Y. (2010) CYCLIZATION OF AROMATIC POLYKETIDES FROM BACTERIA AND FUNGI, *NAT PROD REP 27*, 839-868.
5. JANG, M., CAI, L., UDEANI, G. O., SLOWING, K. V., THOMAS, C. F., BEECHER, C. W., FONG, H. H., FARNSWORTH, N. R., KINGHORN, A. D., MEHTA, R. G., MOON, R. C., AND PEZZUTO, J. M. (1997) CANCER CHEMOPREVENTIVE ACTIVITY OF RESVERATROL, A NATURAL PRODUCT DERIVED FROM GRAPES, *SCIENCE 275*, 218-220.
6. CORTES, J., HAYDOCK, S. F., ROBERTS, G. A., BEVITT, D. J., AND LEADLAY, P. F. (1990) AN UNUSUALLY LARGE MULTIFUNCTIONAL POLYPEPTIDE IN THE ERYTHROMYCIN-PRODUCING POLYKETIDE SYNTHASE OF SACCHAROPOLYSPORA ERYTHRAEA, *NATURE 348*, 176-178.
7. DONADIO, S., STAVER, M. J., MCALPINE, J. B., SWANSON, S. J., AND KATZ, L. (1991) MODULAR ORGANIZATION OF GENES REQUIRED FOR COMPLEX POLYKETIDE BIOSYNTHESIS, *SCIENCE 252*, 675-679.
8. ROHR, J., AND THIERICKE, R. (1992) ANGUCYCLINE GROUP ANTIBIOTICS, *NAT PROD REP 9*, 103-137.
9. ALBERTS, A. W., CHEN, J., KURON, G., HUNT, V., HUFF, J., HOFFMAN, C., ROTHROCK, J., LOPEZ, M., JOSHUA, H., HARRIS, E., PATCHETT, A., MONAGHAN, R., CURRIE, S., STAPLEY, E., ALBERS-SCHONBERG, G., HENSENS, O., HIRSHFIELD, J., HOOGSTEEN, K., LIESCH, J., AND SPRINGER, J. (1980) MEVINOLIN: A HIGHLY POTENT COMPETITIVE INHIBITOR OF HYDROXYMETHYLGLUTARYL-COENZYME A REDUCTASE AND A CHOLESTEROL-LOWERING AGENT, *PROC NATL ACAD SCI U S A 77*, 3957-3961.
10. MA, S. M., LI, J. W., CHOI, J. W., ZHOU, H., LEE, K. K., MOORTHIE, V. A., XIE, X., KEALEY, J. T., DA SILVA, N. A., VEDERAS, J. C., AND TANG, Y. (2009) COMPLETE RECONSTITUTION OF A HIGHLY REDUCING ITERATIVE POLYKETIDE SYNTHASE, *SCIENCE 326*, 589-592.
11. ZAWADA, R. J., AND KHOSLA, C. (1999) HETEROLOGOUS EXPRESSION, PURIFICATION, RECONSTITUTION AND KINETIC ANALYSIS OF AN EXTENDED TYPE II POLYKETIDE SYNTHASE, *CHEM BIOL 6*, 607-615.
12. MALPARTIDA, F., AND HOPWOOD, D. A. (1984) MOLECULAR CLONING OF THE WHOLE BIOSYNTHETIC PATHWAY OF A *STREPTOMYCES* ANTIBIOTIC AND ITS EXPRESSION IN A HETEROLOGOUS HOST, *NATURE 309*, 462-464.

13. MCDANIEL, R., EBERT-KHOSLA, S., FU, H., HOPWOOD, D. A., AND KHOSLA, C. (1994) ENGINEERED BIOSYNTHESIS OF NOVEL POLYKETIDES: INFLUENCE OF A DOWNSTREAM ENZYME ON THE CATALYTIC SPECIFICITY OF A MINIMAL AROMATIC POLYKETIDE SYNTHASE, *PROC NATL ACAD SCI U S A 91*, 11542-11546.
14. RAWLINGS, B. J. (2001A) TYPE I POLYKETIDE BIOSYNTHESIS IN BACTERIA (PART A-ERYTHROMYCIN BIOSYNTHESIS), *NAT. PORD. REP. 18*, 190-227.
15. ZHANG, W. J., LI, Y. R., AND TANG, Y. (2008) ENGINEERED BIOSYNTHESIS OF BACTERIAL AROMATIC POLYKETIDES IN *ESCHERICHIA COLI*, *PROC. NATL. ACAD. SCI. USA 105*, 20683-20688.
16. KEATINGE-CLAY, A. T., MALTBY, D. A., MEDZIHRADSZKY, K. F., KHOSLA, C., AND STROUD, R. M. (2004) AN ANTIBIOTIC FACTORY CAUGHT IN ACTION, *NAT STRUCT MOL BIOL 11*, 888-893.
17. GREGORY, M. A., PETKOVIC, H., LILL, R. E., MOSS, S. J., WILKINSON, B., GAISSER, S., LEADLAY, P. F., AND SHERIDAN, R. M. (2005) MUTASYNTHESIS OF RAPAMYCIN ANALOGUES THROUGH THE MANIPULATION OF A GENE GOVERNING STARTER UNIT BIOSYNTHESIS, *ANGEW. CHEM. INTL. ED. 44*, 4757-4760.
18. GU, L. C., GEDERS, T. W., WANG, B., GERWICK, W. H., HAKANSSON, K., SMITH, J. L., AND SHERMAN, D. H. (2007) GNAT-LIKE STRATEGY FOR POLYKETIDE CHAIN INITIATION, *SCIENCE 318*, 970-974.
19. ZHANG, X., ALERNANY, L. B., FIEDLER, H. P., GOODFELLOW, M., AND PARRY, R. J. (2008) BIOSYNTHETIC INVESTIGATIONS OF LACTONAMYCIN AND LACTONAMYCIN Z: CLONING OF THE BIOSYNTHETIC GENE CLUSTERS AND DISCOVERY OF AN UNUSUAL STARTER UNIT, *ANTIMICROB. AGENTS CHEMOTHER. 52*, 574-585.
20. PAN, H., TSAI, S., MEADOWS, E. S., MIERCKE, L. J., KEATINGE-CLAY, A. T., O'CONNELL, J., KHOSLA, C., AND STROUD, R. M. (2002) CRYSTAL STRUCTURE OF THE PRIMING BETA-KETOSYNTHASE FROM THE R1128 POLYKETIDE BIOSYNTHETIC PATHWAY, *STRUCTURE 10*, 1559-1568.
21. PICKENS, L. B., KIM, W., WANG, P., ZHOU, H., WATANABE, K., GOMI, S., AND TANG, Y. (2009) BIOCHEMICAL ANALYSIS OF THE BIOSYNTHETIC PATHWAY OF AN ANTICANCER TETRACYCLINE SF2575, *J AM CHEM SOC 131*, 17677-17689.
22. ZHANG, W., WATANABE, K., WANG, C. C., AND TANG, Y. (2007) INVESTIGATION OF EARLY TAILORING REACTIONS IN THE OXYTETRACYCLINE BIOSYNTHETIC PATHWAY, *J BIOL CHEM 282*, 25717-25725.
23. LOZANO, M. J., REMSING, L. L., QUIROS, L. M., BRANA, A. F., FERNANDEZ, E., SANCHEZ, C., MENDEZ, C., ROHR, J., AND SALAS, J. A. (2000) CHARACTERIZATION OF TWO POLYKETIDE METHYLTRANSFERASES INVOLVED IN THE BIOSYNTHESIS OF THE ANTITUMOR DRUG MITHRAMYCIN BY STREPTOMYCES ARGILLACEUS, *J BIOL CHEM 275*, 3065-3074.

24. ABDELFATTAH, M. S., AND ROHR, J. (2006) PREMITHRAMYCINONE G, AN EARLY SHUNT PRODUCT OF THE MITHRAMYCIN BIOSYNTHETIC PATHWAY ACCUMULATED UPON INACTIVATION OF OXYGENASE MTMOII, *ANGEW CHEM INT ED ENGL 45*, 5685-5689.
25. ABE, I., AND MORITA, H. (2010) STRUCTURE AND FUNCTION OF THE CHALCONE SYNTHASE SUPERFAMILY OF PLANT TYPE III POLYKETIDE SYNTHASES, *NAT PROD REP 27*, 809-838.
26. OLANO, C., MENDEZ, C., AND SALAS, J. A. (2010) POST-PKS TAILORING STEPS IN NATURAL PRODUCT-PRODUCING ACTINOMYCETES FROM THE PERSPECTIVE OF COMBINATORIAL BIOSYNTHESIS, *NAT PROD REP 27*, 571-616.
27. RIX, U., FISCHER, C., REMSING, L. L., AND ROHR, J. (2002) MODIFICATION OF POST-PKS TAILORING STEPS THROUGH COMBINATORIAL BIOSYNTHESIS, *NAT. PROD. REP. 19*, 542-580.
28. EHRLICH, K. C., LI, P., SCHARFENSTEIN, L., AND CHANG, P. K. (2010) HYPC, THE ANTHRONE OXIDASE INVOLVED IN AFLATOXIN BIOSYNTHESIS, *APPL ENVIRON MICROBIOL 76*, 3374-3377.
29. DICKENS, M. L., PRIESTLEY, N. D., AND STROHL, W. R. (1997) IN VIVO AND IN VITRO BIOCONVERSION OF EPSILON-RHODOMYCINONE GLYCOSIDE TO DOXORUBICIN: FUNCTIONS OF DAUP, DAUK, AND DOXA, *J. BACTERIOL. 179*, 2641-2650.
30. KHAREL, M. K., NYBO, S. E., SHEPHERD, M. D., AND ROHR, J. (2010) CLONING AND CHARACTERIZATION OF THE RAVIDOMYCIN AND CHRYSOMYCIN BIOSYNTHETIC GENE CLUSTERS, *CHEMBIOCHEM 11*, 523-532.
31. ZHANG, W., WATANABE, K., CAI, X., JUNG, M. E., TANG, Y., AND ZHAN, J. (2008) IDENTIFYING THE MINIMAL ENZYMES REQUIRED FOR ANHYDROTETRACYCLINE BIOSYNTHESIS, *J AM CHEM SOC 130*, 6068-6069.
32. THIBODEAUX, C. J., MELANCON, C. E., AND LIU, H. W. (2007) UNUSUAL SUGAR BIOSYNTHESIS AND NATURAL PRODUCT GLYCODIVERSIFICATION, *NATURE 446*, 1008-1016.
33. PARK, S. H., PARK, H. Y., SOHNG, J. K., LEE, H. C., LIOU, K., YOON, Y. J., AND KIM, B. G. (2009) EXPANDING SUBSTRATE SPECIFICITY OF GT-B FOLD GLYCOSYLTRANSFERASE VIA DOMAIN SWAPPING AND HIGH-THROUGHPUT SCREENING, *BIOTECHNOL. BIOENG. 102*, 988-994.
34. HU, Y., AND WALKER, S. (2002) REMARKABLE STRUCTURAL SIMILARITIES BETWEEN DIVERSE GLYCOSYLTRANSFERASES, *CHEM BIOL 9*, 1287-1296.
35. MULICHAK, A. M., LU, W., LOSEY, H. C., WALSH, C. T., AND GARAVITO, R. M. (2004) CRYSTAL STRUCTURE OF VANCOSAMINYLTRANSFERASE GTFD FROM THE VANCOMYCIN BIOSYNTHETIC PATHWAY: INTERACTIONS WITH ACCEPTOR AND NUCLEOTIDE LIGANDS, *BIOCHEMISTRY 43*, 5170-5180.
36. KLYNE, W. (1950) THE CONFIGURATION OF THE ANOMERIC CARBON ATOMS IN SOME CARDIAC GLYCOSIDES, *BIOCHEM J 47*, XLI-II.

37. HE, X. M. M., AND LIU, H. W. (2002) FORMATION OF UNUSUAL SUGARS: MECHANISTIC STUDIES AND BIOSYNTHETIC APPLICATIONS, *ANNU. REV. BIOCHEM. 71*, 701-754.
38. DECKER, H., GAISSER, S., PELZER, S., SCHNEIDER, P., WESTRICH, L., WOHLLEBEN, W., AND BECHTHOLD, A. (1996) A GENERAL APPROACH FOR CLONING AND CHARACTERIZING DNDP-GLUCOSE DEHYDRATASE GENES FROM ACTINOMYCETES, *FEMS MICROBIOL. LETT. 141*, 195-201.
39. RODRIGUEZ, L., AGUIRREZABALAGA, I., ALLENDE, N., BRANA, A. F., MENDEZ, C., AND SALAS, J. A. (2002) ENGINEERING DEOXYSUGAR BIOSYNTHETIC PATHWAYS FROM ANTIBIOTIC-PRODUCING MICROORGANISMS: A TOOL TO PRODUCE NOVEL GLYCOSYLATED BIOACTIVE COMPOUNDS, *CHEM. BIOL. 9*, 721-729.
40. NAKANO, H., MATSUDA, Y., ITO, K., OHKUBO, S., MORIMOTO, M., AND TOMITA, F. (1981) GILVOCARCINS, NEW ANTITUMOR ANTIBIOTICS. 1.TAXONOMY, FERMENTATION, ISOLATION AND BIOLOGICAL ACTIVITIES., *J. ANTIBIOT. 34*, 266-270.
41. BREIDING-MACK, S., AND ZEECK, A. (1987) SECONDARY METABOLITES BY CHEMICAL SCREENING. I. CALCIUM 3-HYDROXYQUINOLINE-2-CARBOXYLATE FROM A STREPTOMYCES, *J ANTIBIOT (TOKYO) 40*, 953-960.
42. BALITZ, D. M., OHERRON, F. A., BUSH, J., VYAS, D. M., NETTLETON, D. E., GRULICH, R. E., BRADNER, W. T., DOYLE, T. W., ARNOLD, E., AND CLARDY, J. (1981) ANTI-TUMOR AGENTS FROM *STREPTOMYCES ANANDII* -GILVOCARCIN-V, GILVOCARCIN-M AND GILVOCARCIN-E, *J. ANTIBIOT. 34*, 1544-1555.
43. MORIMOTO, M. O., S.; TOMITA, F.; MARUMO, H.;. (1981) GILVOCARCINS, NEW ANTITUMOR ANTIBIOTICS. 3. ANTITUMOR ACTIVITY, *J. ANTIBIOT. 34*, 701-707.
44. ELESPURU, R. K., AND GONDA, S. K. (1984) ACTIVATION OF ANTITUMOR AGENT GILVOCARCINS BY VISIBLE LIGHT, *SCIENCE 223*, 69-71.
45. TOMITA, F., TAKAHASHI, K., AND TAMAOKI, T. (1982) GILVOCARCINS, NEW ANTITUMOR ANTIBIOTICS. 4. MODE OF ACTION, *J ANTIBIOT (TOKYO) 35*, 1038-1041.
46. MATSUMOTO, A., AND HANAWALT, P. C. (2000) HISTONE H3 AND HEAT SHOCK PROTEIN GRP78 ARE SELECTIVELY CROSS-LINKED TO DNA BY PHOTOACTIVATED GILVOCARCIN V IN HUMAN FIBROBLASTS, *CANCER RES 60*, 3921-3926.
47. ALEGRIA, A. E., ZAYAS, L., AND GUEVARA, N. (1995) A COMPARATIVE STUDY OF THE VISIBLE LIGHT PHOTOCHEMISTRY OF GILVOCARCINS V AND M, *PHOTOCHEM PHOTOBIOL 62*, 409-415.
48. SEHGAL, S. N., CZERKAWSKI, H., KUDELSKI, A., PANDEV, K., SAUCIER, R., AND VEZINA, C. (1983) RAVIDOMYCIN (AY-25,545), A NEW ANTI-TUMOR ANTIBIOTIC, *J. ANTIBIOT. 36*, 355-361.

49. STRELITZ, F. F., H; ASHESHOV, I. N. (1955) CHRYSOMYCIN: A NEW ANTIBIOTIC SUBSTANCE FOR BACTERIAL VIRUSES, *J. BACTERIOL. 69*, 280-283.
50. WEISS, U., YOSHIHIRA, K., HIGHET, R. J., WHITE, R. J., AND WEI, T. T. (1982) THE CHEMISTRY OF THE ANTIBIOTICS CHRYSOMYCIN-A AND CHRYSOMYCIN-B ANTI-TUMOR ACTIVITY OF CHRYSOMYCIN-A, *J. ANTIBIOT. 35*, 1194-1201.
51. STRELITZ, F., FLON, H., AND ASHESHOV, I. N. (1955) CHRYSOMYCIN: A NEW ANTIBIOTIC SUBSTANCE FOR BACTERIAL VIRUSES, *J BACTERIOL 69*, 280-283.
52. BRAZHNIKOVA, M. G., KUDINOVA, M. K., KULIAEVA, V. V., POTAPOVA, N. P., AND RUBASHEVA, L. M. (1984) [STRUCTURE OF THE ANTIBIOTIC VIRENOMYCIN], *ANTIBIOTIKI 29*, 884-892.
53. YAMASHITA, N., SHIN-YA, K., FURIHATA, K., HAYAKAWA, Y., AND SETO, H. (1998) NEW RAVIDOMYCIN ANALOGUES, FE35A AND FE35B, APOPTOSIS INDUCERS PRODUCED BY STREPTOMYCES ROCHEI, *J ANTIBIOT (TOKYO) 51*, 1105-1108.
54. KOJIRI, K., ARAKAWA, H., SATOH, F., KAWAMURA, K., OKURA, A., SUDA, H., AND OKANISHI, M. (1991) NEW ANTITUMOR SUBSTANCES, BE-12406A AND BE-12406B, PRODUCED BY A STREPTOMYCETE. I. TAXONOMY, FERMENTATION, ISOLATION, PHYSICO-CHEMICAL AND BIOLOGICAL PROPERTIES, *J ANTIBIOT (TOKYO) 44*, 1054-1060.
55. NAKAJIMA, S., KOJIRI, K., SUDA, H., AND OKANISHI, M. (1991) NEW ANTITUMOR SUBSTANCES, BE-12406A AND BE-12406B, PRODUCED BY A STREPTOMYCETE. II. STRUCTURE DETERMINATION, *J ANTIBIOT (TOKYO) 44*, 1061-1064.
56. LI, Y. Q., HUANG, X. S., ISHIDA, K., MAIER, A., KELTER, G., JIANG, Y., PESCHEL, G., MENZEL, K. D., LI, M. G., WEN, M. L., XU, L. H., GRABLEY, S., FIEBIG, H. H., JIANG, C. L., HERTWECK, C., AND SATTLER, I. (2008) PLASTICITY IN GILVOCARCIN-TYPE C-GLYCOSIDE PATHWAYS: DISCOVERY AND ANTITUMORAL EVALUATION OF POLYCARCIN V FROM STREPTOMYCES POLYFORMUS, *ORG BIOMOL CHEM 6*, 3601-3605.
57. NAKASHIMA, T., TADASHI FUJII, KAZUYA SAKAI, TOMOHIRO SAMESHIMA, HIROYUKI KUMAGAI, TAKEO YOSHIOKA. (07/08/1999) CHRYSOMYCIN DERIVATIVE COMPOUNDS AND USE AS ANTITUMOR AGENTS, P 9, MERCIAN CORPORATION.
58. TAKAHASHI, K., AND TOMITA, F. (1983) GILVOCARCINS, NEW ANTITUMOR ANTIBIOTICS. 5. BIOSYNTHESIS OF GILVOCARCINS: INCORPORATION OF 13C-LABELED COMPOUNDS INTO GILVOCARCIN AGLYCONES, *J ANTIBIOT (TOKYO) 36*, 1531-1535.
59. CARTER, G. T., FANTINI, A. A., JAMES, J. C., BORDERS, D. B., AND WHITE, R. J. (1985) BIOSYNTHESIS OF CHRYSOMYCINS A AND B. ORIGIN OF THE CHROMOPHORE, *J ANTIBIOT (TOKYO) 38*, 242-248.

60. LIU, T., FISCHER, C., BENINGA, C., AND ROHR, J. (2004) OXIDATIVE REARRANGEMENT PROCESSES IN THE BIOSYNTHESIS OF GILVOCARCIN V, *J AM CHEM SOC 126*, 12262-12263.
61. FISCHER, C., LIPATA, F., AND ROHR, J. (2003) THE COMPLETE GENE CLUSTER OF THE ANTITUMOR AGENT GILVOCARCIN V AND ITS IMPLICATION FOR THE BIOSYNTHESIS OF THE GILVOCARCINS, *J AM CHEM SOC 125*, 7818-7819.
62. LIU, T., KHAREL, M. K., FISCHER, C., MCCORMICK, A., AND ROHR, J. (2006) INACTIVATION OF GILGT, ENCODING A C-GLYCOSYLTRANSFERASE, AND GILOIII, ENCODING A P450 ENZYME, ALLOWS THE DETAILS OF THE LATE BIOSYNTHETIC PATHWAY TO GILVOCARCIN V TO BE DELINEATED, *CHEMBIOCHEM 7*, 1070-1077.
63. KHAREL, M. K., ZHU, L., LIU, T., AND ROHR, J. (2007) MULTI-OXYGENASE COMPLEXES OF THE GILVOCARCIN AND JADOMYCIN BIOSYNTHESES, *J AM CHEM SOC 129*, 3780-3781.
64. LIU, T., KHAREL, M. K., ZHU, L., BRIGHT, S. A., MATTINGLY, C., ADAMS, V. R., AND ROHR, J. (2008) INACTIVATION OF THE KETOREDUCTASE GILU GENE OF THE GILVOCARCIN BIOSYNTHETIC GENE CLUSTER YIELDS NEW ANALOGUES WITH PARTLY IMPROVED BIOLOGICAL ACTIVITY, *CHEMBIOCHEM*.
65. SHEPHERD, M. D., KHAREL, M. K., ZHU, L. L., VAN LANEN, S. G., AND ROHR, J. (2010) DELINEATING THE EARLIEST STEPS OF GILVOCARCIN BIOSYNTHESIS: ROLE OF GILP AND GILQ IN STARTER UNIT SPECIFICITY, *ORG BIOMOL CHEM 8*, 3851-3856.
66. KHAREL, M. K., PAHARI, P., LIAN, H., AND ROHR, J. (2010) ENZYMATIC TOTAL SYNTHESIS OF RABELOMYCIN, AN ANGUCYCLINE GROUP ANTIBIOTIC, *ORG LETT 12*, 2814-2817.
67. RIX, U., WANG, C. C., CHEN, Y. H., LIPATA, F. M., RIX, L. L. R., GREENWELL, L. M., VINING, L. C., YANG, K. Q., AND ROHR, J. (2005) THE OXIDATIVE RING CLEAVAGE IN JADOMYCIN BIOSYNTHESIS: A MULTISTEP OXYGENATION CASCADE IN A BIOSYNTHETIC BLACK BOX, *CHEMBIOCHEM 6*, 838-835.
68. KHAREL, M. K., ZHU, L. L., LIU, T., AND ROHR, J. (2007) MULTI-OXYGENASE COMPLEXES OF THE GILVOCARCIN AND JADOMYCIN BIOSYNTHESES, *J. AM. CHEM. SOC. 129*, 3780-3781.
69. CHEN, Y., FAN, K., HE, Y., XU, X., PENG, Y., YU, T., JIA, C., AND YANG, K. (2010) CHARACTERIZATION OF JADH AS AN FAD- AND NAD(P)H-DEPENDENT BIFUNCTIONAL HYDROXYLASE/DEHYDRASE IN JADOMYCIN BIOSYNTHESIS, *CHEMBIOCHEM 11*, 1055-1060.
70. LIU, T., KHAREL, M. K., FISCHER, C., MCCORMICK, A., AND ROHR, J. (2006) INACTIVATION OF *GILGT*, ENCODING A C-GLYCOSYLTRANSFERASE, AND *GILOLLL*, ENCODING A P450 ENZYME, ALLOWS THE DETAILS OF THE LATE BIOSYNTHETIC PATHWAY TO GILVOCARCIN V TO BE DELINEATED, *CHEMBIOCHEM 7*, 1070-1077.

71. KHAREL, M. K., PAHARI, P., LIAN, H., AND ROHR, J. (2009) GILR, AN UNUSUAL LACTONE-FORMING ENZYME INVOLVED IN GILVOCARCIN BIOSYNTHESIS, *CHEMBIOCHEM 10*, 1305-1308.
72. LIU, T., KHAREL, M. K., ZHU, L., BRIGHT, S., AND ROHR, J. (2009) INACTIVATION OF THE KETOREDUCTASE *GILU* GENE OF THE GILVOCARCIN BIOSYNTHETIC GENE CLUSTER YIELDS NEW ANALOGUES WITH PARTLY IMPROVED BIOLOGICAL ACTIVITY., *CHEMBIOCHEM 10*, 278-286.
73. LOMBO, F., MENENDEZ, N., SALAS, J. A., AND MENDEZ, C. (2006) THE AUREOLIC ACID FAMILY OF ANTITUMOR COMPOUNDS: STRUCTURE, MODE OF ACTION, BIOSYNTHESIS, AND NOVEL DERIVATIVES, *APPL MICROBIOL BIOTECHNOL 73*, 1-14.
74. GRUNDY, W. E., GOLDSTEIN, A. W., RICKHER, C. J., HANES, M. E., WARREN, H. B., JR., AND SYLVESTER, J. C. (1953) AUREOLIC ACID, A NEW ANTIBIOTIC. I. MICROBIOLOGIC STUDIES, *ANTIBIOT. CHEMOTHER. (WASHINGTON, D. C.) 3*, 1215-1217.
75. KATAHIRA, R., UOSAKI, Y., OGAWA, H., YAMASHITA, Y., NAKANO, H., AND YOSHIDA, M. (1998) UCH9, A NEW ANTITUMOR ANTIBIOTIC PRODUCED BY STREPTOMYCES. II. STRUCTURE ELUCIDATION OF UCH9 BY MASS AND NMR SPECTROSCOPY, *J ANTIBIOT (TOKYO) 51*, 267-274.
76. OGAWA, H., YAMASHITA, Y., KATAHIRA, R., CHIBA, S., IWASAKI, T., ASHIZAWA, T., AND NAKANO, H. (1998) UCH9, A NEW ANTITUMOR ANTIBIOTIC PRODUCED BY STREPTOMYCES: I. PRODUCING ORGANISM, FERMENTATION, ISOLATION AND BIOLOGICAL ACTIVITIES, *J ANTIBIOT (TOKYO) 51*, 261-266.
77. PRAGANI, R., AND ROUSH, W. R. (2008) STUDIES ON THE SYNTHESIS OF DURHAMYCIN A: STEREOSELECTIVE SYNTHESIS OF A MODEL AGLYCONE, *ORG LETT 10*, 4613-4616.
78. WOHLERT, S. E., KUNZEL, E., MACHINEK, R., MENDEZ, C., SALAS, J. A., AND ROHR, J. (1999) THE STRUCTURE OF MITHRAMYCIN REINVESTIGATED, *J NAT PROD 62*, 119-121.
79. SANDBERG-WOLLHEIM, M., YARBRO, J. W., AND KENNEDY, B. J. (1968) EFFECT OF MITHRAMYCIN ON HELA CELLS, *CANCER 21*, 22-25.
80. KENNEDY, B. J., YARBRO, J. W., KICKERTZ, V., AND SANDBERG-WOLLHEIM, M. (1968) EFFECT OF MITHRAMYCIN ON A MOUSE GLIOMA, *CANCER RES 28*, 91-97.
81. KENNEDY, B. J., SANDBERG-WOLLHEIM, M., LOKEN, M., AND YARBRO, J. W. (1967) STUDIES WITH TRITIATED MITHRAMYCIN IN C3H MICE, *CANCER RES 27*, 1534-1538.
82. YARBRO, J. W., KENNEDY, B. J., AND BARNUM, C. P. (1966) MITHRAMYCIN INHIBITION OF RIBONUCLEIC ACID SYNTHESIS, *CANCER RES 26*, 36-39.
83. BROWN, J. H., AND KENNEDY, B. J. (1965) MITHRAMYCIN IN THE TREATMENT OF DISSEMINATED TESTICULAR NEOPLASMS, *N ENGL J MED 272*, 111-118.

84. KENNEDY, B. J., BROWN, J. H., AND YARBRO, J. W. (1965) MITHRAMYCIN (NSC-24559) THERAPY FOR PRIMARY GLIOBLASTOMAS, *CANCER CHEMOTHER REP 48*, 59-63.
85. KENNEDY, B. J., GRIFFEN, W. O., JR., AND LOBER, P. (1965) SPECIFIC EFFECT OF MITHRAMYCIN ON EMBRYONAL CARCINOMA OF THE TESTIS, *CANCER 18*, 1631-1636.
86. REMSING, L. L., BAHADORI, H. R., CARBONE, G. M., MCGUFFIE, E. M., CATAPANO, C. V., AND ROHR, J. (2003) INHIBITION OF C-SRC TRANSCRIPTION BY MITHRAMYCIN: STRUCTURE-ACTIVITY RELATIONSHIPS OF BIOSYNTHETICALLY PRODUCED MITHRAMYCIN ANALOGUES USING THE C-SRC PROMOTER AS TARGET, *BIOCHEMISTRY 42*, 8313-8324.
87. PREVIDI, S., MALEK, A., ALBERTINI, V., RIVA, C., CAPELLA, C., BROGGINI, M., CARBONE, G. M., ROHR, J., AND CATAPANO, C. V. (2010) INHIBITION OF SP1-DEPENDENT TRANSCRIPTION AND ANTITUMOR ACTIVITY OF THE NEW AUREOLIC ACID ANALOGUES MITHRAMYCIN SDK AND SK IN HUMAN OVARIAN CANCER XENOGRAFTS, *GYNECOL ONCOL 118*, 182-188.
88. BATALLER, M., MENDEZ, C., SALAS, J. A., AND PORTUGAL, J. (2008) MITHRAMYCIN SK MODULATES POLYPLOIDY AND CELL DEATH IN COLON CARCINOMA CELLS, *MOL CANCER THER 7*, 2988-2997.
89. ALBERTINI, V., JAIN, A., VIGNATI, S., NAPOLI, S., RINALDI, A., KWEE, I., NUR-E-ALAM, M., BERGANT, J., BERTONI, F., CARBONE, G. M., ROHR, J., AND CATAPANO, C. V. (2006) NOVEL GC-RICH DNA-BINDING COMPOUND PRODUCED BY A GENETICALLY ENGINEERED MUTANT OF THE MITHRAMYCIN PRODUCER STREPTOMYCES ARGILLACEUS EXHIBITS IMPROVED TRANSCRIPTIONAL REPRESSOR ACTIVITY: IMPLICATIONS FOR CANCER THERAPY, *NUCLEIC ACIDS RES 34*, 1721-1734.
90. VOISINE, C., VARMA, H., WALKER, N., BATES, E. A., STOCKWELL, B. R., AND HART, A. C. (2007) IDENTIFICATION OF POTENTIAL THERAPEUTIC DRUGS FOR HUNTINGTON'S DISEASE USING CAENORHABDITIS ELEGANS, *PLOS ONE 2*, E504.
91. QIU, Z., NORFLUS, F., SINGH, B., SWINDELL, M. K., BUZESCU, R., BEJARANO, M., CHOPRA, R., ZUCKER, B., BENN, C. L., DIROCCO, D. P., CHA, J. H., FERRANTE, R. J., AND HERSCH, S. M. (2006) SP1 IS UP-REGULATED IN CELLULAR AND TRANSGENIC MODELS OF HUNTINGTON DISEASE, AND ITS REDUCTION IS NEUROPROTECTIVE, *J BIOL CHEM 281*, 16672-16680.
92. RYU, H., LEE, J., HAGERTY, S. W., SOH, B. Y., MCALPIN, S. E., CORMIER, K. A., SMITH, K. M., AND FERRANTE, R. J. (2006) ESET/SETDB1 GENE EXPRESSION AND HISTONE H3 (K9) TRIMETHYLATION IN HUNTINGTON'S DISEASE, *PROC NATL ACAD SCI U S A 103*, 19176-19181.

93. FERRANTE, R. J., RYU, H., KUBILUS, J. K., D'MELLO, S., SUGARS, K. L., LEE, J., LU, P., SMITH, K., BROWNE, S., BEAL, M. F., KRISTAL, B. S., STAVROVSKAYA, I. G., HEWETT, S., RUBINSZTEIN, D. C., LANGLEY, B., AND RATAN, R. R. (2004) CHEMOTHERAPY FOR THE BRAIN: THE ANTITUMOR ANTIBIOTIC MITHRAMYCIN PROLONGS SURVIVAL IN A MOUSE MODEL OF HUNTINGTON'S DISEASE, *J NEUROSCI 24*, 10335-10342.
94. CHRISTENSEN, M. A., ZHOU, W., QING, H., LEHMAN, A., PHILIPSEN, S., AND SONG, W. (2004) TRANSCRIPTIONAL REGULATION OF BACE1, THE BETA-AMYLOID PRECURSOR PROTEIN BETA-SECRETASE, BY SP1, *MOL CELL BIOL 24*, 865-874.
95. BEAM, M. P., BOSSERMAN, M. A., NOINAJ, N., WEHENKEL, M., AND ROHR, J. (2009) CRYSTAL STRUCTURE OF BAEYER-VILLIGER MONOOXYGENASE MTMOIV, THE KEY ENZYME OF THE MITHRAMYCIN BIOSYNTHETIC PATHWAY, *BIOCHEMISTRY 48*, 4476-4487.
96. NUR-E-ALAM, M., MENDEZ, C., SALAS, J. A., AND ROHR, J. (2005) ELUCIDATION OF THE GLYCOSYLATION SEQUENCE OF MITHRAMYCIN BIOSYNTHESIS: ISOLATION OF 3A-DEOLIVOSYLPREMITHRAMYCIN B AND ITS CONVERSION TO PREMITHRAMYCIN B BY GLYCOSYLTRANSFERASE MTMGII, *CHEMBIOCHEM 6*, 632-636.
97. REMSING, L. L., GONZALEZ, A. M., NUR-E-ALAM, M., FERNANDEZ-LOZANO, M. J., BRANA, A. F., RIX, U., OLIVEIRA, M. A., MENDEZ, C., SALAS, J. A., AND ROHR, J. (2003) MITHRAMYCIN SK, A NOVEL ANTITUMOR DRUG WITH IMPROVED THERAPEUTIC INDEX, MITHRAMYCIN SA, AND DEMYCAROSYL-MITHRAMYCIN SK: THREE NEW PRODUCTS GENERATED IN THE MITHRAMYCIN PRODUCER *STREPTOMYCES ARGILLACEUS* THROUGH COMBINATORIAL BIOSYNTHESIS, *J. AM. CHEM. SOC. 125*, 5745-5753.
98. REMSING, L. L., GARCIA-BERNARDO, J., GONZALEZ, A., KUNZEL, E., RIX, U., BRANA, A. F., BEARDEN, D. W., MENDEZ, C., SALAS, J. A., AND ROHR, J. (2002) KETOPREMITHRAMYCINS AND KETOMITHRAMYCINS, FOUR NEW AUREOLIC ACID-TYPE COMPOUNDS OBTAINED UPON INACTIVATION OF TWO GENES INVOLVED IN THE BIOSYNTHESIS OF THE DEOXYSUGAR MOIETIES OF THE ANTITUMOR DRUG MITHRAMYCIN BY *STREPTOMYCES ARGILLACEUS*, REVEAL NOVEL INSIGHTS INTO POST-PKS TAILORING STEPS OF THE MITHRAMYCIN BIOSYNTHETIC PATHWAY, *J. AM. CHEM. SOC. 124*, 1606-1614.
99. GONZALEZ, A., REMSING, L. L., LOMBO, F., FERNANDEZ, M. J., PRADO, L., BRANA, A. F., KUNZEL, E., ROHR, J., MENDEZ, C., AND SALAS, J. A. (2001) THE MTMVUC GENES OF THE MITHRAMYCIN GENE CLUSTER IN STREPTOMYCES ARGILLACEUS ARE INVOLVED IN THE BIOSYNTHESIS OF THE SUGAR MOIETIES, *MOL GEN GENET 264*, 827-835.

100. BLANCO, G., FERNANDEZ, E., FERNANDEZ, M. J., BRANA, A. F., WEISSBACH, U., KUNZEL, E., ROHR, J., MENDEZ, C., AND SALAS, J. A. (2000) CHARACTERIZATION OF TWO GLYCOSYLTRANSFERASES INVOLVED IN EARLY GLYCOSYLATION STEPS DURING BIOSYNTHESIS OF THE ANTITUMOR POLYKETIDE MITHRAMYCIN BY STREPTOMYCES ARGILLACEUS, *MOL GEN GENET 262*, 991-1000.
101. LOMBO, F., KUNZEL, E., PRADO, L., BRANA, A. F., BINDSEIL, K. U., FREVERT, J., BEARDEN, D., MENDEZ, C., SALAS, J. A., AND ROHR, J. (2000) THE NOVEL HYBRID ANTITUMOR COMPOUND PREMITHRAMYCINONE H PROVIDES INDIRECT EVIDENCE FOR A TRICYCLIC INTERMEDIATE OF THE BIOSYNTHESIS OF THE AUREOLIC ACID ANTIBIOTIC MITHRAMYCIN, *ANGEW CHEM INT ED ENGL 39*, 796-799.
102. PRADO, L., LOMBO, F., BRANA, A. F., MENDEZ, C., ROHR, J., AND SALAS, J. A. (1999) ANALYSIS OF TWO CHROMOSOMAL REGIONS ADJACENT TO GENES FOR A TYPE II POLYKETIDE SYNTHASE INVOLVED IN THE BIOSYNTHESIS OF THE ANTITUMOR POLYKETIDE MITHRAMYCIN IN STREPTOMYCES ARGILLACEUS, *MOL GEN GENET 261*, 216-225.
103. PRADO, L., FERNANDEZ, E., WEISSBACH, U., BLANCO, G., QUIROS, L. M., BRANA, A. F., MENDEZ, C., ROHR, J., AND SALAS, J. A. (1999) OXIDATIVE CLEAVAGE OF PREMITHRAMYCIN B IS ONE OF THE LAST STEPS IN THE BIOSYNTHESIS OF THE ANTITUMOR DRUG MITHRAMYCIN, *CHEM BIOL 6*, 19-30.
104. LOMBO, F., BRANA, A. F., MENDEZ, C., AND SALAS, J. A. (1999) THE MITHRAMYCIN GENE CLUSTER OF STREPTOMYCES ARGILLACEUS CONTAINS A POSITIVE REGULATORY GENE AND TWO REPEATED DNA SEQUENCES THAT ARE LOCATED AT BOTH ENDS OF THE CLUSTER, *J BACTERIOL 181*, 642-647.
105. FERNANDEZ, E., WEISSBACH, U., SANCHEZ REILLO, C., BRANA, A. F., MENDEZ, C., ROHR, J., AND SALAS, J. A. (1998) IDENTIFICATION OF TWO GENES FROM STREPTOMYCES ARGILLACEUS ENCODING GLYCOSYLTRANSFERASES INVOLVED IN TRANSFER OF A DISACCHARIDE DURING BIOSYNTHESIS OF THE ANTITUMOR DRUG MITHRAMYCIN, *J BACTERIOL 180*, 4929-4937.
106. LOMBO, F., SIEMS, K., BRANA, A. F., MENDEZ, C., BINDSEIL, K., AND SALAS, J. A. (1997) CLONING AND INSERTIONAL INACTIVATION OF *STREPTOMYCES ARGILLACEUS* GENES INVOLVED IN THE EARLIEST STEPS OF BIOSYNTHESIS OF THE SUGAR MOIETIES OF THE ANTITUMOR POLYKETIDE MITHRAMYCIN, *J. BACTERIOL. 179*, 3354-3357.
107. KANTOLA, J., BLANCO, G., HAUTALA, A., KUNNARI, T., HAKALA, J., MENDEZ, C., YLIHONKO, K., MANTSALA, P., AND SALAS, J. (1997) FOLDING OF THE POLYKETIDE CHAIN IS NOT DICTATED BY MINIMAL POLYKETIDE SYNTHASE IN THE BIOSYNTHESIS OF MITHRAMYCIN AND ANTHRACYCLINE, *CHEM BIOL 4*, 751-755.

108. LOMBO, F., BLANCO, G., FERNANDEZ, E., MENDEZ, C., AND SALAS, J. A. (1996) CHARACTERIZATION OF STREPTOMYCES ARGILLACEUS GENES ENCODING A POLYKETIDE SYNTHASE INVOLVED IN THE BIOSYNTHESIS OF THE ANTITUMOR MITHRAMYCIN, *GENE 172*, 87-91.
109. GIBSON, M., NUR-E-ALAM, M., LIPATA, F., OLIVEIRA, M. A., AND ROHR, J. (2005) CHARACTERIZATION OF KINETICS AND PRODUCTS OF THE BAEYER-VILLIGER OXYGENASE MTMOIV, THE KEY ENZYME OF THE BIOSYNTHETIC PATHWAY TOWARD THE NATURAL PRODUCT ANTICANCER DRUG MITHRAMYCIN FROM *STREPTOMYCES ARGILLACEUS*, *J. AM. CHEM. SOC. 127*, 17594-17595.
110. WANG, C. C., GIBSON, M., ROHR, J., AND OLIVEIRA, M. A. (2005) CRYSTALLIZATION AND X-RAY DIFFRACTION PROPERTIES OF BAEYER-VILLIGER MONOOXYGENASE MTMOIV FROM THE MITHRAMYCIN BIOSYNTHETIC PATHWAY IN *STREPTOMYCES ARGILLACEUS*, *ACTA. CRYSTALLOGR., SECT. F-STRUCT. BIOL.CRYST. COMMUN. 61*, 1023-1026.
111. PEREZ, M., BAIG, I., BRANA, A. F., SALAS, J. A., ROHR, J., AND MENDEZ, C. (2008) GENERATION OF NEW DERIVATIVES OF THE ANTITUMOR ANTIBIOTIC MITHRAMYCIN BY ALTERING THE GLYCOSYLATION PATTERN THROUGH COMBINATORIAL BIOSYNTHESIS, *CHEMBIOCHEM 9*, 2295-2304.
112. BAIG, I., PEREZ, M., BRANA, A. F., GOMATHINAYAGAM, R., DAMODARAN, C., SALAS, J. A., MENDEZ, C., AND ROHR, J. (2008) MITHRAMYCIN ANALOGUES GENERATED BY COMBINATORIAL BIOSYNTHESIS SHOW IMPROVED BIOACTIVITY, *J. NAT. PROD. 71*, 199-207.
113. TREFZER, A., BLANCO, G., REMSING, L., KUNZEL, E., RIX, U., LIPATA, F., BRANA, A. F., MENDEZ, C., ROHR, J., BECHTHOLD, A., AND SALAS, J. A. (2002) RATIONALLY DESIGNED GLYCOSYLATED PREMITHRAMYCINS: HYBRID AROMATIC POLYKETIDES USING GENES FROM THREE DIFFERENT BIOSYNTHETIC PATHWAYS, *J. AM. CHEM. SOC. 124*, 6056-6062.
114. DURHAM, T. B., AND ROUSH, W. R. (2003) STEREOSELECTIVE SYNTHESIS OF FUNCTIONALIZED PRECURSORS OF THE CDEF AND CDE 2,6-DIDEOXY-TETRA- AND TRISACCHARIDE UNITS OF DURHAMYCINS A AND B, *ORG LETT 5*, 1875-1878.
115. LORICO, A., AND LONG, B. H. (1993) BIOCHEMICAL CHARACTERIZATION OF ELSAMICIN AND OTHER COUMARIN-RELATED ANTITUMOR AGENTS AS POTENT INHIBITORS OF HUMAN TOPOISOMERASE II, *EUR. J. CANCER 29A*, 1985-1991.
116. WEI, T. T., BYRNE, K. M., WARNICKPICKLE, D., AND GREENSTEIN, M. (1982) STUDIES ON THE MECHANISM OF ACTION OF GILVOCARCIN V AND CHRYSOMYCIN A, *J. ANTIBIOT. 35*, 545-548.

117. MATSUMOTO, A., AND HANAWALT, P. C. (2000) HISTONE H3 AND HEAT SHOCK PROTEIN GRP78 ARE SELECTIVELY CROSS-LINKED TO DNA BY PHOTOACTIVATED GILVOCARCIN V IN HUMAN FIBROBLASTS, *CANCER RES. 60*, 3921-3926.
118. MATSON, J. A., ROSE, W. C., BUSH, J. A., MYLLYMAKI, R., BRADNER, W. T., AND DOYLE, T. W. (1989) ANTITUMOR-ACTIVITY OF CHRYSOMYCIN-M AND CHRYSOMYCIN-V, *J. ANTIBIOT. 42*, 1446-1448.
119. SHEPHERD, M. D., LIU, T., MENDEZ, C., SALAS, J. A., AND ROHR, J. (2010) ENGINEERED BIOSYNTHESIS OF GILVOCARCIN ANALOGUES WITH ALTERED DEOXYHEXOPYRANOSE MOIETIES, *APPL ENVIRON MICROBIOL*.
120. BENTLEY, S. D., CHATER, K. F., CERDENO-TARRAGA, A. M., CHALLIS, G. L., THOMSON, N. R., JAMES, K. D., HARRIS, D. E., QUAIL, M. A., KIESER, H., HARPER, D., BATEMAN, A., BROWN, S., CHANDRA, G., CHEN, C. W., COLLINS, M., CRONIN, A., FRASER, A., GOBLE, A., HIDALGO, J., HORNSBY, T., HOWARTH, S., HUANG, C. H., KIESER, T., LARKE, L., MURPHY, L., OLIVER, K., O'NEIL, S., RABBINOWITSCH, E., RAJANDREAM, M. A., RUTHERFORD, K., RUTTER, S., SEEGER, K., SAUNDERS, D., SHARP, S., SQUARES, R., SQUARES, S., TAYLOR, K., WARREN, T., WIETZORREK, A., WOODWARD, J., BARRELL, B. G., PARKHILL, J., AND HOPWOOD, D. A. (2002) COMPLETE GENOME SEQUENCE OF THE MODEL ACTINOMYCETE STREPTOMYCES COELICOLOR A3(2), *NATURE 417*, 141-147.
121. BECHTHOLD, A., SOHNG, J. K., SMITH, T. M., CHU, X., AND FLOSS, H. G. (1995) IDENTIFICATION OF STREPTOMYCES VIOLACEORUBER TU22 GENES INVOLVED IN THE BIOSYNTHESIS OF GRANATICIN, *MOL GEN GENET 248*, 610-620.
122. XU, Z., JAKOBI, K., WELZEL, K., AND HERTWECK, C. (2005) BIOSYNTHESIS OF THE ANTITUMOR AGENT CHARTREUSIN INVOLVES THE OXIDATIVE REARRANGEMENT OF AN ANTHRACYCLIC POLYKETIDE, *CHEM BIOL 12*, 579-588.
123. KOBRYN, K., WATSON, M. A., ALLISON, R. G., AND CHACONAS, G. (2002) THE MU THREE-SITE SYNAPSE: A STRAINED ASSEMBLY PLATFORM IN WHICH DELIVERY OF THE L1 TRANSPOSASE BINDING SITE TRIGGERS CATALYTIC COMMITMENT, *MOLECULAR CELL 10*, 659-669.
124. BUTTERFIELD, Y. S. N., MARRA, M. A., ASANO, J. K., CHAN, S. Y., GUIN, R., KRZYWINSKI, M. I., LEE, S. S., MACDONALD, K. W. K., MATHEWSON, C. A., OLSON, T. E., PANDOH, P. K., PRABHU, A. L., SCHNERCH, A., SKALSKA, U., SMAILUS, D. E., STOTT, J. M., TSAI, M. I., YANG, G. S., ZUYDERDUYN, S. D., SCHEIN, J. E., AND JONES, S. J. M. (2002) AN EFFICIENT STRATEGY FOR LARGE-SCALE HIGH-THROUGHPUT TRANSPOSON-MEDIATED SEQUENCING OF CDNA CLONES, *NUCLEIC ACIDS RESEARCH 30*, 2460-2468.

125. WIDBOOM, P. F., FIELDING, E. N., LIU, Y., AND BRUNER, S. D. (2007) STRUCTURAL BASIS FOR COFACTOR-INDEPENDENT DIOXYGENATION IN VANCOMYCIN BIOSYNTHESIS, *NATURE 447*, 342-345.
126. RAMOS, A., LOMBO, F., BRANA, A. F., ROHR, J., MENDEZ, C., AND SALAS, J. A. (2008) BIOSYNTHESIS OF ELLORAMYCIN IN STREPTOMYCES OLIVACEUS REQUIRES GLYCOSYLATION BY ENZYMES ENCODED OUTSIDE THE AGLYCON CLUSTER, *MICROBIOLOGY 154*, 781-788.
127. BIERMAN, M., LOGAN, R., OBRIEN, K., SENO, E. T., RAO, R. N., AND SCHONER, B. E. (1992) PLASMID CLONING VECTORS FOR THE CONJUGAL TRANSFER OF DNA FROM *E. COLI* TO *STREPTOMYCES* SPP., *GENE 116*, 43-49.
128. QUIROS, L. M., AGUIRREZABALAGA, I., OLANO, C., MENDEZ, C., AND SALAS, J. A. (1998) TWO GLYCOSYLTRANSFERASES AND A GLYCOSIDASE ARE INVOLVED IN OLEANDOMYCIN MODIFICATION DURING ITS BIOSYNTHESIS BY STREPTOMYCES ANTIBIOTICUS, *MOL MICROBIOL 28*, 1177-1185.
129. MACNEIL, D. J., OCCI, J. L., GEWAIN, K. M., MACNEIL, T., GIBBONS, P. H., RUBY, C. L., AND DANIS, S. J. (1992) COMPLEX ORGANIZATION OF THE *STREPTOMYCES AVERMITILIS* GENES ENCODING THE AVERMECTIN POLYKETIDE SYNTHASE, *GENE 115*, 119-125.
130. LIU, T., FISCHER, C., BENINGA, C., AND ROHR, J. (2004) OXIDATIVE REARRANGEMENT PROCESSES IN THE BIOSYNTHESIS OF GILVOCARCIN V, *J. AM. CHEM. SOC. 126*, 12262-12263.
131. WANG, Q., DING, P., PEREPELOV, A. V., XU, Y., WANG, Y., KNIREL, Y. A., WANG, L., AND FENG, L. (2008) CHARACTERIZATION OF THE DTDP-D-FUCOFURANOSE BIOSYNTHETIC PATHWAY IN ESCHERICHIA COLI O52, *MOL MICROBIOL 70*, 1358-1367.
132. SLABA, K., HUSSEIN, A., PALKOVIC, P., HORVATH, V., AND TOMAN, R. (2003) STUDIES ON THE IMMUNOLOGICAL ROLE OF VIRENOSE AND DIHYDROHYDROXYSTREPTOSE PRESENT IN THE COXIELLA BURNETII PHASE I LIPOPOLYSACCHARIDE, *ANN N Y ACAD SCI 990*, 505-509.
133. TOMAN, R., SKULTETY, L., FTACEK, P., AND HRICOVINI, M. (1998) NMR STUDY OF VIRENOSE AND DIHYDROHYDROXYSTREPTOSE ISOLATED FROM COXIELLA BURNETII PHASE I LIPOPOLYSACCHARIDE, *CARBOHYDR RES 306*, 291-296.
134. LOMBO, F., GIBSON, M., GREENWELL, L., BRANA, A. F., ROHR, J., SALAS, J. A., AND MENDEZ, C. (2004) ENGINEERING BIOSYNTHETIC PATHWAYS FOR DEOXYSUGARS: BRANCHED-CHAIN SUGAR PATHWAYS AND DERIVATIVES FROM THE ANTITUMOR TETRACENOMYCIN, *CHEM BIOL 11*, 1709-1718.

135. RODRIGUEZ, L., AGUIRREZABALAGA, I., ALLENDE, N., BRANA, A. F., MENDEZ, C., AND SALAS, J. A. (2002) ENGINEERING DEOXYSUGAR BIOSYNTHETIC PATHWAYS FROM ANTIBIOTIC-PRODUCING MICROORGANISMS. A TOOL TO PRODUCE NOVEL GLYCOSYLATED BIOACTIVE COMPOUNDS, *CHEM BIOL 9*, 721-729.
136. PAULULAT, T., ZEECK, A., GUTTERER, J. M., AND FIEDLER, H. P. (1999) BIOSYNTHESIS OF POLYKETOMYCIN PRODUCED BY STREPTOMYCES DIASTATOCHROMOGENES TU 6028, *J ANTIBIOT (TOKYO) 52*, 96-101.
137. CHEN, H., ZHAO, Z., HALLIS, T. M., GUO, Z., AND LIU HW, H. (2001) INSIGHTS INTO THE BRANCHED-CHAIN FORMATION OF MYCAROSE: METHYLATION CATALYZED BY AN (S)-ADENOSYLMETHIONINE-DEPENDENT METHYLTRANSFERASE WE ARE GRATEFUL TO DR. EUGENE SENO AND THE LILLY RESEARCH LABORATORIES FOR THEIR GENEROUS GIFT OF THE PLASMID PHJL311 AND TO THE NATIONAL INSTITUTES OF HEALTH FOR GRANTS (GM 35 906 AND 54 346). H.-W.L. ALSO THANKS THE NATIONAL INSTITUTE OF GENERAL MEDICAL SCIENCES FOR A MERIT AWARD. T.M.H. WAS A TRAINEE OF THE NATIONAL INSTITUTE OF GENERAL MEDICAL SCIENCES (BIOTECHNOLOGY TRAINING GRANT: 2 T32 GM08347), *ANGEW CHEM INT ED ENGL 40*, 607-610.
138. BEIS, K., SRIKANNATHASAN, V., LIU, H., FULLERTON, S. W., BAMFORD, V. A., SANDERS, D. A., WHITFIELD, C., MCNEIL, M. R., AND NAISMITH, J. H. (2005) CRYSTAL STRUCTURES OF MYCOBACTERIA TUBERCULOSIS AND KLEBSIELLA PNEUMONIAE UDP-GALACTOPYRANOSE MUTASE IN THE OXIDISED STATE AND KLEBSIELLA PNEUMONIAE UDP-GALACTOPYRANOSE MUTASE IN THE (ACTIVE) REDUCED STATE, *J MOL BIOL 348*, 971-982.
139. PARTHA, S. K., VAN STRAATEN, K. E., AND SANDERS, D. A. (2009) STRUCTURAL BASIS OF SUBSTRATE BINDING TO UDP-GALACTOPYRANOSE MUTASE: CRYSTAL STRUCTURES IN THE REDUCED AND OXIDIZED STATE COMPLEXED WITH UDP-GALACTOPYRANOSE AND UDP, *J MOL BIOL 394*, 864-877.
140. JAIN, T. C., SIMOLIKE, G. C., AND JACKMAN, L. M. (1983) STRUCTURE AND STEREOCHEMISTRY OF TOROMYCIN; STUDIES OF ITS ACID-CATALYZED REARRANGEMENT, *TETRAHEDRON 39*, 599-605.
141. OLANO, C., ABDELFATTAH, M. S., GULLON, S., BRANA, A. F., ROHR, J., MENDEZ, C., AND SALAS, J. A. (2008) GLYCOSYLATED DERIVATIVES OF STEFFIMYCIN: INSIGHTS INTO THE ROLE OF THE SUGAR MOIETIES FOR THE BIOLOGICAL ACTIVITY, *CHEMBIOCHEM 9*, 624-633.
142. DOUMITH, M., WEINGARTEN, P., WEHMEIER, U. F., SALAH-BEY, K., BENHAMOU, B., CAPDEVILA, C., MICHEL, J. M., PIEPERSBERG, W., AND RAYNAL, M. C. (2000) ANALYSIS OF GENES INVOLVED IN 6-DEOXYHEXOSE BIOSYNTHESIS AND TRANSFER IN SACCHAROPOLYSPORA ERYTHRAEA, *MOL GEN GENET 264*, 477-485.

143. KHAREL, M. K., LIAN, H., AND ROHR, J. (2011) CHARACTERIZATION OF THE TDP-D-RAVIDOSAMINE BIOSYNTHETIC PATHWAY: ONE-POT ENZYMATIC SYNTHESIS OF TDP-D-RAVIDOSAMINE FROM THYMIDINE-5-PHOSPHATE AND GLUCOSE-1-PHOSPHATE, *ORG BIOMOL CHEM*.
144. DOUMITH, M., WEINGARTEN, P., WEHMEIER, U. F., SALAH-BEY, K., BENHAMOU, B., CAPDEVILA, C., MICHEL, J. M., PIEPERSBERG, W., AND RAYNAL, M. C. (2000) ANALYSIS OF GENES INVOLVED IN 6-DEOXYHEXOSE BIOSYNTHESIS AND TRANSFER IN *SACCHAROPOLYSPORA ERYTHRAEA*, *MOL. GEN. GENET. 264*, 477-485.
145. QUIROS, L. M., AGUIRREZABALAGA, I., OLANO, C., MENDEZ, C., AND SALAS, J. A. (1998) TWO GLYCOSYLTRANSFERASES AND A GLYCOSIDASE ARE INVOLVED IN OLEANDOMYCIN MODIFICATION DURING ITS BIOSYNTHESIS BY *STREPTOMYCES ANTIBIOTICUS*, *MOL. MICROBIOL. 28*, 1177-1185.
146. DRAUTZ, H., REUSCHENBACH, P., ZAHNER, H., ROHR, J., AND ZEECK, A. (1985) METABOLIC PRODUCTS OF MICROORGANISMS. 225. ELLORAMYCIN, A NEW ANTHRACYCLINE-LIKE ANTIBIOTIC FROM STREPTOMYCES OLIVACEUS. ISOLATION, CHARACTERIZATION, STRUCTURE AND BIOLOGICAL PROPERTIES, *J ANTIBIOT (TOKYO) 38*, 1291-1301.
147. WEBER, W., ZAHNER, H., SIEBERS, J., SCHRODER, K., AND ZEECK, A. (1979) [METABOLIC PRODUCTS OF MICROORGANISMS. 175. TETRACENOMYCIN C (AUTHOR'S TRANSL)], *ARCH MICROBIOL 121*, 111-116.
148. MOTAMEDI, H., AND HUTCHINSON, C. R. (1987) CLONING AND HETEROLOGOUS EXPRESSION OF A GENE CLUSTER FOR THE BIOSYNTHESIS OF TETRACENOMYCIN C, THE ANTHRACYCLINE ANTITUMOR ANTIBIOTIC OF STREPTOMYCES GLAUCESCENS, *PROC NATL ACAD SCI U S A 84*, 4445-4449.
149. DECKER, H., ROHR, J., MOTAMEDI, H., ZAHNER, H., AND HUTCHINSON, C. R. (1995) IDENTIFICATION OF STREPTOMYCES OLIVACEUS TU 2353 GENES INVOLVED IN THE PRODUCTION OF THE POLYKETIDE ELLORAMYCIN, *GENE 166*, 121-126.
150. BAO, W. L., WENDT-PIENKOWSKI, E., AND HUTCHINSON, C. R. (1998) RECONSTITUTION OF THE ITERATIVE TYPE II POLYKETIDE SYNTHASE FOR TETRACENOMYCIN F2 BIOSYNTHESIS, *BIOCHEMISTRY 37*, 8132-8138.
151. SUMMERS, R. G., ALI, A., SHEN, B., WESSEL, W. A., AND HUTCHINSON, C. R. (1995) MALONYL-COENZYME A:ACYL CARRIER PROTEIN ACYLTRANSFERASE OF *STREPTOMYCES GLAUCESCENS*: A POSSIBLE LINK BETWEEN FATTY ACID AND POLYKETIDE BIOSYNTHESIS, *BIOCHEMISTRY 34*, 9389-9402.

152. FU, H., MCDANIEL, R., HOPWOOD, D. A., AND KHOSLA, C. (1994) ENGINEERED BIOSYNTHESIS OF NOVEL POLYKETIDES - STEREOCHEMICAL COURSE OF 2 REACTIONS CATALYZED BY A POLYKETIDE SYNTHASE, *BIOCHEMISTRY 33*, 9321-9326.
153. SUMMERS, R. G., WENDTPIENKOWSKI, E., MOTAMEDI, H., AND HUTCHINSON, C. R. (1992) NUCLEOTIDE SEQUENCE OF THE *TCMII-TCMIV* REGION OF THE TETRACENOMYCIN C BIOSYNTHETIC GENE CLUSTER OF *STREPTOMYCES GLAUCESCENS* AND EVIDENCE THAT THE *TCMN* GENE ENCODES A MULTIFUNCTIONAL CYCLASE-DEHYDRATASE-O-METHYL TRANSFERASE, *J. BACTERIOL. 174*, 1810-1820.
154. ROHR, J., EICK, S., ZEECK, A., REUSCHENBACH, P., ZAHNER, H., AND FIEDLER, H. P. (1988) METABOLIC PRODUCTS OF MICROORGANISMS. 249. TETRACENOMYCINS B3 AND D3, KEY INTERMEDIATES OF THE ELLORAMYCIN AND TETRACENOMYCIN C BIOSYNTHESIS, *J ANTIBIOT (TOKYO) 41*, 1066-1073.
155. RAFANAN, E. R., JR., HUTCHINSON, C. R., AND SHEN, B. (2000) TRIPLE HYDROXYLATION OF TETRACENOMYCIN A2 TO TETRACENOMYCIN C INVOLVING TWO MOLECULES OF O(2) AND ONE MOLECULE OF H(2)O, *ORG LETT 2*, 3225-3227.
156. PATALLO, E. P., BLANCO, G., FISCHER, C., BRANA, A. F., ROHR, J., MENDEZ, C., AND SALAS, J. A. (2001) DEOXYSUGAR METHYLATION DURING BIOSYNTHESIS OF THE ANTITUMOR POLYKETIDE ELLORAMYCIN BY STREPTOMYCES OLIVACEUS. CHARACTERIZATION OF THREE METHYLTRANSFERASE GENES, *J BIOL CHEM 276*, 18765-18774.
157. BLANCO, G., PATALLO, E. P., BRANA, A. F., TREFZER, A., BECHTHOLD, A., ROHR, J., MENDEZ, C., AND SALAS, J. A. (2001) IDENTIFICATION OF A SUGAR FLEXIBLE GLYCOSYLTRANSFERASE FROM *STREPTOMYCES OLIVACEUS*, THE PRODUCER OF THE ANTITUMOR POLYKETIDE ELLORAMYCIN, *CHEM. BIOL. 8*, 253-263.
158. WOHLERT, S. E., BLANCO, G., LOMBÓ, F., FERNÁNDEZ, E., BRAÑA, A. F., REICH, S., UDVARNOKI, G., MÉNDEZ, C., DECKER, H., FREVERT, J., SALAS, J. A., AND ROHR, J. (1998) NOVEL HYBRID TETRACENOMYCINS THROUGH COMBINATORIAL BIOSYNTHESIS USING A GLYCOSYLTRANSFERASE ENCODED BY THE ELM GENES IN COSMID 16F4 AND WHICH SHOWS A BROAD SUGAR SUBSTRATE SPECIFICITY, *JOURNAL OF THE AMERICAN CHEMICAL SOCIETY 120*, 10596-10601.
159. RODRIGUEZ, L., OELKERS, C., AGUIRREZABALAGA, I., BRANA, A. F., ROHR, J., MENDEZ, C., AND SALAS, J. A. (2000) GENERATION OF HYBRID ELLORAMYCIN ANALOGS BY COMBINATORIAL BIOSYNTHESIS USING GENES FROM ANTHRACYCLINE-TYPE AND MACROLIDE BIOSYNTHETIC PATHWAYS, *J MOL MICROBIOL BIOTECHNOL 2*, 271-276.

160. PEREZ, M., LOMBO, F., BAIG, I., BRANA, A. F., ROHR, J., SALAS, J. A., AND MENDEZ, C. (2006) COMBINATORIAL BIOSYNTHESIS OF ANTITUMOR DEOXYSUGAR PATHWAYS IN *STREPTOMYCES GRISEUS*: RECONSTITUTION OF "UNNATURAL NATURAL GENE CLUSTERS" FOR THE BIOSYNTHESIS OF FOUR 2,6-D-DIDEOXYHEXOSES, *APPL. ENVIRON. MICROBIOL. 72*, 6644-6652.
161. PEREZ, M., LOMBO, F., ZHU, L. L., GIBSON, M., BRANA, A. F., ROHR, R., SALAS, J. A., AND MENDEZ, C. (2005) COMBINING SUGAR BIOSYNTHESIS GENES FOR THE GENERATION OF L- AND D-AMICETOSE AND FORMATION OF TWO NOVEL ANTITUMOR TETRACENOMYCINS, *CHEM.COMMUN.*, 1604-1606.
162. LOMBO, F., GIBSON, M., GREENWELL, L., BRANA, A. F., ROHR, J., SALAS, J. A., AND MENDEZ, C. (2004) ENGINEERING BIOSYNTHETIC PATHWAYS FOR DEOXYSUGARS: BRANCHED-CHAIN SUGAR PATHWAYS AND DERIVATIVES FROM THE ANTITUMOR TETRACENOMYCIN, *CHEM. BIOL. 11*, 1709-1718.
163. FISCHER, C., RODRIGUEZ, L., PATALLO, E. P., LIPATA, F., BRANA, A. F., MENDEZ, C., SALAS, J. A., AND ROHR, J. (2002) DIGITOXOSYLTETRACENOMYCIN C AND GLUCOSYLTETRACENOMYCIN C, TWO NOVEL ELLORAMYCIN ANALOGUES OBTAINED BY EXPLORING THE SUGAR DONOR SUBSTRATE SPECIFICITY OF GLYCOSYLTRANSFERASE ELMGT, *J. NAT. PROD. 65*, 1685-1689.
164. RAMOS, A., OLANO, C., BRANA, A. F., MENDEZ, C., AND SALAS, J. A. (2009) MODULATION OF DEOXYSUGAR TRANSFER BY THE ELLORAMYCIN GLYCOSYLTRANSFERASE ELMGT THROUGH SITE-DIRECTED MUTAGENESIS, *J BACTERIOL 191*, 2871-2875.
165. SALAH-BEY, K., DOUMITH, M., MICHEL, J. M., HAYDOCK, S., CORTES, J., LEADLAY, P. F., AND RAYNAL, M. C. (1998) TARGETED GENE INACTIVATION FOR THE ELUCIDATION OF DEOXYSUGAR BIOSYNTHESIS IN THE ERYTHROMYCIN PRODUCER SACCHAROPOLYSPORA ERYTHRAEA, *MOL GEN GENET 257*, 542-553.
166. CHEN, H. W., YAMASE, H., MURAKAMI, K., CHANG, C. W., ZHAO, L. S., ZHAO, Z. B., AND LIU, H. W. (2002) EXPRESSION, PURIFICATION, AND CHARACTERIZATION OF TWO N,N-DIMETHYLTRANSFERASES, TYLM1 AND DESVI, INVOLVED IN THE BIOSYNTHESIS OF MYCAMINOSE AND DESOSAMINE, *BIOCHEMISTRY 41*, 9165-9183.
167. CHANG, C. W., ZHAO, L. H., YAMASE, H., AND LIU, H. W. (2000) DESVI: A NEW MEMBER OF THE SUGAR N,N-DIMETHYLTRANSFERASE FAMILY INVOLVED IN THE BIOSYNTHESIS OF DESOSAMINE, *ANGEW. CHEM. INT. ED. ENGL. 39*, 2160-2163.
168. BORISOVA, S. A., ZHAO, L., SHERMAN, D. H., AND LIU, H. W. (1999) BIOSYNTHESIS OF DESOSAMINE: CONSTRUCTION OF A NEW MACROLIDE CARRYING A GENETICALLY DESIGNED SUGAR MOIETY, *ORG LETT 1*, 133-136.

169. XUE, Y. Q., ZHAO, L. S., LIU, H. W., AND SHERMAN, D. H. (1998) A GENE CLUSTER FOR MACROLIDE ANTIBIOTIC BIOSYNTHESIS IN *STREPTOMYCES VENEZUELAE*: ARCHITECTURE OF METABOLIC DIVERSITY, *PROC. NATL. ACAD. SCI. U.S.A. 95*, 12111-12116.
170. ZHAO, L. S., QUE, N. L. S., XUE, Y. Q., SHERMAN, D. H., AND LIU, H. W. (1998) MECHANISTIC STUDIES OF DESOSAMINE BIOSYNTHESIS: C-4 DEOXYGENATION PRECEDES C-3 TRANSAMINATION, *J. AM. CHEM. SOC. 120*, 12159-12160.
171. MADDURI, K., KENNEDY, J., RIVOLA, G., INVENTI-SOLARI, A., FILIPPINI, S., ZANUSO, G., COLOMBO, A. L., GEWAIN, K. M., OCCI, J. L., MACNEIL, D. J., AND HUTCHINSON, C. R. (1998) PRODUCTION OF THE ANTITUMOR DRUG EPIRUBICIN (4'-EPIDOXORUBICIN) AND ITS PRECURSOR BY A GENETICALLY ENGINEERED STRAIN OF STREPTOMYCES PEUCETIUS, *NAT BIOTECHNOL 16*, 69-74.
172. WOHLERT, S. E., BLANCO, G., LOMBÃ³, F., FERNÃ¡NDEZ, E., BRAÃ±A, A. F., REICH, S., UDVARNOKI, G., MÃ©NDEZ, C., DECKER, H., FREVERT, J., SALAS, J. A., AND ROHR, J. (1998) NOVEL HYBRID TETRACENOMYCINS THROUGH COMBINATORIAL BIOSYNTHESIS USING A GLYCOSYLTRANSFERASE ENCODED BY THE ELM GENES IN COSMID 16F4 AND WHICH SHOWS A BROAD SUGAR SUBSTRATE SPECIFICITY, *JOURNAL OF THE AMERICAN CHEMICAL SOCIETY 120*, 10596-10601.
173. BORISOVA, S. A., AND LIU, H. W. (2010) CHARACTERIZATION OF GLYCOSYLTRANSFERASE DESVII AND ITS AUXILIARY PARTNER PROTEIN DESVIII IN THE METHYMYCIN/PICROMYCIN BIOSYNTHETIC PATHWAY, *BIOCHEMISTRY 49*, 8071-8084.
174. NYBO, S. E., SHEPHERD, M. D., BOSSERMAN, M. A., AND ROHR, J. (2010) GENETIC MANIPULATION OF STREPTOMYCES SPECIES, *CURR PROTOC MICROBIOL CHAPTER 10*, UNIT 10E 13.
175. WANG, C., GIBSON, M., ROHR, J., AND OLIVEIRA, M. A. (2005) CRYSTALLIZATION AND X-RAY DIFFRACTION PROPERTIES OF BAEYER-VILLIGER MONOOXYGENASE MTMOIV FROM THE MITHRAMYCIN BIOSYNTHETIC PATHWAY IN STREPTOMYCES ARGILLACEUS, *ACTA CRYSTALLOGR SECT F STRUCT BIOL CRYST COMMUN 61*, 1023-1026.
176. BOSSERMAN, M. A., FLOREZ, A. B., SHAABAN, K. A., BRANA, A. F., SALAS, J. A., MENDEZ, C., AND ROHR, J. (2011) CHARACTERIZATION OF THE TERMINAL ACTIVATION STEP CATALYZED BY OXYGENASE CMMOIV OF THE CHROMOMYCIN BIOSYNTHETIC PATHWAY FROM STREPTOMYCES GRISEUS, *BIOCHEMISTRY 50*, 1421-1428.
177. HOFFMEISTER, D., DRAGER, G., ICHINOSE, K., ROHR, J., AND BECHTHOLD, A. (2003) THE C-GLYCOSYLTRANSFERASE URDGT2 IS UNSELECTIVE TOWARD D- AND L-CONFIGURED NUCLEOTIDE-BOUND RHODINOSES, *J AM CHEM SOC 125*, 4678-4679.

Stephen Eric Nybo

VITA

BORN: December 9, 1983 Nashville, TN

EDUCATION:

2006-Present Doctoral Candidate at University of Kentucky, Lexington, KY.
Cumulative GPA: 3.67
GRE Scores: Verbal: 570 (77%), Quantitative: 710 (71%), Analytical Writing: 6.0 (96%)
2006 B.A.,Biology and Classics, with honors, Transylvania University, Lexington, KY.

POSITIONS and TRAINING:

2006-2010 5th year Doctoral Candidate, Department of Pharmaceutical Sciences, College of Pharmacy, University of Kentucky, Lexington, KY.
Advisor: Jurgen Rohr, Ph.D.
Project: Study of the chrysomycin biosynthetic pathway through characterization of the gene cluster bioinformatically and *in vivo* characterization. Glycodiversification of elloramycin and mithramycin biosyntheses using combinatorial biosynthetic methodology.
Dissertation Title: *Isolation and elucidation of the chrysomycin biosynthetic gene cluster and altering the glycosylation patterns of tetracenomycins and mithramycin-pathway molecules.*
Anticipated Graduation Date: Fall, 2011

2006-2007 Graduate Student, Department of Pharmaceutical Sciences, College of Pharmacy, University of Kentucky, Lexington, KY.
Rotations:

- Kyung-Bo Kim, Ph.D., Department of Pharmaceutical Sciences. Synthesized epoxomycin derivative using PROTAC-based synthetic methodology.
- Jurgen Rohr, Ph.D. Department of Pharmaceutical Sciences. Extracted premithramycins A1 and A2; extracted saquayamycin derivatives from soil samples and analyzed metabolites via HPLC chromatography.

2002-2006 Undergraduate, Transylvania University, Lexington, KY.
Thesis Title: Vaccination as an Effective Means to Combat Emerging Infectious Diseases
Project: General studies in immunology, microbiology, cell biology, organic chemistry, animal behavior, genetics, and physiology. Also, training in Greco-Roman history and Latin grammar.

AWARDS AND RECOGNITION:

2010 Kentucky Opportunity Fellowship. One year fellowship, University of Kentucky.
2010 Graduate School Academic Year Fellowship. One year fellowship, University of Kentucky.

2006 Daniel R. Reedy Quality Fellowship. Three year fellowship, University of Kentucky.

2004 "Who's Who Among Students in American Universities and Colleges?" Recognized in annual publication.

2003 Member of Biology and Latin honoraries at Transylvania University.

2002 Transylvania University Pioneer Scholarship, partial tuition 4 year scholarship.

UNIVERSITY SERVICE:

2010 Reviewed several documents and letters for grammar and syntax for student(s) applying for green card and dissertations.
2009 Picked up post-doc and student from airport for study in our lab.
2008 Picked up prospective graduate student at airport for interview with the program.
Attended pot luck to answer questions for prospective graduate students about the department.
2007 Indirectly assisted summer student/rotation students with questions, helped with protocols in the lab, and generated enthusiasm for drug discovery division.
2007 Assisted with the graduate school's open house and fielded questions of interviewing students.

PEER REVIEWED PUBLICATIONS:

First co-author paper/First author

1) Nybo SE, Shaaban K, Scott D, Rohr J. Generation of A New Mithramycin Analogue by Incorporating Two Beneficial Bioisosteres through Combinatorial Biosynthesis. *In preparation.*

2) **Nybo SE**, Shaaban K, Kharel MK, Salas JA, Méndez C, Sutardjo H, and Rohr J**. Ketoolivosyl-tetracenomycin C: A new ketosugar-bearing tetracenomycin generated by combinatorial biosynthesis in a recombinant *Streptomyces* strain. *Submitted,* Oct. 2011.

3) Kharel MK*, **Nybo SE***, Shepherd MD*, and Rohr J**. Cloning and characterization of the ravidomycin and chrysomycin biosynthetic gene clusters. *Chembiochem.* 2010 Mar 1;11(4):523-32.

4) **Nybo SE**, Shepherd MD, Bosserman MA, and Rohr J**. Genetic manipulation of *Streptomyces* sp. *Curr Protoc Microbiol.* 2010 Nov;Chapter 10:Unit 10E.3.

Co-author manuscript

5) Kharel MK., Shepherd MD, **Nybo SE**, Smith ML, Bosserman MA, Rohr J**. Isolation of streptomyces species from soil. *Curr Protoc Microbiol*. 2010 Nov; Chapter 10:Unit 10E.4

6) Madan K. Kharel, **Nybo SE**, Pahari P, Shaaban KA, Shepherd MD, Tibrewal N, and Rohr J**. Angucyclines: Biosynthesis, Mode-of-Action, Synthesis, and New Natural Products. *Nat. Prod. Report.* In preparation.

*These authors contributed equally to this work.

** Primary Investigator.

MEETINGS

1) Kharel, Madan K., **S. Eric Nybo**, Micah D. Shepherd, Jurgen Rohr**. "Genetic Investigation of Chrysomycin and Ravidomycin Biosynthesis." Abstracts, 39th Central Regional Meeting of the American Chemical Society, Covington, KY, United States, May 20-23 (2007), CRM-257.

2) Clements, Joseph S., Eva Csuhai, Gerald L. Seebach, **S. Eric Nybo,** Zackary R. Edens. "Anthrapyridone syntheses: Electronic effects, part II." Abstracts of papers, 227th ACS National Meeting, Anaheim, CA, United States, March 28-April 1 (2004), CHED-796.